Detection and Mapping of Cannabis Use in Hair Samples Using Mass Spectrometry

Emma Elizabeth Beasley MSci

A thesis submitted in partial fulfilment of the requirements of

Sheffield Hallam University

for the degree of Doctor of Philosophy

December 2018

Acknowledgements

Firstly, I would like to thank my director of studies, Dr Thomas Bassindale, for the opportunity to undertake this project and for the help and guidance along the way. You always had faith that the project would come through in the end; hopefully it has. I would also like to thank the rest of my supervisory team, Dr Simona Francese and Dr Caroline Dalton, for your expert guidance and support.

Thank you to Professor Nicola Woodroofe for putting myself and the project forward for the Vice Chancellor's Scholarship without which this project would not have been possible. Your kind words and nods of encouragement through presentations were always a comfort.

Thank you to Professor Ron Heeren for the opportunity to work at M4I within the University of Maastricht. Working in your laboratory and witnessing the cutting edge of mass spectrometry research was awe inspiring and is an experience I will never forget.

I would also like to thank Dr Bryn Flinders for all your help and encouragement, the company in the lab on late nights, and for loaning a bike to me to get around Maastricht. It was lovely to have a friend in an unfamiliar place and I am truly grateful for your kindness and support.

I would like to thank Dr David Douce and Gareth Rhys Jones for the invitation to work at Waters, and for the hospitality and expertise shared.

I would like to extend a special thank you to Alex Andrews. You stopped working on your thesis (several times) to help with formatting mine. I hope your new life in Australia is all you wish for and more.

Thank you to my fellow PhD students, Ieva and Becky, for being there with me through the highs of our trip to New York to the lows of the frustrations that come with mass spectrometry research. I love you both and pass or fail I will always be grateful that I met you. Thank you also to Cristina for being the perfect antidote to the second-year blues. Watching you tackle the special language that is the Yorkshire dialect was a joy. I

have seen you grow so much from the first day you arrived in the UK and I wish you every success in your future career.

I would like to thank my husband, Lee, for putting up with my work schedule for the last four years. You truly have been on this journey with me from day one. You are the only one who knows just how close I came to quitting, and you are the one that encouraged me to keep going. You said that I could fail but I was not allowed to quit; this is a mantra I have kept with me since that day. You have adapted Figures, checked references, and been there for me every step of the way. I could not have got this far without you. I love you with all my heart.

Finally, I would like to thank my mum and dad, Hilary and Ron, for being my biggest cheerleaders. I love you both. You have an unfathomable amount of faith in my abilities and I am truly grateful for everything you have done for me. I know that pass or fail you are both proud of me, and that means the world.

Dad, I love you. In the past few months you have faced the most difficult time of your life with unimaginable strength. You are amazed by the science and technology that surrounds you. I now know where I got this special trait, and so this thesis is dedicated to you.

Abstract

Hair differs from other human materials used for toxicological analysis, such as blood or urine, because of its substantially longer window of detection (months to years) enabling retrospective investigations of drug consumption. Due to its solid and durable nature, hair may be analysed centuries after growth with little degradation. Other advantages of hair analysis include the non-invasiveness of its collection, which is of particular importance in infant/child investigations and the ease of sample storage.

Although hair analysis offers the potential to reveal information which is not possible with other biological matrices, it also suffers from some unique limitations that can make interpretation of findings challenging. These are largely due to exposure of hair to the environment before analysis can take place.

Current analytical techniques allow detection and quantification of cannabinoids in hair samples. Frequently used techniques include gas chromatography mass spectrometry and liquid chromatography mass spectrometry. The majority of studies exclusively analyse the natural products Δ9-tetrahydrocannabinol (THC), Cannabinol (CBN), cannabidiol (CBD) or the metabolite 11-nor-9-carboxy-tetrahydrocannabinol (THC-COOH).

In this thesis THC, CBD, CBN, THC-COOH and the additional metabolite 11-Hydroxy-delta-9-tetrahydrocannabinol (11-OH-THC) have been simultaneously detected and quantified in authentic hair samples using a novel atmospheric pressure chemical ionisation method coupled to gas chromatography mass spectrometry. The results of these findings are compared to self-report data and are largely found to be in concordance, with some anomalies. In addition, several strategies to overcome the complication of external contamination of hair samples were trialled and compared to self-report data.

In this thesis there is also an investigation presented to demonstrate the *in-situ* derivatisation of cannabinoids using matrix-assisted laser desorption ionisation (MALDI). This is the first time a hair has been analysed for cannabinoids using MALDI and the first example of *in situ* derivatisation for hair samples.

The addition of an N-methylpyridium group results in improved ionisation efficiency, permitting both detection and mapping of Δ9-tetrahydrocannabinol (THC), Cannabinol (CBN), cannabidiol (CBD) and the metabolites 11-nor-9-carboxy-tetrahydrocannabinol (THC-COOH), 11-Hydroxy-delta-9-tetrahydrocannabinol (11-OH-THC) and 11-nor-delta(9)-carboxy-tetrahydrocannabinol glucuronide (THC-COO-gluc) in single hair samples.

Additionally, for the first time an in-source re-arrangement of THC is reported and characterised in this thesis, thus contributing new knowledge in the analysis of this drug by MALDI mass spectrometry.

Contents

List of Tables

List of Figures

Abbreviations

11-OH-THC	11-Hydroxy-Δ^9-tetrahydrocannabinol
2D-GC	two-dimensional gas chromatography
3-HC	3-hydroxycoumarin
ACN	acetonitrile
APCI	atmospheric pressure chemical ionisation
APGC	atmospheric pressure gas chromatography
ATT	6-aza-2-thiothymine
BSTFA	N,O-Bis(trimethylsilyl)trifluoroacetamide
CB_1	cannabinoid receptor 1
CB_2	cannabinoid receptor 2
CBD	cannabidiol
CBN	cannabinol
CHCA	α-Cyano-4-hydroxycinnamic
CID	collision-induced dissociation
CNS	central nervous system
CTAB	cetyltrimethylammonium bromide
DEA	drug enforcement administration
DHB	2,5-Dihydroxybenzoic acid
ECCI	electron capture chemical ionisation
ECS	endocannabinoid System
EI	electron impact ionisation
ESI	electrospray ionisation
FMPTS	2-Fluoro-1-methylpyridinium-p-toluene-sulfonate
GC	gas chromatography
GC-MS	gas chromatography mass spectrometry
GC-MS/MS	gas chromatography tandem mass spectrometry
ICR	incorporation rate
LC	liquid chromatography
LC-MS	liquid chromatography-mass spectrometry
LiTFA	lithium trifluoroacetate

LLE	Liquid-liquid extraction
LOD	limit of detection
LOQ	limit of quantitation
m/z	mass to charge ratio
MALDI-MSP	matrix assisted laser desorption ionisation-mass spectrometry profiling
MALDI-MSI	matrix assisted laser desorption ionisation- mass spectrometry imaging
MDMA	3,4-Methylenedioxymethamphetamine
MIPSE	molecularly imprinted solid phase extraction
MS/MS	tandem mass spectrometry
MTBSTFA	N-Methyl-N-tert-butyldimethylsilyltrifluoroacetamide
ND	not detected
NICE	national institute for heal and care excellence
PFOH	2,2,3,3,3-pentafluoropropanol
PFPA	Pentafluoropropionic anhydride
Q	quadrupole
QqQ	triple quadrupole
Q-ToF	quadrupole time-of-flight
QUALY	quality adjusted life years
RT	retention time
SAMHSA	substance abuse and mental health services administrator
SoHT	society of hair testing
SCRA	synthetic cannabinoid receptor agonists
SPE	solid phase extraction
TFA	trifluoroacetic acid
TFAA	trifluoracetic acid anhydride
THC	Δ^9-tetrahydrocannabinol
THCA-A	Δ^9-Tetrahydrocannabinolic Acid A
THC-COO-glu	Δ^9-Tetrahydrocannabinolic acid-glucuronide
THC-COOH	11-Nor-9-carboxy-Δ^9-tetrahydrocannabinol
TMS	trimethylsilyl
TOF	time of flight
UPLC-MS/MS	ultra-performance liquid chromatography tandem mass spectrometry

Matrix (Disambiguation)

In relation to matrix assisted laser desorption ionisation the term matrix refers to a solvent containing one or more small organic molecules which is fundamental to the ionisation process.

In toxicology (in this thesis in relation to the use of gas chromatography-mass spectrometry) the term matrix refers to hair extracts.

Chapter 1. General introduction

The field of forensic toxicology encompasses analysis of biological specimens for substances such as alcohol, drugs and poisons, which are related to a medico-legal investigation.

Recent Home Office data indicates that, in England and Wales, cannabis remains the most commonly encountered illicit drug, where it accounted for 72% of the 138,955 drug samples seized by police in the financial year ending March 2017 [1]. As in previous years, cannabis was the most commonly used drug in 2016/17, with an estimated 6.6% of adults aged 16 to 59 having used it in the last year (around 2.2 million people) [2]. Due to its widespread use and popularity, the detection of cannabis use is important in the field of forensic toxicology.

In this introductory chapter, cannabis, including its mechanism of action and interpretational issues will be discussed in detail. In addition, the use of hair as an alternative biological matrix with advantages and pitfalls will also be discussed. Finally, current analytical techniques used to detect cannabis use in hair samples will be described.

1.1 Cannabis

Cannabis is a highly variable plant species in terms of botany, genetics, and chemical constituents. The precise number of species in the Cannabis genus has long been disputed [3]. Some reports proposed Cannabis as a polytypic genus, however, based on morphological, anatomical, phytochemical, and genetic studies, it is generally accepted as having a single, highly polymorphic species known as *Cannabis sativa Linnaeus* [4].

Cannabis has been used for recreational and medicinal purposes for centuries. For the purpose of this research, the term cannabis refers to the dried flower tops of the female plant. This product is also commonly known as marijuana or marihuana. The most common way to administer cannabis is by smoking, although it can also be ingested [5].

1.1.1 Chemical components of cannabis

The *cannabis sativa L.* plant contains more than 500 chemicals of which 61 are cannabinoids, a further 1500 compounds are produced by pyrolysis during smoking of cannabis [6]. Of the naturally occurring compounds delta-9-tetrahydrocannabinol (THC) is considered to be the main psychoactive component.

The THC content in cannabis plant material is extremely variable. In America the mean concentration of THC in plant material seized by the Drug Enforcement Agency (DEA) has increased year-on-year from 4 to 12% in the years 1995 to 2014, although concentration ranges are not reported [7].

In 2005 a study of 247 cannabis samples collected from street level users in the UK revealed a wide concentration range of 1.16-23% with a median level of 14% [8]. In a more recent UK study conducted in 2016, the concentration range was highly variable, from 1.9% to 22.5%, with a median value of 14.2% for the 400 samples tested [9].

1.1.2 Tetrahydrocannabinol formation and metabolism

In the growing *Cannabis sativa* plant, most cannabinoids are initially formed as carboxylic acids (e.g., Δ9-THCA and CBDA) that are decarboxylated to their corresponding neutral forms as a consequence of drying, heating, combustion, or aging [10] (Figure 1-1). CBN is often analysed in hair samples. It is not formed biosynthetically but is an oxidative degradant of Δ9-THC [11].

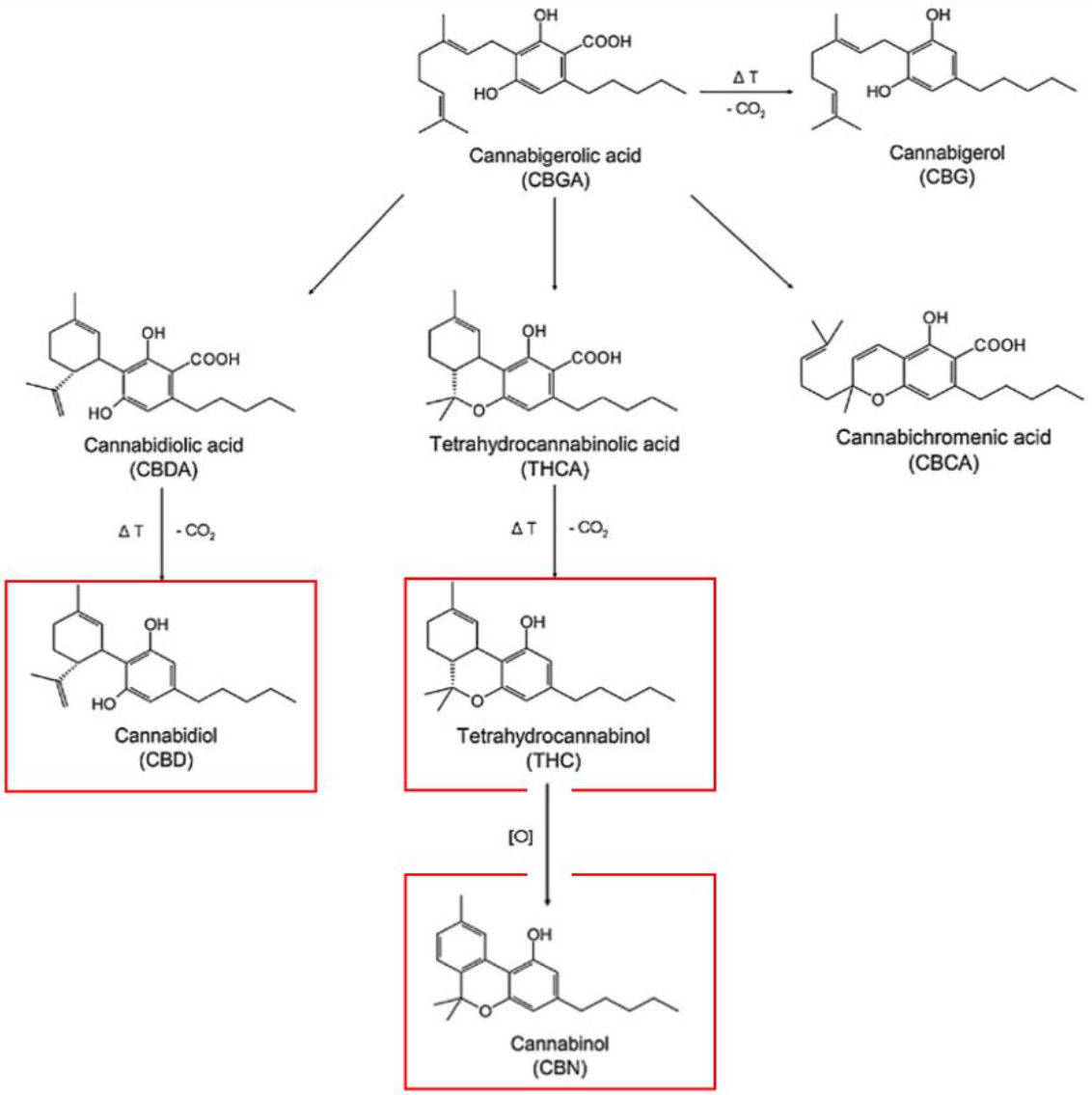

Figure 1-1. The biosynthetic pathway for the production of cannabinoids and breakdown products of THC. Compounds highlighted with a red box are target analytes in this research project.

When ingested or inhaled, THC undergoes complex hepatic metabolism based on oxidation and subsequent glucuronidation [6]. Since this is an enzymatic pathway only present *in vivo*, metabolite detection has been suggested as a solution to external contamination difficulties associated with solely analysing THC, CBD and CBN content in hair samples (see Section 1.3.7). The main oxidative metabolites of THC are 11-hydroxy-delta-9-tetrahydrocannabinol (11-OH-THC) and 11-nor-9-carboxy-delta-9-tetrahydrocannbinol (THC-COOH) which are shown in Figure 1-2. THC-COOH subsequently undergoes glucuronidation to form 11-nor-delta(9)-carboxy-tetrahydrocannabinol glucuronide (THC-COO-gluc).

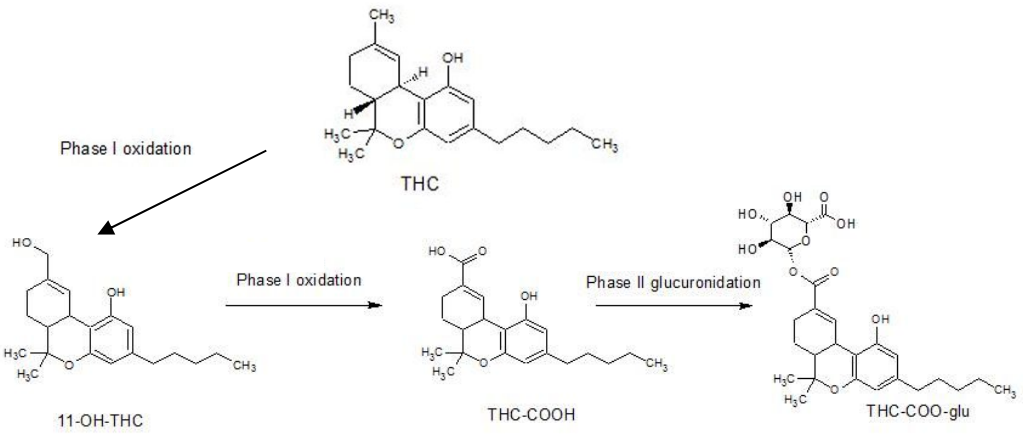

Figure 1-2. The *in vivo* metabolic pathway of THC.

1.1.3 Mechanism of action

The effects of THC are triggered by the compound binding to receptors in the endogenous cannabinoid system.

The endocannabinoid system (ECS) is a widespread neuromodulatory system that plays important roles in central nervous system development, synaptic plasticity, and the

response to endogenous and external stimuli [12]. The ECS comprises of cannabinoid receptors, endogenous cannabinoids, and the enzymes responsible for the synthesis and degradation of the endocannabinoids.

Two cannabinoid receptors have been identified in humans (CB_1 and CB_2) [13]. CB_1 receptors are found mainly on neurons in the brain and are present in high densities in other areas of the central nervous system (CNS). CB_1 is activated by the endogenous cannabinoids anandamide and 2-arachidonylglycerol (shown in Figure 1-3), among others. The pre-synaptic CB_1 receptor inhibits the release of both excitatory and inhibitory neurotransmitters in the CNS and peripheral nervous system. Activation of the CB_1 receptor produces a sensation of euphoria, along with other effects such as antiemetic and analgesic [14] which will be discussed further in Section 1.1.4.

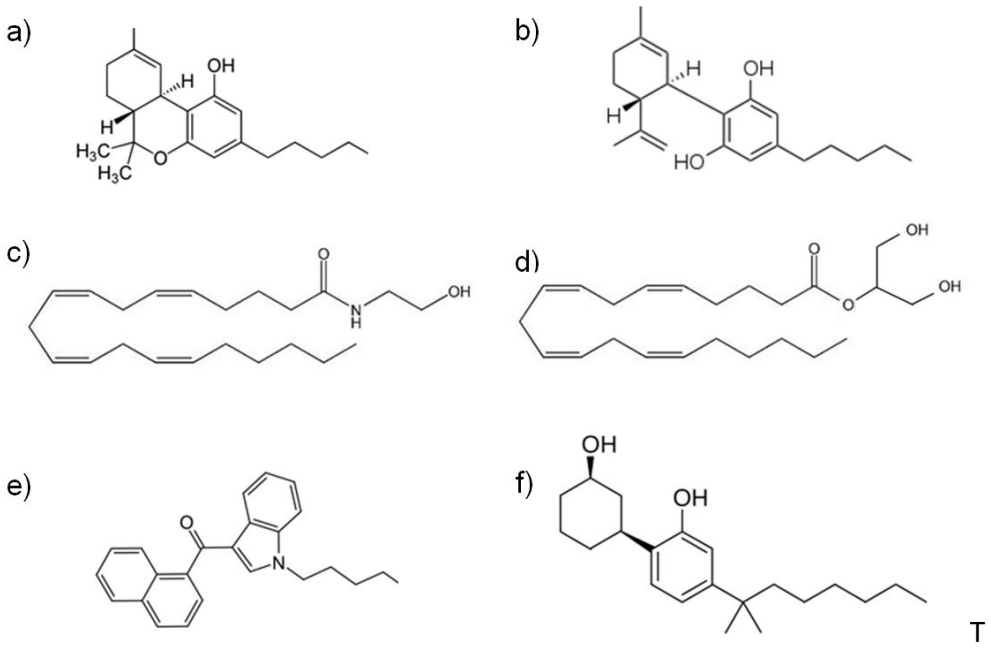

Figure 1-3. Structures of cannabinoid receptor agonists. a) plant cannabinoid THC, b) plant cannabinoid CBD, c) endocannabinoid anandamide, d) endocannabinoid 2-arachidonylglycerol e) synthetic cannabinoid JWH-018 f) synthetic cannabinoid CP47,497

The CB_2 receptor is predominantly expressed in the immune system, for example in the tonsils and spleen. CB_2 receptors appear to be involved in inflammatory processes [15], and so targeting this receptor may be a new approach to treat inflammatory diseases. Whilst activation of the CB_1 receptor produces psychotropic effects, the activation of the CB_2 receptor does not [16]. THC has approximately equal affinity for the CB_1 and CB_2 receptor whilst CBD has a very low affinity for both cannabinoid receptors. Interestingly, CBD antagonizes cannabinoid receptor agonists [16].

Recently there has been a rapid growth in the detection of synthetic cannabinoid receptor agonists (SCRAs). These are becoming increasingly chemically diverse, with 169 detected from 2008 to 2016. In 2015, just over 22 000 seizures of synthetic cannabinoids were reported across Europe [17]. These seizures amounted to more than 2.5 tonnes of the substances.

SCRAs were originally developed to research the CB_1 and CB_2 receptors. SCRAs include compounds such as JWH-018 and CP47,497 (shown in Figure 1-3) which are now sold under the brand names such as “spice”,” K2”, and “black mamba” for recreational use. Many SCRAs have a higher CB_1 binding affinity than THC, and so have been known to cause severe adverse effects [18].

A more detailed review on downstream cellular responses to CB_1 and CB_2 activation can be found by Ibsen *et al.*[19].

1.1.4 Desired effects and therapeutic uses of cannabis

It is widely accepted that cannabis can have many therapeutic properties including as a treatment for chronic pain [20–22], muscle spasticity in multiple sclerosis patients [23,24] and as an anti-sickness (antiemetic) treatment for patients undertaking chemotherapy [25,26]. There is also some evidence to suggest cannabis can be used as a treatment for Tourette's syndrome [27]. In light of these findings, the use of medical marijuana has been legalised in several American states, and in September 2018 the law in the UK was changed to allow its use in some specific treatments [28].

In 2010, GW Pharmaceuticals released a cannabis-derived medicine in the form of an oromucosal spray marketed under the brand name of Sativex. It is used to treat muscle stiffness/spasm due to multiple sclerosis. The formulation contains a 1:1 ratio of THC and CBD as active ingredients and can be prescribed in the UK [29]. However, NICE (National Institute for Health and Care Excellence) recommend that Sativex should not be prescribed as it is not cost effective [30].

In 2018, Epidiolex was approved as a prescription medicine by the FDA. Epidiolex is used to treat severe forms of epilepsy and is also produced by GW Pharmaceuticals. In contrast to Sativex, the active ingredient of Epidiolex is solely CBD [31].

1.1.5 Adverse effects of cannabis use

The recreational use of cannabis is illegal in most countries (including the UK). This is due to the adverse effects associated with cannabis usage including anxiety, depression, panic reactions and psychotic symptoms including an increased risk of developing schizophrenia [32]. However, despite some recent sensationalist media coverage, it is important to highlight the fact that cannabis consumption alone is not

enough to cause mental health problems, but in combination with other compounding factors such as a family history of mental health issues, the age of exposure to cannabis, and genetic factors cannabis can increase the risk of developing mental health problems. A detailed review of the link between cannabis use and mental health problems can be found by Radhakrishnan *et al.* [33]. Some studies suggest that CBD intake may mitigate adverse effects of THC usage including hallucinations/delusions and social withdrawal (introvertive anhedonia) [34].

In addition to possible adverse effects on mental health, a link between cannabis consumption and reaction time impairment has been established and it is thought that people who drive under the influence of cannabis are around twice as likely to be involved in a serious car accident [35–38]. Other negative traits associated with cannabis use include risk taking, antisocial behaviour, and poor academic performance [39].

1.2 Biological matrices for the detection of cannabis use

The biological matrices blood, urine, hair, oral fluid and sweat have been proposed for the detection of cannabis use. Each matrix has its own advantages and limitations associated with it, as summarised in Table 1-1. A detailed review of biological matrices used for determining cannabis use can be found by Musshoff and Madea [40].

Biological sample	Advantages	Limitations
Blood	Preferred for the interpretation of acute effects after cannabis abuse. Able to distinguish between occasional and regular users [41].	Invasive. Sample collection needs to be performed by a trained medical professional. Shortest window of detection compared to other biological samples. Blood samples should be stored at -20°C [42].
Urine	Non-invasive. Commonly used in workplace testing, well-established technique.	Procedure is limited to samples obtained within a few days after the last consumption [40] (up to months if sample is taken from a chronic user). Concerns around privacy during collection. Samples must be stored at -20°C[43].
Sweat	Non-invasive. Usually collected weekly over several weeks, giving a long detection window and insights into drug use patterns [44].	Possibility of time-dependent drug loss from the patch by drug degradation on the patch or skin, reabsorption into the skin and volatile losses through the covering membrane of the patch [44].
Hair	Non-invasive, long window of detection (depending on hair length) stored at room temperature.	Possibility of external contamination. Low incorporation rates of metabolites [45] .
Oral fluid	Non-invasive. Fast, simple sample collection. Compatible with point-of-collection-testing making rapid analysis possible at the roadside [46].	Only able to detect recent cannabis use unless sample is provided by a chronic cannabis smoker [47]. THC can reduce salivation, leading to reduced sample volume. Confirmatory testing still needed after a roadside positive test.

Table 1-1. Advantages and limitations of several biological matrices used for the detection of recent or ongoing cannabis use.

1.3 Hair testing for the analysis of cannabis use

1.3.1 Hair

Hair is a feature common to all mammals. Its main biological function is to facilitate thermoregulation, but additional functions include camouflage and increasing sensory perception. The main function of human hair is for protection (eyelashes stop things entering and irritating the eyes whilst scalp hair prevents physical damage from sunlight to the head and neck) [48].

As described in Table 1-1, hair differs from other human materials used for toxicological analysis such as blood or urine because of its substantially longer detection window (months to years) enabling retrospective investigation of chronic and past consumption. Because of its solid and durable nature, hair analysis can be performed even centuries after growth [49]. Other advantages of hair analysis include the non-invasiveness of its collection; eradicating the need for special restroom facilities and same-sex collectors (as with urinalysis) or medically trained sample collectors (as with blood analysis). Finally, the ease of sample storage is an additional benefit of hair analysis as samples can be stored at room temperature and take up relatively little storage space.

1.3.2 Applications of hair testing

Despite the analytical pitfalls of hair testing with regards to external contamination, there are many applications which call for retrospective intake analysis which is not possible with other testing methods such as blood, urine or saliva analysis.

The first report of this type of retrospective analysis came in 1858 when arsenic was detected in the hair of a corpse exhumed 11 years after burial [50]. Perhaps one of the most famous uses of elemental analysis in hair was arsenic found in the hair of Emperor Napoleon Bonaparte over 100 years after his death [51]. Whilst elemental analysis of hair is still an important tool in forensic science today, modern hair analysis has much wider applications since the advent of chromatographic techniques allow for the detection of a wide variety of compounds.

Applications of modern hair testing include workplace drug testing programmes [52], drug facilitated crime investigations [53,54], post-mortem investigations [55–59], driving licence renewals [60] and even the detection of chemical warfare agents [61].

One of the most common reasons for undertaking hair testing in the UK is for evidence in family courts as to whether a parent has abstained from drugs and/or alcohol. The Times newspaper claimed that in 2010 over 10,000 hair tests had been conducted for UK family courts over the course of a year [62].

Clinical applications of hair testing have become more prevalent in recent years. This includes investigating patient compliance to prescribed medications. To date, research has primarily focused on the detection of drugs used to treat HIV [63–67]. The testing of neonatal hair to determine in-utero exposure has also been studied for both alcohol [68–70], nicotine [71] and illicit drugs [71–81]. Another possible clinical application of hair testing is to determine the suitability of a patient to receive an organ transplantation by determining drug and alcohol use or abstinence [82,83]. It has also been suggested that hair cortisol levels can be used as a biomarker for chronic stress, and a recent review article by Steudte-Schmiedgen concluded that hair cortisol

analysis is a promising addition to trauma and posttraumatic stress disorder (PTSD) related research [84].

1.3.3 Anatomy of hair

To understand the incorporation of xenobiotics into hair, an understanding of the anatomy of hair is also needed. Initially hair can be divided into two main sub groups, the hair shaft which is seen externally as flexible tubes of dead, fully keratinized epithelial cells and the living hair follicle which is located 3-5 mm below the surface of the skin.

1.3.3.1 Anatomy of the hair shaft

The hair shaft has three structural areas; the innermost of these is the medulla as can be seen in Figure 1-4. It may be continuous across the hair shaft, discontinuous or even completely absent. The cortex represents the majority of the hair fibre composition and plays an important role in the physical and mechanical properties of hair [85]. The outermost region of the hair shaft is the cuticle; it covers the hair from the root to the tip of the epidermis and is formed of 5-10 layers of flat overlapping cells. The cuticle can become damaged due to hair treatments, such as bleaching, dying, perming and the use of styling techniques such as straightening and curling which exposes the hair to intense heat.

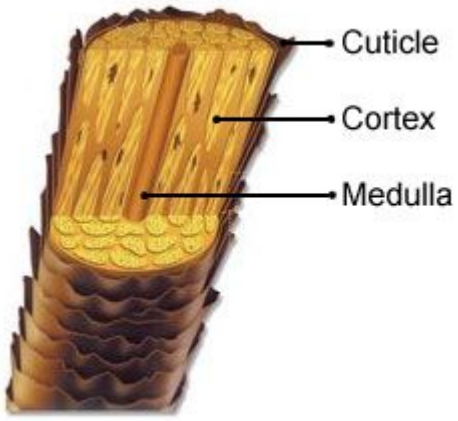

Figure 1-4. The anatomy of the hair shaft showing the three distinct areas. Reproduced from [86].

1.3.3.2 Anatomy of the hair follicle

The structure of the hair follicle can be seen in Figure 1-5. At the base of the hair bulb is the dermal papilla which contains the blood supply to the follicle. This is the main source for transport and supply of metabolic fuel and hence of drug molecules. The cell membranes of the matrix cells (that are localized in a cone-shaped region around the papilla) and the cell membranes of the melanocytes (that are situated at the apex of the papilla) are exposed to the circulating blood, lymph and extracellular fluids [87]. As the hair grows from the bulb it dehydrates and keratinisation takes place.

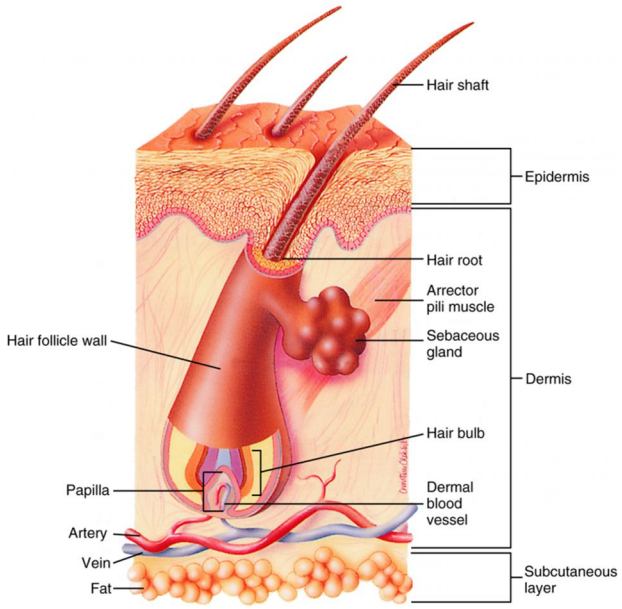

Figure 1-5. The structure of the hair follice. Reproduced from [88].

1.3.4 Hair growth rates and hair growth cycle

Other important factors in the interpretation of hair analysis results include the hair growth rate and the hair growth cycle. Hair grows in a cycle composed of the anagen (active growing), catagen (transition) and telogen (resting) stages. At any one time, approximately 85% of adult scalp hair is in the growing phase (anagen) with the remaining 15% in the resting phase (telogen). In the telogen phase the dermal papilla contains no capillaries [89]. The rate of hair growth can vary between individuals, with studies showing a five-fold difference in head hair growth rate from 0.6 to 3.36 cm per month [89]. However, as can be seen in Table 1-2 reproduced from the review article by LeBau *et al.*, the average growth rate is approximately 1 cm per month [90]. Despite the wide range in growth rates between individuals the Society of Hair Testing (SoHT) recommends using the 1 cm per month average when interpreting results for head hair [91]. This can cause assessments of a timeline of usage/abstinence to be inaccurate. For example, for an individual with a hair growth rate of 0.65 cm per

month a 1 cm section would equate to approximately 47 days of usage. However, for an individual with a hair growth rate of 2.2 cm per month a 1 cm section would equate to approximately 14 days of usage.

Year of publication	**Growth rate (cm/month)**			
	Minimum	Maximum	Average	Reference
1951	0.84	1.15	0.98	[92]
1964	0.76	0.96	0.86	[93]
1992	0.84	1.37	1.12	[94]
1993	0.6	3.36	Not reported	[89]
1996	0.65	2.2	1.4	[95]
2004	0.95	1.12	1.04	[96]
2007	0.73	1.48	1.11	[97]

Table 1-2. Published growth rates of human head hair, adapted from a review article by LeBeau *et al.* [98].

It is worth noting that other hair types such as chest, pubic, axillary, beard, arm and leg can be used in testing however head hair is preferred because it has the fastest growth rate with the highest percentage of follicles in the anagen phase [99].

1.3.5 Mechanisms of drug incorporation into hair

There are several possible mechanisms of incorporation of drug compounds into hair. Whilst for interpretational purposes it would be advantageous for compounds only to be incorporated from the blood stream, there are several other possible mechanisms. These include sweat, sebum, smoke, contaminated hands and secondary transfer (Figure 1-6). In this section each model will be discussed, including an evaluation of

how each possible route of incorporation can affect the interpretation of hair testing results.

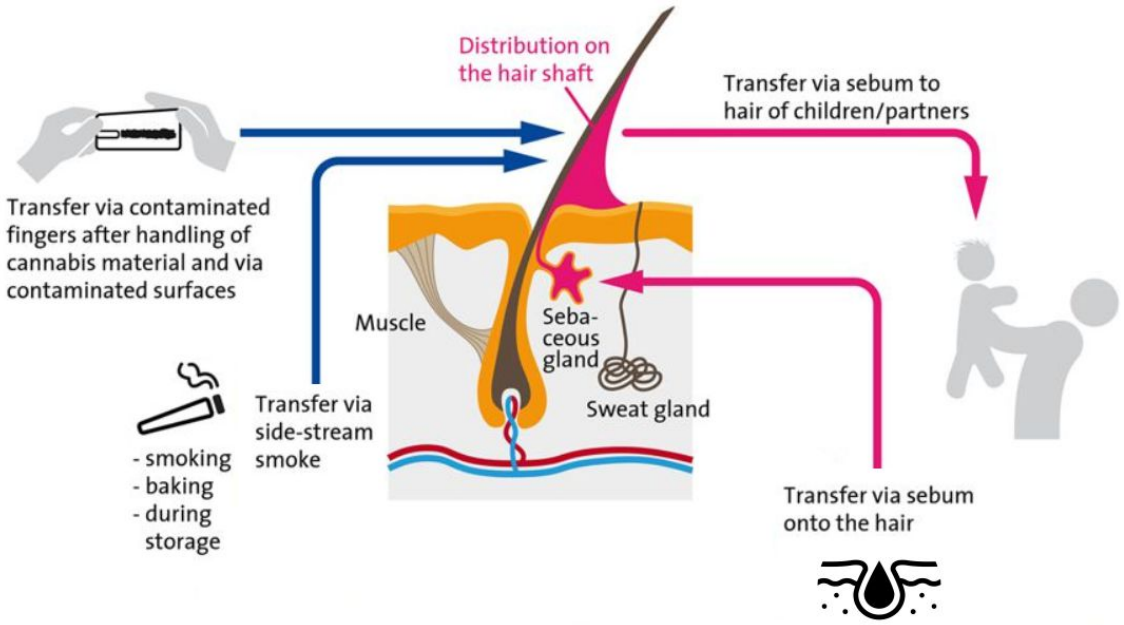

Figure 1-6. Possible methods of cannabinoid incorporation into hair samples, in addition to incorporation via the bloodstream. Adapted from [100].

1.3.5.1 Incorporation from blood

Incorporation models typically assume that drugs or chemicals enter hair by passive diffusion from blood capillaries into growing cells within the hair bulb and then becomes "trapped" in the keratinised cells as the hair dehydrates [101].

For a drug molecule to permeate a cell it must cross the plasma membrane. Therefore, the physicochemical properties of both the cell membrane and drug molecule largely dictate the amount of drug which is incorporated into the hair from the bloodstream. Nakahara *et al.* studied the effects of melanin affinity and lipophilicity on the incorporation rate (ICR) of twenty drugs of abuse using a rat model. They concluded

that both melanin affinity and lipophilicity were positively correlated with the ICR, except for in the case of 11-nor-9-carboxy-THC (THC-COOH) where the ICR was low despite having high lipophilicity [45].

The pKa of the drug molecule is also important in the passage of the drug from the plasma into the melanocytes of the hair bulb as the molecule must be non-ionised to cross the cell membrane. There is a pH gradient from plasma (pH 7.3) to the melanocytes of the hair bulb (pH 3-5) [99] this in turn means that basic compounds incorporate preferentially to acidic compounds. This is described in more detail in Figure 1-7 reproduced from Pragst *et al.* [99].

It should be noted that it is only possible for drugs to be incorporated into the hair bulb when the hair is in the anagen phase of the growth cycle (see Section 1.3.3).

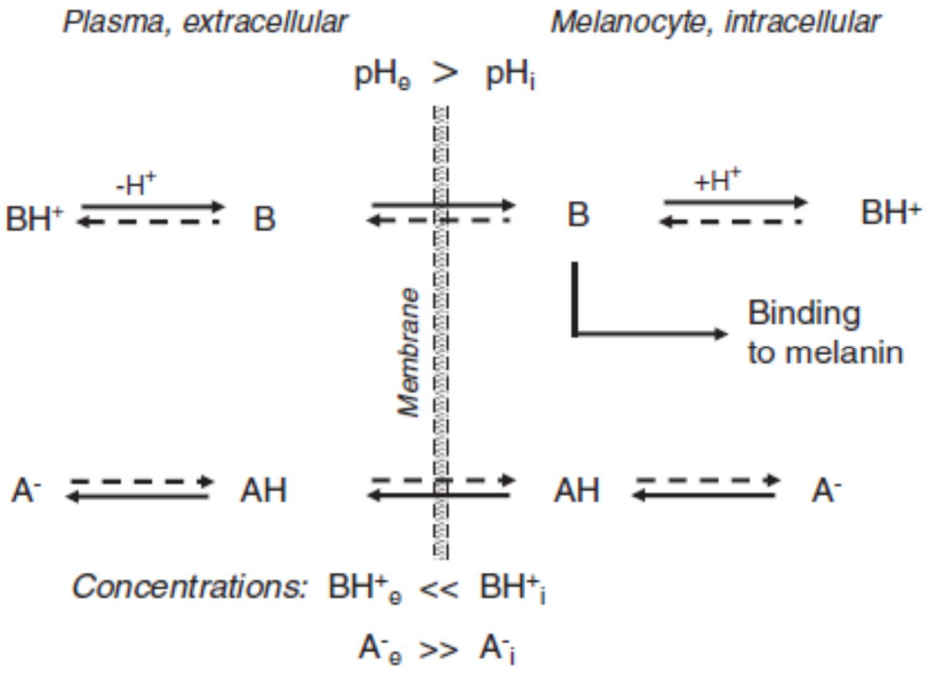

Figure 1-7. Influnce of acidic/basic properties of drugs on the incorporation of xenobiotics from the bloodstream into the cells of the hair bulb reproduced from [99].

Ideally, the passage from blood to the hair follicle would be the only incorporation route of xenobiotics into hair, allowing for a clear dose-response correlation; however, this is not the case, and interpretational issues arising from this are summarised in Section 1.3.6.1

1.3.5.2 Incorporation from sebum and sweat

As sebum is secreted directly on to the hair surface this is thought to play a role in the detection of drugs in hair samples [99]. Stout and Ruth found that sebum had a nominal effect on incorporation in their study of cocaine, nicotine and flunitrazepam in mouse hair [102], however there is a lack of literature of the effect of sebum on incorporation of cannabinoids.

It is well known that drugs and their metabolites are excreted in sweat. In fact, sweat-testing is becoming a popular alternative sampling technique [103] (see Section 1.2). Sweat bathes scalp and other hair and this presents interpretational difficulties in the context of hair analysis, as it is difficult to determine whether drugs came from incorporation via the blood stream or via sweat. Whilst this may not seem problematic; as drugs present in sweat are a direct consequence of intake, it could lead to elevated levels detected in hair (possibly taking samples beyond a cut-off). In addition, it will skew the results of segmental analysis, as shown by Henderson *et al.,* where deuterated cocaine was detected in multiple hair segments suggesting multiple intakes of the drug however only a single dose of the drug was administered [104]. This was found in 74% of the 23 individuals tested, despite washing the hair prior to analysis.

1.3.5.3 Incorporation from external sources

In addition to incorporation from the bloodstream and sweat, external sources of contamination must also be considered when analysing hair since the hair shaft is exposed to the environment.

Likely sources of external contamination include powders from drugs such as cocaine and smoke contamination from drugs such as crack cocaine, heroin and cannabis. It is possible that contamination can also occur from touching drugs and then touching hair directly after [100,105]. In fact, in 2009 the FBI ceased all hair testing for cocaine citing the likelihood of external contamination as the reason [106]. Testing was then re-instated in 2014 due to new guidelines which included extensive wash protocols and the detection of metabolites [107].

Washing procedures have been used to help eliminate externally bound drugs, along with monitoring of metabolites. These can be useful in reducing false positives, however may not prevent them entirely. This is discussed further in Section 1.3.8.

1.3.6 Analysis of hair to detect cannabis use

Several cannabinoids, including THC and its metabolites can be detected in hair samples using standard analytical techniques such GC-MS and LC-MS. Between the year 2000 and 2014 there was just one publication on the detection of cannabinoids using LC-MS and 15 publications using GC-MS. These and their findings are summarised Table 1-3.

There are a wide range of concentrations of each cannabinoid detected in the hair of cannabis users. Differences in amounts and frequency of usage and in individual smoking style (depth of inhalation, puff duration, and breathhold) will be a factor.

Analytical reasons for variations could also include differing sample preparation, analytical technique, and differing concentration of cannabinoids in the original plant material.

In most studies summarised in Table 1-3 the concentration of THC is greater than other cannabinoids. This is not always the case, as some studies found CBD to be at higher concentration than THC [108,109]. In the study conducted by Salomone *et al.* 29% of individuals had CBD concentrations higher than THC [110].

In all cases where both THC and THC-COOH are analysed in the same sample, the concentration of THC is much higher. This could be explained by the fact that peak plasma concentrations are approximately three times higher for THC than for THC-COOH after cannabis is smoked, as shown in Figure 1-8. However THC-COOH was detected for on average 11 times longer in blood than THC in a study conducted by Heustis *et al.* [111].

Some studies found that samples had low THC concentrations but high CBN concentrations [108,112,113]. This may be explained by the pyrolytic degradation of THC to CBN when cannabis is smoked [112,114].

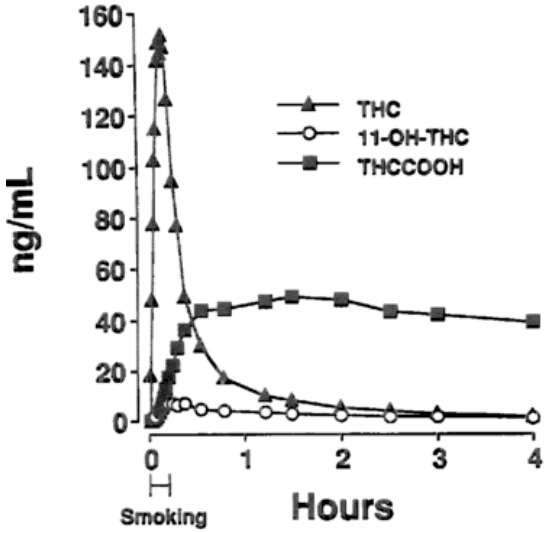

Figure 1-8. Mean plasma levels of THC, 11-OH-THC and THC-COOH during and after smoking a single 3.55% THC marijuana cigarette reproduced from [111].

THC (ng/mg)	CBD (ng/mg)	CBN (ng/mg)	THC-COOH (pg/mg)	No. of samples	Mass of sample used (mg)	Instrumentation	LOD/**LOQ** THC (ng/mg)	LOD/**LOQ** CBD (ng/mg)	LOD/**LOQ** CBN (ng/mg)	LOD/**LOQ** THC-COOH (pg/mg)	Ref
<LOQ-0.070	0.013-0.02	0.031-0.300	N/A	10	10	GC–EI-MS/MS	0.031, **0.062**	0.007, **0.012**	0.011, **0.030**	N/A	[115]
0.02-0.232	<LOQ-0.018	0.009-0.107	N/A	23	10	GC-EI-MS/MS	0.015, **0.20**	0.0005, **0.001**	0.0005, **0.001**	N/A	[113]
<LOQ-4.2	<LOQ-12.1	<LOQ-0.85	N/A	77	50	GC-EI-MS	0.012, **0.037**	0.013, **0.038**	0.016, **0.048**	N/A	[116]
0.09-0.72	ND-0.57	<LOQ-0.34	N/A	12	50	GC-EI-MS	Not reported	Not reported	Not reported	N/A	[117]
0.06-0.27	<LOQ-0.05	0.05-1.38	N/A	22	50	GC-EI-MS	0.006, **0.05**	0.005, **0.05**	0.002, **0.05**	N/A	[118]
<LOQ-0.73	0.81-19.02	0.12-1.48	N/A	20	10	GC-EI-MS	0.05, **0.27**	0.08, **0.27**	0.14, **0.51**	N/A	[109]
0.29-2.2	0.53-18.36	0.55-4.54	N/A	25	10	GC-EI-MS	0.05, **0.27**	0.08, **0.27**	0.14, **0.51**	N/A	[108]
0.13-7.25	0.23-2.79	0.05-2.27	N/A	9	Not reported	GC-MS	0.001 **Not reported**	0.02 **Not reported**	0.02 **Not reported**	N/A	[119]
0.054-0.553	0.018-1.862	0.031-0.205	N/A	14	50	UHPLC-MS/MS	0.0012, **0.0039**	0.0054, **0.018**	0.0016, **0.0053**	N/A	[110]
0.003-0.438	N/A	N/A	0.03 -1.53	93	70-100 strands	GC-NCI-MS/MS	Not reported	N/A	N/A	not reported	[120]
ND-0.11	N/A	N/A	ND-7.3	53	20	GC-NCI-MS/MS	0.001	N/A	N/A	0.1	[121]
N/A	N/A	N/A	ND-9.01	18	20	GC-NCI-MS/MS	N/A	N/A	N/A	0.025, **0.05**	[122]
N/A	N/A	N/A	0.05-9.38	224	25	GC-NCI-MS/MS	N/A	N/A	N/A	0.015, **0.05**	[123]
N/A	N/A	N/A	0.6-1.39	4	20	GC-NCI-MS	N/A	N/A	N/A	0.3, **0.4**	[124]
N/A	N/A	N/A	0.09-1.94	12	20	GC-GC-ECCI-MS	N/A	N/A	N/A	Not reported **0.05**	[125]
N/A	N/A	N/A	0.06-14.23	23	20	GC-NCI-MS/MS	N/A	N/A	N/A	0.025, **0.5**	[126]

Table 1-3. Summarised results from publications investigating cannabinoid detection in user hair samples, including reported Limits of Detection (LOD), limits of quantification (LOQ) and concentration ranges of various cannabinoids(N/A= cannabinoid not included in the study ND= not detected).

1.3.6.1 Dose/concentration correlation studies

Often in the context of medical or legal settings, toxicologists are asked to determine how much, or how often, a drug was used. To give an accurate answer to this question there must be a strong dose-concentration correlation for the biological sample being analysed.

In a study conducted by Huestis *et al.* it was found that 36% of confirmed cannabis users by urinalysis and self-report (n=38) had no detectable levels of THC or THC-COOH in their hair samples (LOQ 1.0 and 0.1 pg/mg of hair respectively). They also discovered that the median concentrations of THC and THC-COOH were not statistically different between daily and non-daily cannabis users [121]. Whilst a link between dose and concentration of cannabinoids in hair was not found, it should be noted that it was more likely for THC and THC-COOH to be detected in daily user's hair than in non-daily users.

Similarly, in 157 cases where cannabinoids were detected in hair samples as part of a study conducted by Sachs and Dressler [127] they concluded that: *"a dose-concentration relationship does not exist either for THC or THC-COOH, or even both".*

Despite Sachs and Dressler publishing these findings in the year 2000, the interpretation issue of a lack of dose/concentration correlation is still heavily debated today. For example, in the 2016 SoHT annual meeting one attendee asked the following question: *"What actually is the merit of quantification? Why do we strive to quantify we cannot compare inter-person, we cannot compare inter-lab? We cannot say the higher dose will give a higher result."*

The President of the SoHT, Markus Baumgartner replied: *"I think we should apply what the SoHT suggested many many years ago and that is low, medium or high range, not to say anything about the doses but to compare low medium or high. I think this is very helpful from my viewpoint."*

Without further investigation it is difficult to know if low, medium or high concentrations can be reliably reported. For this type of reporting to be effective there would need to be a uniform approach to sample preparation and analysis techniques. In addition, a shared database of results from all laboratories undertaking hair analysis would need to be available to overcome the problem of small or non-representative databases, which is not yet the case.

1.3.7 External contamination studies

As one of the main methods of drugs becoming incorporated into the hair is through external contamination, it is important to have an evidence base to aid in interpretation of analytical results. There are few studies that have been conducted in this area of research, as summarized below.

1.3.7.1 Contamination due to cannabis smoke

Since THC is present in the smoke produced when the plant material is combusted, the presence of THC in body fluids can be due to passive exposure to smoke, and not necessarily direct or intentional usage. As a result of this passive exposure to cannabis smoke has successfully been used as a defence in UK courts [128].

Several studies have been conducted into the passive exposure of cannabis smoke in relation to cannabinoid levels in blood [129–133] , urine [129–138] and oral fluid [139–142]. Early studies suggested that passive exposure to cannabis smoke could give

positive results, however these studies were heavily criticised due to the extreme, unrealistic conditions used [143]. This included the simultaneous burning of multiple marijuana cigarettes and the use of very small, unventilated rooms. In some studies participants even had to wear goggles to prevent eye irritation [133,136].

One recent study conducted by Röhrich *et al.* focused on investigating more realistic conditions of passive exposure on blood and urine samples [132]. The study was carried out in a Netherlands coffee shop where cannabis was legally being smoked. Eight non-smoking participants stayed in the coffee shop for three hours. The results showed that none of the urine samples produced immunoassay results higher than the cut-off concentration of 25 ng/mL, therefore none of the participants would be accused of cannabis use in a routine drug screen. GC-MS analysis revealed trace amounts of THC and THC-COOH in both urine and plasma. However, the highest concentration of THC-COOH found in urine was less than half of the cut-off concentration recommended by the Substance Abuse and Mental Health Services Administration (SAMHSA) guidelines for federal workplace drug testing programmes of 15 ng/mL, and so again, none of the eight participants would be reported positive for cannabis consumption.

Whilst it has been widely reported that marijuana smoke elevates the THC levels found in hair samples, investigations into the level of incorporation and/or factors effecting this incorporation are extremely limited as discussed below:

The first *in vitro s*tudy was performed by Strano-Rossi and Chiarotti where hair samples were exposed to marijuana smoke to evaluate decontamination procedures [112]. Further to this Thorspecken *et al.* adapted a desiccator to contaminate hair

samples with marijuana smoke to investigate the effect of moistening the hair and hair treatments on the level of THC detected. The authors concluded that moistening the hair before exposure raised the concentration of THC and CBN, whilst bleaching and perming the hair lowered the concentration of THC and CBN. This study was limited by that fact that only one, pooled sample of dark blonde hair of Caucasian origin was used, and similarly only one time point was used (sixty minutes of exposure).

The first and as yet only *in vivo* marijuana smoke contamination study was conducted in 2014 by Moosmann *et al*. In this study three participants were exposed to the smoke of one marijuana cigarette whilst breathing through SCUBA regulators [144]. The exposure was repeated every weekday over a three-week period in a relatively small room (2.5 m^2).

The authors stated that the degree of contamination differed with length of hair, with shorter hair being less affected by contamination than medium and longer hair. However, it should be noted that the sample size was small (n=1 for each hair length) and differences could also be due to personal washing technique of the hair as neither this nor the brand of shampoo used was standardised in the study.

The authors also cast doubt over the Society of Hair Testing recommended sampling site of the posterior vertex region [145] , claiming that this sampling site suffers from the highest degree of contamination. However, again it must be noted that only one participant was used for this part of the study, and personal hair washing procedure of this individual could contribute to the finding.

Interestingly, THC was detected in all three of the participant's hair samples after the exposure period with a concentration range of 140-1700 pg/mg of hair. This is well

above the SoHT cut-off of 50 pg/mg. Two out of the three participants had levels of THC above the cut-off four weeks after exposure and one participant even had levels above the cut off seven weeks after exposure, despite daily washing of the hair with shampoo and a decontamination procedure prior to analysis.

1.3.7.2 Contamination due to handling of cannabis plant material

Since THC is present in plant material, it is reasonable to assume that contamination of hair samples could be due to touching plant material or contaminated surfaces. Moosmann *et al.* showed that THC could be detected in the hair samples of non-cannabis users after the handling of plant material, even after extensive washing for four weeks post exposure [146].

Contamination of synthetic cannabinoids was further investigated by Moosmann *et al.*. Hair samples of laboratory analysts who had been in contact with synthetic cannabinoid herb mixtures were tested. All of the hair samples were positive for at least one synthetic cannabinoid, despite the implementation of a decontamination wash procedure and gloves and laboratory coats being worn throughout the handling period [147].

Concentrations of synthetic cannabinoids in hair samples ranged from trace amounts up to a maximum of 170 pg/mg. It was also shown that subjects without direct contact with the synthetic cannabinoids, but who were co-habiting with the analysts also had cannabinoids detected in their hair. One of the analysts had a concentration less than 0.5 pg/mg in his hair, his girlfriend who did not have direct contact with the synthetic cannabinoids had a concentration of 11 pg/mg in her hair. This could be partially

explained by previous findings showing that longer hair is more susceptible to external contamination [144], however, much more research into the secondary transfer of cannabis plant/synthetic cannabinoid herb material needs to be conducted to fully understand the implications when interpreting results. One other possible explanation for the result is usage of the drug, as participants were not screened for drug use prior to the study.

Interestingly, it was also shown in this study that hair samples from other parts of the body (leg, chest and pubic region) tested positive for the synthetic cannabinoids, despite being completely covered up during the handling experiment. It should be noted that not all the participants gave a positive result for the same sampling site. A limitation is that and only three individuals took part in this part of the study. Further studies are clearly needed for a better understanding of this type of contamination for both synthetic and non-synthetic cannabinoids.

1.3.8 Strategies to overcome the issue of external contamination of cannabinoids

As mentioned previously in Section 1.3.7, external contamination is one of the main causes of interpretational issues in relation to hair analysis. In this section a review of literature citing a variety of published strategies to overcome this issue is presented.

1.3.8.1 Identification of metabolites

One strategy to reduce the number of false positives test results is to also identify THC metabolites, since these are only produced *in vivo*, as discussed in Section 1.1.2).

THC-COOH is by far the most frequently targeted metabolite of THC in hair samples. The Society of Hair Testing recommend that this is the metabolite detected to confirm cannabis usage [145]. In many cases THC-COOH is the only metabolite that is targeted for detection [121,148–151]. Recently there has been some debate as to the suitability of THC-COOH to identify THC usage in hair samples since Moosmann *et al.* reported that THC-COOH could be detected in segments correlating to a period 2-3 months before THC was orally ingested (n=2) [100]. The authors attributed this to contamination from sweat/sebum as sweat patches remained positive for THC-COOH for up to 25 days after oral intake of THC. However, Gambelunghe *et al.* did not detect THC-COOH in the sweat patches of cannabis users [152] which was also the finding of Kintz *et al.* [153].

Moosmann *et al.* postulated that since THC-COOH is present in sweat, it could be transferred from the hair of a user to the hair of another person, through touch contamination or from sleeping on the same pillow[100]. Hill *et al*. recently tested this theory [154] and concluded:

"Our experiments attempting to transfer THC-COOH in the presence of moisture from THC-COOH positive hair to either fabric or negative hair have shown that such transfer does not occur easily and, if it should occur, is readily removed by an extended aqueous washing procedure".

THC-COOH is not the only metabolite to be detected in hair; 11-OH-THC was first reported to be detected by Wicks and Tsanaclis [155]. In a large study (n=1272), 11-OH-THC was detected in 77 samples (6%) where the metabolite THC-COOH was not. THC-COOH was detected in a total of 543 samples.

In a further study of 6838 samples by Tsanaclis and Wicks, 11-OH-THC was again detected in a large number of hair samples (n=2016). In this study, THC-COOH was detected in more samples (n=2303) and at a higher median concentration (0.003 ng/mg) than 11-OH-THC (0.002 ng/mg) [156].

Pinchini *et al.* have recently reported a method to detect THC-COO-gluc in cannabis user hair samples (n=20) using UPLC-MS-MS [157]. Interestingly, this metabolite was found to be at least three times more concentrated than THC-COOH and was detected in four cases where THC-COOH was not. Whilst the authors warn that this data is "absolutely preliminary" the use of THC-COO-gluc as a biomarker for cannabis use in hair samples seems promising.

1.3.8.2 Limitations of metabolite analysis

The main limitation with metabolite analysis is that metabolites are not always detected, even when cannabis consumption is confirmed [158,159]. This has been attributed to poor incorporation rates of the metabolites into the hair [45]. Conversely, there are several examples where hair samples are considered to be positive for THC metabolites, yet negative for the parent drug [120,160]. The likelihood of the presence of THC metabolites in hair after passive exposure to cannabis smoke has yet to be fully understood since studies to date have either been conducted *in vitro* or such that participants were not able to inhale the second-hand smoke produced [144], which is unrealistic.

1.3.8.3 Decontamination/ Wash analysis

Washing hair samples before analysis is suggested by the SoHT to be a mandatory process. Ideally, this step should remove any trace of drugs present on the exterior of

the hair shaft but not remove any drug compounds that are incorporated into the cortex of the hair.

A comprehensive review into the many different washing procedures was recently conducted by Vogliardi *et al.* They concluded that the washing procedures most frequently used are those which utilise one or two washes with non-protic solvents, such as dichloromethane or a single short wash with a protic solvent such as methanol. However, some laboratories reverse the washing procedure, using a sequence of non-protic solvent followed by a protic one [161]. Additional solvents routinely used for the decontamination of hair samples for the analysis of cannabinoids include isopropanol, water, ether and acetone [161]. There is no universally recognised procedure for the decontamination of hair samples, nor is there any indication of which procedure is most or least optimal for removing external contamination whilst keeping internally bound cannabinoids in place.

Tsanaclis and Wicks proposed analysing the wash residue obtained from the decontamination procedure as a strategy to differentiate between external contamination cannabis use when metabolites are not detected [162]. The concentration of THC in the wash residue was compared to the concentration of THC in the hair after the completion of washing procedures. The authors suggest that wash: hair ratios of zero (i.e. no drug found in the wash procedure) suggested drug use was likely, while ratios greater than 0.1 and less than 0.5 indicated drug use was 'possible' and ratios greater than 0.5 meant that drug use was 'questionable'.

In a larger study conducted by Tsanaclis *et al.* 46 samples from the medico-legal sector were analysed for cannabis consumption [163]. In 21 of these samples (45.7%) THC

and THC-COOH were detected above the cut-off level and so consumption was confirmed. Wash ratio analysis was then performed on the samples where THC was detected but THC-COOH was not. Of these 21.7% were in the category of drug use 'likely', 17.4% were in the category drug use 'possible' and 15.7% were in the category of drug use 'questionable'.

1.3.8.4 Limitations with the assessment of wash residue

The Society of Hair Testing recognise that there is no standard washing procedure and accept that "different washing procedures will affect the remaining amount of drug in the hair" [145]. This will almost certainly affect the THC wash to hair ratio. In addition, the fact that metabolites of THC were found in wash residues in this study (see Section 4.4.2) could suggest that the wash procedure used by Tsanaclis and co-workers caused leaching of the metabolites that are incorporated into the hair into the wash residue. If this is also the case for THC, the wash residue concentration could be greater simply due to greater amounts being removed from the hair cortex. In addition, the authors recognise that the bands 0-0.1, 0.1-0.5 and greater than 0.5 are arbitrary numbers, which are not based on studies conducted to determine which ratio correlates to which usage conclusions.

Results from hair wash analysis can still only be put into three categories; 'likely', 'possible' and ‘questionable'. Arguably this is no better than reporting an ‘inconclusive’ result. However, this approach could prove useful in cases where a ruling is made on the ‘balance of probability’ (i.e. a civil case) rather than ‘beyond reasonable doubt’ (i.e. a criminal case). The validity of the wash analysis approach would also depend on case

circumstances and other evidence available, for example urine analysis would also need to be taken into consideration.

Others have also suggested wash values have limited validity. Thorspecken *et al.* stated that a positive cannabinoid finding in the last wash step of the solution did not imply a positive cannabinoid finding in hair. In contrast a negative result in the last wash solution did not always entail a negative result in the hair. Therefore the criterion that a negative wash solution assures a complete removal of external contamination does not seem universally valid [164].

Moosmann *et al.* studied the hair/wash ratio for synthetic cannabinoids after participants had handled herbal mixtures [147]. The results showed that whilst some samples had a high ratio (correctly suggesting external contamination) others had a negative wash result and a positive hair result (wrongfully suggesting drug use). This study shows that the notion of a wash to hair ratio may be too simplistic. The authors advise the concurrent analysis of additional body fluids to prove drug usage in cases where metabolites are not detected in hair.

1.3.8.5 THCA-A as an indication of "touch" contamination

The biogenetic precursor of THC, Δ9-tetrahydrocannabinolic acid A (THCA-A) has been identified as a possible marker of contamination due to the touching of marijuana plant material. This is because THCA-A is not incorporated significantly into hair through the bloodstream after oral intake of THCA-A [165], and it is only detected in negligible amounts in cannabis smoke [144]. As a consequence of this Moosmann *et al.* postulated that the presence of high THCA-A concentrations in the hair samples of

known cannabis users could be linked to handling plant material or touching contaminated surfaces, and then touching head hair [146].

This hypothesis was tested in a recent study where ten volunteers rolled one cannabis cigarette each day for five consecutive days whilst refraining from smoking or being in contact with cannabis for the rest of the study period. At the end of the exposure period all hair samples tested positive for THC and THCA-A.

Four weeks after the first exposure period nine out of ten hair samples were still positive for THCA-A and five out of ten were still positive for THC [146]. One limitation with this study however is that the participants self-reported not to have used or been exposed to cannabis smoke within the last six months. Unfortunately, the usage of cannabis cannot be ruled out as body fluid analysis was not carried out prior to the study being conducted, nor was it carried out during the study period.

In a previous study conducted by Moosmann *et al.* hair samples from children and their cannabis consuming parents were analysed [159]. The authors found that there was no significant difference in the concentration ratio THCA-A/THC between the two separate groups of adults and children if the specific relationship between child and caregiver was not considered. However, comparison of the THCA-A/THC concentration ratio within families showed that in 9 out of the 10 cases studied there was a significant statistical difference with the ratio being greater for the children than the adults. The authors concluded that the higher the THCA-A /THC ratio in relation to their caregivers, the more likely that THC is present due to external contamination. This could be possibly from adults touching plant material and then touching the child's hair.

It was suggested that this method could not only be useful in the case of child exposure, but also in law enforcement handling or in the case of cannabis growers. However, the main limitation of this method is the varying amounts of THCA-A and THC found within the plant material itself [159] and so unfortunately one general cut-off value to differentiate between this type of contamination and usage in terms of a THCA-A/THC ratio is not yet feasible.

1.4 Instrumentation for drug testing in hair

In this section the current methodology in hair analysis of chromatographic separation followed by detection using a mass spectrometer will be discussed. A review of methods previously used was shown in Table 1-3.

1.4.1 Chromatographic separation

Since hair samples are complex matrices (containing many compounds in addition to analytes of interest), they generally require the separation of their components by liquid chromatography (LC) or gas chromatography (GC) prior to their introduction to the ion source.

In chromatography, separation is based on different affinities to a mobile and stationary phase.

1.4.1.1 Gas Chromatography

In gas chromatography (GC) the process of separation is based on a two-step sequence. First, the components of a mixture are adsorbed onto a coating that lines the inner wall of a column located in an oven. Next, the oven is progressively heated, and the adsorbed components are sequentially transferred into a gaseous mobile phase before moving into the mass spectrometer (Figure 1-9). The temperature at

which a compound elutes from the column is a function of the vapour pressure of the compound. The higher the vapour pressure of the compound the more rapidly it will transverse the column, carried by the mobile phase.

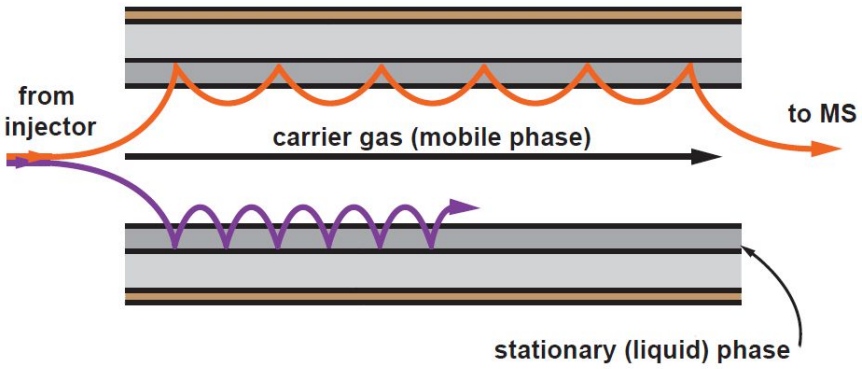

Figure 1-9. Separation process on a capillary GC column adapted from [166]. The orange path represents a compound of high volatility. The purple path represents a compound of relatively low volatility,

1.4.1.2 Liquid Chromatography

Liquid chromatography (LC) was first developed to expand the range of compounds that could be analysed as its predecessor, GC, is not suitable for involatile, polar and high molecular mass analytes.

The principle of separation in LC is that organic compounds in an aqueous mobile phase will adsorb preferentially onto an organic stationary phase. Compounds are then eluted sequentially using a gradient of the composition of the mobile phase from aqueous to organic (e.g. from water to acetonitrile). The order of elution of the components is a function of the preference of the particular compound to be associated with either the stationary or the mobile phase as the composition of the mobile phase changes during the gradient [166].

The column used in liquid chromatography is different to that used in GC as it contains porous particles coated with an organic stationary phase. The mobile phase carries analytes around and through the particles. The order of elution is determined by the length of time individual analytes remain adsorbed on the stationary phase.

1.4.2 Mass Spectrometry (MS)

Mass spectrometry is an analytical technique which has far reaching applications. Ions are produced in the gas phase which can then be analysed in term of a mass to charge (*m/z*) ratio. This mass to charge ratio along with additional information such as fragmentation pattern can then be used to identify the analyte. Many different mass spectrometry instruments are used for the analysis of elements, isotopes, small molecules (such as drug compounds) and macromolecules (such as proteins). In this section the theory behind the different mass spectrometry techniques used in this thesis will be discussed.

A basic diagram of a mass spectrometer is depicted in Figure 1-10. MS instruments generally have at least four main features; a) an inlet (sample introduction) b) an ionisation source (production of ions from an analyte) c) one or multiple mass analysers (for separation of ions based on a mass-to-charge ratio) and d) a mass detector (for conversion of separated ions into electrical signals that can be represented in the form of a mass spectrum [167].

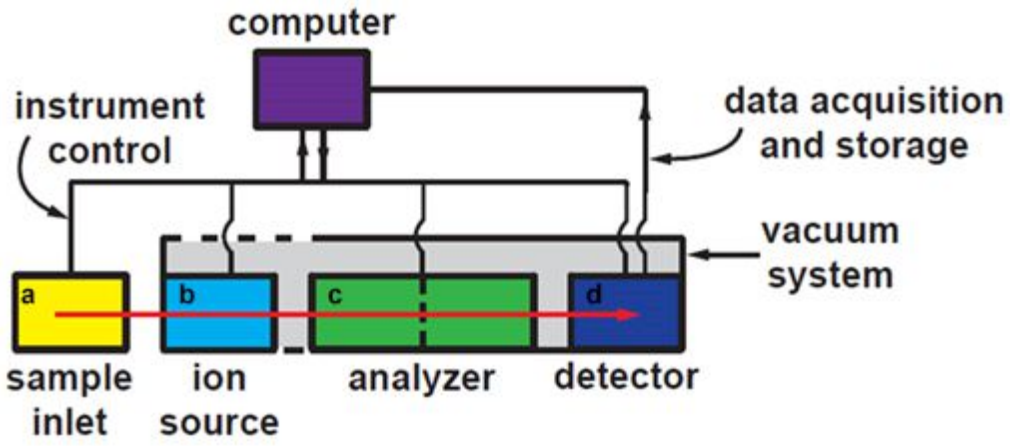

Figure 1-10. The general layout and main components of any mass spectrometer, including; (a) sample inlet, (b) an ionisation source, (c) one or more mass analysers, (d) a mass detector along with a data system displaying the mass spectrum. Adapted from [166].

1.4.2.1 Ionisation

For analytes to be detected they must first be ionised. Ions can be formed using a variety of methods, the choice of technique varies depending on the target analyte and application (see Figure 1-11). In this section the ionisation techniques used in this thesis will be discussed. Namely Electron Ionisation (EI), Matrix-Assisted Laser Desorption Ionisation (MALDI), Atmospheric Pressure Chemical ionisation (APCI) and Electrospray Ionisation (ESI).

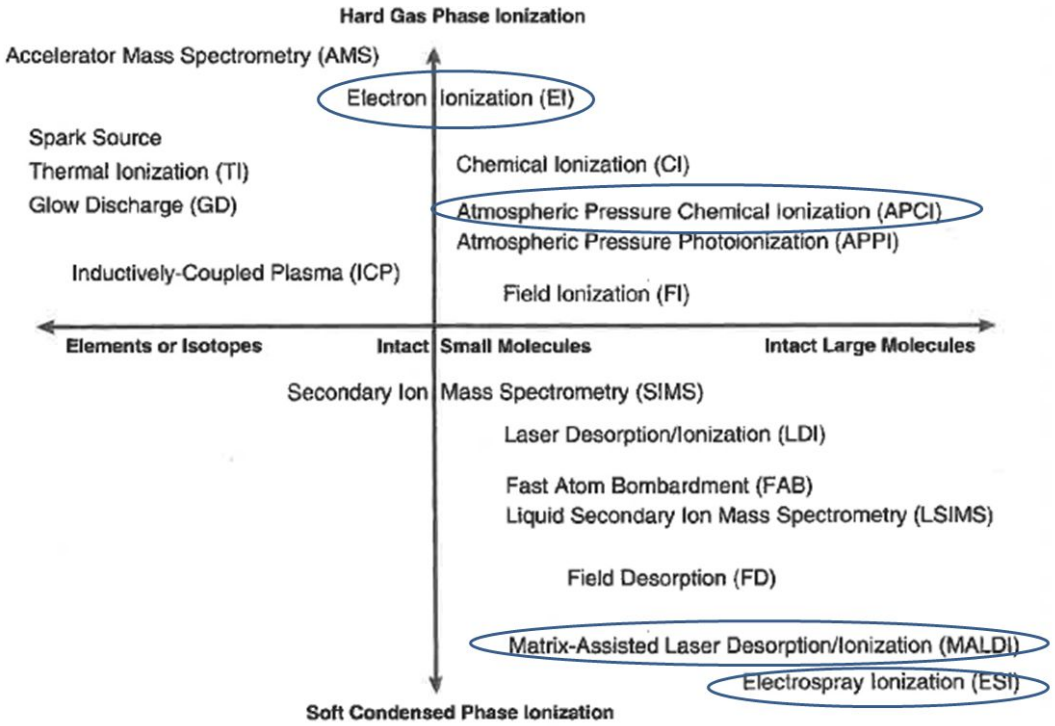

Figure 1-11. Mass spectrometric techniques for different needs arranged by main fields of application and estimated relative hardness or softness reproduced from [168]. Techniques used in this PhD project have been circled.

1.4.2.1.1 Electron Ionisation

Electron ionisation (EI), sometimes referred to as electron impact, was first developed by A.J Dempster in 1918 [169]. EI was the first commercially available ionisation method and is still widely used today, often in the analysis of small organic molecules. It is known as a "hard" ionisation technique, high energy impacts mean more fragmentation of the analyte. This means that molecular ion peaks are not always observed in mass spectra. This makes the technique unfavourable in the analysis of large molecules or trace levels.

In EI, molecules in the gas phase are bombarded with energetic electrons obtained from a heated filament located inside the vacuum. The bombardment removes an electron from the sample molecules, thus ionising them. The initial product is a

positively charged molecular ion, a radical cation $[M]^{+\cdot}$. The more common annotation is $[M]^{+}$ and will be used hereafter to denote a positively charged molecular ion. Excess energy imparted during the ionisation process is distributed along the bonds of the ions formed and often leads to fragmentation of the parent molecule [167]. Fragmentation is generally predictable and provides information on the structure of the analyte. A major disadvantage of EI is that it is limited to molecules with molecular masses of <1kDa.

Ion Formation $M + e^- \rightarrow M^{+\cdot} + 2e^-$

Fragmentation $M^{+\cdot} \rightarrow m_1^{+} + n^{\cdot}$ or $m_1^{+\cdot} + n$

1.4.2.1.2 Electrospray ionisation

Electrospray ionisation (ESI) was first introduced by Dole and co-workers in 1968 [170] and was later coupled to a quadrupole mass analyser in 1984 by Yamashita and Fenn [171].

ESI is accomplished by passing a solution of analyte through a needle held at high electrical potential into a chamber at atmospheric pressure. The high electrical potential in the range of 2-5kV is applied between the capillary and cone and causes an accumulation of positively charged ions at the tip of the capillary, to form what is known as a Taylor cone [167]. When the imposed electric field is high enough the cone elongates which then breaks and forms a spray of charged droplets. The solvent component of the droplet begins to evaporate with the aid of a stream of nitrogen gas and the diameter of the droplets is reduced, until eventually only charged analyte molecules remain. A schematic of an ESI source is shown in Figure 1-12.

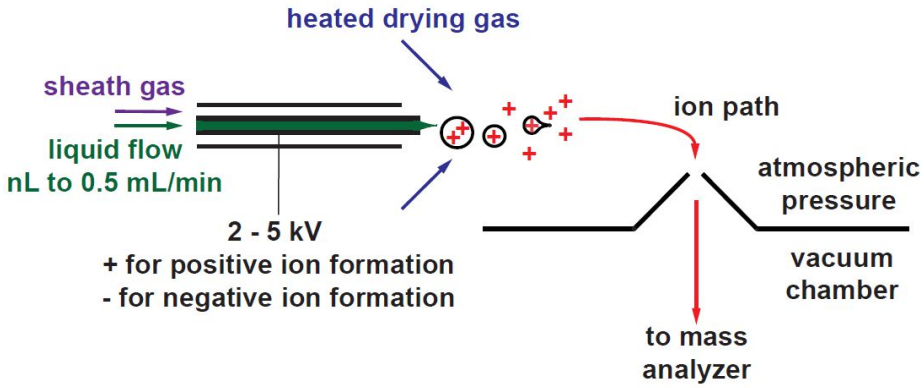

Figure 1-12. Schematic representation of an electrospray ionisation source reproduced with permission from [166].

1.4.2.1.3 Atmospheric Pressure Chemical Ionisation

Atmospheric Pressure Chemical Ionisation (APCI) was developed in the 1970s by the Horning group [172]. APCI is an ionisation technique which utilises gas-phase ion-molecule reactions at atmospheric pressure. In APCI, primary ions are produced by a corona discharge.

When using nitrogen, nitrogen plasma is created by the corona discharge needle. $N_2^{+\cdot}$ and $N_4^{+\cdot}$ ions react directly with analyte molecules [173] (Figure 1-13). Each ionisation event liberates a further electron and can thereby initiate a chain of ionisation events, sustaining the corona discharge.

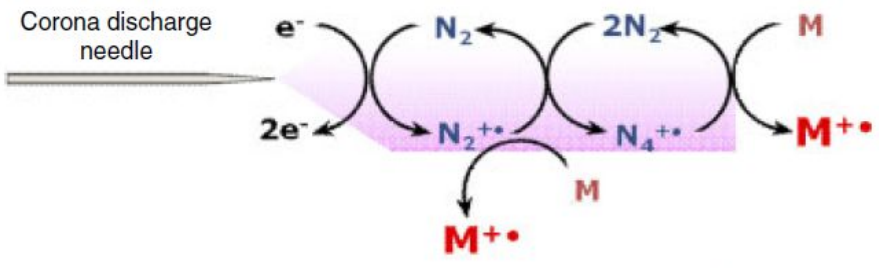

Figure 1-13. Ion formation when using nitrogen in an APCI source. Reproduced from Portoles *et al.* [174].

The same sequence of reactions, although initiated by different sources of primary ionisation, is observed not only in APCI but also in atmospheric pressure photonisation (APPI) and direct analysis in real time (DART)[175].

1.4.2.1.4 Matrix-Assisted Laser Desorption Ionisation

Matrix-Assisted Laser Desorption ionisation (MALDI) was first introduced in the late 1980s [176,177]. The main purpose of the work at that time was to develop a mass spectrometric technique that employed "soft" ionisation, decreasing the fragmentation of analytes and increasing the range of masses to be successfully analysed.

MALDI makes use of the absorption of laser light by a solid sample layer. The energy uptake upon laser irradiation then causes desorption and ionisation of the sample in a two-step process (Figure 1-14). Although lasers of both ultraviolet (UV) and infrared (IR) wavelengths are available, UV lasers are most commonly used. Of these nitrogen lasers and frequency tripled or quadrupled Nd:Yag lasers serve the majority of applications [178].

In MALDI-MS profiling (MALDI-MSP) analysis, the analyte is first co-crystallised with an excess of matrix that has a constituent aromatic component able to absorb photons from a UV laser beam (a more detailed discussion of matrix compounds can be found in Chapter 2). When dried the analyte-matrix mixture is exposed to a sudden input of energy from a laser pulse, the matrix evaporates carrying with it the analyte molecules which then enter the mass analyser. A schematic of this process can be found in Figure 1-14.

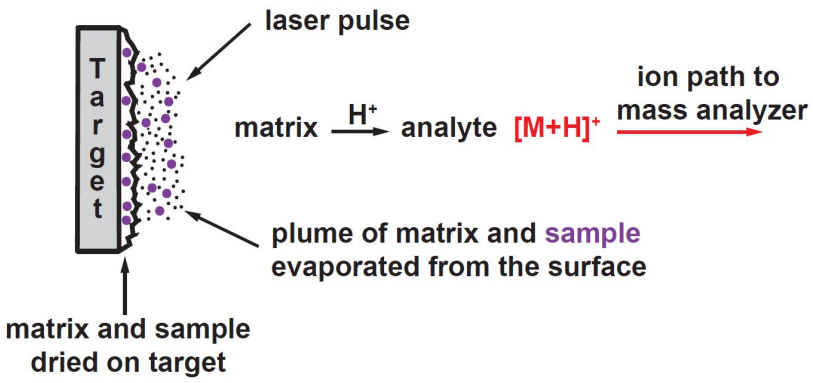

Figure 1-14. A schematic diagram of the process of MALDI-MS showing laser irradiation, desorption and subsequent ionisation of matrix and analyte molecules. Reproduced with permission from [166].

MALDI MSP experiments generate mass spectra in discrete areas of a sample. MALDI-MSP can be performed on sample solutions which are co-crystallised with matrix on a MALDI target as shown in Figure 1-15 A and directly on biological tissues which are co-crystallised with matrix as shown in Figure 1-15 B.

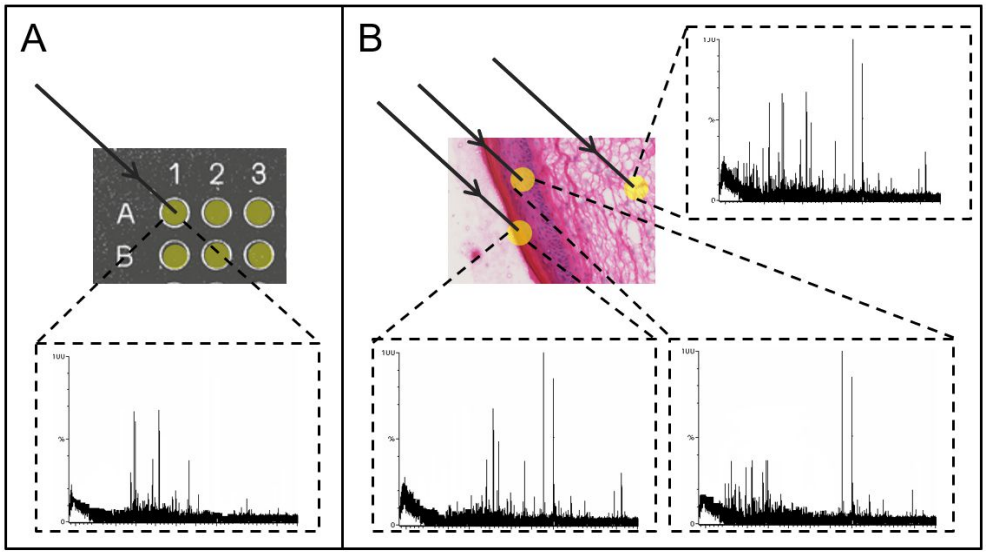

Figure 1-15. The principle of MALDI MS profiling from A) dried sample spots on a target plate and B) dried sample spots deposited directly onto a biological sample. Arrows represent laser shots. Reproduced with permission from [179].

The ionisation mechanisms in MALDI are not fully understood, with several proposed theories of ionisation [180–183]. Originally, it was thought that positively charged ions

were produced solely by a proton transfer reaction since most ions generated in MALDI are singly charged. However, it is now thought to be a complex process involving several stages

A two-step framework is generally accepted as useful model for many MALDI experiments. The steps are primary ionisation during or shortly after the laser pulse, followed by secondary reactions in the expanding plume of desorbed material [184]. Molecules generate a dense gas plume as they desorb from the surface. Collisions in the gas plume may result in additional reactions.

Charge transfer takes place from the protonated matrix to any compound with a higher proton affinity yielding protonated molecules, $[M+H]^+$. The reactions likely to occur in the gas phase are ion generation and ion-ion recombination. Ion recombination leads to a proposed "lucky survivor" model [182]. Most ions resulting from excitation by the laser are re-neutralised as cationic and anionic components re-combine. Therefore, singly charged ions are the lucky survivors of the re-neutralisation conflict. Neutralization probability strongly increases with the charge state and so singly charged ions have the greatest chance of "surviving". The model developed by Karas *et al.* offers an explanation to the phenomenon of almost exclusively M+H peak in MALDI spectra. A more detailed review of alternative MALDI ionisation theories can be found by Lu *et al.* [183].

1.4.2.1.5 MALDI imaging (MALDI MSI)

MALDI-MSI was first reported in 1997 by the Caprioli group [185]. This technique utilises the sensitivity and selectivity of MS to provide information on chemical composition.

Unlike with traditional techniques such as GC-MS and LC-MS (the most commonly used mass spectrometry method in the analysis of hair samples), MSI can give spatial information on the compounds observed in the mass spectrum as homogenisation of the hair sample is not required. This feature has made MSI an unique tool for clinical, pharmacological, and forensic science research.

The MALDI-MS images presented within this thesis were acquired in raster mode which was developed by AB Sciex. This method of data acquisition is achieved by continuously firing the laser in rows across a sample. The sample preparation is similar to MALDI-MSP; however, the matrix is sprayed rather than spotted on top of the sample. A schematic of MALDI-imaging workflow can be seen in Figure 1-16.

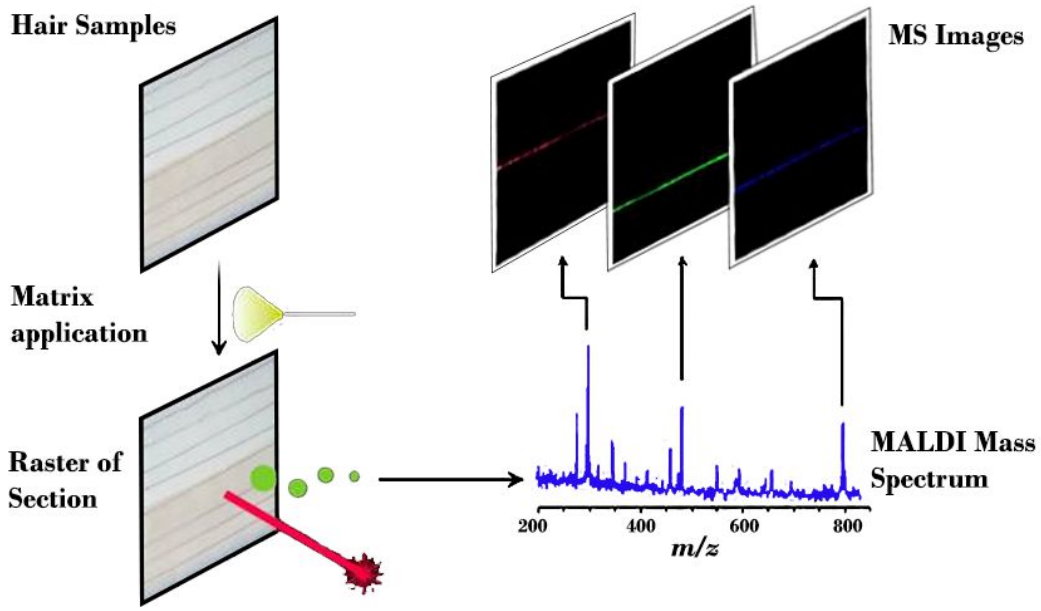

Figure 1-16. The MALDI MSI workflow showing a) matrix application b) laser irradiation c) the reconstruction of molecular image maps from specific ions.

1.4.2.2 **Mass analysers**

Following ionisation, ions are then separated based on their mass to charge ratio *(m/z)* by one or more mass analysers. The principles of the mass analysers used in this PhD project (quadrupole and time-of-flight) as well as their hybrid and tandem couplings (quadrupole time-of-flight and triple quadrupole) will be detailed in this section.

1.4.2.2.1 Quadrupole

Quadrupole (Q) analysers consist of a set of four rods. The rods, which are metal or metal-coated ceramic are placed parallel to each other with opposite pairs connected electrically (Figure 1-17). The voltage placed on one pair of rods is comprised of a positive direct current (dc) combined with a superimposed radio frequency (rf) voltage. The other pair of rods carries a negative dc voltage with an rf component that is 180˚ out of phase with that of the first pair. Whilst for simplicity Figure 1-17 represents the rods as either positive or negative, the rods in fact constantly oscillate between positive and negative polarities.

Mass separation is based on the fact that ions begin to oscillate upon entering the field produced by the superimposed rf and dc voltages. For any field derived from the combination of voltages, only ions with one specific *m/z* value have a stable trajectory along the axis of the quadrupole to the detector. All other ions with different *m/z* values develop unstable oscillation patterns perpendicular to the flight path and are lost by collision with, and discharge onto, the rods. Changing the dc and rf voltages progressively while keeping their ratio constant, enables the scanning of a mass range yielding spectra comprised of different *m/z* values.

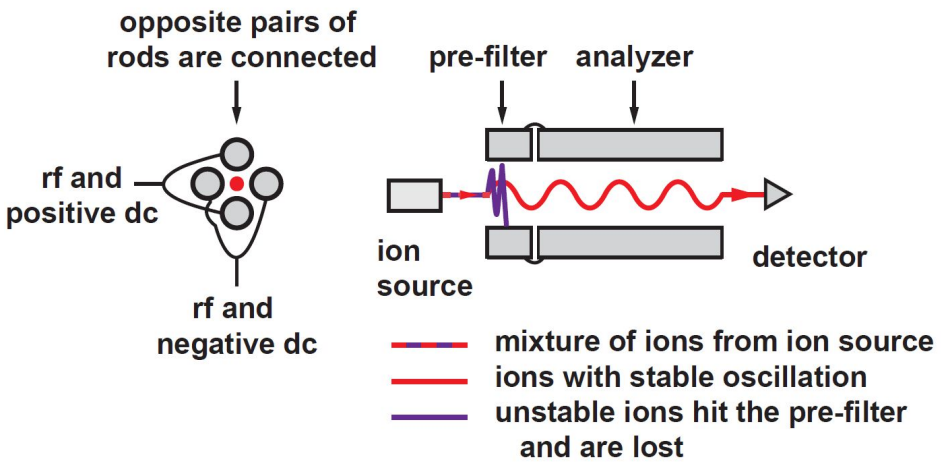

Figure 1-17. Schematic representation of quadrupole mass analyser; ions pass through four parallel rods, those with a stable trajectory (red line) pass through to the detector whereas ion with an unstable trajectory (purple line) collide with the rods. Reproduced with permission from [166].

1.4.2.2.2 Triple quadrupole

The triple quadrupole (QqQ) consists of two quadrupole analysers (Q1 and Q3), and a central section between Q1 and Q3 that is an Rf-only component (designated with a lower-case q) as shown in Figure 1-18. The rf field in q2 acts to constrain the ions, enabling their transfer between the two analytical quadrupoles. The central cell is the location where the collision gas is introduced to effect collision-induced dissociation (CID). The products of the CID process are analysed in Q3 by scanning to collect full spectra or by recording the intensity of a specific ion.

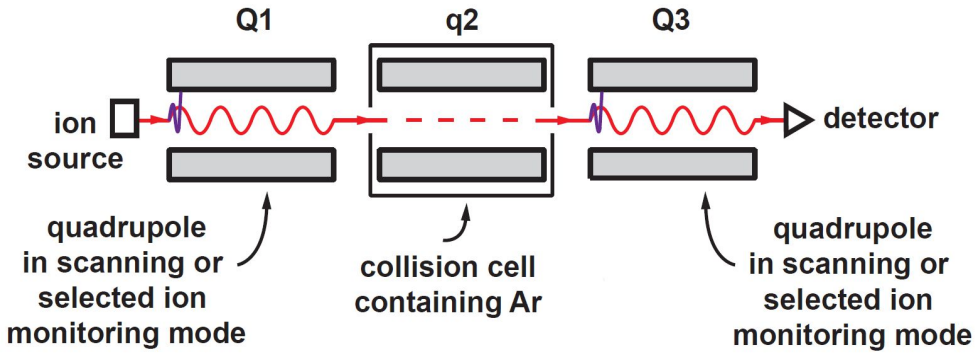

Figure 1-18. Schematic of a triple quadrupole mass analyser. Reproduced with permission from [166].

QqQ instruments are versatile because the Q1 and Q3 analysers can be used in conjunction with each other in either scanning or static (selected ion monitoring mode). The various scan modes are shown in Figure 1-19.

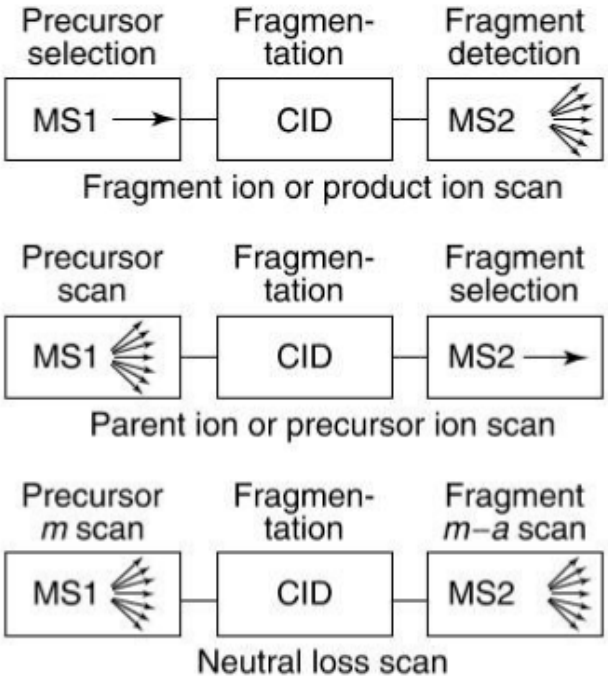

Figure 1-19. Representation of the different scan modes available for a triple quadrupole mass analyser reproduced from [167].

1.4.2.2.3 Quadrupole-Time of flight

In this PhD project, when a time-of-flight (ToF) mass analyser in reflectron mode was used it was solely used coupled to a quadrupole mass analyser. Therefore, the description that follows is written with this application in mind. A schematic of the Q-ToF analyser is shown in Figure 1-20.

The basic principle of a linear time-of-flight mass analyser is that ions formed in the MALDI source are accelerated towards a flight tube by a potential applied between the sample plate and the extraction grid. This imparts a constant kinetic energy on the ions

as they enter the field-free flight tube. The ions will then separate according to their velocities which will depend on their respective mass before reaching the detector [167]. Briefly, ions will a lower mass will have a shorter flight time than ions with a higher mass. The relationship between velocity (v), mass (m) and kinetic energy (E_k) is shown below:

$$E_K = \frac{1}{2}mv^2$$

In reflectron mode, an ion mirror corrects for the small variations in kinetic energy imparted to individual ions and helps to re-focus the ions before they reach the detector.

For conventional ToF-MS analysis all three quadrupoles are operated in RF-only mode and act as ion guides allowing the passage of ions with a pre-selected range of *m/z* values. The ions are then focused into the orthogonal time-of-flight mass spectrometer for detection [167].

For ToF-MS/MS analysis the quadrupoles are used as described in the previous section before the resulting product ions are focused into the orthogonal time-of-flight mass spectrometer and detected [186].

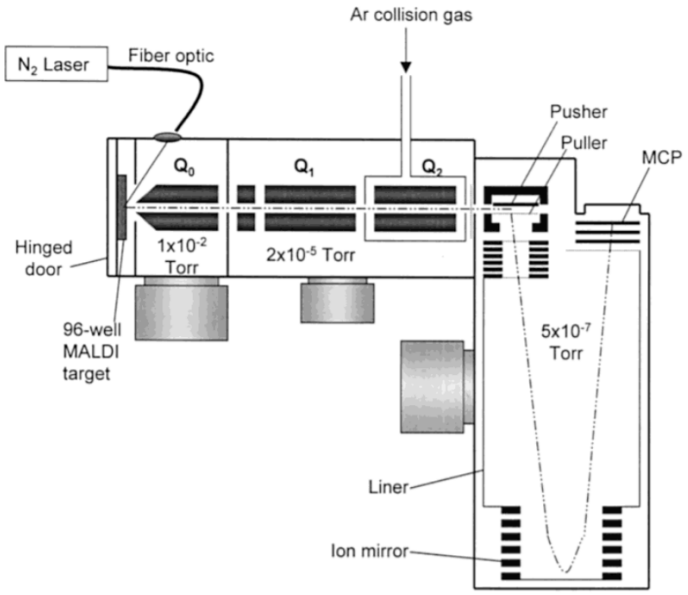

Figure 1-20. Schematic of a hybrid Quadrupole Time-of-flight hybrid mass analyser. The red line represents the path of ions through the quadrupoles and time-of-flight mass analyser. Reproduced from [187].

1.5 Aims of this project

Despite cannabis being the most commonly used illicit drug, at commencement of this study there were no methods published for detection of cannabinoids using MALDI, in hair or in other biological matrices. Since MALDI-MSI can provide unique information regarding the spatial distribution of cannabinoids within a sample, it is important that a method is established.

There was also a lack of consistency in the traditional GC-MS/MS methods available for cannabinoid detection in hair samples, with some methods describing detection of parent compounds only, and others detecting only a single metabolite. Often it was reported that metabolites could not be detected due to poor incorporation into the hair matrix, and so trace analysis with low detection limits is needed.

In addition, there was no consensus in the interpretation of cannabinoid findings in hair samples, with several different methods of determining whether a sample contained cannabinoids due to cannabis use or due to external contamination. Since the implications of false positive and false negative samples can be life changing, this inconsistent area of practice needs to be addressed.

This project sought to investigate the above issues by:

1. developing a method to detect cannabinoids in intact hair samples using both MALDI profiling and MALDI imaging techniques
2. applying the developed methods to hair exposed to cannabis smoke contamination

3. developing a GC-MS/MS method to simultaneously detect and quantify THC, CBN, CBD, THC-COOH and the rarely studied 11-OH-THC metabolite simultaneously in hair samples

4. applying this method to cannabis user and non-user hair samples to study the correlation between the results of mass spectrometric analysis and self-report data with a variety of methods of interpretation

Chapter 2. Development of Matrix-Assisted laser desorption ionisation Mass Spectrometry to detect cannabinoids in hair samples

2.1 Introduction

Matrix Assisted Laser Desorption Ionisation-Mass Spectrometry (MALDI-MS) has been highlighted as a potential hair analysis method due several advantages over current techniques including improved chronological information [188], simpler sample preparation and less sample needed compared to traditional GC-MS and LC-MS methods of analysis. Several drugs have already been analysed in hair samples using MALDI imaging techniques including methamphetamine [189], cocaine [190], ketamine [191], zolpidem, [192] and nicotine[193].

For analytes to be ionised and detected using MALDI-MS, a matrix (a solvent containing small organic molecules) must be applied. The matrix must have two main properties: it must have the ability to absorb at the wavelength of the laser used and have the ability to transfer protons during the ionisation process [194]. Selection of the correct matrix for MALDI-MS detection is of utmost importance as using the optimal matrix can improve the sensitivity of a method, whilst using an unsuitable matrix can lead to the inability to detect an analyte which is present, even in high concentration. The selection of the correct matrix is of particular importance in this study due to the extremely low concentration of cannabinoids and metabolites found in hair samples.

In a recent review into MALDI approaches for the analysis of low molecular weight compounds Bergman *et al.* concluded that there is no easy way to determine which matrices or methods will work and without a set president of the analysis of similar molecules, a "trial and error" approach is often needed [195].

In this study several different approaches including matrix selection, the use of additives (see Section 2.4.1) and derivatisation (see Section 2.5) were investigated to

develop a suitable method to detect cannabinoids in hair samples using MALDI-MS. In addition to this an in-source re-arrangement of the THC is reported for the first time, confirmed with the use of LC-MS.

In addition, the developed method was applied to cannabis smoke contaminated hair. Since THC is present in the smoke produced when the plant material is combusted, the presence of THC in hair can be due to exposure to cannabis smoke, and not necessarily direct or intentional usage. The exact mechanism of smoke contamination is not yet understood as discussed in detail in Section 1.3.7.1.

2.2 Methods and Materials

2.2.1 Chemicals and reagents

Matrices. α-Cyano-4-hydroxycinnamic acid (CHCA), 2,5-Dihydroxybenzoic acid (DHB), 6-Aza-2-thiothymine (ATT), 3-Hydroxycoumarin (3-HC) and were purchased from Sigma-Aldrich (Poole, UK).

Additives. trifluoroacetic acid (TFA), Lithium chloride (LiCl), lithium trifluoroacetate (LiTFA), Hexadecyltrimethylamnium bromide (CTAB) and aniline were purchased from Sigma-Aldrich (Poole, UK).

Derivatisation reagents. 2-Fluoro-1-methylpyridinium-p-toluene-sulfonate (FMPTS) and triethylamine (TEA) were both purchased from Sigma-Aldrich (Poole, UK).

Drug Standards. Cannabinol (CBN), cannabidiol (CBD) Δ9-tetrahydrocannabinol (THC), 11-nor-9-carboxy-tetrahydrocannabinol (THC-COOH) 11-Hydroxy-delta-9-

tetrahydrocannabinol (11-OH-THC) and 11-nor-delta(9)-carboxy-tetrahydrocannabinol glucuronide (THC-COO-gluc) were purchased as analytical references from Cerilliant (Sigma-Aldrich, Zwijndrecht, The Netherlands).

Solvents. Acetonitrile (ACN) and Methanol were purchased from Fisher Scientific.

2.2.2 Sample Preparation

2.2.2.1 Matrix Preparations

CHCA was prepared at either 10 mg/mL or 5mg/mL concentrations with the solvent composition being ACN:0.2% aqueous TFA (70:30).

DHB was prepared at 10 mg/mL dissolved in acetonitrile and 0.2% aqueous TFA (1:1).

3-HC was prepared at 10 mg/mL in 50% ACN with 0.2% aqueous TFA. ATT was prepared at 10 mg/mL in 50% ACN with 0.2% aqueous TFA.

The 3-HC ATT binary matrix was prepared according to Shanta *et al.* with 10 mg/mL of both ATT and 3-HC matrices dissolved in 50% acetonitrile (ACN) with 0.2% TFA [196].

Cannabinoid standards (100 µg/mL unless otherwise stated) were mixed 1:1 with matrix solutions and deposited in triplicate on the MALDI target. The spots were left to dry at ambient temperature before analysis.

2.2.2.2 Addition of Additives to the matrix

Aniline was added in equimolar amounts to CHCA. Two different matrix compositions with added aniline were prepared; ACN:0.5% TFA (70:30) as suggested by Groeneveld *et al.*[197] and ACN:0.5% TFA (75:25) as proposed by Kuyawama *et al.*[198].

CTAB was added to the CHCA matrix mixture in a ratio of 1:1000 in a water-acetonitrile solution (50/50, v/v) as described by Su *et al*.[199]

Lithium salts were added as described by Cerruti *et al.*[200]. Briefly, CHCA was prepared at 10 mg/mL in acetonitrile/ water/trifluoroacetic acid (70/30/0.1, v/v/v) and Lithium solutions at 25, 50 and 100 mM were mixed with the matrix solution for each lithium salt.

2.2.3 Derivatisation

Derivatisation was carried out according to Thieme *et al.*[201]. Briefly, 40 µl of 10 mg/mL 2-Fluoro-1-methylpyridinium-p-toluene-sulfonate (FMPTS) and 10 µl of trimethylamine was mixed using a vortex. This caused the colourless solution to turn "canary yellow" as previously observed by Thieme *et al.* THC standard (20 µL, 0.1 µg/µL) was added to the mixture and left at room temperature for five minutes before spotting (1 µL) onto a target plate.

2.2.4 Microscopy of hair samples

Hair samples were placed on glass slide using double-sided Sellotape® Super Clear tape before imaging with an Olympus BX60 microscope.

2.2.5 Spiking of hair

Hair samples from an individual who reported not to have used any illicit drugs were collected by cutting and washed with methanol and water by vortexing. The samples were then cut into 5 cm sections and placed into the bottom of a well in a 24-well cell culture plate to keep the spiking solution volume to a minimum whilst still submerging

the hairs. Spiked samples were prepared by soaking in cannabinoid standard solutions (300 µL, 0.5 µg/mL). Blank hair samples were prepared by soaking in methanol (300 µL). The plate was sealed with tape to avoid evaporation of the standards. All hairs were soaked for two hours, removed and allowed to dry for one hour at room temperature.

2.2.6 *In situ* derivatisation of cannabinoids

The hair was placed on glass slide using double-sided Sellotape® Super Clear tape. Derivatisation reagent (2.5 mL) was then sprayed using a neo for Iwata® air-brush at a pressure of 30 psi onto an area of 9 cm^2 with the sample in the centre of the area. This step was carried out in a fume hood due to hazards associated with the use of the triethylamine catalyst.

2.2.7 Deposition of matrix for imaging

The hairs were coated in CHCA (5 mg/mL) with the solvent composition ACN:0.2% Aqueous TFA (70:30) using the SunCollect autospraying system (SunChrom GmbH, Friedrichsdorf, Germany). Fifteen layers were sprayed at a flow rate of 2 µL/min.

2.3 Instrumentation

2.3.1 MALDI Instrumentation and analytical conditions

All data was acquired in positive ion mode on an Applied Biosystems/MDS Sciex hybrid quadrupole time-of-flight mass spectrometer (Q-Star Pulsar-*i*) with an orthogonal MALDI ion source (Applied Biosystems, Foster City, CA, USA) and a Neodymium-doped yttrium aluminium garnet (Nd: YAG) laser (355 nm, 1 KHz). The laser power was 30 % (1000 Hz, 3.2 µJ), which had an elliptical spot size of 100 × 150 µm [202]. Image acquisition was performed using the "raster image" mode [203]. The MALDI-MS/MS images were obtained using argon as the collision gas; the collision energy and the collision gas pressure were set at 20 and 5 arbitrary units, respectively.

Images were acquired using 'oMALDI Server 5.1' software supplied by MDS Sciex (Concord, Ontario, Canada) and processed using Biomap 3.7.5 software (www.maldi-msi.org) to generate black and white images for each *m/z* ratio of interest. Further Image analysis and processing was performed using the public domain software ImageJ (http://rsb.info.nih.gov/ij); where the previous black and white images were assigned different colours and overlaid to create one final image.

2.3.2 LC-MS/MS Instrumentation and analytical conditions

All experiments were performed on a Thermo Finnigan LCQ™ 'classic' quadrupole ion trap liquid chromatography mass spectrometer with electrospray ionisation (ESI) interfaced to a liquid chromatography system. The system used also consisted of an auto sampler and auto injector. The column used was a Phemonex Lunar® C18 (150 mm x 1 mm, 5 µm) with a corresponding guard column. LC-MS/MS Chromatographic separation was realised using gradient elution according to a previously published method by Roth *et al.* [204]. Briefly, 0.1% HCOOH in water was used as mobile phase A and ACN+ 0.1% HCOOH was used as mobile phase B. Mobile phase A was gradually reduced over time whilst mobile phase B was increased from 20 to 95%. The total run time was 15 minutes with the THC molecule eluting at 4 minutes.

All experiments were performed on a Thermo Finnigan LCQ™ 'classic' quadrupole ion trap liquid chromatography mass spectrometer equipped with an electrospray ionisation (ESI) source, interfaced to a liquid chromatography system. The system used also consisted of an auto sampler and auto injector.

2.4 Profiling of THC with multiple matrices

The use of α-Cyano-4-hydroxycinnamic acid (CHCA) resulted in the greatest intensity response as shown in Figure 2-1. However, upon inspection of the mass spectra it is evident that a peak associated with the matrix is unresolved with the peak associated with THC (*m/z* 315). This could explain why using 10 mg/mL CHCA decreased the THC intensity observed as with larger concentrations of the matrix present, a greater

suppressant effect from the matrix peak will be observed. This finding is in agreement with Zhang *et al.* who also observed a suppressant effect and much stronger matrix clusters at concentrations higher than 5 mg/mL when analysing peptides [205].

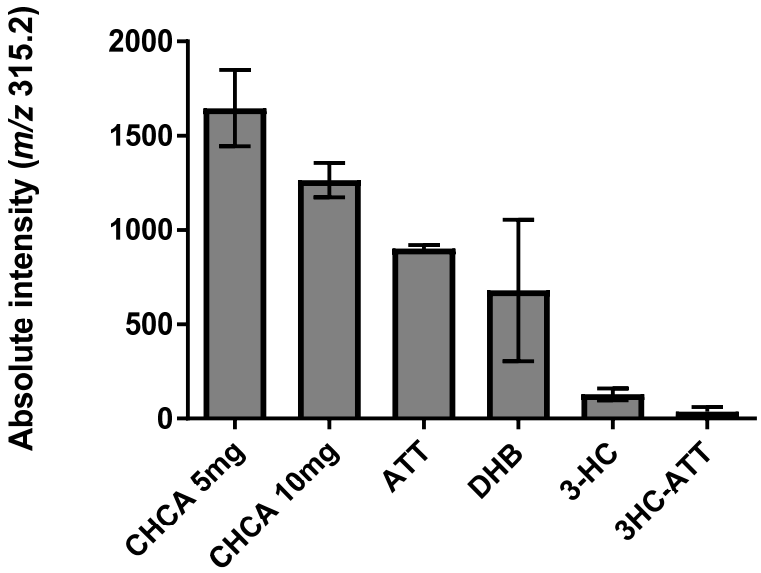

Figure 2-1. Absolute intensity of THC peak (*m/z* 315.2) with a range of different matrices.

The binary matrix of 6-aza-2-thiothymine (ATT) and 3-hydroxycoumarin (3-HC) proposed by Shanta *et al.* as a new combination matrix for the analysis of small molecules [196] gave the lowest intensity response. 2,5-Dihydroxybenzoic acid (DHB) did not crystallise uniformly and this is reflected in the large standard deviation of intensities observed. Crystal inhomogeneity is a well-documented problem with using the DHB matrix [206].

2.4.1 The use of matrix additives

Matrices can cause signal interference, or suppression of the analyte signal in the region below 1,000 Da [207]. This is due to the most frequently used matrices, e.g., CHCA and DHB, being small organic molecules themselves. When ionized, the matrix

usually forms clusters at low masses, which can interfere with the detection of low molecular weight analytes [195]. In MALDI, an additive is any compound which is added to the matrix/solvent composition. Additives have been proposed to eliminate or reduce ion suppression effects [208], and thereby improve the signal-to-background ratio. Some examples of additives include sugars [209], acids [210], surfactants, [211,212] and weak bases [213].

2.4.1.1 Addition of CTAB

The addition of the surfactant cetrimonium bromide (CTAB) to the CHCA matrix has previously been reported to supress CHCA-related ion signals in the low mass region[211]. However, in this study it was found that the relative intensity of the THC peak decreased with the addition of CTAB as can be seen in Figure 2-2, the absolute intensity also decreased with the addition of CTAB. One explanation for the fact that the CHCA-CTAB matrix performed poorly with the THC is that it does not contain an amine group, this method has been successfully used to analyse compounds found in clandestine tablets, however all compounds reported contained amine groups such as MDMA[199]. Guo *et al.* also reported that non-amine containing drugs such as benzoin and warfarin gave weaker peak intensities than drugs containing amine groups using the CHCA-CTAB matrix [211].

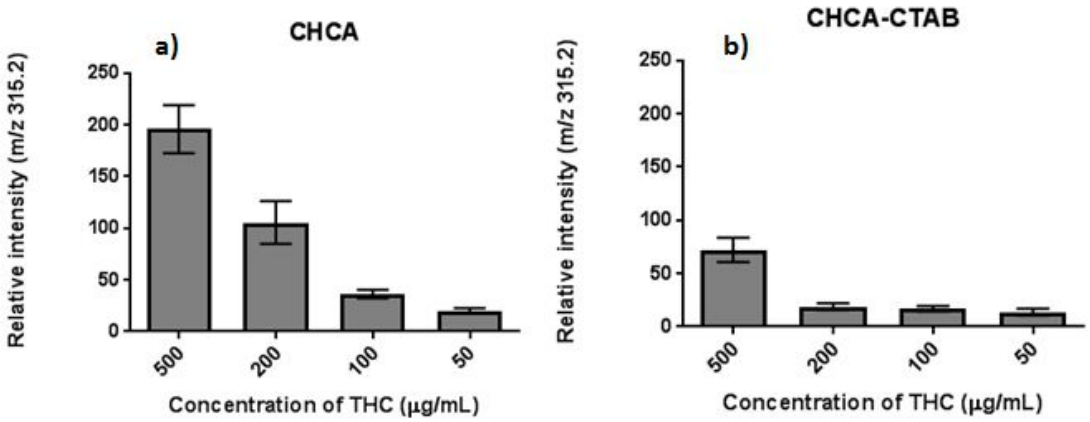

Figure 2-2. a) Relative intensity of THC peak (*m/z* 315) with CHCA used as the matrix. b) Relative intensity of THC peak with CHCA-CTAB used as the matrix. THC peak intensities were normalised with the $[CHCA+H]^+$ peak of *m/z* 190.05.

2.4.2 Addition of aniline and matrix composition

As shown in Figure 2-3, the relative intensity of the peak corresponding to THC (*m/z* 315.2) was greater when using 5 mg/mL CHCA rather than 10 mg/mL CHCA.

At both CHCA concentrations the addition of the ionic liquid aniline improved the relative intensity of the THC peak. This was not entirely unexpected as improved signal intensity using CHCA-Aniline has previously been reported for a range of compounds including proteins, peptides and amino acids [206,214]. However, this is the first time this matrix additive has been reported for the use of cannabinoid detection.

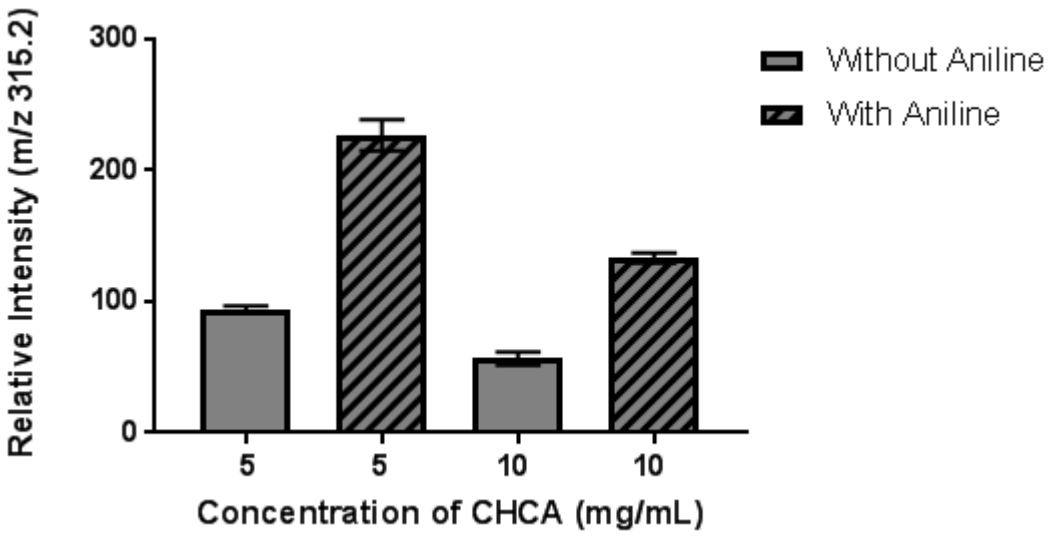

Figure 2-3. Effect of matrix composition and the addition of aniline on the relative intensity of the THC peak normalised to the CHCA dimer of *m/z* 379.

2.4.3 Addition of Lithium Salts

The addition of lithium salts to CHCA in order generate lithium-analyte adducts to improve the detection of lipids both in profiling and imaging experiments is well documented [200,214,215]. In this study two common lithium salts, LiCl and LiTFA were added to CHCA and analysed with THC. As shown in Figure 2-4, the addition of either salt decreased the THC signal intensity greatly. Figure 2-4a shows that an increase in lithium chloride concentration had little effect on the intensity of the THC signal. Figure 2-4b shows that an increase in lithium trifluoroacetate concentration caused the THC signal intensity to decrease. However, the expected peak of the Lithium adduct $[M+Li]^+$ (*m/z* 321) was not observed with either lithium salt, suggesting that the adduct had not formed. This was also the case when CHCA without the addition of aniline was used as the matrix (data not shown).

This could be explained by the lack of a phosphate group in THC molecule, as it is thought that the lithium ion exhibits a high affinity to phospholipids due to the presence of an exchangeable hydrogen on the phosphate group forming strong ion-dipole interactions with a strong covalent character [200]. This result suggests that the lithium ion does not have a high affinity for the hydroxyl group of the THC molecule, but that the addition of lithium salts supresses the THC signal.

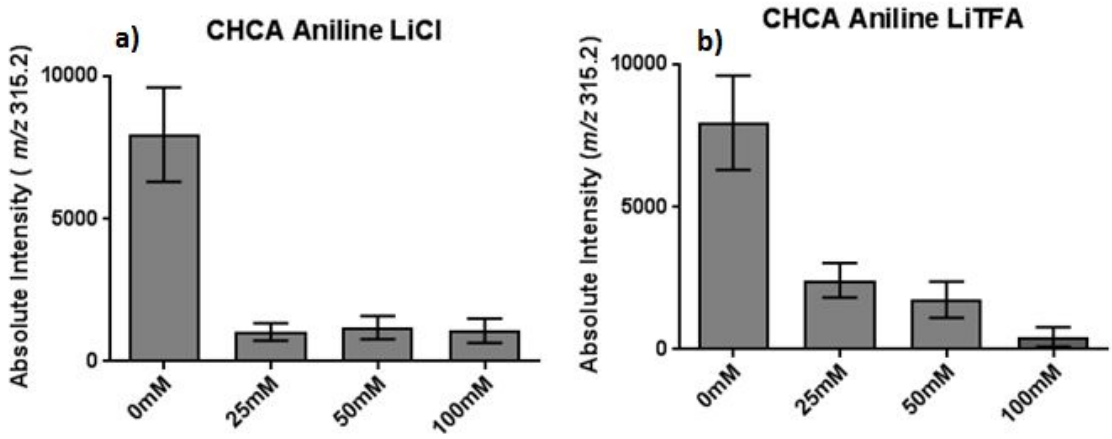

Figure 2-4. Intensity of THC peak (*m/z* 315.2) after the addition of lithium chloride (a) lithium trifluoacetate (b) to CHCA matrix in a range of different concentrations.

2.4.4 The laser-induced rearrangement of THC

Whilst investigating the optimum matrix compositions it was noted that there was not a singular peak associated with THC at *m/z* 315 as expected, but rather a "cluster" of peaks as shown in Figure 2-5A. Whilst peaks at *m/z* 316 and 317 can be partially explained by the presence of ^{13}C isotopes within the molecule, the origin of the peaks observed at *m/z* 311-314 are not apparent. The lack of these peaks in the matrix blanks and the similar spectrum obtained with DHB matrix shown in figure 2-5B supports the theory that the peaks are associated with the THC molecule.

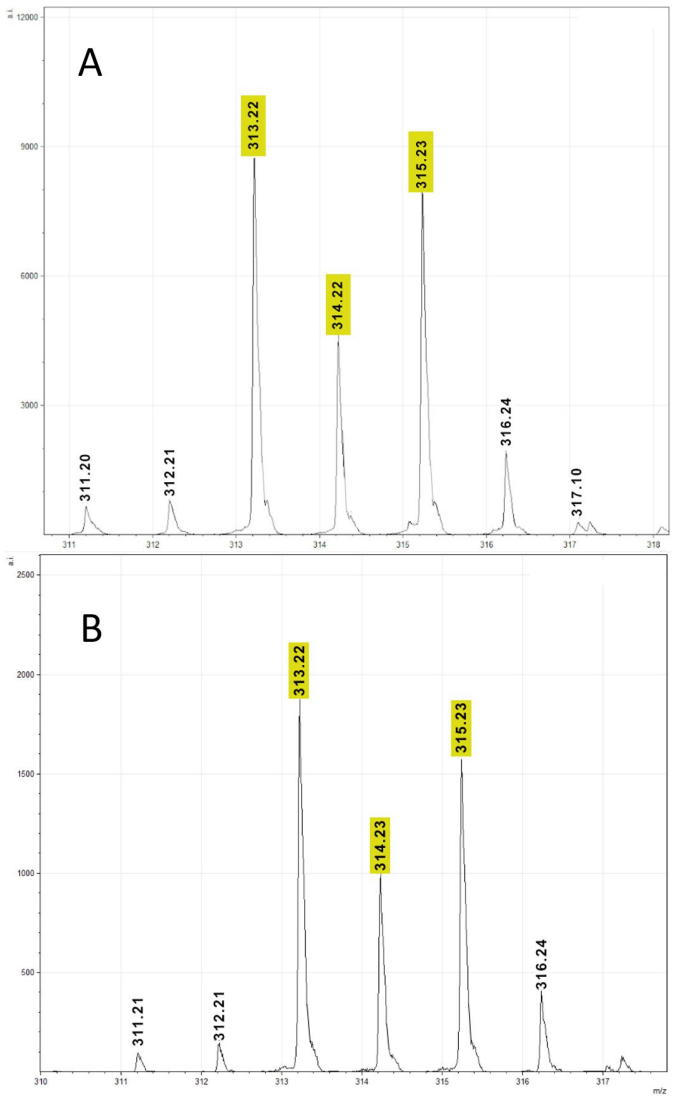

Figure 2-5. A- *m/z* region 310-318 of THC with CHCA matrix. B- *m/z* region 310-318 THC with DHB matrix.

To investigate this phenomenon further, LC-MS/MS analysis of the THC standard was carried out.

A single peak in the chromatogram confirmed the purity of the THC standard. The mass spectrum of the peak can be seen in Figure 2-6, showing the M+H at *m/z* 315. Interestingly, the peak previously seen at *m/z* 314 is no longer present. In addition to this the peak at *m/z* 313 has now reduced to 3% of the intensity of the *m/z* 315 peak (previously seen at 50-110% of the 315 peak depending on matrix used, see Figure 2-5B and 5C). Since this LC-MS system uses a softer ionisation source it is reasonable to

assume that the cause of the THC "cluster" is the MALDI ionisation process, in particular the use of laser energy. To further investigate the influence of laser power on the molecule an experiment was carried out with increasing laser power. It can be seen in Figure 2-7 that increasing laser power causes the ratio of *m/z* 313 to 315 signal intensity to increase, showing increasing *m/z* 313 formation.

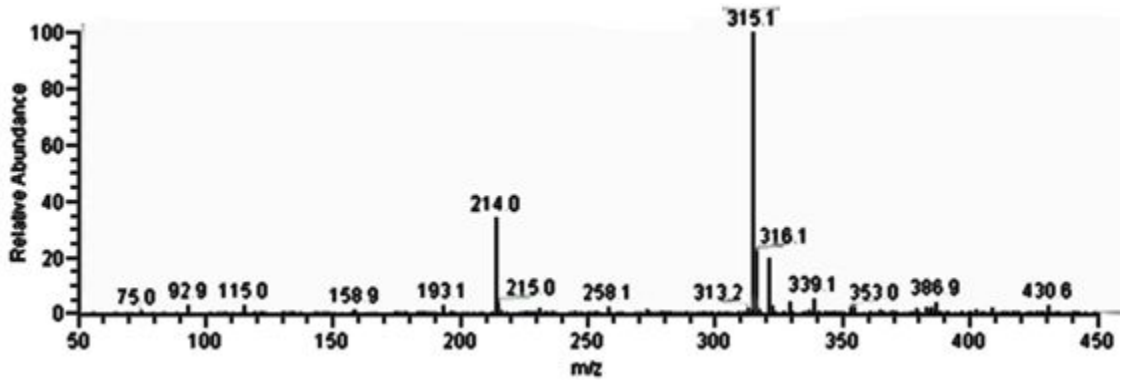

Figure 2-6. LC-MS mass spectrum of THC standard.

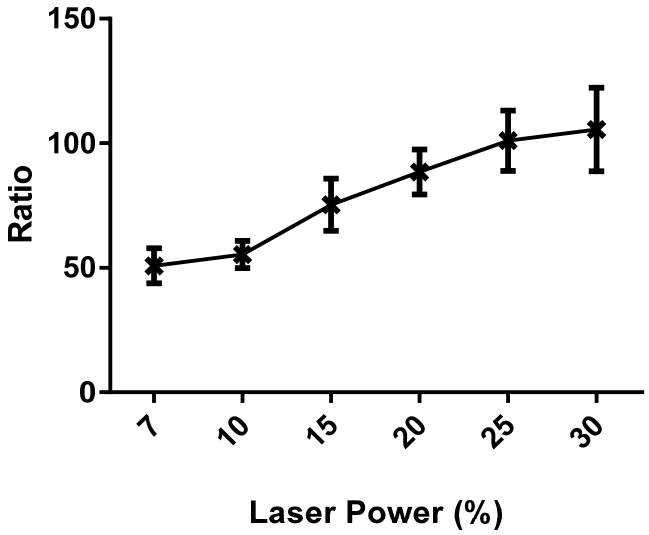

Figure 2-7. Ratio of signal intensity of *m/z* 313.2 to 315.2 at increasing laser energies (n=3 per point).

One possible explanation for this observation is a laser induced re-arrangement of the THC molecule as depicted in Figure 2-8. The loss of hydrogens as free radicals would

increase the conjugation of the THC molecule, making the molecule more stable and the reaction favourable. MS/MS spectra obtained by direct infusion shown in Figure 2-9 also support this theory.

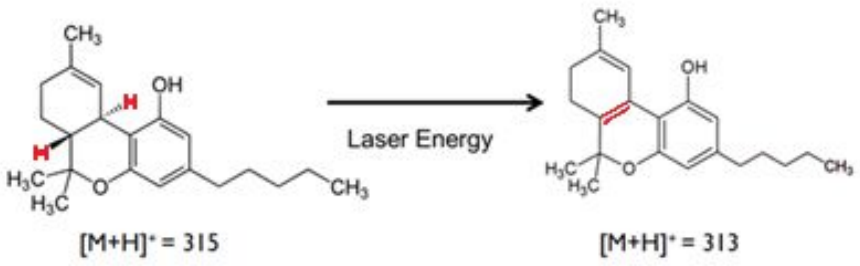

Figure 2-8. Re-arrangement of THC molecule.

The MS/MS spectra of the parent ion at *m/z* 315.1 is shown in Figure 2-9A and the MS/MS spectra of the re-arranged parent ion at *m/z* 313.1 is t is shown in Figure 2-9B. The spectra are very similar with many fragments forming from common mass losses (peaks labelled with a star). These peaks have a mass shift of -2 from spectrum A to spectrum B, reaffirming the loss of two hydrogens from the THC molecule. One notable difference between the spectra is a shift of -2 from *m/z* 259.1 in spectrum 2-9A to *m/z* 257.1 in spectrum 2-9B. The suggested structures of these fragments can be seen the insert of Figures 2-9A and 2-9B, the latter of which was first proposed by Bijlsma *et al.* based on MS^E accurate mass data[216]. These structures agree with the proposed re-arrangement shown in Figure 2-8. In addition to this both mass spectra have a common fragment ion at *m/z* 193, the structure of which is shown in Figure 2-9-B. The fragment does not contain the re-arrangement, so appears identical in each MS/MS experiment.

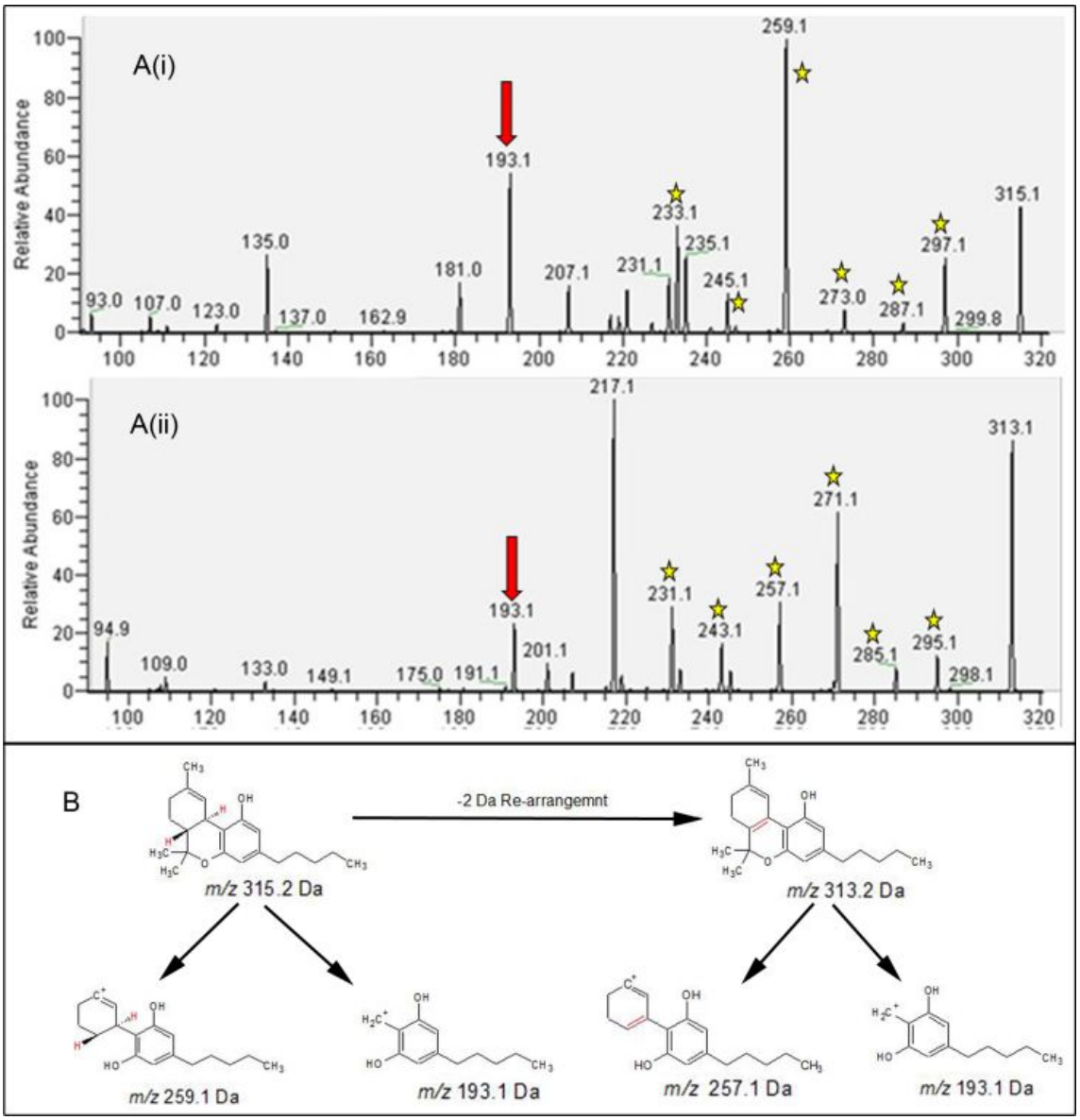

Figure 2-9. (A) MS/MS spectra of THC. Product ion mass spectrum of (i) *m/z* 315 and (ii) m/z 313 are shown. Both spectra were obtained by direct infusion. Peaks with a star symbol denote a mass shift of 2 Da. (B) Proposed re-arrangement of THC and structures of fragments present at *m/z* 259 and 257 and 193.

2.5 Derivatisation of cannabinoids

Since the laser is an essential component in MALDI-MS, the only way to analyse THC and avoid the unwanted re-arrangement is to chemically modify THC before analysis. Derivatisation of analytes has previously been identified as a possible strategy to improve signal strength when analysing small molecules using MALDI [195], however this approach had not previously been investigated for cannabinoids.

Whilst derivatisation of analytes is undesirable due the additional time and reagents needed, this approach can be highly advantageous. Derivatisation results in analyte peaks shifted to a higher mass region, and so by use of a suitable reagent, it is possible to avoid matrix peak interferences for the analyte signal.

Moreover, derivatisation with a reagent that can provide a permanent charge is particularly useful for non-charged compounds, which may not be possible to analyse otherwise [195]. Another advantage of derivatisation is that the signal strength can be increased, because the derivatised compound may have different chemical and physical properties, which can provide beneficial changes in volatility and higher ionization efficiency.

In this study, the target for the derivatisation was the hydroxyl group, since all cannabinoids of interest contain this functional group. After carefully reviewing the literature, the derivatisation method using 2-Fluoro-1-Methylpyridinium *p*-tolunesulfonate (FMPTS) to form an N-methylpyridinium derivative (shown in Figure 2-10), as reported by Quirke *et al.* for the detection of alcohols using electrospray ionisation mass spectrometry, was chosen [217]. FMPTS derivatisation has previously been reported to improve the detection of a range of compounds with alcohol

moieties, in various sample types including surfactants [218], oestrogens [219] and the narcotic analgesic buprenorphine [220], using LC-MS analysis, and polyamides [221] and sterols [222] in MALDI profiling experiments.

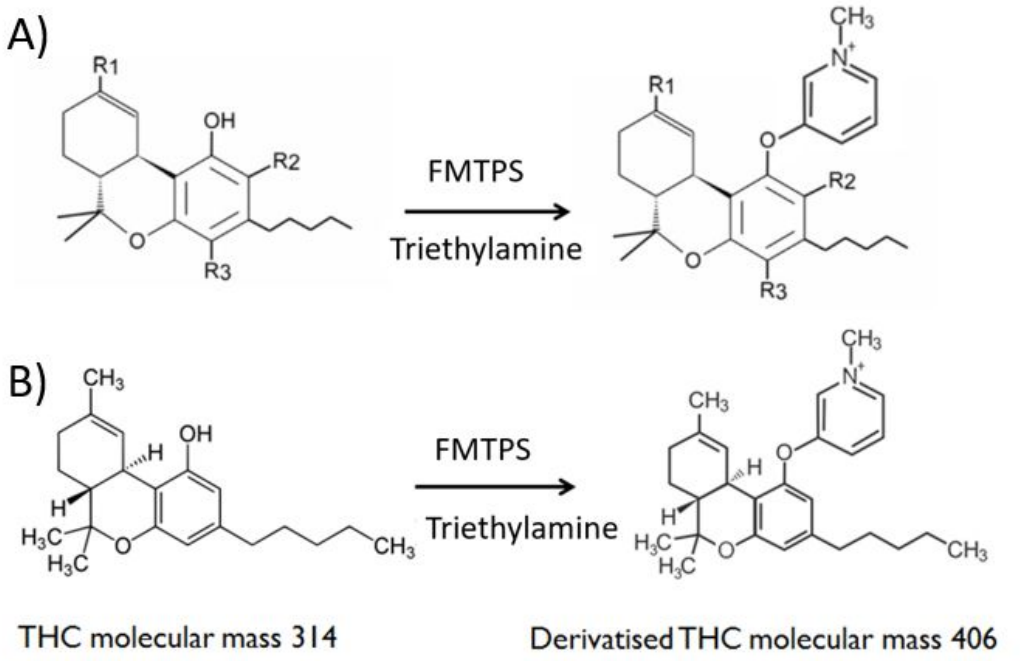

Figure 2-10. Expected FMTPS derivatisation scheme with A) generic cannabinoid and B) THC.

This strategy was selected due to the simplicity of the nucleophilic substitution reaction which occurs readily at room temperature [223], the stability of the products formed [218,224] and also the addition of a permanent charge to the analytes. This is of particular importance as it allows all cannabinoids to be analysed in positive mode analysis (despite the non-derivatised THC-COOH being theoretically more suited to negative mode) [225].

Derivatisation was successful for all cannabinoids of interest, with all expected peaks being observed and in agreement with the expected monoisotopic *m/z* values (Table 2-1). The derivatised species show an addition of 92 a.m.u. as first observed by Quirke *et al.* [217] and confirmed by others [219,222].

Cannabinoid	[M+H] Theoretical	[M+H] Experimental	Derivatised [M+92] Theoretical	Derivatised [M+92] Experimental
THC	315.23	315.23	406.27	406.28
CBN	311.20	311.20	402.24	402.24
CBD	315.23	315.23	406.27	406.28
11-OH-THC	331.23	331.23	422.27	422.26
THC-COOH	345.21	345.21	436.25	436.25
THC-COO-gluc	521.24	521.25	612.28	612.28

Table 2-1. Theoretical and experimental *m/z* ratios for derivatised and non-derivatised cannabinoid standards.

After derivatisation the ions corresponding to non-derivatised cannabinoids were not observed, suggesting that reaction went to completion (or such that non-derivatised cannabinoids remained present at concentrations below the limit of detection). The expected derivatised THC peak at *m/z* 406.28 was the most abundant in the spectrum (Figure 2-11a). However, there was evidence that rearrangement still occurred as the peak at *m/z* 404.27 was observed, though it was present at only 6% of the intensity of the *m/z* 406.28 peak, as opposed to approximately 100% when analysed without derivatisation. This suggests that the derivatisation largely protects THC from the re-arrangement, possibly due to steric hindrance, or increasing the required amount of laser energy to re-arrange the molecule.

The peak at *m/z* 406.28 was also observed in the mass spectrum of the derivatised CBD molecule. This was anticipated as THC and CBD are isobaric species, however an additional peak at *m/z* 483.32 was also detected in the CBD spectrum (Figure 2-11b); CBD gains two N-methyl-pyridinium groups as it has two hydroxyl groups, rather than the one for THC. The peak at *m/z* 483.32 corresponds to the loss of a methyl group from the doubly-derivatised molecule expected to be observed at *m/z* 498.32.

CBN was detected at the expected mass of 402.24 (Figure 2-11c).

Whilst theoretically there could be two additions of the N-methyl-pyridinium group to 11-OH-THC only one addition was observed corresponding to a mass of 422.26 (Figure 2-11d).

THC-COOH was observed at the expected mass of 436.26. However, an additional peak at *m/z* 450.27 was observed in greater abundance (Figure 2-11e). This peak is not observed in the mass spectrum of the FMPTS derivatisation reagent with CHCA and so it is assumed that it is associated with the THC-COOH analyte. The mass does not correlate to a doubly derivatised THC-COOH molecule and so the structure of the compound correlating to this mass is unknown.

The THC-COO-gluc molecule could have up to five N-methyl-pyridinium additions on molecule because of multiple hydroxyl groups being present, though only the corresponding *m/z* value for one addition, at *m/z* 612.28 was observed (Figure 2-11f). The peak at *m/z* 436.25 was more abundant, suggesting the glucuronide group readily fragments from the parent molecule during analysis resulting in the detection of THC-COOH.

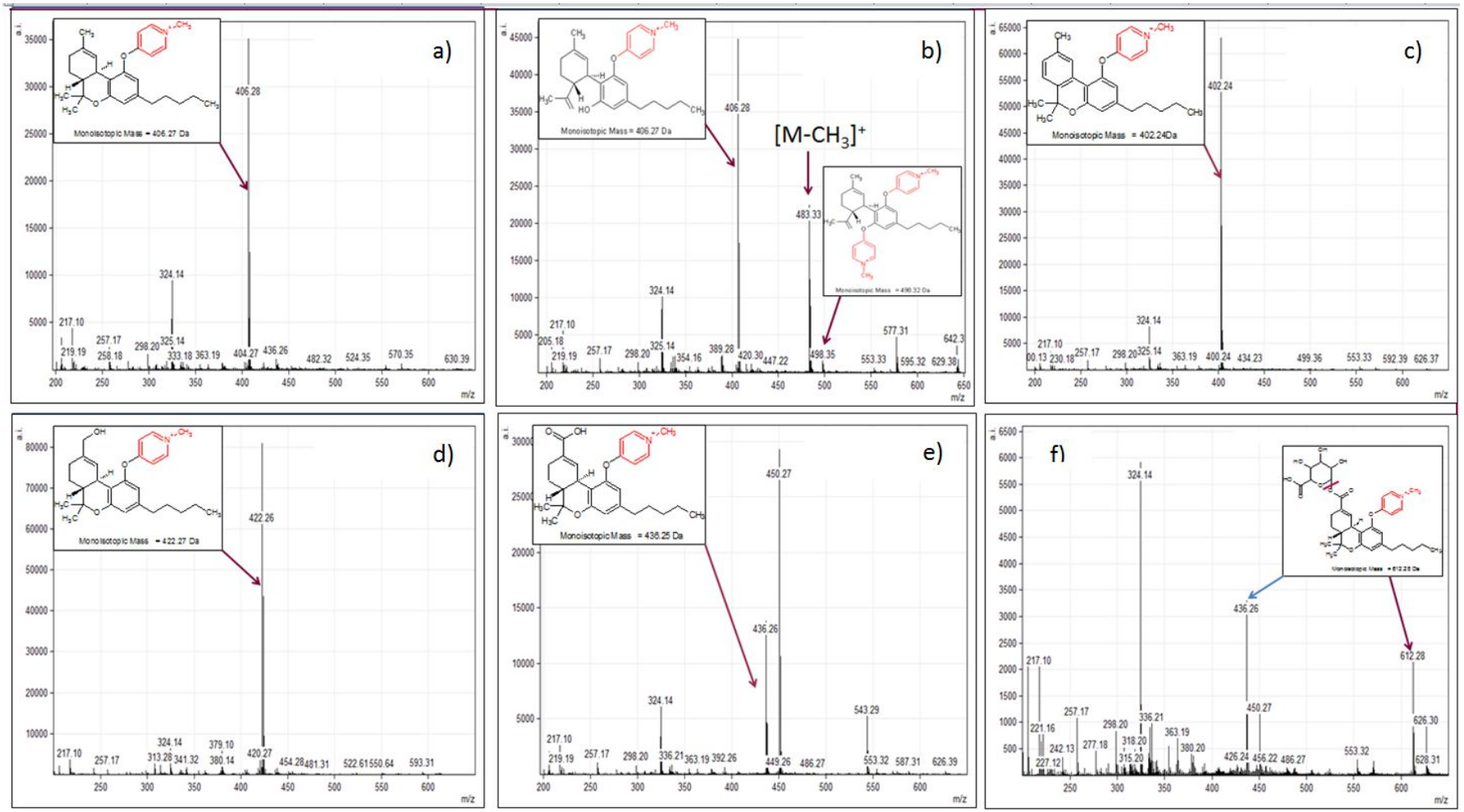

Figure 2-11. Mass Spectra of derivatized cannabinoids a) THC b) CBD, c) CBN, d) 11-OH-THC, e) THC-COOH and f) THC-COO-glucuronide standards derivatised with FMPTS.

A further experiment increasing the laser power used for analysis showed that the ratio of the peak pertaining to THC-COO-gluc to the peak corresponding to THC-COOH decreased sharply from 10 to 20% with an overall decrease of 28% when the laser power was increased from 15 to 30%, suggesting laser energy is at least partially responsible for the fragmentation observed (Figure 2-12).

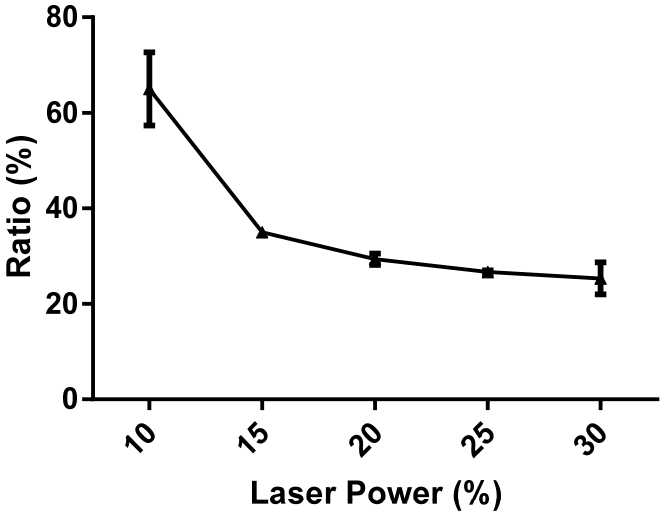

Figure 2-12. The effect of laser power on fragmentation of THC-COO-gluc to THC-COOH (n=3).

2.5.1 Profiling of derivatised analytes with a range of matrices

Since derivatisation changes the structure and functional groups of the cannabinoids, matrix selection was re-investigated. The addition of aniline to the derivatised THC molecule no longer improved the signal intensity when using the matrix CHCA. This could be because the addition of 92 a.m.u. means that the THC peak is no longer supressed by a matrix peak, as was previously observed.

Following the results from the underivatised THC compound with a range of matrices (Figure 2-1), CHCA, ATT and a binary THC-DHB matrix proposed by Laugesen and

Roepstorff to improve crystal inhomogeneity [226] were spotted with all derivatised cannabinoids and metabolite standards and profiled.

The ATT matrix gave low intensities of analytes or had large standard deviations and so was excluded from future experiments, as shown in Figure 2-13. CHCA gave the highest intensities for CBD, CBN, and THC-COOH. The CHCA-DHB combined matrix gave the highest intensity for THC and 11-OH-THC, with CHCA only slightly lower. Following these results, the CHCA matrix was selected for future experiments.

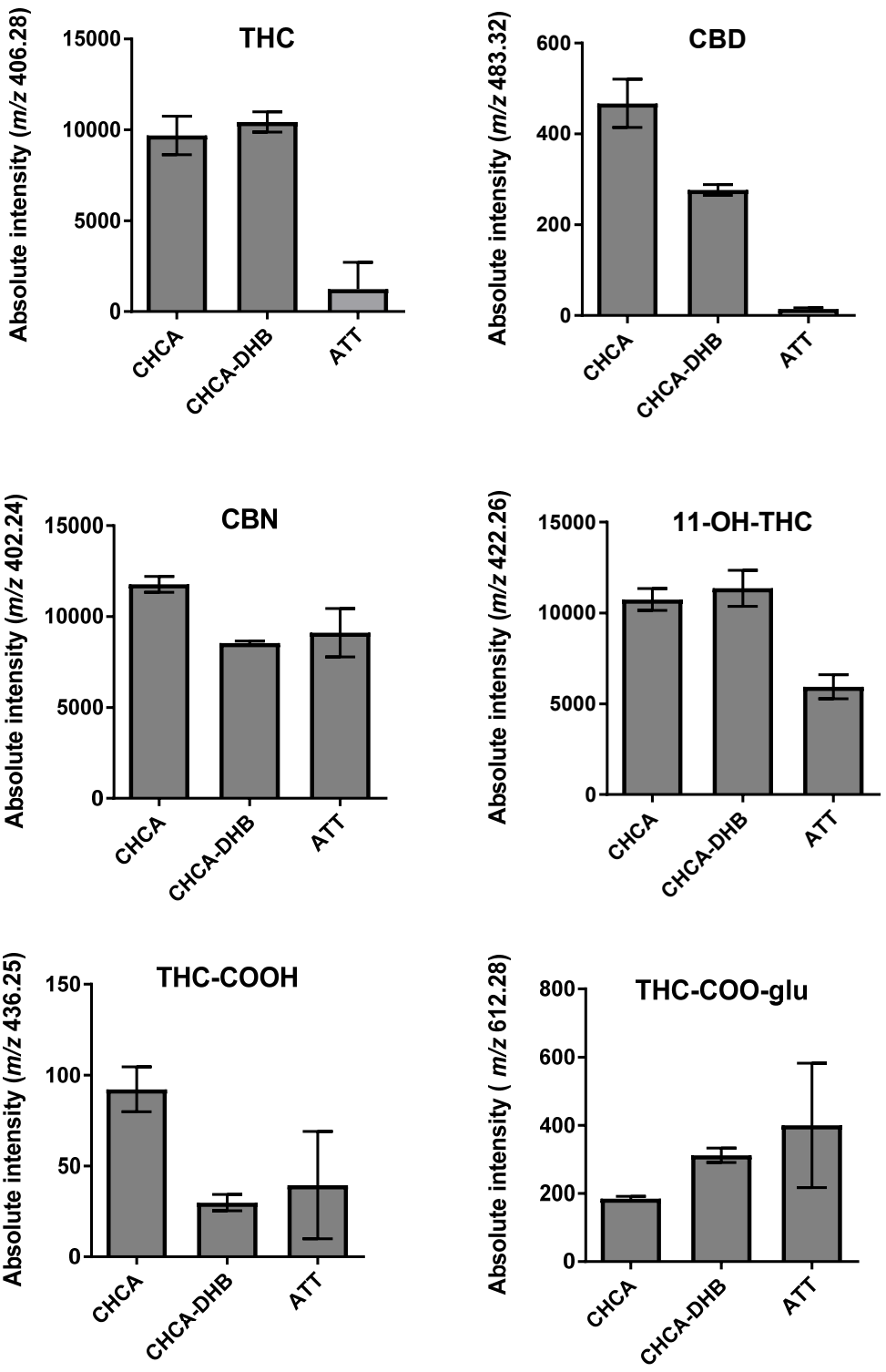

Figure 2-13. Absolute intensity of peaks pertaining to derivatised cannabinoids and metabolites with a range of different matrices.

2.6 On-hair derivatisation

Following the development of a method for detection of the derivatised cannabinoid standards, this section will discuss application of the method to hair samples.

2.6.1 Microscopy of derivatised hair samples

The derivatisation of THC was performed on spiked hair samples by spotting 1 µL of derivatisation reagent on top of the hair, followed by 1 µL of the 5 mg/mL CHCA matrix. Without derivatisation, profiling experiments indicated that 5 mg/mL concentration of CHCA was found to be optimal (see Figures 2-1 and 2-3). However, there was very little instrumental response for any *m/z* value on the derivatised hair sample.

Microscopy of the hair showed that at a CHCA concentration of 5 mg/mL there was very little matrix crystallisation (Figure 2-14), explaining the absence of instrumental response. Further investigations were conducted in order to ascertain the optimum matrix concentration and volume placed directly onto the hair are presented in Figure 2-14.

Using 5 mg/mL CHCA there were very few matrix crystals on the hair sample, whilst increasing the concentration of CHCA to 15 and 20 mg/mL led to the formation of crystals. Usefully it was seen that the addition of the derivatisation reagent appeared to help the CHCA matrix adhere to the hair sample (Figure 2-15).

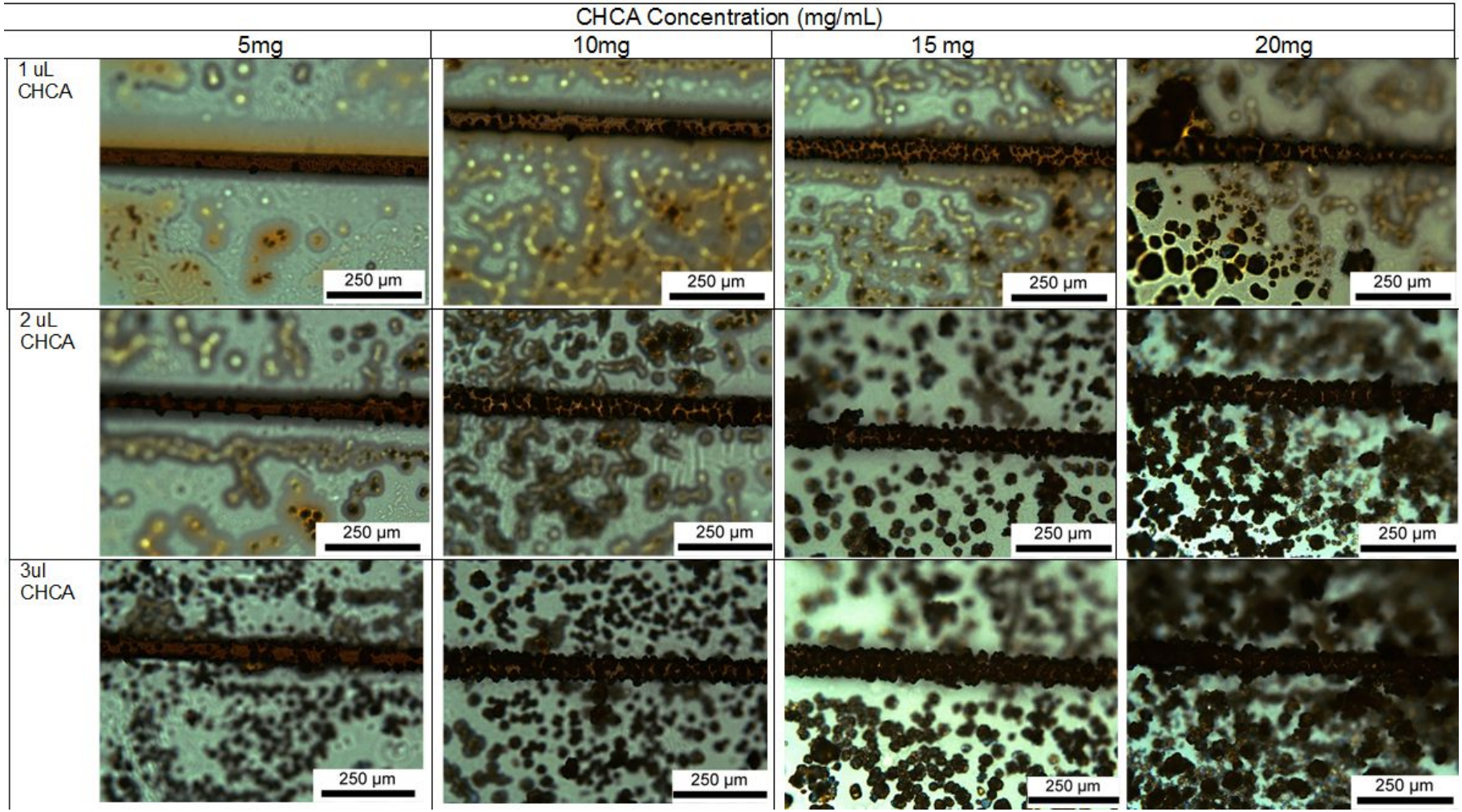

Figure 2-14. Microscope images of derivatised hair samples with different concentration and volumes of matrix applied

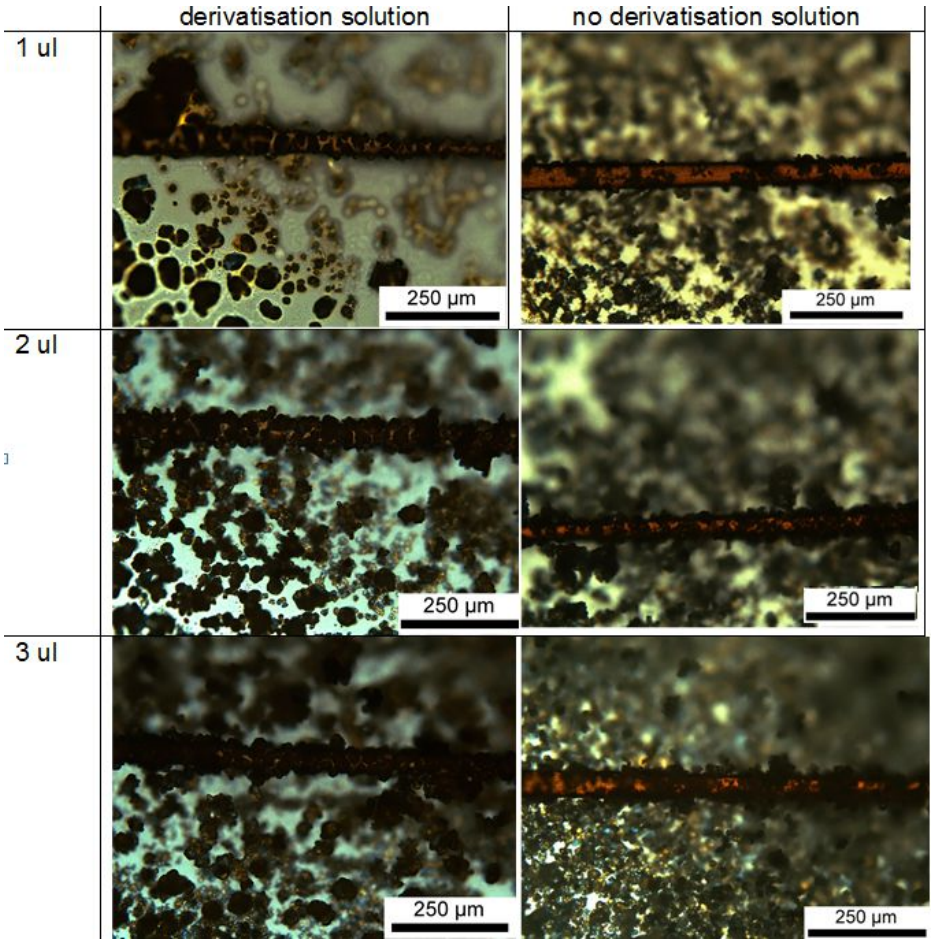

Figure 2-15. Derivatised and underivatised hair with 20 mg/mL CHCA matrix spotted on top.

2.7 Profiling and imaging of cannabinoids in hair samples

Following the evaluation of the matrix application under the microscope, CHCA (2 µL, 20 mg/mL) was used as the matrix to analyse hair spiked with THC. Unlike with previous experiments where CHCA (1 µL, 5 mg/mL) was used, the analyte could now be detected during profiling experiments.

Following the evaluation of microscopy and profiling experiments, 15 mg/mL and 20 mg/mL concentrations of CHCA were selected and a MALDI-MSI experiment was performed. Samples were prepared as described in Section 2.2.5. A schematic of the experiment can be seen in Figure 2-16 and the mass spectrometry image can be seen in Figure 2-17.

At all concentrations and volumes of CHCA the THC compound had been delocalised from the hair and into the surrounding matrix. This can be seen most prominently in the first hair sample with 15 mg/mL CHCA where signal intensities directly on top of the hair are lower than those in the surrounding area. However, signal intensities for THC were also highest at the 1 µL volume 15 mg/mL CHCA concentration.

Delocalisation of the THC compound could be due to THC being soluble in the derivatisation reagent and so it spreads out as far as the spot of the derivatisation solution.

The delocalisation of analytes is undesirable as it may lead to interpretational difficulties. For example, the analyte may delocalise into a region of the hair that originally did not contain the analyte. This could lead to misleading results when trying to estimate a timeline of usage.

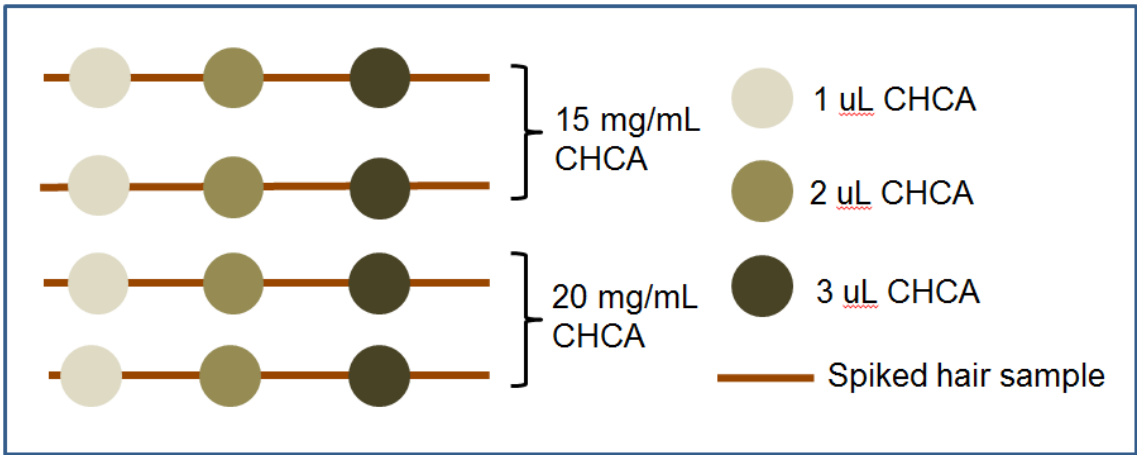

Figure 2-16. Schematic of imaging experiment.

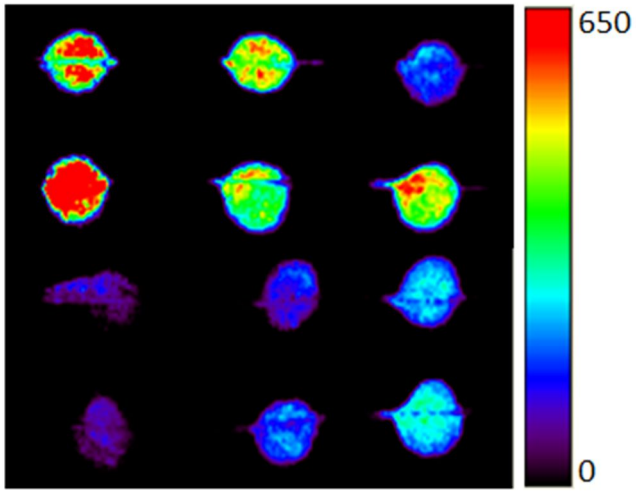

Figure 2-17. MALDI image of peak 406.2 corresponding to derivatised THC.

2.7.1 Spraying of derivatisation reagent

It was hypothesised that the delocalisation of the analyte could be due to the relatively large volume of derivatisation reagent being spotted. To test this hypothesis a hand sprayer (see Section 2.2.6) was used to supply a fine mist of the derivatisation reagent before spraying the sample with CHCA matrix using an automated sprayer (see Section 2.2.7). A hand sprayer was chosen due to hazards associated with the trimethylamine component of the derivatisation reagent, as it was easily used in a fume hood. The result of using a spray for the derivatisation reagent can be seen in Figure 2-18. Since

previously the delocalisation was equal in all directions (see Figure 2-17) it is reasonable to assume that delocalisation is not occurring along the hair sample, although this cannot be ruled out.

Once the derivatisation and spraying of analytes was optimised blank and cannabinoid spiked hairs were imaged to verify efficiency of the derivatisation method for imaging purposes and were compared to hairs which had not gone through the derivatisation step, the results of which can be found in Figure 2-18.

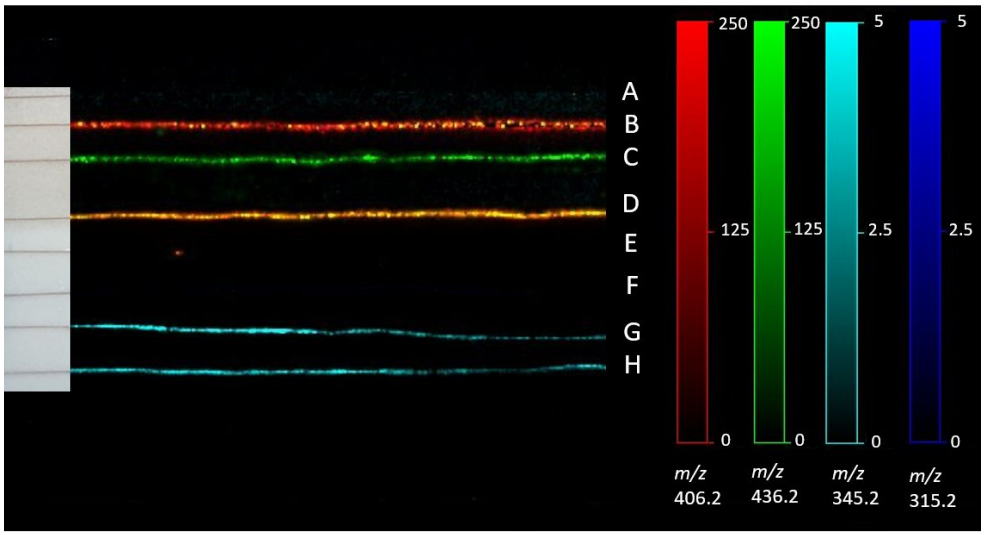

Figure 2-18. Comparison between derivatised and non-derivatised hairs. Hair A soaked in methanol and derivatised. Hair B soaked in THC standard then derivatised. Hair C soaked in THC-COOH standard and derivatised. Hair D soaked in a 1:1 mixture of THC standard and THC-COOH standard and derivatised. Hair E soaked in methanol and not derivatised. Hair F soaked in THC standard and not derivatised. Hair G soaked in THC-COOH standard and not derivatised. Hair H soaked in a mixture of THC and THC-COOH and not derivatised.

Unless dramatic modifications are made to contrast and brightness, underivatised hairs soaked in THC standard could not be visualised in the 2D molecular map as the ion signals of the underivatised THC were of extremely low intensity. Interestingly THC-COOH could be visualised in the 2D molecular ion map (Cyan colour) in hairs G and H which were soaked in THC-COOH standard and a mixture of THC and THC-COOH standard respectively, however this was also at relatively low intensity. The peak at *m/z* 406.2 corresponding to derivatised THC is clearly seen in the hair that was spiked with

THC and subsequently derivatised (red in colour). Similarly, the expected ion at *m/z* 436.2 was observed in the hair spiked with THC-COOH and subsequently derivatised (green colour); the hair which was spiked with a mixture of THC and THC-COOH and then derivatised appears yellow in colour as both THC and THC-COOH ions are present (a mixture of red and green gives yellow).

Since it was established that derivatisation enhances both the THC and THC-COOH signal in imaging experiments (as shown in Figure 2-18), a second mapping experiment with the other cannabinoids shown in was carried out (Figure 2-19). The peak at *m/z* 406.2 corresponding to derivatised THC is clearly seen in the hair which was spiked with THC and then derivatised (red *m/z* map), the peak at *m/z* 483.2 was observed in the hair spiked with CBD and derivatised (yellow *m/z* map), the peak at *m/z* 402.2 was corresponding to the derivatised CBN was observed in the hair which was spiked with CBN and derivatised (blue *m/z* map), the peak at *m/z* 436.2 corresponding to the derivatised THC-COOH was observed in the hair which was spiked with THC-COOH and derivatised (green *m/z* map) and finally the peak at *m/z* 422.2 corresponding to the derivatised 11-OH-THC was observed in the hair which was spiked with 11-OH-THC and derivatised (magenta *m/z* map). As with the profiling experiments, THC-COO-gluc fragmented to give THC-COOH at a *m/z* of 436.2 (green *m/z* map) and its image intensity reflect a 5X lower concentration compared to the other standards due to the concentration in which it is supplied.

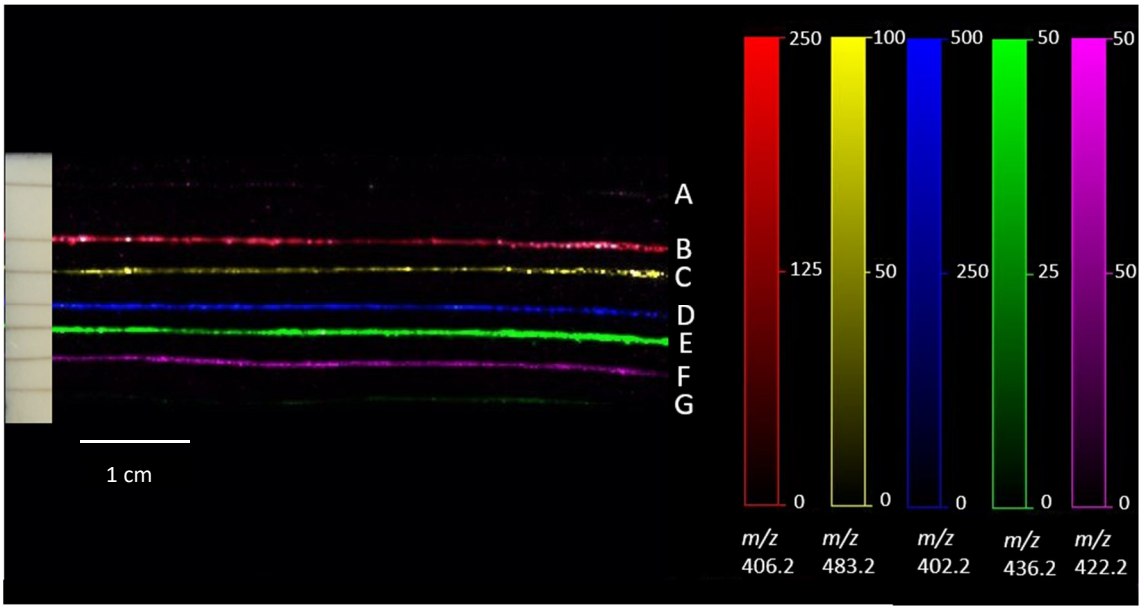

Figure 2-19. Simultaneous imaging of several cannabinoids of interest. Hair A soaked in Methanol. Hair B soaked in THC. Hair C soaked in THC. Hair D hair soaked in CBD. Hair E soaked in THC-COOH. Hair F soaked in 11-OH-THC. Hair G soaked in THC-COO-gluc. All hairs were derivatised with FMTPS prior to analysis.

Once verified the efficiency of the derivatisation method coupled with the MALDI MSI analyses, users' hair was investigated employing this optimised method. MALDI MS/MS images were obtained of hairs collected from a volunteer who self-reported to use cannabis once a week and the transition *m/z* 406.2 derivatised THC parent ion compound to *m/z* 110.0 was monitored (Figure 2-20). The product ion at *m/z* 110.0 corresponds to the hydrated methylpyridinium fragment which is common to all FTMPS derivatives and have previously been used for confirmation [218].

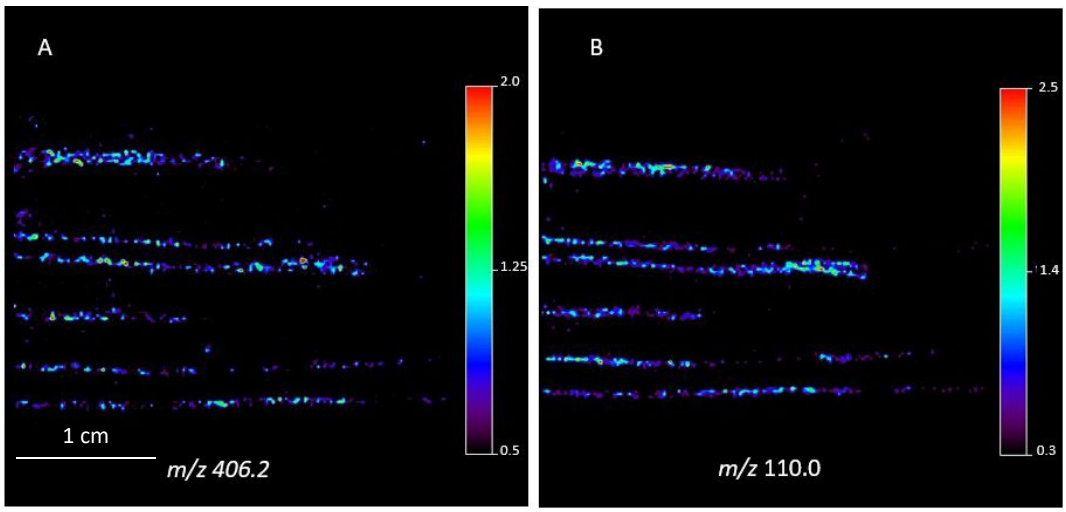

Figure 2-20. MS/MS image of user hairs. 6A shows derivatised THC parent ion at *m/z* 406.2 6B shows the map of the fragment ion at *m/z* 110.

2.8 MALDI Imaging to detect hair exposure to cannabis smoke

Since THC is present in the smoke produced when the plant material is combusted, the presence of THC in hair can be due to exposure to smoke, and not necessarily direct or intentional usage. The exact mechanism of smoke contamination is not yet fully understood. Mapping the THC compound and its location in the hair sample after exposure to cannabis smoke could therefore offer new insights into the mechanism of contamination and the most appropriate procedure to remove external contamination. In this section preliminary results of hairs exposed to cannabis smoke and subsequently analysed using MALDI-MSP and the MALDI-MSI methods developed in Section 2.7 will be presented.

2.8.1 Methods and Materials

Methods for the matrix preparation, deposition of matrix, spiking of samples hair samples, and derivatisation were performed as previously described in Section 2.2. The

instrumentation was also used as described in Section 2.3. Additional methods and materials unique to this section can be found below.

2.8.1.1 Spraying of derivatisation reagent

For imaging experiments in this section the derivatisation reagent was sprayed using a Bruker ImagePrep (Bruker Daltonics, Bremen, Germany).

2.8.1.2 Preparation of plant extracts

The plant extract was prepared according to De Backer *et al.* [227]. The plant material (purchased from a coffee shop in Maastricht, The Netherlands) shown in Figure 2-21A was dried for 24 h in a 35 °C forced ventilation oven. The sample was then ground to a fine powder. 200 mg of powder (shown in Figure 2-21C) was extracted with a mixture of 20 mL mixture methanol/chloroform (v/v: 9/1) by agitation for 30 minutes. The extract was then filtered (shown in Figure 2-21D) and used for subsequent analysis.

In addition to the "fresh" plant extract a 3-year-old plant extract which had been stored at 5°C was also analysed. The origin of the plant and process of extraction for this sample is unknown.

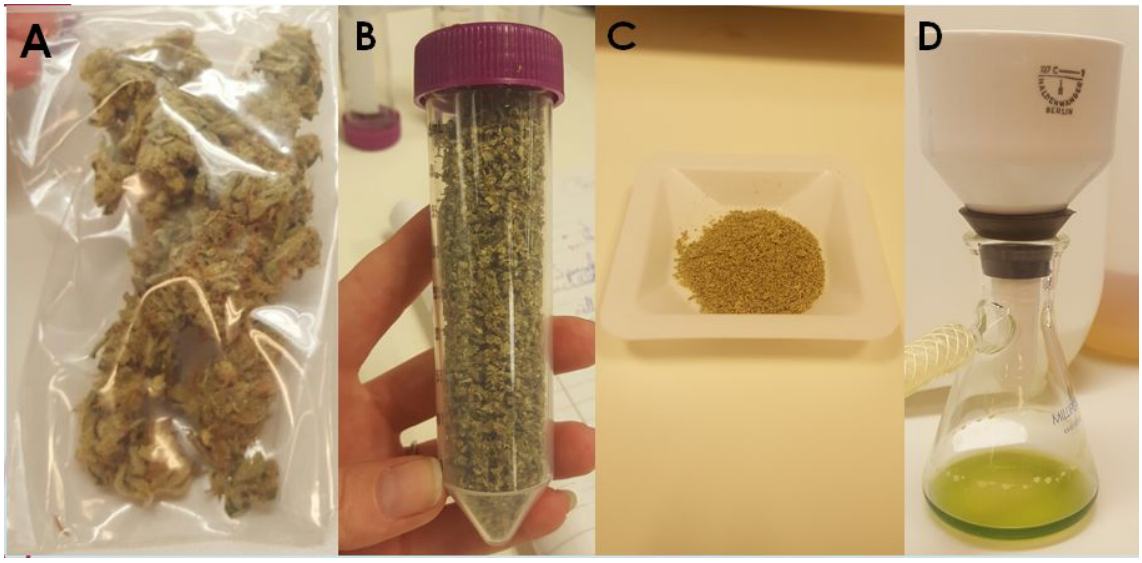

Figure 2-21. A-Cannabis plant material as bought from a coffee shop. B-Cannabis plant material after grinding. C-Cannabis plant material after drying at 30 °C for 24hr and grinding with pestle and mortar. D-Cannabis plant material filtrate.

2.8.1.3 Preparation of cannabis cigarettes

Cannabis cigarettes were prepared by a regular user, who was asked to make cigarettes as they normally would. Briefly, the plant material shown in Figure 2-21A was ground using a herb grinder to separate the cannabis bud from small stems which were still attached. This resulted in a consistency that is more amenable to rolling into a cigarette (Figure 2-21B). Each cannabis cigarette contained approximately 130 mg of plant material and 700 mg of Lucky Strike tobacco and was rolled using Rizla green regular rolling paper.

2.8.1.4 Smoke exposure conditions

A hair sample (approximately 5 g) from an individual who reported that they did not use cannabis was placed inside a desiccator. Hairs were approximately 12 cm in length. The cannabis cigarette was placed inside the tap of the desiccator as shown in Figure 2-22. The contents were then placed under vacuum and the cigarette was then lit. The

tap was turned on and off at regular intervals to mimic inhalation and keep the cigarette alight. After 15 minutes in the desiccator under smoke conditions the hair was removed and stored in foil at room temperature before analysis.

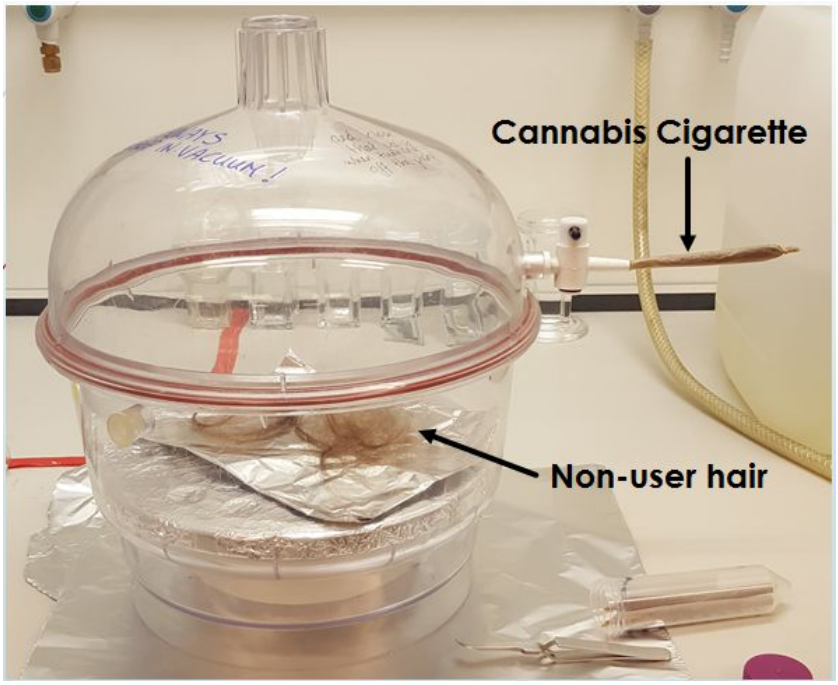

Figure 2-22. Experimental set up of cannabis smoke exposure experiments.

2.8.2 Instrumentation

Profiling and high-speed imaging was performed on a Bruker RapifleX MALDI Tissuetyper™ system (Bruker Daltonik GmbH, Bremen, Germany). The instrument was operated in reflectron mode in positive ion mode in the mass range *m/z* 100-600. The instrument was calibrated prior to analysis using red phosphorus clusters. Images were acquired using a 50 × 50 µm raster (25 × 25 µm beam scan area). The images were generated using the FlexImaging 5.0 software (Bruker Daltonik GmbH) and were normalized to the total ion current (TIC).

2.8.3 Results

2.8.3.1 Profiling of plant extracts and hair samples

In the three-year-old plant extract, peaks at *m/z* 406 and 402 were detected which correspond to FMTPS derivatised THC and CBN respectively (Figure 2-23A). The relative intensities of the peaks were high, being the largest two peaks in the spectrum. The peak corresponding to THC was also detected in the fresh plant extract; however, the peak corresponding to CBN was not (Figure 2-23B). This could be due to the fact the THC is known to degrade to CBN [228–230], or that the two extracts were of different plant strains (discussed in detail in Section 1.1.2). The three-year-old plant extract mass spectrum also contained an additional peak at *m/z* 438 which was not detected in the fresh plant extract and is of unknown origin. It does not correspond to theoretical values of FMTPS derivatised cannabis plant constituents reported in the study from which the extraction procedure was reproduced [227].

The profile of a hair exposed to THC smoke also contained *m/z* 406 in the mass spectrum. Interestingly, the peak corresponding to CBN is also detected (denoted with an arrow on Figure 2-23C) but at a much lower abundance than in the aged plant extract. This suggests that the degradation of THC to CBN is accelerated due to exposure to high temperature when burned in the cigarette.

The peak at *m/z* 438 is detected in the hair sample exposed to cannabis smoke and the aged plant extract, but not in the fresh plant extract, suggesting it also may be a degradation product of the plant material induced by pyrolysis.

A peak was observed at *m/z* 420 in the hair sample that was exposed to cannabis smoke but was not detected in either the plant material extracts or the blank hair

sample. It is hypothesised that this corresponds to a compound in the tobacco or the rolling paper used to make the cannabis cigarette.

Peaks corresponding THC, CBD and CBN were not detected in the blank hair sample from the non-user (Figure 2-23D). The peak corresponding to the doubly-derivatised CBD (*m/z* 483) was not detected in any sample.

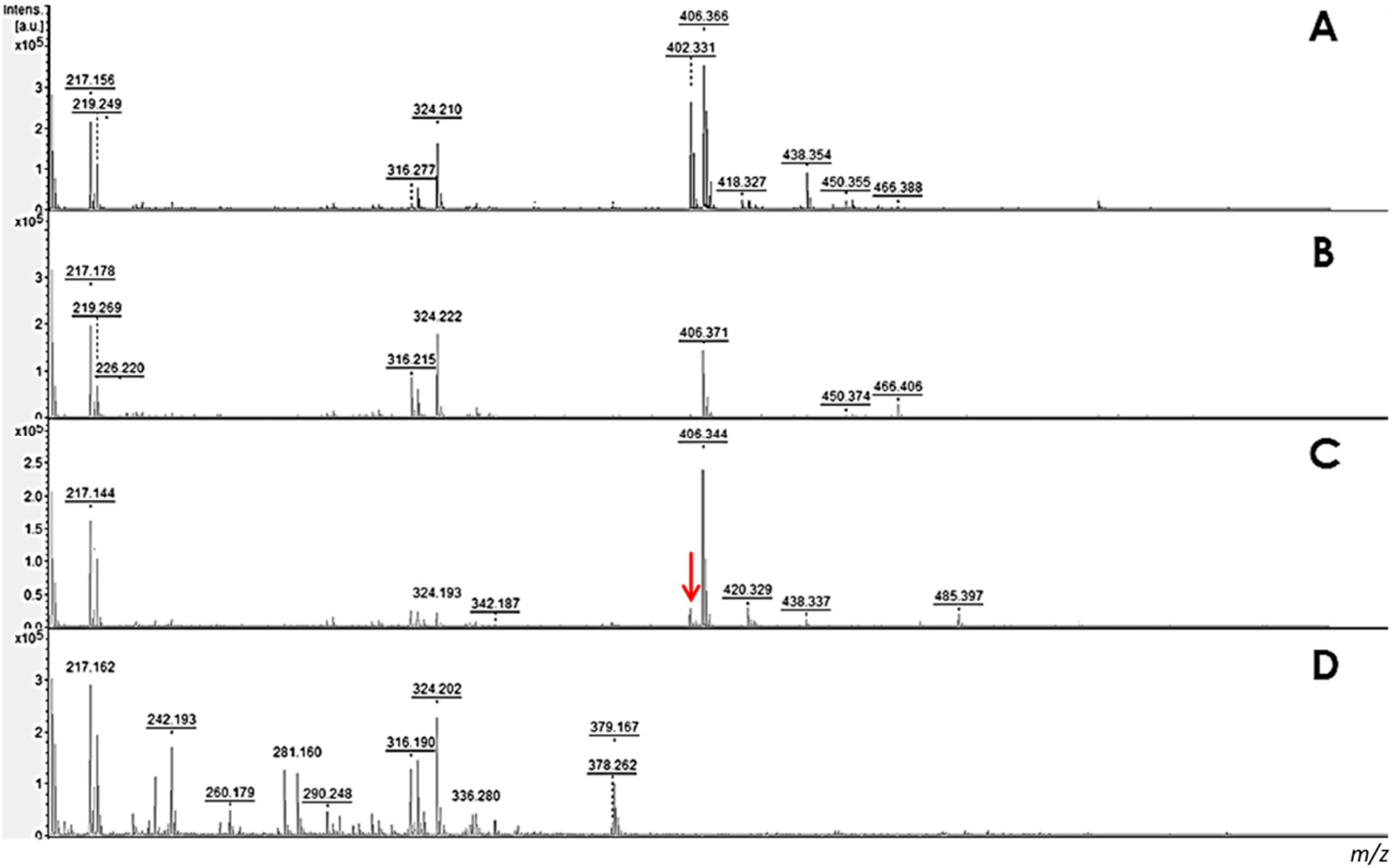

Figure 2-23. MALDI-MSP mass spectrum of A) 3-year-old plant extract. B) Freshly prepared plant extract. C) cannabis smoke contaminated hair sample. D) hair sample not exposed to cannabis smoke

2.8.3.2 Imaging of smoke contaminated hairs

In addition to a smoke contaminated hair prepared as described in the previous section, a blank hair from the non-user and a hair spiked with fresh plant extract as described in Section 2.2.5 were subsequently imaged using MALDI-MSI. During spray optimisation experiments the peak at *m/z* 324 was found to be a suitable marker for the derivatisation reagent due to high signal intensity, and was used to deduce whether the derivatisation reagent was sprayed heterogeneously on the sample. The results from Figure 2-24A suggests a good coverage of the derivatisation reagent on the hairs; however, there are some regions where the mass correlating to the derivatisation reagent has a lower intensity due to inhomogeneity in the spraying of the derivatisation reagent. This is reflected in lower abundance of analytes in the regions where the derivatisation is at a lower intensity as seen in Figure 2-24B and 2-24C.

As with the profiling experiments, *m/z* 406 corresponding to THC was observed in both the plant extract spiked hair and the hair exposed to cannabis smoke. *m/z* 420 was only detected in the smoke contaminated hair. As before, the hair not exposed to cannabis smoke (control) did not have *m/z* 406 or *m/z* 420 detected.

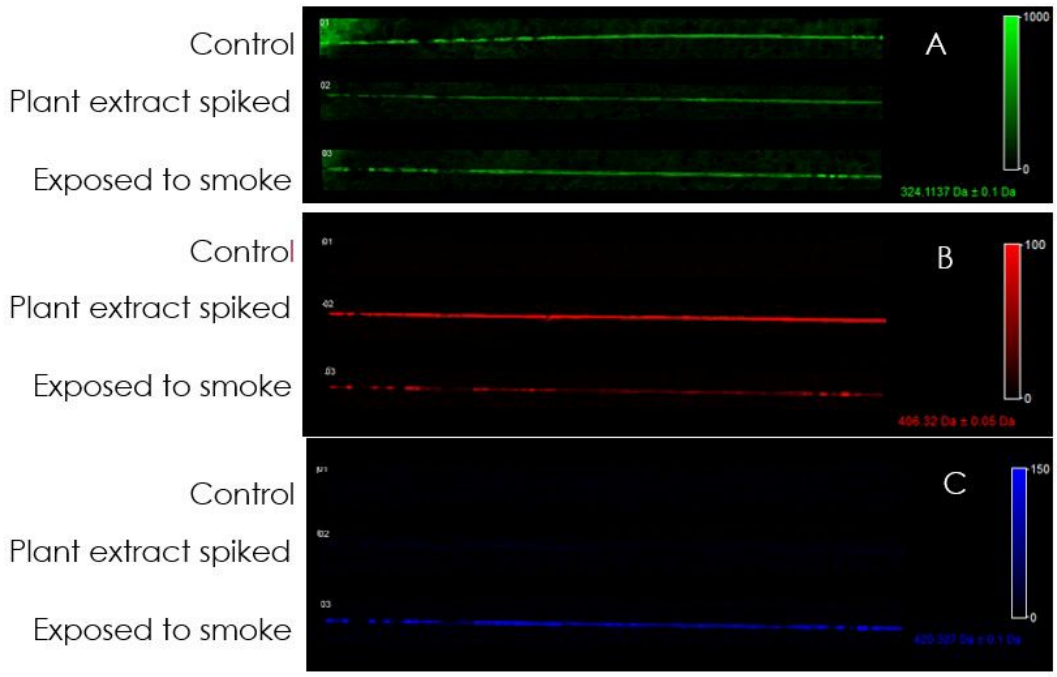

Figure 22-24. MALDI-MSI A) map of derivatisation reagent (*m/z* 324). B) map of THC (*m/z* 406). C) map of *m/z* 420.

2.9 Further work

2.9.1 Optimisation of FMTPS spray

At present, the spray method can cause inhomogeneities in the volume of derivatisation reagent across the hair sample. Therefore, additional optimisation of the FMTPS spray method should be conducted. A homogeneous spray is needed to reliably identify relative intensities within the sample so that any assignment of high or low intensities of cannabinoid peaks are in fact due to the relative abundance of compounds in that area, and not due to inhomogeneity of the derivatisation reagent.

If homogenous spraying of the derivatisation reagent is not achieved, investigations into normalising any image to a peak associated with the derivatisation reagent should be investigated.

2.9.2 Longitudinal sectioning of hair samples

The methods developed in this study have been applied to intact hairs, however there are limitations associated with this type of analysis. As drugs are considered to be entrapped inside the keratin matrix of the hair (described in detail in Section 1.3.5), it is difficult to know whether a) the drug is completely extracted out of the hair by the MALDI matrix solution or b) if the detected drug originates from external contamination or metabolic incorporation [231].

To be able to make a distinction between external contamination and intake, examination of drug distribution inside the hair itself is required and so should be investigated in future work. Whilst methods for the preparation of longitudinal sections of hair samples have previously been described [189,191,193,231,232] analysis of cannabinoids in sliced hair samples has not yet been reported.

In relation to smoke contamination, an assessment of whether the cannabinoids found in cannabis smoke remain on the cuticle of the hair (indicating external contamination) or are found inside the cortex (indicating usage) should be a priority along with an assessment of the effectiveness of current decontamination procedures.

2.9.3 Quantification of cannabinoids in hair samples

Quantification of analytes was not attempted in this study and is a logical next step for future work. This may be achieved by utilising a method developed in collaboration with Flinders *et al.* during the course of this study to determine the amount of cocaine detected in hair samples [233]. The full text of this article can be found in Appendix II.

2.9.4 Use of realistic smoke contamination procedures

Realistic smoke contamination conditions should be used in future studies, with additional investigations into whether the method is sensitive enough to detect cannabinoids under these conditions.

One such exemplar method was conducted by Röhrich *et al.* to investigate the levels of cannabinoids in urine and blood after exposure to cannabis smoke. The exposure to cannabis smoke by non-users took place in a coffee shop in Maastricht in the Netherlands. Coffee shops in the Netherlands are pubs where cannabis can be consumed legally. The coffee shop in which exposure took place had no windows but relatively efficient ventilation and, therefore, was not very smoky during the exposure.

This type of experiment would create a more realistic method of contaminating hair samples than the one used currently used in this PhD study. Findings form a realistic experiment would be more applicable to interpretation of cannabinoid findings in authentic hair samples.

2.9.5 Analysis of different hair types

The hair cuticle is the region affected by stress caused by the external environmental and physical factors. Undamaged hair has a smooth cuticle and outer layer, while damaged hair has a dull and dry cuticle with a rough outer layer [234]. Morphological characteristics such as roughness, pores, pits, and cracks, holes, or overall severe peeling (desquamation) occur in the cuticle layers and can be observed and classified using scanning electron microscopy (SEM) [235].

In relation to cannabinoid detection in hair samples, future work should focus on establishing whether there is a link between hair damage and cannabinoid concentrations found in hair samples after exposure to cannabis smoke by analysing samples using both SEM and MALDI-Imaging.

2.9.6 Further Analysis of user hairs

Finally, prior to integration into a toxicology workflow a much larger sample of user hairs, from different levels of users and with different hair types should be analysed and the relative levels of each metabolite reported. Initially these analyses should be carried out in parallel with well-established techniques such as GC-MS/MS to assess whether the techniques are comparable.

2.10 MALDI-MS optimisation discussion and Conclusions

In this study several approaches to detecting cannabinoids using MALDI Mass spectrometry were investigated. A range of different matrices and matrix compositions were evaluated, and it was shown that CHCA yielded the greatest signal intensity for the THC molecule at a concentration of 5 mg/mL in a solution of 70:30 ACN:0.2% aqueous TFA. It was also shown that the neither the addition of cetrimonium bromide nor lithium salts improved the detection of THC. In contrast, the addition of the ionic liquid aniline did improve the relative intensity of the THC peak significantly.

During the development of this method an interesting, laser induced, THC rearrangement was detected and reported. This resulted in two peaks which corresponded to the THC molecule (*m/z* 131 and *m/z* 315) and hence lower ability to detect the molecule without derivatisation.

The derivatisation of several cannabinoids and metabolites of interest with the addition of N-methylpyridium was found to be successful.

The novel *in situ* derivatisation, completed in minutes at room temperature using FMPTS, showed a greatly increased signal intensity over the non-derivatised analytes, enhancing the ability to detect THC, CBD, CBN and THC metabolites. The ability to

detect the metabolites of THC only formed *in vivo* THC-COOH, 11-OH-THC and THC-COO-gluc will enhance the ability of the analyst to distinguish between use and exposure. During analysis the THC-COO-gluc fragments to form THC-COOH, with the consequence that if the *m/z 436.2* is detected it cannot be determined which of the analytes was present. The *m/z* 612 is however unique to the THC-COO-gluc. This is an advantage over traditional GC-MS methods where the glucuronide is not generally detected as a parent compound due to the common practice of hydrolysis or digestion of the hair sample which converts it into the THC-COOH [236].

Due to the processing in this method the limits of detection for the analysis are not reported. The main limitation of the study the inability to assess LODs due to the spiking procedure as it is not possible to ascertain how much of the spiking solution the hair has taken up.

The method reports a sample preparation workflow, notwithstanding the derivatisation step, which is less complicated than the traditional GC-MS or LC-MS methods. This method also gives the opportunity to simultaneously detect THC and metabolites in a single workup and analysis. Application to a single user hair has shown applicability to real life samples. The traditional method of segmenting the sample into 1 cm pieces means a one-month history can be obtained, using MALDI-IMS experiments the resolution will be much smaller than that, allowing possibly isolating use on a single day.

2.11 Smoke contamination discussion and conclusion

The preliminary findings in this study suggest that MALDI-MS could be a useful tool to differentiate between the THC and CBN content in plant extracts which can be an indicator of degradation. This could be an advantage over commonly used techniques such as LC-MS due to the rapid nature of MALDI-MSP analysis.

THC was detected on hair contaminated with cannabis smoke using MALDI-MSP and MALDI-MSI. This is an important finding as MALDI-MSI could also be used to distinguish whether a compound is in the cortex or cuticle of the hair, which is not possible in current analysis techniques as GC-MS and LC-MS. This may be beneficial as the major pitfall of hair analysis is the presence of external contamination, making interpretation of analytical findings problematic.

Chapter 3. Development of Gas Chromatography-Mass Spectrometry to detect cannabinoids in hair samples

This chapter includes a discussion of current GC-MS methodologies used to analyse hair for cannabis use. The novel work in this chapter introduces a sample preparation technique optimised for the simultaneous detection and quantification of THC, CBD, CBN, 11-OH-THC and THC-COOH using GC-MS in hair samples. Additionally, the use of atmospheric pressure chemical ionisation (APCI) for detection and quantification of cannabinoids in hair samples will be investigated for the first time.

3.1 Introduction

GC-MS was first used to detect cannabinoids in hair samples in the 1990s, specifically THC and THC-COOH were initially targeted [237]. A comprehensive review of sample preparation methods from literature published between 2000 to 2014 was conducted by Vogliardi *et al.* [161] and is summarised in Table 3-1. Ideally a method would simultaneously detect THC, CBD and metabolites. This review revealed that only 12% of studies analysed both the parent compound THC and the metabolite THC-COOH. Without the analysis of metabolites cannabis consumption cannot be confirmed due to potential contamination issues which are outlined in Section 1.3.7. Similarly, only a third of studies detected both THC and CBD. The detection and quantification of CBD is becoming increasingly relevant due to possible clinical applications of CBD (see Section 1.1.4) and changes in the potency of cannabis plants.

There are no published methods included in the review article which analyse the metabolite 11-OH-THC, or simultaneously analyse THC, CBD and THC-COOH. This amounts to a distinct lack of scope in current methodology, possibly limiting the amount of information gained before the difficult process of interpretation of analytical findings can take place.

This lack of coverage of analytes is also reflected in more recent literature [238]. The previously reported limits of detection and quantitation of several instrumental methods can be seen in Table 1-2 of Chapter 1.

Compound(s) Analysed	Number of studies	References
THC	3	[239–241]
THC, CBD and CBN	8	[108,109,113,115–117,119,242]
THC and THC-COOH	3	[121,165,243]
THC-COOH	12	[122–127,160,244–248]
11-OH-THC	0	
Total	**26**	

Table 3-1. Total number of published methods for each combination of cannabinoids and/or metabolites taken from the years 2000-2014.

Due to low incorporation rates of THC metabolites [45], highly sensitive instrumentation is needed for successful analysis. Many GC methods utilise EI ionisation, however this this considered to be a "hard" ionisation technique which is prone to fragmentation of analytes. This can result in sub-optimal amounts of the intact compound reaching the detector, making the method less sensitive.

In contrast, APCI is considered a low energy "soft" ionisation technique. This promotes ionisation with very little fragmentation, resulting in the formation of $M+H^+$ or M^+ ions as the base peaks of the mass spectrum (see Section 1.4.2. for more information). The reduced fragmentation observed by using this relatively new source can have a significant impact on target analysis at trace levels. In recent years the usefulness of the interface has been demonstrated in several fields including environmental analysis [249,250], food safety [251–253], and metabolic profiling [254]. However, it has not

been applied to the detection of cannabinoids in any sample type. It has also not been evaluated for the detection of any compounds in hair samples.

3.2 Sample preparation

There are several sample preparation steps that are required before a hair sample can be analysed using GC-MS. Briefly, this includes:

- washing of the hair to remove external contamination (see Section 1.3.8 for more information)
- digestion of hair to liquify the sample or soaking the hair to extract the drugs
- clean up and extraction of analytes from the digest (see Section 3.2.6)
- derivatisation to make the analytes more amenable to GC (see Section 3.2.3)

3.2.1 Decontamination of hair samples

The wash protocol chosen for decontamination of hair samples was taken from a recent study conducted by Duvier *et al.* [255]. After extensive testing of both single and sequential decontamination protocols, the authors concluded that three sequential wash protocols were found to perform equally well regarding the removal of external cannabis contamination originating from smoke or indirect contact. In addition, these methods did not remove incorporated THC. These steps were: (1) methanol, SDS; (2) methanol, SDS, methanol and (3) methanol, methanol. Due to reagent availability and the additional preparation time needed for a 3-step

decontamination procedure, the methanol-methanol decontamination step reported by Duvier *et al.* was chosen for future experiments in this PhD project.

Hair samples were washed with MeOH (5 mL) before drying at room temperature and washing with a further 5 mL. After vortexing (10 s) and ensuring that all the hairs were in the solvent, the test tubes were shaken (15 min at 100 rpm). The hair samples were then removed from the test tube using tweezers and placed on paper to dry in a fume hood.

It is, however, important to note that the main limitation of the above study is that only THC was analysed.

3.2.2 Digestion of hair samples

For substances that are stable in alkaline conditions, a useful method for extraction of analytes from the hair matrix consists of digestion in an aqueous solution of NaOH. Under these conditions, there is complete dissolution of the hair. Whilst the hydrolysis of morphine, heroin and cocaine occurs in alkaline conditions, cannabinoids have been found to be stable [161]. Since this is a well-established method it was chosen for use without alteration.

Figure 3-1. 20 mg of hair a) before and b) after 30 minutes at 70°C with NaOH (1 mL, 1 M).

3.2.3 Derivatisation

Derivatisation of cannabinoids before GC analysis is necessary to increase their volatility. A recent literature review into plant cannabinoid derivatisation techniques by Monlár and Molnár-perl showed that alkylsilyation of cannabinoids was the most common technique, followed by acylation and/or esterification [256]. In this section a range of derivatisation reagents, taken from published methods or potentially of use for cannabinoids will be assessed to identify the most suitable for further experiments. Before derivatisation experiments analytical standards (10 ng/µL) were dried under a flow of nitrogen at 45°C and reconstituted in ethyl acetate (50 µL). Experiments were conducted without derivatisation by reconstituting analytical standards in ethyl acetate (50 µL).

3.2.3.1 Derivatisation methods

The expected *m/z* of derivatised analytes using different derivatisation reagents can be found in Table 3-2. The ion of greatest abundance for each compound was used, where this is not the [M]+ ion, [M]+ ions were also monitored for confirmatory purposes. Illustrative examples of THC and THC-COOH derivatised with each regent used in this study can be found in Figure 3-2.

Derivatisation reagent	THC	THCOOH
None	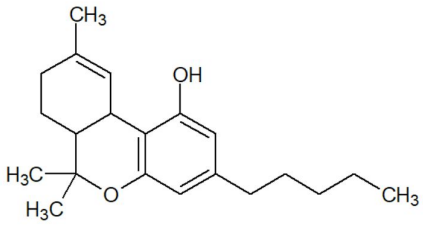	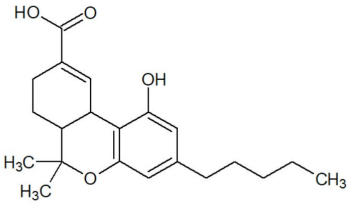
BSTFA	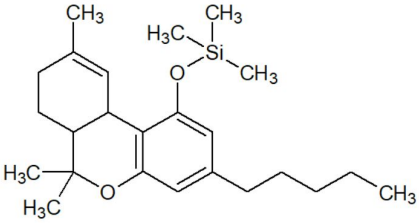	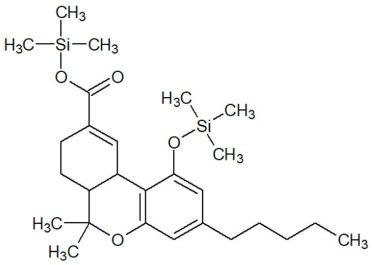
MTBSTFA	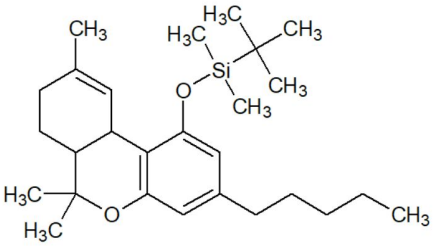	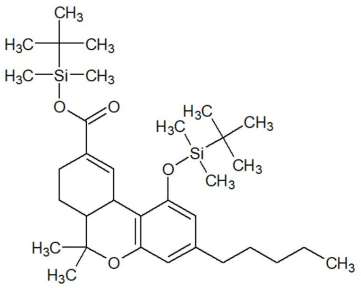
BSTFA/MTBSTFA	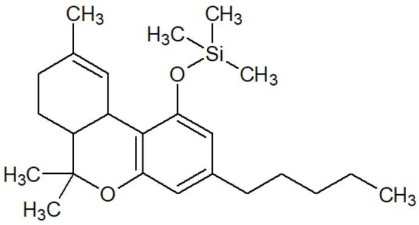	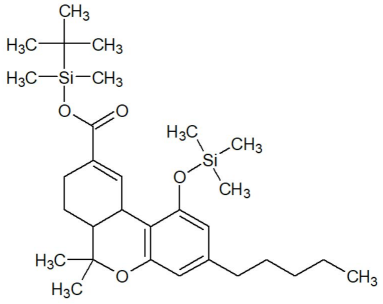
PFPOH/PFOH	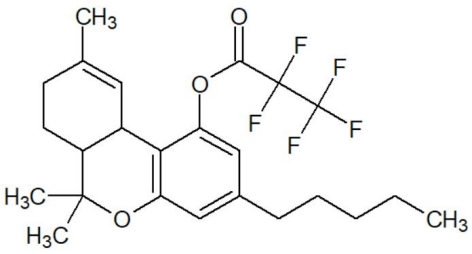	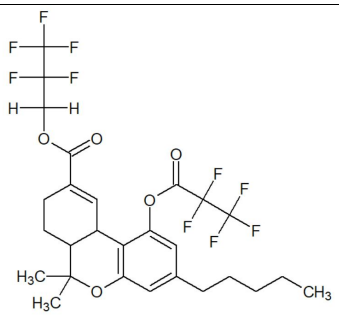

Figure 3-2. Representative structures of THC and THC-COOH after derivatisation with BSTFA, MTBSTFA, a mixture of BSTFA and MTBSTFA and a mixture of PFPOH and PFOH.

	Ions monitored				
Compound	No Reagent	BSTFA	MTBSTFA	BSTFA/MTBSTFA mix	PFPA/PFOH
THC	299	371	371	371	377
CBD	231	390	371	390	377
CBN	295	367	424	367	295
11-OH-THC	330	371	444	374	622
THC-COOH	344	371	515	371	489

Table 3-2. *m/z* values monitored for each compound with different derivatisation reagents

3.2.3.2 **BSTFA**

BSTFA derivatisation was performed as per Han *et al.* Extracts were reconstituted in BSTFA (50 µL) and heated at 70°C for 30 min. The sample was then dried under N_2 and reconstituted in ethyl acetate (50 µL) [257].

3.2.3.3 **MTBSTFA**

MTBSTFA derivatisation was performed according to Uhl and Sachs. Dried extracts were heated in MTBSTFA (75 µL) at 90°C for 1 hour. The sample was dried under N_2 and reconstituted in ethyl acetate (50 µL) [160].

3.2.3.4 **BSTFA/MTBSTFA mixture**

The BSTFA/MTBSTFA mixture was prepared according to Brewer *et al.* Dried extracts were reconstituted in equal parts of BSTFA:MTBSTFA:ACN (50 µL) at 90°C for 1 hour [258]. The sample was dried under N_2 and reconstituted in ethyl acetate (50 µL) prior to analysis.

3.2.3.5 **PFPA/PFOH**

For derivatisation with PFPA/PFOH, dried extracts were heated in PFPA (50 µL) and PFPOH (25 µL) at 65°C for 30 min. The sample was dried under N_2 and reconstituted in L ethyl acetate (50 µL) prior to analysis. This method was proposed by Baptista *et al.* [259].

3.2.4 Instrumental parameters

All analyses were conducted using the following method:

A 1 µl sample was injected into a Hewlett Packard (HP) GC/MS system: HP 6890 series GC system (USA) with an Agilent Technologies DB-5MS column (crosslinked 5% phenyl methylsiloxane, 30 m x 250 µm x 0.25 µm film thickness) coupled to a Waters Micromass® Quattro Micro™ GC tandem mass spectrometer (Manchester, UK) using an Agilent Technologies 7683B series autosampler (CA, USA)

The inlet temperature was 220°C with a splitless injection. The carrier gas was helium (1.0 mL/min). The column oven temperature was programmed to rise from an initial temperature of 150°C, held for 1 minute, to 270°C, at 20°C per minute and then held for 5 min. To determine the retention times and characteristic mass fragments, the primary electron ionization (EI) mass spectra were recorded in full-scan mode (*m/z* 50–650).

3.2.5 Results of derivatisation experiments

Whist THC, CBD and CBN could be detected without derivatisation, the metabolites 11-OH-THC and THC-COOH could not. Once derivatised THC and CBD showed increased peak areas, whilst 11-OH-THC and THC-COOH could be detected, with all reagents when compared to no derivatisation. CBD showed an increase in peak area with all derivatisation reagents compared to without, except PFPA/PFOH. BSTFA derivatisation gave the largest peak area for all cannabinoids, as shown in Table 3-3. BSTFA also gave the largest peak height for all analytes. As an illustrative example, an overlaid chromatogram of THC under all the investigated derivatisation conditions can be seen in Figure 3-3.

	Peak areas with varying derivatisation reagents				
Compound	No Reagent	BSTFA	MTBSTFA	BSTFA/MTBSTFA mix	PFPA/PFOH
THC	55600	761000	261000	97800	103000
CBD	50100	1100000	304000	292000	45300
CBN	517000	4850000	867000	184000	813000
11-OH-THC	ND	1390000	50800	219000	288000
THC-COOH	ND	590000	355000	359000	209000

Table 3-3. Summary of the peak area of analyte when injected underivatised and under different derivatisation methods (10 ng/µL) to three significant Figures (n=3).

THC and CBD both have the same retention time and mass spectrum with PFPA/PFOH derivatisation, this also reported by Baptista *et al.*[259]. Andrews and Paterson also reported this phenomenon with HFIP/TFAA derivatisation [260]. This is thought to be due to conversion of CBD to THC under acidic conditions [260].

The importance of measuring THC/CBD ratios to establish potency and due to possible clinical applications of CBD (described in detail in Section 1.1.8) means differentiation between the two compounds is highly desirable in any current method of analysis. In

addition, the conversion of CBD to THC raises the possibility of over-estimation of the true value of THC in a sample as the value obtained is in fact THC+CBD [259,261].

For the above reasons, derivatisation with PFPA/PFOH and HFIP/TFAA reagents were excluded from further investigation in this study.

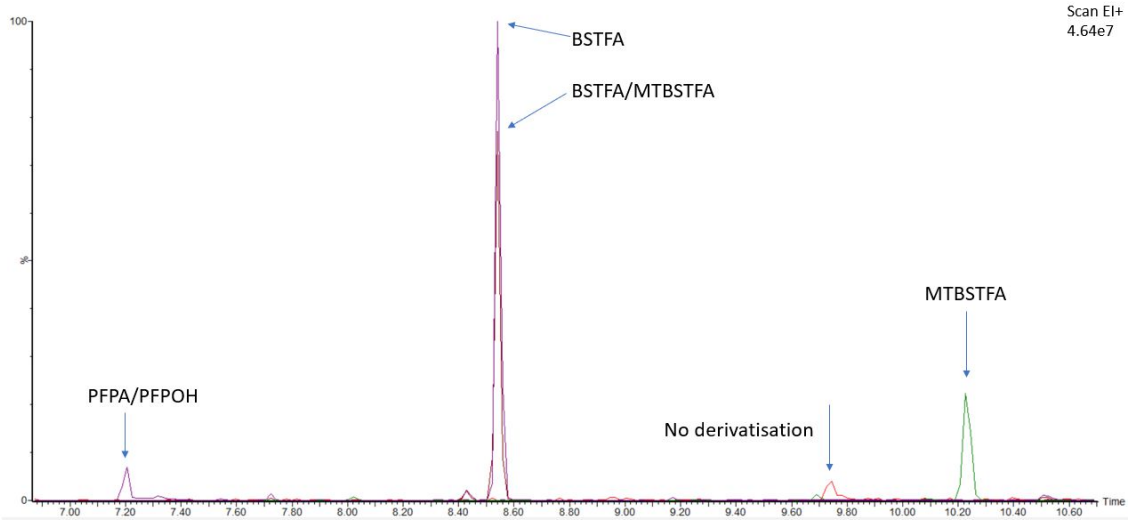

Figure 3-3. Overlay of chromatograms obtained from the derivatisation of THC with a variety of reagents

Based on peak shape, retention time and response BSTFA was chosen as the derivatisation reagent for future experiments.

3.2.6 Extraction of analytes from hair

The purpose of the extraction procedure is to selectively extract and concentrate the analytes of interest from the hair digest. This is necessary to reduce the presence of possible interference caused by organic compounds in high abundance from the hair matrix. This is generally carried out by liquid-liquid extraction (LLE) or solid phase extraction (SPE) [161].

Initially the hair digest was extracted using SPE cartridges (Bond Elut Certify, Varian Inc., Palo Alto, CA, USA). The method was adapted from Sears [262] with the addition

of a conditioning step taken from Guthery *et al*. to buffer the sample to pH 7 before extraction [263]. THC, CBD, CBN and 11-OH-THC could be extracted using this protocol. However, THC-COOH was not detected after SPE extraction, despite the utilisation of separate elution steps as described by Sears [262].

Considering this, an LLE extraction protocol was then selected after careful review of the literature. The chosen method was developed by Han *et al.* [243] and allowed for the sequential extraction of neutral and acidic analytes.

Briefly, hair digests were extracted with n-hexane:ethyl acetate (2 mL 9:1) for 10 minutes by quick mechanical shaking (250 rpm) for the extraction of THC, CBD, CBN and 11-OH-THC. The organic layer was then transferred into a screw-cap tube. This procedure was performed twice.

For the extraction of THC-COOH buffer (1 mL of 0.1M sodium acetate buffer, pH 4.5) and acetic acid (200 µL) were added. Hair digests were re-extracted with n-hexane:ethyl acetate (2 mL, 9:1) and the organic extract was transferred into the screw cap tube. Hair samples were extracted with n-hexane:ethyl acetate (2 mL, 9:1) one more time and the organic extract was transferred into the same screw-cap tube and evaporated to dryness at 45°C under a gentle stream of nitrogen.

This method of extraction allowed for the detection of all analytes of interest.

3.3 GC-EI-MS/MS method development

In this section the optimisation of GC oven temperature and development of a selected reaction monitoring (SRM) method will be discussed.

3.3.1 Oven temperature parameters.

A review of literature revealed a range in GC oven temperature parameters for the separation of trimethylsilyl derivatives of cannabinoids [108,160,241,248]. Start temperatures ranged from 60 °C [160] to 120 °C [248] depending which cannabinoids were analysed. Final oven temperatures ranged from 250 °C [241] to 300 °C [108,160]. At the commencement of this work no studies had been conducted on simultaneous detection of THC, CBD, CBN, THC-COOH and 11-OH-THC in hair samples, and so oven temperature parameters were optimised for peak shape, peak separation and total run time.

Figure 3-4 demonstrates the chromatographic separation of analytes at A) 300°C final temperature and B) 320°C final temperature. All analytes are well separated with both oven temperature parameters; however, at a 300°C end temperature the latest eluting peak THC-COOH (5) is broad. This can be seen in Figure 3-4Aii. At a final temperature of 320°C peak 5 becomes narrower and is now much closer in peak height to analyte 11-OH-THC (4). The narrowing of the peak also means that signal to noise increases, improving the limit of detection (LOD) of the analyte. This is imperative since metabolites are found in low concentrations in hair samples. Increasing the starting temperature from 40°C to 150°C decreased the retention time of the latest eluting peak (THC-COOH) from 15.4 minutes to 9.7 minutes, reducing the overall time for each run, which is very advantageous in a high throughput laboratory.

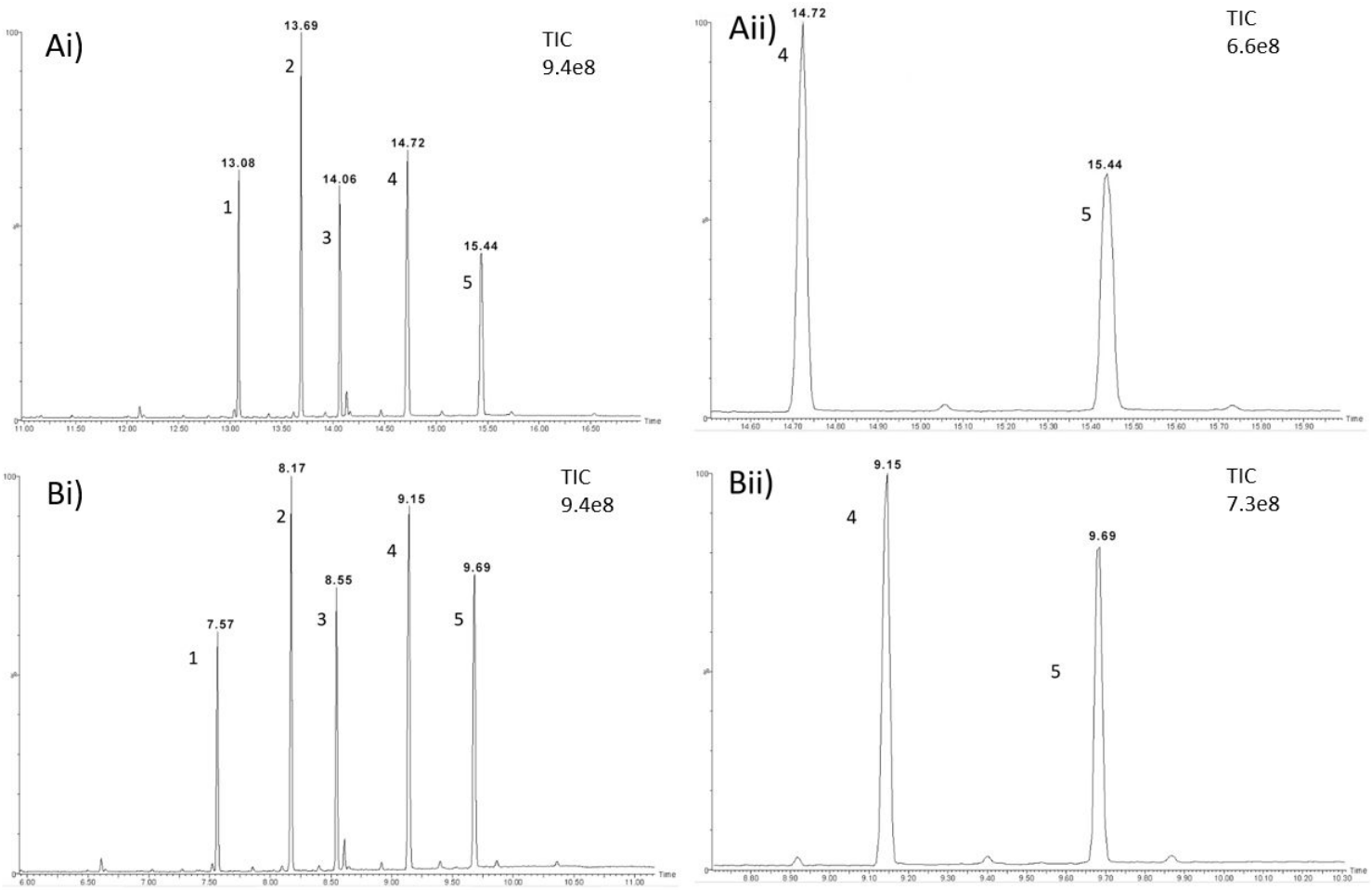

Figure 3-4. GC oven programme starting A) 40°C start ending at 300°C at 20°C/min (B) 150°C start ending at 320°C degrees 20°C/min. 1- CBD 2-THC 3-CBN 4-11-OH-THC 5-THCCOOH i) full chromatogram ii) compounds 4 and 5.

3.3.2 Tandem mass spectrometry analysis

The use of tandem mass spectrometry (MS/MS) greatly increases selectivity and sensitivity, especially when analysing complex matrices such as hair. This then enables low limits of detection for the analytes (see Section 1.4.2 for more information). The precursor ion in tandem MS is ideally of relatively high mass and abundance to obtain a product ion mas spectrum of analytical significance. This allows for identification of the analyte and will help to achieve a good signal-to-noise ratio with low detection limits.

The selected reaction monitoring (SRM) transitions for CBN, THC, and CBD previously reported by Lachenmeier *et al.* [264] were found to give a high response, as shown in Figure 3-5c, 3-5d and 3-5e respectively. Similarly, the SRM transition for THC-COOH, reported by Niedbala *et al.* gave a relatively high response (Figure 3-5a).

No SRM transition for 11-OH-THC had been previously reported; however target ions of *m/z* 459 and *m/z* 371 had previously been described by Sears [262]. Based on the literature and the successful transition of 488 → 371 for the structurally similar THC-COOH compound, for 11-OH-THC an SRM transition of 459 → 371 was chosen. However, it yielded a relatively low response (Figure 3-5b) and so required further optimisation.

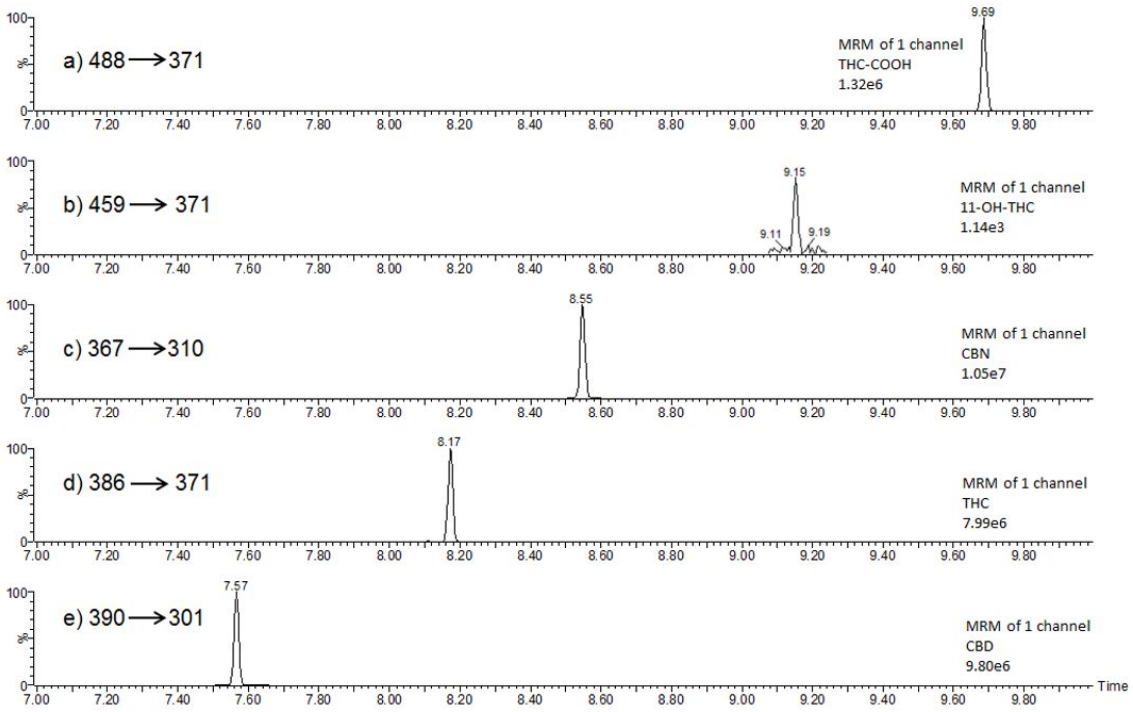

Figure 3-5. SRM chromatograms of 10 ng/µL of a) THC-COOH, b) 11-OH-THC, c) CBN, d) THC, e) CBD. On each chromatogram the MS/MS transition (quadrupole 1 to quadrupole 3) *m/z* can be found.

3.3.2.1 Optimisation of selected reaction monitoring for 11-OH-THC

Upon inspection of the full scan mass spectrum for 11-OH-THC, it was observed that the $[M]^+$ ion at *m/z* 459 was in relatively low abundance (circled in Figure 3-5A). The ion of the greatest abundance in the mass spectrum was *m/z* 73, however, this ion has low specificity as it is also observed in septa bleed [265]. As 73 is a low *m/z* it is also doubtful that significant further fragmentation, or unique fragmentation, would occur. Consequently, the second most abundant peak in the spectrum at *m/z* 371 was selected to undergo a product ion scan, shown in Figure 3-5B. The most abundant ion in the product ion scan was at *m/z* 305, and so the chosen SRM transition was 371 → 305, a chromatogram of which can be seen in Figure 3-6.

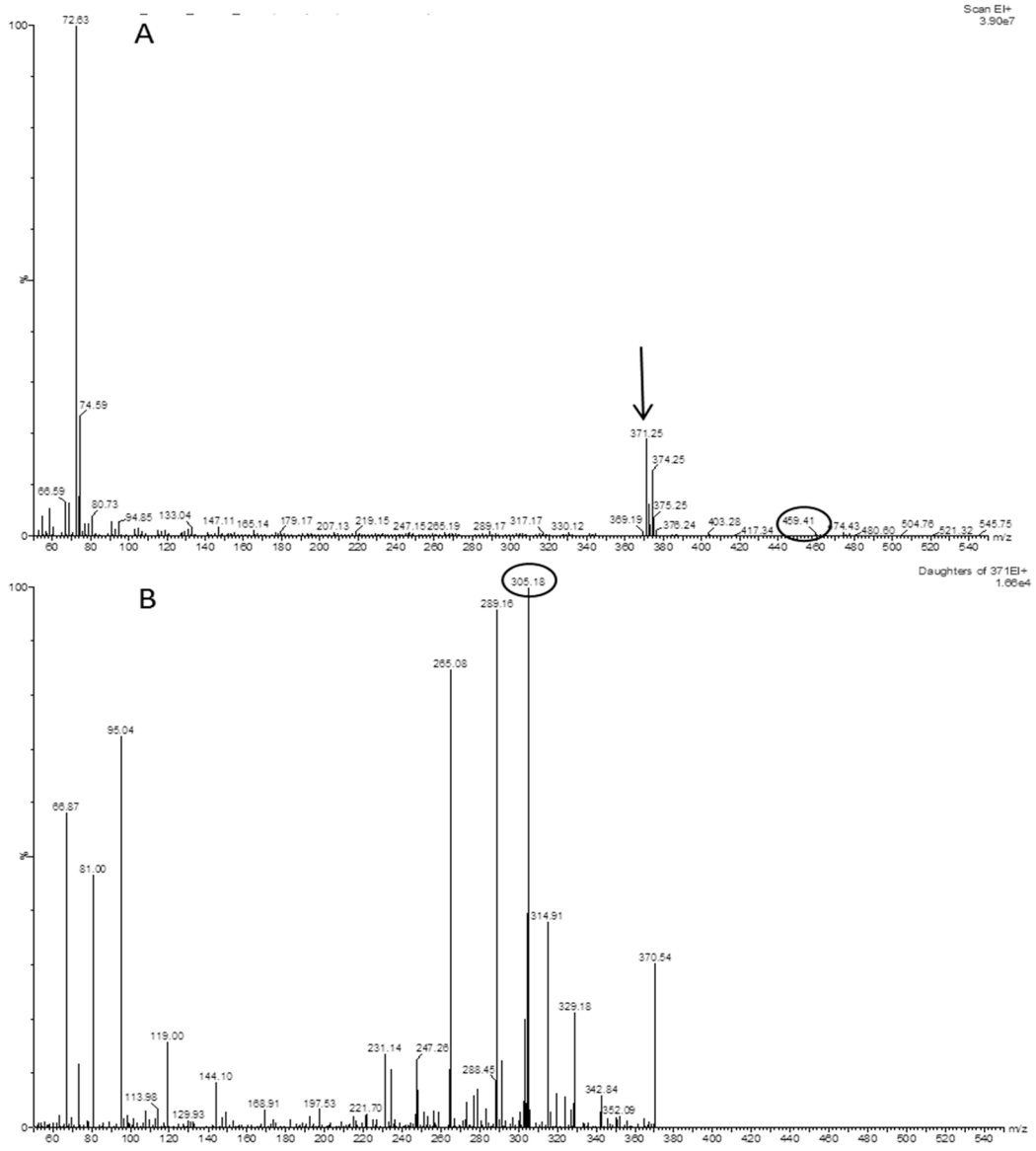

Figure 3-6. A) Full scan mass spectrum of 11-OH-THC, the $M^{+\cdot}$ ion *m/z* 459 is circled. The second most abundant peak *m/z* 371 is indicated with an arrow. B) product ion scan of *m/z* 371. The most abundant peak *m/z* 305 is circled.

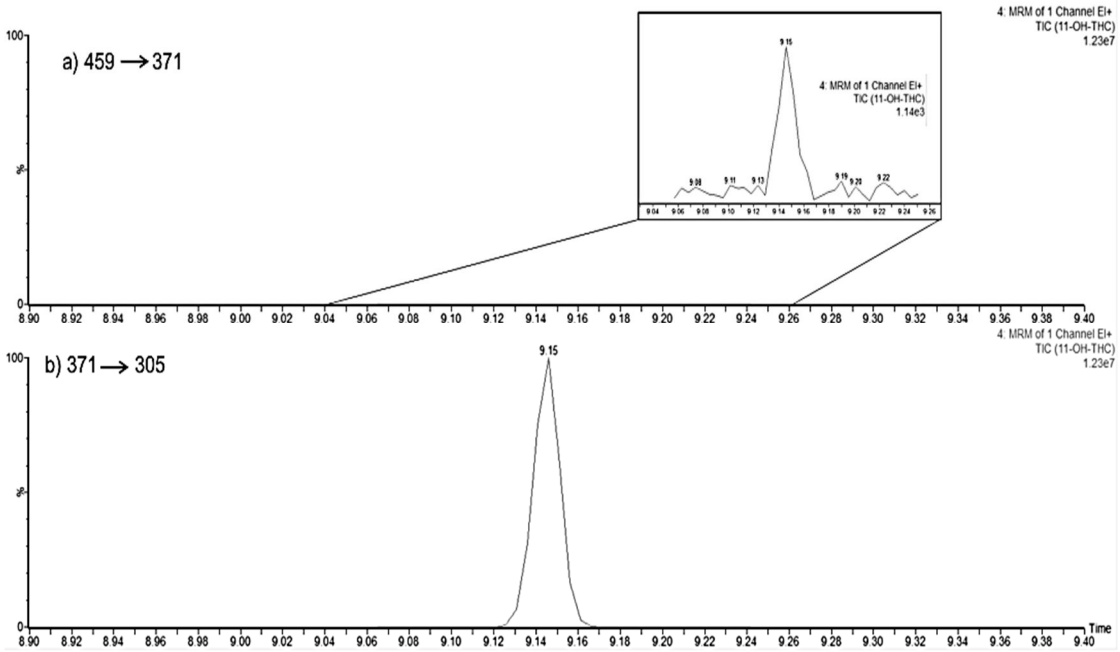

Figure 3-7. Comparison of 11-OH-THC chromatograms of SRM a) the original transition 459→371 and b) the optimised transition 371→305

The optimised precursor and production ions selected for SRM along with retention times for each analyte, including isotopically standards, using the GC temperatures as optimised in Section 3.3.1 can be found in Table 3-4.

Compound name	Precursor ion (*m/z*)	Product ion (*m/z*)	RT (min)
THC	386	371	8.17
CBD	390	301	7.57
CBN	387	310	8.54
11-OH-THC	371	304	9.15
THC-COOH	488	371	9.69
THC-d3	389	374	8.16
CBD-d3	393	304	7.55
CBN-d3	340	313	8.52
11-OH-THC-d3	374	308	9.13
THC-COOH-d3	491	374	9.67

Table 3-4. Precursor and product ions chosen for SRM and retention times for all analytes

3.3.3 GC-EI-MS/MS Calibration of spiked hair extracts

A matrix-matched calibration was constructed using hair samples from a self-reporting non-user. Samples (20 mg) were washed, digested, and extracted as described (Section 3.2). The extracts were then spiked with THC, CBD and CBN at 0.02, 0.05, 1, 2.5, 5, 7.5 and 10 ng/mg. In addition, samples were spiked with the metabolites 11-OH-THC and THC-COOH at 0.1, 0.2, 0.5, 1, 2, 5 and 10 pg/mg. Deuterated internal standards were added to each sample, one per analyte. THC-d3, CBD-d3, CBN-d3 were added at a concentration of 2.5 ng/mg per sample whilst 11-OH-THC-d3 and THC-COOH-d3 were added at 2 pg/mg.

The calibration ranges were based on reported concentrations of cannabinoids the hair of cannabis users (see Table 1-3) and also to be in line with cut-off concentrations recommended by the SoHT [145].

After spiking with analytes and deuterated standards, hair extracts were derivatised with BSTFA as described in Section 3.2.3.

Calibration curves were constructed for each analyte by plotting concentration against response ratio. The response ratio was calculated as the peak area of the analyte divided by the peak area of deuterated standard.

3.3.3.1 Results of GC-EI-MS/MS calibration of spiked hair extracts

The exact limit of detection for THC, CBD and CBN was not determined, as the lowest calibrant (0.02 ng/mg) had a signal to noise ratio greater than three. This is below the SoHT recommended cut-off of 0.05 ng/mg and so was deemed adequate for the application of hair testing. However, when calculated, the linear range (within 15%) did not include the lowest two calibrants. Whilst 11-OH-THC and THC-COOH were both

detected at the SoHT suggested limit of 0.2 pg/mg neither analyte gave a linear response at any three points in the calibration range (r^2=0.566 and 0.724 respectively).

Without the hair matrix 11-OH-THC gave a linear response between 0.16 and 10 pg/µL (r^2 0.998), THC-COOH gave a linear response between 0.31 and 10 pg/µL (r^2 0.996). It is likely that this is due a phenomenon known as the matrix effect.

Matrix effects and selectivity issues have long been associated with bioanalytical techniques. The matrix effect is a change in MS signal of an analyte due to co-eluting matrix [266]. The analyte signal can be enhanced or suppressed resulting in inaccurate performance characteristics of the method. Matrix effect is a parameter of concern during method development and/or validation as it can lead to over or underestimation of the analyte concentration.

It is suggested that the ion interface can also affect matrix effect as physiochemical processes of ion formation vary depending on the ionization technique [266]. However, a comparison of matrix effect with different ionisation modes has not been reported for the analysis of cannabinoids in hair samples.

Analyte	**Linear range (ng/mg)**	**Coefficient of correlation (r^2)**
THC	1-10	0.980
CBD	1-7.5	0.984
CBN	1-10	0.956

Table 3-5. Linear range and coefficient of correlation for THC, CBD and CBN in spiked hair samples

3.4 GC-APCI-MS/MS methods

3.4.1 Sample preparation

Sample preparation was as in Section 3.3.3. Hair samples (20 mg) of a self-reporting non-user were washed, digested and extracted before spiking with analytes and deuterated standards.

3.4.2 Instrumentation

Sample analysis was performed using a Xevo TQ-XS equipped with an atmospheric pressure ionization source coupled to a triple quadrupole mass spectrometer (Waters Corporation, Wilmslow, England), an Agilent 7890A gas chromatograph and 7693 autosampler (Agilent Technologies, Santa Clara, CA), and a Restek Rxi-5Sil (30m x 0.25mm x 0.25µm, Restek UK LTD Buckinghamshire, UK) column was used for the analysis. Samples were injected with a volume of 1 µL. The GC oven parameters were as follows: initial temperature of 150 °C increasing at 20 °C/min to a final temperature of 320 °C. The Xevo TQ-XS triple quadrupole mass spectrometer was operated under dry conditions to promote charge transfer ionisation. Nitrogen was supplied by an INMATEC PN6000 (Inmatec GaseTechnologie, Germany) nitrogen generator and was used as the auxiliary gas, maintained at a flow rate of 200 L/hr. Argon was used as the collision gas and maintained at 0.23 mL/min. Cone gas flow was initially set at 290 L/h. Corona voltage was set at 2.0 µA. The cone voltage was maintained at 10 V for all compounds with a source offset at 30 V. The APGC source was kept at 150°C.

3.4.3 GC-APCI-MS/MS analysis of analytes

The applicability of the "soft" ionisation method of the APCI source was tested using TMS derivatised cannabinoid standards. As an illustrative example, a comparison of the full mass spectrum of THC in EI and APCI ionisation modes can be seen in Figure 3-8. Unlike with EI, the molecular ion peak of THC (*m/z* 386) is the most abundant in the spectrum when APCI is utilised. This was also the case for all other analytes. A comparison of optimised SRM transitions for EI and APCI and their theoretical derivatised mass can be found in Table 3-6.

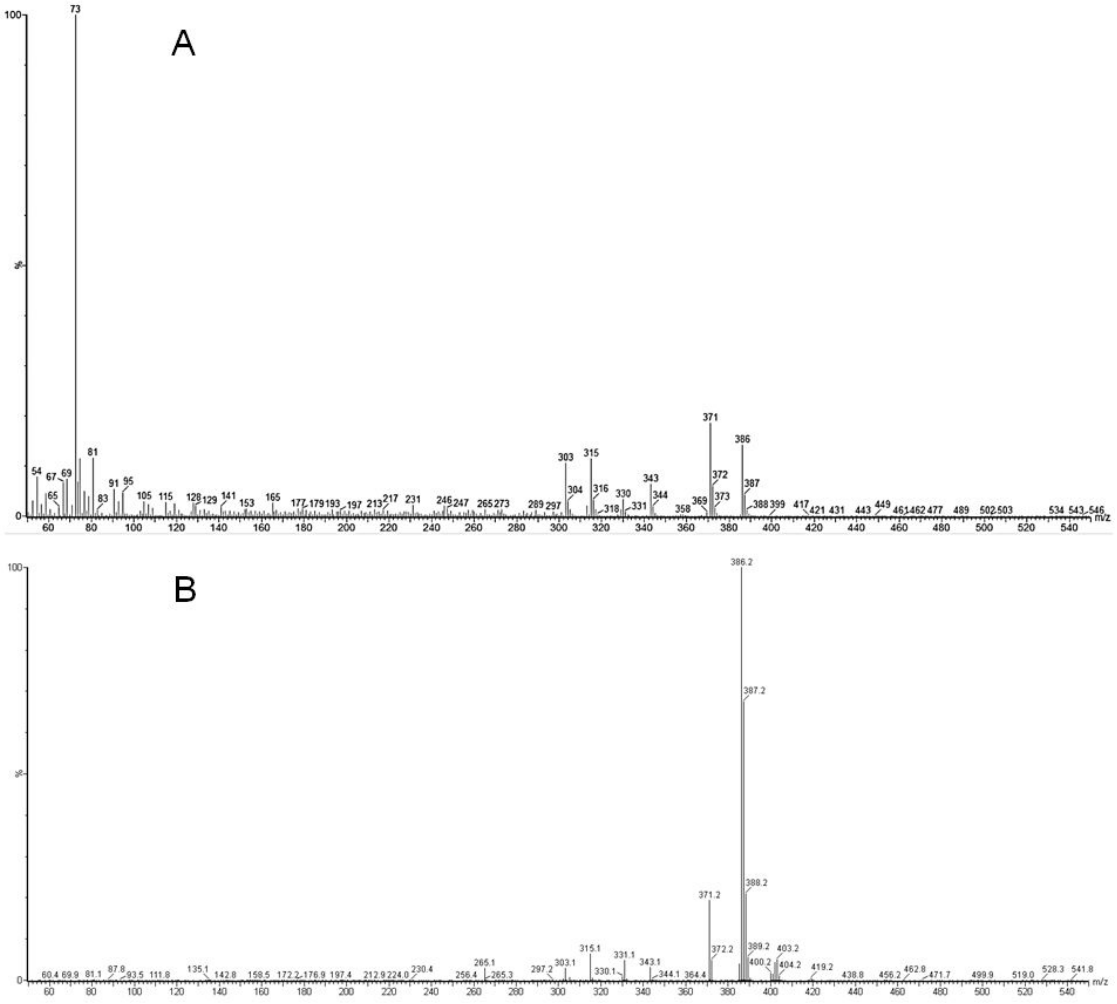

Figure 3-8. A) EI full scan spectrum of THC standard B) APCI full scan spectrum of THC standard

Cannabinoid	Theoretical Derivatised mass *(m/z)*	EI transition *(m/z)*	APCI transition *(m/z)*
THC	386.1	386.1 → 371.1	386.1 → 371.1
CBD	458.3	390.1 → 301.1	458.2 → 390.1
CBN	382.2	367.1 → 310.1	382.1 → 367.1
11-OH-THC	474.3	371.1 → 305.1	474.2 → 371.1
THC-COOH	488.2	488.2 → 371.1	488.2 → 371.1

Table 3-6. Theoretical *m/z* for each alanyte with optimised EI and APCI SRM transitions.

3.4.4 GC-APCI-MS/MS Cannabinoid Standard Calibrations

A calibration rage from 100 ag/µL to 50 pg/µL of all analytes was prepared to assess the LOD, LOQ and linear range of the APCI method. Deuterated standards of each analyte were added to each calibrant at a concentration of 1 pg/µL.

Calibration curves were constructed for each analyte by plotting concentration against response ratio. The response ratio was calculated as peak area of analyte/peak area of d3 standard.

As can be seen in Table 3-7, all analytes had a LOD ≤ 10 fg/µL, with THC and CBN having LODs of 1 fg/µL. All analytes also had a wide linear range across several orders of magnitude; the widest being 25-25000 fg/µL for CBD and the narrowest being 5-1000 fg/µL for THC-COOH and 11-OH-THC. An example of calibration points, standard deviation and % error for THC can be found in Table 3-8, all points being less than ±10%. Figure 3-9 is an example chromatogram of blank BSTFA (a), the derivatised THC standard at 1 fg/µL (b) and 1pg/µL (c).

Analyte	Limit of detection (fg/µL)	Linear range (fg/µL)	Coefficient of correlation
THC	1	25-10000	0.998
CBD	10	25-25000	0.997
CBN	1	25-1000	0.996
11-OH-THC	5	5-1000	0.999
THC-COOH	2.5	5-1000	0.998

Table 3-7. Limits of detection, linear range and coefficient of correlation for THC, CBD, CBN,11-OH-THC and THC-COOH

Analyte	Concentration fg/µL	SD	% Bias
THC	25	0.0006	6.3
	50	0.0006	1.2
	250	0.0029	2.8
	500	0.0076	8.2
	2500	0.0157	0.27
	5000	0.0686	0.13
	10000	0.3400	0.47

Table 3-8. Example of THC standard calibration (n=3)

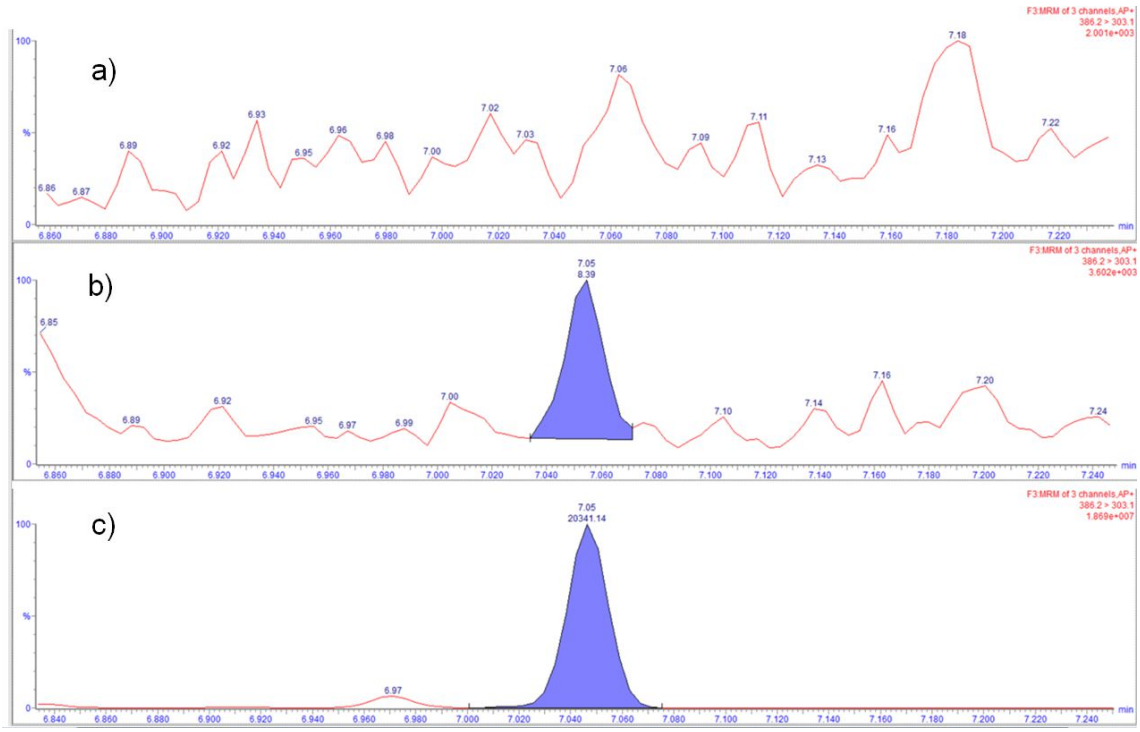

Figure 3-9. Chromatogram SRM transition 378.9→374.2 of a) BSTFA blank (ND) b) 1fg/µL (S:N 8.39), c) 10pg/µL (S:N 20341). Retention time and S/N shown above the peak on each Figure.

3.4.5 Spiked hair calibration with GC-APCI-MS/MS

Washed and dried hair extracts of a self-reporting non-user were spiked to prepare the following concentrations:

THC, CBD, CBN - 50, 100, 250, 500, 2500, 10000 fg/µL

11-OH-THC and THC-COOH - 5, 10, 25, 50, 250, 1000 fg/µL

All d3 analogues were added at a concentration of 1000 fg /µL

3.4.5.1 Results of spiked hair calibration with GC-APCI-MS/MS

In contrast to the standard calibrations in section 3.5.2, the deuterated analogues of the cannabinoids in a matrix-matched calibration did not give a consistent response at 1 pg/µL, sometimes being undetectable. The THC d3 analogue was not detectable in any of the samples, making quantitation unreliable.

One approach proposed to minimise matrix effects is to dilute the final extract to be injected onto the analytical column. In some instances this method has been reported to be effective for reducing signal suppression, while achieving acceptable sensitivity during electrospray ionisation of wastewater [267,268].

In this study diluting the sample from 20 µL to 100 µL improved the signal to noise of all analytes, as can be seen in Table 3-8. However, the values were still much lower than the standards without the hair matrix. As an illustrative example, chromatograms of the d3 analogue without hair matrix (A) in 20mg of hair (B) and diluted 1 in 5 (C) are shown in Figure 3-10.

The hair matrix also affected the retention time of analytes, the most affected being CBD with a shift of 0.06 minutes and the least affected being THC-COOH with a shift of 0.01 minutes.

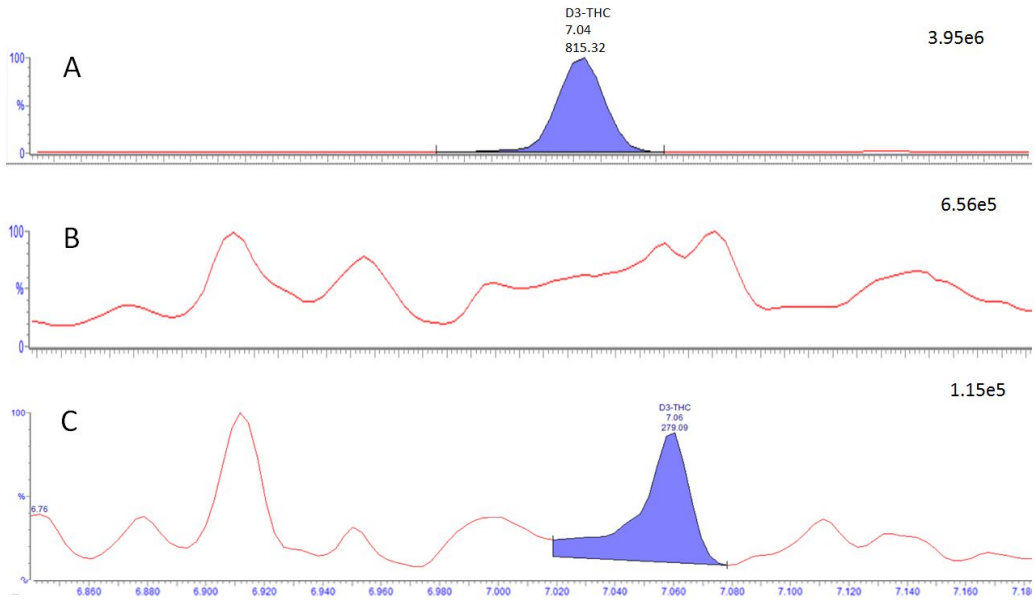

Figure 3-10. A) 1pg/µL THC-d3 standard. B) 20 mg hair extract spiked with 1pg/µL THC-d3 standard. C) sample B diluted 1 in 5. Retention times and signal to noise is shown above each peak.

Analyte	Without hair	Spiked hair sample	Spiked hair sample after 1 in 5 dilution
THC-d3	815	ND	279
CBD-d3	560	13	45
CBN-d3	1440	19	228
11-OH-THC-d3	6869	81	467
THC-COOH-d3	4188	42	127

Table 3-9. Signal to noise ratio (1 pg/µL) cannabinoids without hair, in 20mg hair extract, and after 1 in 5 dilution.

Due to these findings a new six-point calibration was made by spiking 20 mg hair extracts from a self-reporting non-user to the following:

THC, CBD, CBN - 50, 100, 250, 500, 2500, 10000 fg/µL

THC-COOH and 11-OH-THC 25, 50, 100, 500, 5000, 25000 fg/µL

All d3 analogues were added at a concentration of 10000 fg/µL

The final volume of all samples was 100µL. The conversion from fg/µL to pg/mg was calculated using the equations below:

$$Concentration\ (fg/mg) = \frac{Concentration\ (fg/\mu L) \times sample\ volume\ (\mu L)}{mass\ of\ hair\ sample\ (mg)}$$

$$Concentration\ (pg/mg) = \frac{Concentration\ (fg/mg)}{1000}$$

CBD no longer gave a linear response when in the matrix-matched calibration. This suggests that CBD suffers from matrix-related irreproducibility. In addition, repeat injections of the same CBD calibrant gave a high standard deviation. All other analytes (THC, CBN, THC-COOH and 11-OH-THC) gave a linear response as shown in Table 3-10. THC had a limit of detection of 0.5 pg/mg which is lower than the SoHT cut-off of 50 pg/mg. The upper limit of quantification in this method is 50 pg/mg and so user samples may need diluting into the linear range, as THC concentrations in the order of ng/mg have been reported previously (see Table 1-3).

The exact limit of detection for CBD, CBN was not determined, as the lowest calibrant (0.25 pg/mg) had a signal to noise ratio greater than 3. This is well below previously reported limits of detection (see Table 1-3). Similarly, the lowest calibrant (0.125 pg/mg) for metabolites THC-COOH and 11-OH-THC also had a signal to noise ratio greater than 3. This is higher than some previously reported limits of detection but was deemed acceptable as is lower than the SoHT cut-off of 0.2 pg/mg.

As shown in Table 3-10, the analytes CBN and 11-OH-THC were linear across the whole calibration range however, THC and THC-COOH were only linear within the highest 3

calibrants. An example of standard deviation and % error for a THC calibration curve is given in Table 3-11.

Analyte	Linear range (pg/mg)	Coefficient of correlation (r^2)
THC	2.5 -50	0.999
CBD	N/A	0.869
CBN	0.25-50	0.999
11-OH-THC	0.125-125	0.998
THC-COOH	2.5-125	0.992

Table 3-10. Linear ranges and coefficient of correlation of THC, CBD, CBN, 11-OH-THC and THC-COOH in spiked hair samples

Concentration (pg/mg)	SD	% Bias
2.5	0.002	5.9
12.5	0.005	0.26
50	0.016	1.17

Table 3-11. Example of calibration for THC in spiked hair sample (n=3)

3.4.6 Further work

3.4.6.1.1 Investigation and reduction of matrix effect

One area for future investigation is the occurrence of matrix effects and whether these vary substantially between different hair donors. The closeness of a match between the matrix to be used for calibration and the samples to be investigated is of great importance in achieving reliable and accurate results [266]. Matuszewski *et al.* demonstrated a high variability of matrix effect among different lots of plasma and

highlighted the need to investigate the relative matrix effect which can reveal differences in response among various lots of the same matrix [269]. It is reasonable to assume that hair, which is a complex matrix, may also result in variability of matrix effects between different hair types (ethnic groups, colour, damage, heat and chemical treatment) and should be thoroughly investigated before this technique is incorporated into casework.

Another strategy to reduce matrix effects is to ensure that the maximum amount of analyte is extracted from the digest with minimal matrix. This may be achieved by using a more specific extraction method such as molecularly imprinted solid phase extraction (MISPE). A method for the extraction of THC, CBD, CBN and THC-COOH from oral fluid and urine using MIPSE has recently been reported by Cela-Perez *et al*. [270]. In addition, Gonzalez *et al.* have also recently utilised MIPSE to extract THC,CBD,CBN, THC-COOH and 11-OH-THC from plasma and urine [271]. The use of MIPs as SPE sorbent allows a rapid, simple, and effective and selective extraction compared to traditional SPE since they are materials prepared in the presence of a target analyte or closely related species that serves as a mold for the formation of complementary binding sites. Both studies reported increased sensitivity when using MISPE.

Matrix effects may also be reduced by utilising two-dimensional (GCxGC) gas chromatography. Comprehensive GC×GC allows the whole chromatogram to be transferred onto a secondary column. It has been recognised as a technique capable of providing improved resolution of complex matrices compared to conventional single dimensional GC (1D-GC) [272]. This was demonstrated for a variety of drugs (including CBN) in hair samples in a study conducted by Guthery *et al.* In the study, endogenous

compounds, long chain fatty acids, and amides were detected with much greater signal intensities than the drug and metabolite compounds. However, drug compounds were clearly resolved from the interfering matrix compounds when compared to 1D-GC [263].

Prior to introduction into a toxicology workstream there are several steps that need to be taken for the method to be fully validated. These include the determination of inter-day and intra-day accuracy and precision and the use of using quality control (QC) samples. A full review of the steps needed for method validation has been conducted by Peters *et al.*[273].

3.4.7 Discussion and conclusions

The use of APCI has been evaluated as an alternative source for GC-MS/MS analysis of cannabinoids in hair samples. In contrast to EI ionisation, molecular ions were the most abundant in the mass spectrum. The molecular ions are highly favourable as a precursor ion in MS-MS and in this study improved sensitivity compared to GC-EI-MS/MS. Instrumental LODs of between 1 and 10 fg/µL were achieved for all analytes. The response was repeatable and linear (<15% error) over several orders of magnitude.

The hair matrix was found to affect detection for all analytes, causing suppression of signals and a retention time shift. Signal suppression of up to a factor of 85 was observed in certain cases. After dilution, LODs of 0.125 pg/mg could be achieved in matrix-matched samples for some analytes. All analytes were detected at concentrations well below SoHT requirements (50 pg/mg and 0.2 pg/mg for THC and THC-COOH, respectively) and therefore this study demonstrates the advantages and

applicability of APCI as new source for GC-MS/MS detection of cannabinoids in hair sampels. The main limitation of the technique was the fact that CBD could not be quantified due to matrix-related irreproducibility. Reducing matrix effects should therefore be a priority in future investigations.

Chapter 4. Application of atmospheric pressure chemical ionisation gas chromatography mass spectrometry to detect cannabinoids in hair samples

4.1 Introduction

In this section the GC-APCI-MS/MS method developed in Chapter 3 will be applied to participant-derived hair samples. These samples were collected in the context of a study into the age of onset of cannabis use and executive function. The researcher sought to use hair samples to confirm participant answers from lifestyle questionnaires on recent cannabis use.

Recent studies to detect cannabis use in hair samples exclusively analyse THC, CBD, CBN or the metabolite THC-COOH, possibly limiting the amount of information gained before the difficult process of interpretation of analytical findings can begin.

Due to difficulties in simultaneous detection of THC and metabolites several studies have solely analysed THC-COOH [122–125] and so the presence of THC in addition to THC-COOH has not been considered in interpretation of analytical findings.

In this study all the previously detected analytes and an additional THC metabolite (11-OH-THC) are simultaneously analysed and reported for the first time in real user hairs.

There is currently no consensus in the scientific community about what constitutes a positive result for the detection of cannabis use. Therefore, this study will include an evaluation into the different strategies proposed in literature:

- Detection of metabolites
- The use of cut-offs
- Wash residue analysis

4.2 Methods and Materials

Methods for decontamination of hair, extraction of analytes and derivatisation prior to analysis were performed as previously described in chapter 3. The instrumentation was also used as described in Chapter 3. Additional methods and materials unique to this chapter can be found below.

4.2.1 Hair Samples

Hair samples were obtained from individuals in the context of a study into the age of onset of cannabis use and executive function. The hair sample collection was approved by the Sheffield Hallam University Research Ethics committee (SHU ethics number 13-2011). Written and informed consent was obtained from all participants. All results were anonymised.

Some participants had self-reported cannabis use, some had not and were included in the studies' control group. In the interest of preventing bias, self-report data was not available until after GC-APCI-MS/MS analysis.

Hair was stored at room temperature in foil to prevent UV damage for approximately 5 years before analysis. 10-20 mg of hair was analysed, due to a lack of samples weighing 20 mg or more.

Of the 70 samples submitted for analysis, 63% (44) were excluded as sample weighed less than 10 mg which is presumed to be insufficient for analysis [274].

Based on self-report data, samples were divided into three categories for interpretation. Non-user, infrequent user (fewer than 10 lifetime cannabis cigarettes) and frequent users (greater than 10 lifetime cannabis cigarettes, with a mean of 1000).

4.2.2 Preparation of wash residue

The wash residues obtained from the decontamination procedure as described in Section 1.3.8.3 were transferred into a new vial and dried under nitrogen at 45°C before derivatisation with BSTFA as described in Section 4.2.4 prior to analysis.

4.3 Results of hair analysis and concordance with self-report data

Of the 70 participants originally recruited, 26 had hair samples above 10 mg and were included in the analysis. Over one third (43%) of the samples (n=11) were non-users of cannabis, 38% (n=10) were infrequent users and 19 (n=5) were frequent users. Full details of the concentrations of THC, CBD, CBN, 11-OH-THC and THC-COOH in each usage grouping can be found in Appendix I.

The results of the GC-APCI-MS/MS analysis are summarised in Table 4-1. Concentrations of THC and CBN were substantially lower than had been reported previously (in the pg/mg rather than ng/mg range as shown in Table 1-2). The concentration of THC-COOH was also lower than previously reported, with none of the detected concentrations being above 0.5 pg/mg.

It is not possible to compare 11-OH-THC concentration with literature values since this compound is rarely reported in literature. Moreover, where 11-OH-THC has previously been detected in hair samples, the limit of detection was 1 pg/mg of hair [155] which is greater than the concentrations detected in this study. In other studies, the limit of detection was not reported [156].

Analyte	Detected samples	Samples below LLOQ	Concentration ranges (pg/mg hair)	Mean Concentration (pg/mg hair)
THC	18	9	1.28-31.40	9.20
CBN	23	1	1.30-18.19	3.56
11-OH-THC	3	0	0.21-0.32	0.27
THC-COOH	5	0	0.16-0.42	0.32

Table 4-1. Concentration ranges and mean concentrations of THC, CBD, CBN, 11-OH-THC and THC-COOH detected in participant hair samples analysed with GC-APCI-MS/MS.

Out of a total of 26 samples, only three did not have any of the analytes detected. Of these, two were from self-reported non-cannabis users and one was from a self-reported frequent user (an average of 2 joints a day); CBD, CBN and THC-COOH was detected in the wash residue of this sample.

Conversely, only one sample had all analytes detected. This individual had self-reported to use an average of one joint a day and had reported 2-3 days between last use.

In 10 samples THC was detected, however metabolites were not, suggesting external contamination or infrequent usage of cannabis. Of these 30% fell into the frequent cannabis user category, 40% in the infrequent user category and 30% in the non-user category. This suggests that THC detection alone is not a reliable usage discriminator.

No samples had metabolites detected without also having THC detected. However, in three out of the seven samples in this group THC was only detected in trace amounts (below the LOQ). This poses an interesting interpretational dilemma, if the metabolites are only generated *in-vivo* should the detection of these metabolites indicate usage,

even if the parent compound is detected only at trace levels? It is worth noting that two out of three of these samples were from self-report non-users.

CBD was detected in six samples, due to non-linearity of response with hair samples (see Section 3.4.5) quantitation of CBD was not possible. In all cases where CBD was detected, CBN and THC were also detected. Four of these samples were from self-declaring frequent users, however two of these samples were from self-reporting non-users of cannabis.

The metabolite 11-OH-THC was detected in three samples. All samples in this category came from declared cannabis users. In only one of the three samples where the metabolite 11-OH-THC was detected, THC-COOH was also. This would result in a false negative by interpretational methods which only use the results of THC-COOH analysis.

CBN was detected in all but three samples. Whilst CBN is known to be a degradation product of THC in resin [228,229] and plant material [230] it was surprising to detect CBN on 82% of hair samples provided by individuals who self-report never to have used cannabis.

Carryover of CBN was excluded due to the lack of signal in blank samples which were put into the run after every four participant samples. In addition, 12% of samples (n=3) did not have CBN detected, which suggests that the reagents used were not the cause of the signal. Chromatographic separation with additional MS-MS data is thought to be gold standard in compound identification and so further investigations whether the source of CBN is a commonly encountered interference or exposed hairs should be conducted.

There is a lack of research articles on the degradation of THC in hair samples. Skopp *et al.* conducted a study where hair samples were exposed to sunlight for 10 weeks. Contrasting to studies in plant and resin material, the authors found that concentrations of THC, CBD and CBN decreased over the course of the study and hypothesised that CBN was further degraded to other compounds.

There are no studies on the stability of cannabinoids in hair samples stored for 5 years or stored in darkness. In the absence of this literature, it may be reasonable to assume that:

a) the original concentrations of THC in the hair samples decrease over time

b) THC degrades to other products in addition to CBN, therefore the THC and CBN concentration in degraded material will not equal the original THC concentration of the fresh sample

In addition to CBN being a degradation product of THC, several other studies of have reported a higher concentrations of CBN than THC or CBD [108,113,242], possibly due to hair being exposed to sunlight before sample collection.

In two studies which had control groups CBN was not detected, however limits of detection were much higher than the GC-APCI-MS/MS (LODS of 0.025 ng/mg [117] and 0.15 ng/mg [108] compared to 0.00025ng/mg with GC-APCI-MS/MS).

4.4 Discussion of published reporting criteria

4.4.1 Recommended cut-offs. What is their value?

Cut-off levels are essential in any toxicological analysis. The cut-off is the point at which a result is either reported to be positive or negative. This value should optimise drug detection but minimise the number of false positives. It is important to note that a sample which is reported to be negative does not have to be drug-free but it may have the drug detected at a concentration below the defined cut-off.

The society of hair testing recommend a THC-COOH cut off of 0.2 pg/mg [145], the FDA recommends a cut off of 0.1 pg/mg [275] whilst SAMSHA recommend a cut off of 0.05 pg/mg for the detection of THC-COOH [276].

The SoHT also recommend cut off of 50 pg/mg for THC. There are no reported guidelines for CBN, CBD or 11-OH-THC but since CBN and CBD are also found in plant materials and cannabis smoke it is reasonable to assume the cut-off for these analytes would be 50 pg/mg. Similarly, there are no guidelines for the cut-off value of 11-OH-THC. It is assumed the cut off would be 0.2 pg/mg of hair as with the metabolite THC-COOH.

In this study four samples had a THC-COOH concentration greater than 0.2 pg/mg of hair; two of these samples belonged to regular users and two belonged to self-reporting non-users.

Two additional samples had a concentration of 11-OH-THC greater than the assumed 0.2 pg/mg of hair cut off, both samples belonged to self-reporting regular cannabis users.

No samples in this study had a THC, CBD or CBN concentration greater than the recommended cut off for THC, possibly due to the age of the hair samples.

In the case of hair samples, the origin of recommended cut-offs is questionable. The SoHT guidelines state that the cuts offs are:

"Based on previous guidelines and the available literature on drug concentrations in hair from drug users"- Cooper, G.A., Kronstrand, R. and Kintz, P., 2012. Society of Hair Testing guidelines for drug testing in hair. *Forensic Science International*, *218*(1-3), pp.20-24.

It is important to note that these guidelines were published in 2012 and have not been updated since. It is unclear exactly which literature the guidelines were based on, however given the available literature at the time it can be assumed that there was a relatively small number of studies, each with differing wash, extraction, derivatisation, and analytical techniques. Moreover, studies are often based on results of individuals who are suspected to be drug users, and so are not necessarily reflective of the general population. It also appears that the cut-offs are heavily influenced by the sensitivity of instrumental methods at the time of writing, rather than based on scientific evidence as can be seen from the following quote:

"The higher sensitivity of the instrument method enables us to lower the cut off of THC from 0.1 to 0.05 ng" - Nadulski, T. and Pragst, F., 2007. Simple and sensitive determination of Δ9-tetrahydrocannabinol, cannabidiol and cannabinol in hair by combined silylation, headspace solid phase microextraction and gas chromatography–mass spectrometry. *Journal of Chromatography B*, *846*(1-2), pp.78-85.

Since the GC-APCI-MS/MS method reported in this study allows detection of cannabinoids at concentrations much lower than the recommended cut-offs it begs the question, should the recommended cut-offs be amended? Is it possible for an instrument to be too sensitive when it comes to analysing cannabinoids in hair, given the compounds low incorporation rate [45]? It also asks the question what does it

mean to detect such a low level of cannabinoids (usage, association with, or the amount that can be expected in the general population)?

4.4.2 Wash residue analysis

Tsanaclis and Wicks proposed using the wash residue obtained from the decontamination procedure as a strategy to differentiate between external contamination and usage of cannabis when metabolites are not detected [162]. In the study, the concentration of THC in the wash residue was compared to the concentration of THC in the hair after the completion of washing procedures. It was claimed that wash ratios of zero (i.e. no drug found in the wash procedure) suggested drug use was likely, while ratios greater than 0.1 and less than 0.5 indicated drug use was 'possible' and ratios greater than 0.5 meant that drug use was 'questionable' (Table 4-2).

W/H ratio	Drug use	External contamination	Interpretation
0 and <0.1	Likely	Less likely	Used drug
>0.1 and <0.5	Possible	Was wash effective?	Might have used drug; Indicates association with drug
>0.5	Questionable	Was wash effective?	Not sure of drug use; indicates association with drug

Table 4-2. Guidelines for the interpretation of results of the analysis of hair samples and wash residues based on the authors' laboratory results in cases when parent drug is present and the relevant metabolite is not Taken from Tsanaclis and Wicks [162]**.**

The method as proposed by Tsanaclis and Wicks was used to analyse samples in this study and findings are reported below:

4.4.2.1 THC wash residue analysis

Of the eligible samples (n=4) where THC was quantifiable in both wash and hair, three samples had a wash to hair ratio greater that 0.5 therefore have "questionable" drug

use and so the interpretation should be "Not sure of drug use; indicates association with drugs". All the samples in this category were from frequent cannabis users.

One sample had a wash to hair ratio of 0.26 which puts the sample in the "possible" drug use category. The interpretation should be "might have used drug; indicates association with drug". This sample was the only sample to have all 5 analytes detected and was from a frequent cannabis user.

4.4.2.2 CBN Wash residue analysis

Whilst the method in the Tsanaclis and Wicks study was only applied to THC concentrations, in this study the method is also applied to CBN. Since the samples were stored a long time prior to analysis it is possible that THC present in the hair at the time of collection has degraded to CBN (see Section 4.3.2).

CBN was detected in the wash and hair of 23 of the 26 samples. The majority (16) had a hair to wash ratio greater than 0.5 and so were in the "questionable; not sure of drug use" category. These samples belonged to participants in all three groupings of usage. Four samples had a ratio between 0.1 and 0.5 and so were in the "possible" drug use category, both samples were from frequent users.

Three samples had a CBN wash to hair ratio <0.1 and so are in the "drug use likely" category. Two out of three of these samples were from non-users and one was from an infrequent user, suggesting the wash ratio of CBN for aged samples is not an accurate indicator of usage.

4.4.2.3 Metabolite wash residue analysis

Whist THC-COOH was detected in some hair samples, 11-OH-THC was detected in more wash samples, as shown in Figure 4-1. 11-OH-THC was detected in both the wash

residue and hair of some samples whereas THC-COOH was exclusively detected in the hair *or* the wash residue.

Two cannabis users had metabolites present in the wash residue, but not in the corresponding hair sample. On the other hand, three non-users had metabolites in wash residue. Therefore, assuming self-report is correct, wash residue analysis of metabolites is not an accurate indicator of usage.

In this study there was a greater concentration of metabolites found in wash residues than in hair samples as shown in Figure 4-2. Since metabolites are not produced in the cannabis smoke it could be suggested that the detection of metabolites in wash residue is also indicative of cannabis usage, however further investigations with a larger sample size is needed to test this hypothesis.

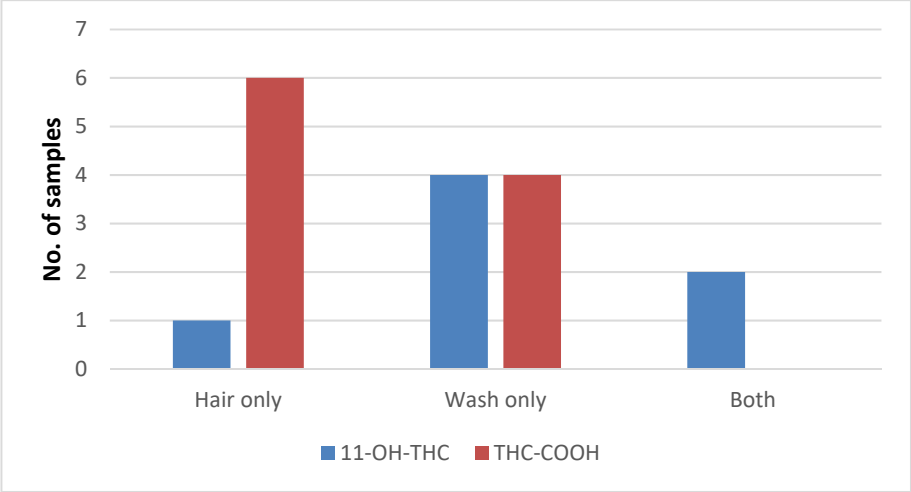

Figure 4-1. Number of samples where THC-COOH and 11-OH-THC are detected in the wash residue, hair sample, and in both hair and wash.

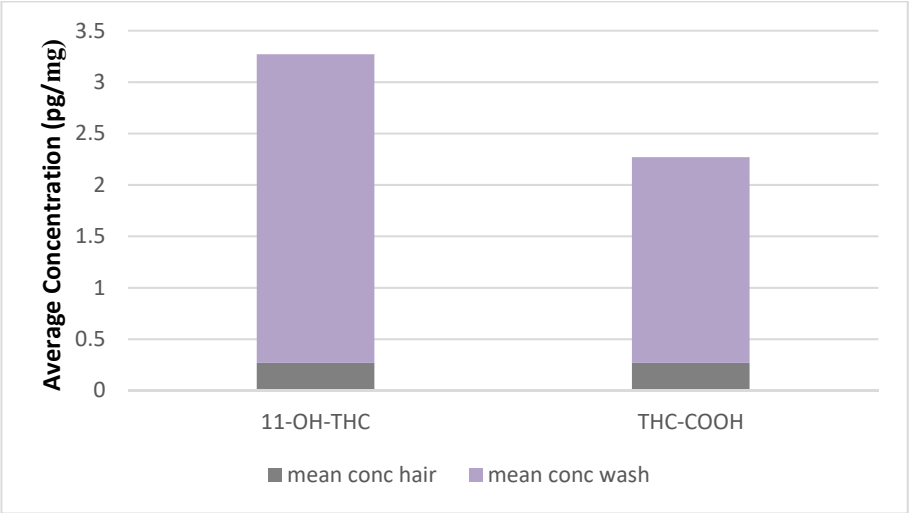

Figure 4-2. Mean concentrations detected of (left) 11-OH-THC in har samples (n=3) and washes (n=6) and (right) THC-COOH hair (n=6) and washes (n=4)

4.5 Determination of positive samples

There are many different methods of interpretation which can make assigning a hair sample as positive or negative for cannabis use problematic. These methods include the detection of metabolites, the use of cut-offs, and the analysis of wash residue. In this study each method of interpretation has been applied to the participants of the psychology study and compared with the self-report data using methods described above. A summary of the evaluations can be seen in Table 4-3.

Of note is detection of metabolites in relation to the number of "positive" samples. Whilst the detection of any metabolite in hair or wash residue yields 12 positive samples, only one of these samples remains positive if both THC-COOH and 11-OH-THC are both detected in the hair sample. This sample belongs to a frequent cannabis user.

On the other hand, five non-users would be reported as having a positive sample if either metabolite was detected in wash or hair, however none of these samples would

remain positive criteria was that both THC-COOH and 11-OH-THC had to be detected in the hair sample.

There is also a discrepancy between the number of positive samples depending on which metabolite cut off is applied. Given the potentially life changing consequences for a positive sample, a consensus based on scientific investigation should be reached.

The THC hair/wash residue analysis technique did not identify any participants and being likely to use drugs. This may in part be due to the time elapsed between sample collection and analysis (5 years).

Interpretation method	Total No. of positive samples	Total No. of positive (frequent users)	Total No. of positive (infrequent users)	Total No. of positive (non-users)
Any Cannabinoid or metabolite detected	23	9	5	9
Any metabolite detected hair or wash	12	6	1	5
Any metabolite detected in hair	7	5	0	2
THC-COOH only detected hair	4	2	0	2
11-OH-THC only detected hair	2	2	0	0
THC-COOH and 11-OH-THC detected in hair	1	1	0	0
Metabolites above SoHT cut-off	6	4	0	2
Metabolites above FDA cut-off	7	5	0	2
Metabolites above SAMHSA cut off	7	5	0	2
THC, CBD and CBN detected in hair	6	4	0	2
THC, CBD, CBN above SoHT cut-off	0	0	0	0
THC Wash ratio >0.1 and <0.5 (possible dug use)	1	1	0	0
THC Wash ratio 0 and <0.1 (likely drug use)	0	0	0	0

Table 4-3. Comparison of self-report data with different methods of interpretation for frequent cannabis users (n=10), infrequent users (n=5) non-users (n=11)

4.5.1 Further work

One area for further research is to investigate whether certain wash protocols remove metabolites from hair, rather than just removing externally bound smoke contamination. As yet there are no specific guidelines on wash protocols for the detection of cannabis use in hair, and the few studies that have been conducted in this area have exclusively investigated THC and not metabolites.

Given the lack of current literature, another avenue for future investigation is to study whether cannabinoids in hair samples are in fact stable, and if so, for how long.

Finally, an additional biomarker of cannabis use (such as urine testing) would be useful in this type of investigation to confirm or refute self-report data as it is known that it can be unreliable.

4.5.2 Conclusions

The GC-APCI-MS/MS method previously optimised in Chapter 3 was successfully applied to authentic user hair samples for the first time. No single analysis method could identify all 10 self-declared users. According to self-report data, 11-OH-THC was the only indicator of cannabis use without also incurring false positives, on the other hand there were many false negatives using this interpretation method (n=7). THC-COOH was detected in 18% (n=2) of the self-reporting non-cannabis users.

Evaluation of the reporting criteria for cannabinoids in hair samples showed that a different number of samples would be considered to be positive for cannabis use depending on which interpretation method was used.

Chapter 5. Overall Conclusions

5.1 Background to investigations

Hair differs from other human materials used for toxicological analysis such as blood or urine because of its substantially longer detection window (months to years) enabling retrospective investigations of drug consumption. Due to its solid and durable nature, hair analysis can be performed even centuries after growth. Other advantages of hair analysis include the non-invasive nature of collection, which is of particular importance in infant/child investigations, and also the ease of sample storage.

Although hair analysis offers the potential to reveal information which is not possible with other biological matrices, it also suffers from some unique limitations that can make interpretation of findings challenging. These are largely due to exposure of hair to the environment before analysis takes place.

Existing analytical techniques allow detection and quantification of cannabinoids in hair samples. These techniques include GC-MS/MS and LC-MS/MS. Recent studies exclusively analyse THC, CBD, CBN or the metabolite THC-COOH, limiting the amount of information gained before the difficult process of interpretation of analytical findings.

Recently, MALDI-MS analysis of hair samples has been suggested as an alternative technique to traditional methods such as GC-MS. This is due to reduced sample preparation, the ability to detect a narrower time frame of drug use and a reduction in sample amount required for analysis. In addition, MALDI-MS offers the unique opportunity of being able to analyse a longitudinally sliced hair to detect xenobiotics inside the hair itself, possibly eliminating the interpretational issues associated with exposure to the environment.

However, despite cannabis being the most commonly used illicit drug worldwide, a MALDI-MS method for the detection of cannabinoids in a single hair had not been reported. At the commencement of this research MALDI-MS had only been applied to the analysis of cocaine, methamphetamine, ketamine and nicotine in relation to hair testing. These compounds are both more readily incorporated into hair [45] and more easily ionisable using MALDI than cannabinoids [277]; posing a difficult challenge in the development of a technique to detect cannabinoids using MALDI-MS.

5.2 MALDI-MS and MALDI-MSI method optimisation

5.2.1 CHCA was the optimal matrix for the detection of THC

An in depth literature review revealed that MALDI matrix is the "key to success" [175], however finding the right matrix for analytes is unfortunately a trial and error process [195]. During this study the matrix selection and the use of additives were investigated to develop a suitable method for detection of cannabinoids in hair samples using MALDI-MS. It was found that CHCA with the additive aniline gave the highest signal intensities for THC, however ionisation efficiencies for underivatised cannabinoids were poor, as also described by Groeneveld *et al.* [197]. This led to an investigation into *in situ* derivatisation.

5.2.2 THC underwent a laser induced in-source re-arrangement

THC underwent an in-source re-arrangement producing another species which was detected at approximately the same intensity as the analyte. This would theoretically

have the effect of impairing detection. To investigate this phenomenon further, LC-MS/MS analysis of the THC standard was performed. A single peak in the chromatogram confirmed the purity of the THC standard and MS/MS analysis support the hypothesis that the THC molecule loses two hydrogens as free radicals during an in-source re-arrangement as a result of the energy from the laser source. To further investigate the influence of the laser on the molecule an experiment was carried out with increasing laser power. As the laser power increased the ratio of *m/z* 313 (corresponding to the re-arranged THC molecule) to 315 (corresponding to THC) signal intensity increased.

5.2.3 Derivatisation of THC improved signal intensity

Derivatisation had been identified as a possible strategy to improve signal strength and decrease matrix interference [142]. Despite the derivatisation of cannabinoids being commonplace for GC-MS analysis, a review of the literature revealed that this approached had not been tried for MALDI-MS.

The target for the derivatization was the hydroxyl group since all cannabinoids of interest contain this functional group. After carefully reviewing the literature, derivatization using 2-Fluoro-1-Methylpyridinium p-tolunesulfonate (FMPTS) to form N-methylpyridinium derivatives was chosen. Derivatisation was successful and improved signal intensities of peaks corresponding to the analytes. CBD has two hydroxyl groups whereas THC has only one, so the detection of a peak at *m/z* 483.32 (related to CBD with the addition of two derivatisation groups) in the CBD spectrum

allowed for differentiation between THC and CBD, which would not be possible without derivatisation.

5.2.4 Spaying of derivatisation reagent allowed *in situ* derivatisation and MALDI-MS-imaging

During initial MALDI-MSI experiments the THC compound had been delocalised from the hair and into the surrounding matrix. It was hypothesised that the delocalisation of the analyte could be due to too large a volume of derivatisation reagent being spotted on top of the hair sample. To test this hypothesis a hand sprayer was used to supply a fine mist of the derivatisation reagent before spraying the sample with CHCA matrix using an automated sprayer. Following this method of derivatisation, delocalisation of the analyte did not occur. Hairs spiked with THC, CBD, CBN, 11-OH-THC, THC-COOH and THC-COO-gluc were successfully derivatised and imaged for the first time.

5.2.4.1 THC can be detected on single hairs exposed to cannabis smoke using MALDI-MSP and MALDI-MSI

In both MALDI-MSP and MALDI-MSI experiments, *m/z* 406 corresponding to THC was observed on hair exposed to cannabis smoke. No *m/z* 406 was detected on blank unexposed hair. Whilst these are preliminary findings in unrealistic smoking conditions, the result suggests that MALDI could be used to investigate how exposure to cannabis smoke affects the levels of cannabinoids found in hair samples. In particular, analysing longitudinal slices of hair exposed to cannabis smoke could give

insight into whether or cannabinoids penetrate the hair cortex, and which decontamination procedures are most effective.

5.2.5 MALDI-MS and MALDI-MSI Further work

5.2.5.1 Matrix selection and application

Whilst several different approaches including matrix selection and the use of additives were investigated in this study to develop a suitable method to detect cannabinoids in hair samples using MALDI-MS, many more remain untried. Of particular interest could be halogen-substituted CHCA [278,279] and other liquid ionic matrices [280]. Investigation into a more suitable matrix could yield greater signal intensities, which could in turn lower the limit of detection.

There are also many matrix application techniques that have not been assessed in this body of work. These include sublimation and acoustic matrix deposition. In future experiments these application techniques should be trailed alongside the automated spraying method described in this work to determine the optimum technique in terms of matrix homogeneity and signal intensity of analytes, whilst avoiding delocalisation of analytes.

5.2.5.2 Derivatisation

Further work includes optimisation of the derivatisation method to assess whether it is possible to completely derivatise CBD. In this current study CBD is detected as both a singularly and doubly derivatised compound. The singular derivatisation *m/z* is

identical to singularly derivatised THC, and so complete derivatisation of CBD is necessary for differentiation of the two analytes. Experiments could include investigating the effect of different time points and reaction temperatures in solution.

5.2.5.3 Quantitation

In the MALDI aspect of this study quantitation of cannabinoids was not attempted. MALDI-MSP and MALDI-MSI both have limitations in terms of quantitation. These include the inability to control for tissue-specific ion suppression and the irreproducibility of ion signals from scan to scan [281]. These limitations can be caused by numerous factors including tissue heterogeneity, matrix crystal heterogeneity and laser power fluctuations.

In recent years the use of internal standards has facilitated the quantitation of a variety of analytes in a range of tissue types [193,282–293] and so quantitation of cannabinoids in hair samples using MALDI-MSI could be possible future line of investigation.

5.2.5.4 Direct comparison with established techniques

Prior to integration into a toxicology workflow a larger sample of user hairs, from different levels of users and with different hair types should be tested and the relative levels of each metabolite reported. Initially these should run in parallel with well-established techniques such as GC-MS/MS or LC-MS/MS to validate the MALSI-MSI method.

5.2.5.5 Smoke and plant material contamination experiments

Preliminary studies suggest that contamination with cannabis smoke can be detected using MALDI-MS and MALDI-MSI. Further investigations using more realistic smoking conditions such as those proposed by Röhrich *et al.* [132] should be conducted. These investigations could lead to the detection of new markers of smoke exposure.

5.2.5.6 Application of technique to other sample types

Further work includes the application of the derivatisation method proposed in this thesis to other compounds and tissue types.

Since derivatisation occurs with phenol moieties, this technique could be extended to other biologically relevant analytes such as oestrogen, or xenobiotics including synthetic cannabinoids.

In addition, the method developed in this study could be used on tissues other than hair. For example, preliminary studies on finger marks suggest that the derivatisation technique enhances the signal from THC that was on the finger, whilst keeping ridge detail intact. Furthermore, finger marks were also shown to contain THC after handling of plant material (data not shown).

5.3 GC-MS/MS method optimisation

Since MALDI-MS is not yet a quantitative method of analysis of cannabinoids in hair samples, the well-established technique of GC-MS/MS was optimised and used to

investigate cannabinoids in hair samples collected for a psychology study. The use of GC-MS/MS also allowed for comparisons with previously reported values.

5.3.1 BSTFA was the optimal derivatisation reagent

Whist THC, CBD and CBN could be detected without derivatisation 11-OH-THC and THC-COOH could not. THC, CBD, 11-OH-THC and THC-COOH showed an increased peak area with all derivatisation techniques compared to no derivatisation. CBN showed an increase in peak area with all derivatisation reagents apart from with PFPA/PFOH. BSTFA derivatisation gave the largest peak area and peak height for all cannabinoids. Based on peak shape, retention time and response BSTFA was chosen as the derivatisation reagent for future experiments.

5.3.2 GC-APCI-MS/MS improved limits of detection and quantitation compared to GC-EI-MS/MS

During GC-EI-MS/MS investigations, the limit of detection for THC, CBD and CBN was below the SoHT recommended cut off. However, the linear range was narrow. Whilst 11-OH-THC and THC-COOH were both detected at the SoHT limit of 0.2 pg/mg, neither analyte gave a linear response using any three points in the calibration range and so quantitation using this method was not possible.

Without the hair matrix 11-OH-THC gave a linear response between 0.16 and 10 pg/µL THC-COOH gave a linear response between 0.31 and 10 pg/µL. This suggests that matrix effects are larger at lower analyte concentrations, and that the higher

concentrations of THC, CBD and CBN mean matrix effects has less of an effect on overall analysis.

During GC-APCI-MS/MS experiments all analytes and were detected and quantifiable in the fg/µL range, with linear ranges spreading several orders of magnitude. However, in spiked hair calibrants matrix effects were apparent as concentrations that could be detected using standards (1 pg/µL) were undetectable when the matrix was added. Matrix effects were in part lessened by the dilution of hair samples. Limits of detection and quantitation were below the suggested SoHT cut off.

5.3.3 THC, CBD, CBN THC-COOH and 11-OH-THC were simultaneously detected in authentic hair samples

Hair samples were collected in the context of a study into the age of onset of cannabis use and executive function.

Out of 26 samples, three did not have any analytes detected. Only one sample had all analytes detected. Concentrations of THC, CBD and CBN were substantially lower than had been reported previously (in the pg/mg rather than ng/mg range). The concentration of THC-COOH was similar to previously published articles with two sample concentrations being above 0.2 pg/mg, the cut off recommended by the society of hair testing.

5.3.3.1 Concordance with self-report

Out of a total of 10 samples in the self-report "cannabis user" group, THC-COOH was detected in just 20%. The metabolite 11-OH-THC was detected in a different 20% of samples whilst 10% of samples had both THC-COOH and 11-OH-THC detected. Therefore, 50% of the samples in the cannabis user group were identified by the presence of THC metabolites in the hair. Analysis of the washes to determine the ratio of cannabinoids in wash residue compared to that detected in the hair samples, proposed as an additional way of identifying positive samples, failed to identify any additional positive samples in this group.

Metabolites were not detected in any of the infrequent cannabis users (n=5) and as above, the wash ratio analysis did not identify any samples as positive.

Surprisingly, metabolites were detected in 2 of the 11 samples provided by individuals who self-reported not to have used cannabis in their lifetimes.

If the self-report data is accurate, this reveals a worrying number of both false positives and false negatives in the various interpretation methods to detect cannabis use. A limitation of this study is that the time since last use was not known beyond one week prior to collection.

5.3.4 Further work for GC-MS/MS analysis

Further work includes an in-depth analysis of matrix effects in hair samples and strategies to reduce them. For example, a lower initial amount of hair may help to

overcome matrix effects, as well as having the practical advantages associated with smaller sample size.

There is a distinct lack of research published relating to how the physical condition of the hair could affect matrix effects. Other aspects such as dyeing, bleaching, heat damage and ethnicity of hair should also be assessed in future work.

Further work may also include investigations into whether two-dimensional-GC could separate hair matrix interferences away from analytes and allow for more efficient ionisation, which is less prone to matrix effects. This was suggested as a potential analytical technique for use in hair samples by Guthery *et al.* [294], however its application to cannabinoids in authentic hair samples has not yet been explored.

Finally, with current technologies allowing for lower limits of detection and quantitation of cannabinoids in hair samples, experiments need to be conducted into assessing scientifically derived cut-offs, rather than instrumental ones.

5.4 Concluding remarks

The scientific findings in this thesis have contributed novel research and furthered knowledge in the fields of matrix-assisted laser desorption mass spectrometry and in the analysis of cannabinoids in hair samples. In addition, the PhD project has raised questions around the reporting criterion for positive hair samples and highlighted new avenues for future study.

Publications, presentations and posters

Peer review publications

Full copies of these publications can be found in Appendix II

Beasley, E., Frances, S. and Bassindale, T., 2016. Detection and mapping of cannabinoids in single hair samples through rapid derivatization and matrix-assisted laser desorption ionisation mass spectrometry. *Analytical chemistry*, *88*(20), pp.10328-10334.

Flinders, B., Beasley, E., Verlaan, R.M., Cuypers, E., Francese, S., Bassindale, T., Clench, M.R. and Heeren, R.M., 2017. Optimization of sample preparation and instrumental parameters for the rapid analysis of drugs of abuse in hair samples by MALDI-MS/MS imaging. *Journal of the American Society for Mass Spectrometry*, *28*(11), pp.2462-2468.

Oral presentations

Rapid derivatisation for the detection of cannabinoids in hair samples using MALDI-Imaging Mass Spectrometry presented at the British Mass Spectrometry Society Special Interest Group meeting for Imaging Mass Spectrometry, Sheffield, UK

5.5 Poster Presentations

Beasley, E., Frances, S. and Bassindale, T. Detection and Mapping of Cannabinoids in Single Hairs Through Rapid derivatisation MALDI-Imaging Mass Spectrometry presented at the International Association of Legal Medicine, Venice, Italy, 2016.

Beasley, E. Morgan G., Bassindale, T. Development of Offline and Fully Automated Sample Preparation Methods for Analysis of Cannabinoids in Hair Samples. Presented at the 65th American Society for Mass Spectrometry, IdIndianapolis, USA.

References

[1] Home Office, Seizures of drugs in England and Wales, financial year ending 2017, (2017). https://assets.publishing.service.gov.uk/government/uploads/system/uploads/attachment_data/file/657872/seizures-drugs-mar2017-hosb2217.pdf.

[2] Home Office, Drug misuse: Findings from the 2016/2017 Crime Survey for England and Wales, (2017). https://assets.publishing.service.gov.uk/government/uploads/system/uploads/attachment_data/file/642738/drug-misuse-2017-hosb1117.pdf.

[3] E. Small, Evolution and Classification of Cannabis sativa (Marijuana, Hemp) in Relation to Human Utilization, The Botanical Review. 81 (2015) 189–294.

[4] B.F. Thomas, M.A. ElSohly, Chapter 1 – The Botany of Cannabis sativa L., in: Anal. Chem. Cannabis, 2016: pp. 1–26.

[5] A. Hazekamp, F. Grotenhermen, Review on clinical studies with cannabis and cannabinoids 2005-2009, Multiple Sclerosis. 5 (2010) 1–21.

[6] P. Sharma, P. Murthy, M.M.S. Bharath, Chemistry, Metabolism, and Toxicology of Cannabis: Clinical Implications, Iranian Journal of Psychiatry. 7 (2012) 149–156.

[7] M.A. ElSohly, Z. Mehmedic, S. Foster, C. Gon, S. Chandra, J.C. Church, Changes in Cannabis Potency Over the Last 2 Decades (1995–2014): Analysis of Current Data in the United States, Biological Psychiatry. 79 (2016) 613–619.

[8] D.J. Potter, P. Clark, M.B. Brown, Potency of Δ9–THC and other cannabinoids in cannabis in England in 2005: Implications for psychoactivity and pharmacology, Journal of Forensic Sciences. 53 (2008) 90–94.

[9] D.J. Potter, K. Hammond, S. Tuffnell, C. Walker, M. Di Forti, Potency of Δ9–tetrahydrocannabinol and other cannabinoids in cannabis in England in 2016: Implications for public health and pharmacology, Drug Testing and Analysis. 10 (2018) 628–635.

[10] G.A. Thakur, R.I. Duclos Jr, A. Makriyannis, Natural cannabinoids: templates for drug discovery, Life Sciences. 78 (2005) 454–466.

[11] A.A.M. Stolker, J. Van Schoonhoven, A.J. De Vries, I. Bobeldijk-Pastorova, W.H.J. Vaes, R. Van Den Berg, Determination of cannabinoids in cannabis products using liquid chromatography–ion trap mass spectrometry, Journal of Chromatography A. 1058 (2004) 143–151.

[12] H. Lu, K. Mackie, An Introduction to the Endogenous Cannabinoid System, Biological Psychiatry. 79 (2016) 516–525.

[13] A.C. Howlett, International Union of Pharmacology. XXVII. Classification of Cannabinoid Receptors, Pharmacological Reviews. 54 (2002) 161–202.

[14] G. Appendino, G. Chianese, O. Taglialatela-Scafati, Cannabinoids: occurrence and medicinal chemistry, Current Medicinal Chemistry. 18 (2011) 1085–1099.

[15] K. Maresz, E.J. Carrier, E.D. Ponomarev, C.J. Hillard, B.N. Dittel, Modulation of the cannabinoid CB2 receptor in microglial cells in response to inflammatory stimuli, Journal of Neurochemistry. 95 (2005) 437–445.

[16] R. Mechoulam, M. Peters, E. Murillo-Rodriguez, L.O. Hanuš, c, Chemistry & Biodiversity. 4 (2007) 1678–1692.

[17] European Monitoring Centre for Drugs and drug Addiction, European Drug Report. Trends and developments, (2017).

[18] S.D. Banister, J. Stuart, R.C. Kevin, A. Edington, M. Longworth, S.M. Wilkinson, C. Beinat, A.S. Buchanan, D.E. Hibbs, M. Glass, Effects of bioisosteric fluorine in synthetic cannabinoid designer drugs JWH-018, AM-2201, UR-144, XLR-11, PB-22, 5F-PB-22, APICA, and STS-135, ACS Chemical Neuroscience. 6 (2015) 1445–1458.

[19] M.S. Ibsen, M. Connor, M. Glass, Cannabinoid CB1 and CB2 Receptor Signaling and Bias, Cannabis and Cannabinoid Research. 2 (2017) 48–60.

[20] E. Martín-Sánchez, T.A. Furukawa, J. Taylor, J.L.R. Martin, Systematic review and meta-analysis of cannabis treatment for chronic pain., Pain Medicine. 10 (2009) 1353–68.

[21] K.P. Hill, Medical Marijuana for Treatment of Chronic Pain and Other Medical and Psychiatric Problems, Journal Of The American Medical Association. 313 (2015) 2474.

[22] L. Degenhardt, N. Lintzeris, G. Campbell, R. Bruno, M. Cohen, M. Farrell, W.D. Hall, Experience of adjunctive cannabis use for chronic non-cancer pain: Findings from the Pain and Opioids IN Treatment (POINT) study, Drug and Alcohol Dependence. 147 (2015) 144–150.

[23] P.F. Smith, Medicinal cannabis extracts for the treatment of multiple sclerosis., Current Opinion in Investigational Drugs (London, England : 2000). 5 (2004) 727–30.

[24] J. Corey-Bloom, T. Wolfson, A. Gamst, S. Jin, T.D. Marcotte, H. Bentley, B. Gouaux, Smoked cannabis for spasticity in multiple sclerosis: A randomized, placebo-controlled trial, Canadian Medical Association Journal. 184 (2012) 1143–1150.

[25] M. Duran, E. Pérez, S. Abanades, X. Vidal, C. Saura, M. Majem, E. Arriola, M. Rabanal, A. Pastor, M. Farré, N. Rams, J.R. Laporte, D. Capellà, Preliminary efficacy and safety of an oromucosal standardized cannabis extract in chemotherapy-induced nausea and vomiting, British Journal of Clinical

Pharmacology. 70 (2010) 656–663.

[26] K.A. Sharkey, N.A. Darmani, L.A. Parker, Regulation of nausea and vomiting by cannabinoids and the endocannabinoid system, European Journal of Pharmacology. 722 (2014) 134–146.

[27] I. Reznik, Medical marijuana/cannabis treatment of Tourette's syndrome: Focus on the quality of life, European Neuropsychopharmacology. 24 (2014) 645–646.

[28] The Home Office, Government announces definition for cannabis-based products for medicinal use, (2018). https://www.gov.uk/government/news/government-announces-definition-for-cannabis-based-products-for-medicinal-use (accessed November 12, 2018).

[29] National institue for health and care excellence, Medicinal forms cannabis extract, National Institue for Health and Care Excellence. (2018). https://bnf.nice.org.uk/medicinal-forms/cannabis-extract.html (accessed October 10, 2018).

[30] New guidance to tackle inequalities in multiple sclerosis care, National Institue for Health and Care Excellence. (2014). https://www.nice.org.uk/news/article/new-guidance-to-tackle-inequalities-in-multiple-sclerosis-care (accessed October 10, 2018).

[31] Food and drug Administration, Perscribing information for Epidiolex, Food and Drug Administration. (2018). https://www.accessdata.fda.gov/drugsatfda_docs/label/2018/210365lbl.pdf (accessed October 10, 2018).

[32] W. Hall, What has research over the past two decades revealed about the adverse health effects of recreational cannabis use?, Addiction. 110 (2014) 19–35.

[33] R. Radhakrishnan, S.T. Wilkinson, D.C. D'Souza, Gone to Pot - A Review of the Association between Cannabis and Psychosis, Frontiers in Psychiatry. 5 (2014) 54.

[34] C.J.A. Morgan, H.V. Curran, Effects of cannabidiol on schizophrenia-like symptoms in people who use cannabis, The British Journal of Psychiatry. 192 (2008) 306–307.

[35] R.L. Hartman, M.A. Huestis, Cannabis effects on driving skills, Clinical Chemistry. 59 (2013) 478–492.

[36] M. Li, J.E. Brady, C.J. DiMaggio, A.R. Lusardi, K.Y. Tzong, G. Li, Marijuana Use and Motor Vehicle Crashes, Epidemiologic Reviews. 34 (2012) 65–72.

[37] M. Asbridge, J.A. Hayden, J.L. Cartwright, Acute cannabis consumption and motor vehicle collision risk: systematic review of observational studies and meta-analysis, British Medical Journal (Clinical Research Ed.). 344 (2012) 536.

[38] S.G. Gerberich, S. Sidney, B.L. Braun, I.S. Tekawa, K.K. Tolan, C.P. Quesenberry,

Marijuana use and injury events resulting in hospitalization, Annals of Epidemiology. 13 (2003) 230–237.

[39] D.M. Fergusson, L.J. Horwood, A.L. Beautrais, Cannabis and educational achievement, Addiction. 98 (2003) 1681–1692.

[40] F. Musshoff, B. Madea, Review of biologic matrices (urine, blood, hair) as indicators of recent or ongoing cannabis use., Therapeutic Drug Monitoring. 28 (2006) 155–163.

[41] T. Daldrup, H. Kaferstein, H. Kohler, R.D. Maier, F. Musshoff, Deciding between one off/occasional and regular cannabis consumption, Blutalkohol. 37 (2000) 39–47.

[42] K.B. Scheidweiler, D.M. Schwope, E.L. Karschner, N.A. Desrosiers, D.A. Gorelick, M.A. Huestis, In vitro stability of free and glucuronidated cannabinoids in blood and plasma following controlled smoked cannabis, Clinical Chemistry. (2013).

[43] G. Skopp, L. Pötsch, Stability of 11-nor-Δ9-carboxy-tetrahydrocannabinol glucuronide in plasma and urine assessed by liquid chromatography-tandem mass spectrometry, Clinical Chemistry. 48 (2002) 301–306.

[44] M.A. Huestis, K.B. Scheidweiler, T. Saito, N. Fortner, T. Abraham, R.A. Gustafson, M.L. Smith, Excretion of Δ9-tetrahydrocannabinol in sweat, Proceedings of the Fourth Symposium of the European Workplace Drug Testing Society (EWDTS). 174 (2008) 173–177.

[45] Y. Nakahara, K. Takahashi, R. Kikura, Hair analysis for drugs of abuse. X. Effect of physicochemical properties of drugs on the incorporation rates into hair., Biological & Pharmaceutical Bulletin. 18 (1995) 1223–1227.

[46] B.D. Plouffe, S.K. Murthy, Fluorescence-based lateral flow assays for rapid oral fluid roadside detection of cannabis use, Electrophoresis. 38 (2017) 501–506.

[47] D. Lee, G. Milman, A.J. Barnes, R.S. Goodwin, J. Hirvonen, M.A. Huestis, Oral fluid cannabinoids in chronic, daily cannabis smokers during sustained, monitored abstinence, Clinical Chemistry. (2011).

[48] C.B. Goodhart, The evolutionary significance of human hair patterns and skin colouring, British Association for the Advancement of Science, 1960.

[49] H. Báez, M.M. Castro, M.A. Benavente, P. Kintz, V. Cirimele, C. Camargo, C. Thomas, Drugs in prehistory: Chemical analysis of ancient human hair, Forensic Science International. 108 (2000) 173–179.

[50] H. Sachs, History of hair analysis, Forensic Science International. 84 (1997) 7–16.

[51] H. Smith, S. Forshufvud, A. Wassen, Distribution of arsenic in Napoleon's hair, Nature. 194 (1962).

[52] L. Tsanaclis, J. Wicks, Chapter 8 - Workplace Drug Testing - Kintz, Pascal, in: A. Salomone, M.B.T.-H.A. in C. and F.T. Vincenti (Eds.), Academic Press, Boston,

2015: pp. 197–239.

[53] M. Villain, Applications of Hair in Drug-Facilitated Crime Evidence, Analytical and Practical Aspects of Drug Testing in Hair. (2006) 255.

[54] K.S. Scott, The use of hair as a toxicological tool in DFC casework., Science & Justice : Journal of the Forensic Science Society. 49 (2009) 250–3.

[55] P. Kintz, Value of hair analysis in postmortem toxicology, Forensic Science International. 142 (2004) 127–134.

[56] P. Kintz, Segmental hair analysis can demonstrate external contamination in postmortem cases, Forensic Science International. 215 (2012) 73–76.

[57] F. Krumbiegel, M. Hastedt, S. Eichberg, N. Correns, R. Gapert, S. Hartwig, S. Herre, M. Tsokos, Hair analysis in the detection of long-term use of non-steroidal anti-inflammatory drugs and its relation to gastrointestinal hemorrhage: an examination of 268 hair and blood samples from autopsy cases, Forensic Science, Medicine, and Pathology. 10 (2014) 18–28.

[58] M.K.K. Nielsen, S.S. Johansen, K. Linnet, Evaluation of poly-drug use in methadone-related fatalities using segmental hair analysis, Forensic Science International. 248 (2015) 134–139.

[59] R. Kegler, A. Büttner, J. Nowotnik, D. Rentsch, Postmortem investigation of 88-cm-long dreadlocks for drugs of abuse: an unusual case report in the northeast of Germany, Forensic Toxicology. 34 (2016) 419–424.

[60] E. Lendoiro, A. de Castro, C. Jiménez-Morigosa, X.A. Gomez-Fraguela, M. López-Rivadulla, A. Cruz, Usefulness of hair analysis and psychological tests for identification of alcohol and drugs of abuse consumption in driving license regranting, Forensic Science International. 286 (2018) 239–244.

[61] M. Spiandore, A. Piram, A. Lacoste, D. Josse, P. Doumenq, Hair analysis as a useful procedure for detection of vapour exposure to chemical warfare agents: Simulation of sulphur mustard with methyl salicylate, Drug Testing and Analysis. 6 (2014) 67–73.

[62] H. Devlin, Science Correspondent, Unreliable drugs tests leave families a hair's breadth away from break-up, The Times (London, England). (2011) 26.

[63] M. Gandhi, Q. Yang, P. Bacchetti, Y. Huang, Short communication: A low-cost method for analyzing nevirapine levels in hair as a marker of adherence in resource-limited settings, AIDS Research and Human Retroviruses. 30 (2014) 25–28.

[64] A.Y. Liu, Q. Yang, Y. Huang, P. Bacchetti, P.L. Anderson, C. Jin, K. Goggin, K. Stojanovski, R. Grant, S.P. Buchbinder, Strong relationship between oral dose and tenofovir hair levels in a randomized trial: hair as a potential adherence measure for pre-exposure prophylaxis (PrEP), PloS One. 9 (2014).

[65] S.M. Baxi, A. Liu, P. Bacchetti, G. Mutua, E.J. Sanders, F.M. Kibengo, J.E. Haberer,

J. Rooney, C.W. Hendrix, P.L. Anderson, Comparing the novel method of assessing PrEP adherence/exposure using hair samples to other pharmacologic and traditional measures, JAIDS Journal of Acquired Immune Deficiency Syndromes. 68 (2015) 13–20.

[66] E.P. Rosen, C.G. Thompson, M.T. Bokhart, H.M.A. Prince, C. Sykes, D.C. Muddiman, A.D.M. Kashuba, Analysis of Antiretrovirals in Single Hair Strands for Evaluation of Drug Adherence with Infrared-Matrix-Assisted Laser Desorption Electrospray Ionization Mass Spectrometry Imaging, Analytical Chemistry. 88 (2016) 1336–1344.

[67] S.A.B. Shah, R. Mullin, G. Jones, I. Shah, J. Barker, A. Petroczi, D.P. Naughton, Simultaneous analysis of antiretroviral drugs abacavir and tenofovir in human hair by liquid chromatography–tandem mass spectrometry, Journal of Pharmaceutical and Biomedical Analysis. 74 (2013) 308–313.

[68] D.L. Caprara, J. Klein, G. Koren, Diagnosis of fetal alcohol spectrum disorder (FASD): fatty acid ethyl esters and neonatal hair analysis, ANNALI-ISTITUTO SUPERIORE DI SANITA. 42 (2006) 39.

[69] M. Baber, G. Koren, J. Gareri, Development And Validation Of Neonatal Hair Analysis Of Fatty Acid Ethyl Esters To Detect Prenatal Alcohol Exposure, Alcoholism Clinical & Experimental Research. 38 (2014) 32A–32A.

[70] J. Klein, D. Chan, G. Koren, Neonatal hair analysis as a biomarker for in utero alcohol exposure, New England Journal of Medicine. 347 (2002) 2086.

[71] J. Fujii, A. Higashi, I. Matsuda, M. Nakano, Measurement of concentrations of nicotine and cotinine in maternal and neonatal hair, Japanese Journal of Clinical Pharmacology and Therapeutics. 32 (2001) 119–125.

[72] G. Koren, Hair Analysis II Measurement of drugs in neonatal hair; a window to fetal exposure, Forensic Science International. 70 (1995) 77–82.

[73] E. Lendoiro, E. González-Colmenero, A. Concheiro-Guisán, A. De Castro, A. Cruz, M. López-Rivadulla, M. Concheiro, Maternal hair analysis for the detection of illicit drugs, medicines, and alcohol exposure during pregnancy, Therapeutic Drug Monitoring. 35 (2013) 296–304.

[74] F. Garcia-Bournissen, B. Rokach, T. Karaskov, G. Koren, Cocaine detection in maternal and neonatal hair: Implications to fetal toxicology, Therapeutic Drug Monitoring. 29 (2007) 71–76.

[75] S. Pichini, L. Cortes, E. Marchei, R. Solimini, R. Pacifici, M.D. Gomez-Roig, O. García-Algar, Ultra-high-pressure liquid chromatography tandem mass spectrometry determination of antidepressant and anxiolytic drugs in neonatal meconium and maternal hair, Journal of Pharmaceutical and Biomedical Analysis. 118 (2016) 9–16.

[76] K. Graham, J. Klein, R. Forman, G. Koren, Potential Misclassification of a Case of SIDS: Maternal and Neonatal Hair Analysis for Cocaine and Heroin, Journal of

Maternal-Fetal Medicine. 2 (1993) 91–93.

[77] M. Moller, T. Karaskov, G. Koren, Opioid detection in maternal and neonatal hair and meconium: characterization of an at-risk population and implications to fetal toxicology., Therapeutic Drug Monitoring. 32 (2010) 318–23.

[78] L.D. Katikaneni, F.R. Salle, T.C. Hulsey, Neonatal hair analysis for benzoylecgonine: a sensitive and semiquantitative biological marker for chronic gestational cocaine exposure, Neonatology. 81 (2002) 29–37.

[79] M. Wada, Y. Sugimoto, R. Ikeda, K. Isono, N. Kuroda, K. Nakashima, Determination of methamphetamine in neonatal hair and meconium samples: Estimation of fetal drug abuse during pregnancy, Forensic Toxicology. 30 (2012) 80–83.

[80] C. Moore, D. Deitermann, D. Lewis, The analysis of neonatal hair for drugs of abuse: A case study, Clinical Chemistry. 42 (1996) 455.

[81] E. Vinner, J. Vignau, D. Thibault, X. Codaccioni, C. Brassart, L. Humbert, M. Lhermitte, Neonatal hair analysis contribution to establishing a gestational drug exposure profile and predicting a withdrawal syndrome, Therapeutic Drug Monitoring. 25 (2003) 421–432.

[82] D.L. Haller, M.C. Acosta, D. Lewis, D.R. Miles, T. Schiano, P.A. Shapiro, J. Gomez, S. Sabag-Cohen, H. Newville, Hair analysis versus conventional methods of drug testing in substance abusers seeking organ transplantation, American Journal of Transplantation. 10 (2010) 1305–1311.

[83] M. Beckmann, G. Paslakis, M. Böttcher, A. Helander, Y. Erim, Integration of Clinical Examination, Self-Report, and Hair Ethyl Glucuronide Analysis for Evaluation of Patients With Alcoholic Liver Disease Prior to Liver Transplantation, Progress in Transplantation. 26 (2016) 40–46.

[84] S. Steudte-Schmiedgen, C. Kirschbaum, N. Alexander, T. Stalder, An integrative model linking traumatization, cortisol dysregulation and posttraumatic stress disorder: Insight from recent hair cortisol findings, Neuroscience & Biobehavioral Reviews. 69 (2016) 124–135.

[85] B. Buffoli, F. Rinaldi, M. Labanca, E. Sorbellini, A. Trink, E. Guanziroli, R. Rezzani, L.F. Rodella, The human hair: from anatomy to physiology, International Journal of Dermatology. 53 (2014) 331–341.

[86] people's blog, The anatomy of hair, (2014). http://blog.peoples.bm/anatomy-hair/ (accessed November 3, 2018).

[87] L. Pötsch, G. Skopp, M.R. Moeller, Proceedings of the 1st European Meeting on Hair Analysis. Clinical, Occupational and Forensic Application Biochemical approach on the conservation of drug molecules during hair fiber formation, Forensic Science International. 84 (1997) 25–35.

[88] Koreesa group, The hair follicle, (n.d.). http://koreesa.co.uk/hair-follicle/

(accessed November 3, 2018).

[89] M.R. Harkey, Anatomy and physiology of hair, Forensic Science International. 63 (1993) 9–18.

[90] M.A. LeBeau, M.A. Montgomery, J.D. Brewer, The role of variations in growth rate and sample collection on interpreting results of segmental analyses of hair, Forensic Science International. 210 (2016) 110–116.

[91] Society of Hair Testing, Recommendations for hair testing in forensic cases, Forensic Science International. 145 (2004) 83–84.

[92] R.J. Myers, J.B. Hamilton, Regeneration and rate of growth of hairs in man, Annals of the New York Academy of Sciences. 53 (1951) 562–568.

[93] V. Pecoraro, I. Astore, J. Barman, C. Ignacioaraujo, THE NORMAL TRICHOGRAM IN THE CHILD BEFORE THE AGE OF PUBERTY., The Journal of Investigative Dermatology. 42 (1964) 427.

[94] N. Miyazawa, T. Uematsu, Analysis of ofloxacin in hair as a measure of hair growth and as a time marker for hair analysis., Therapeutic Drug Monitoring. 14 (1992) 525–528.

[95] L. Pötsch, A discourse on human hair fibers and reflections on the conservation of drug molecules, International Journal of Legal Medicine. 108 (1996) 285–293.

[96] D. Van Neste, Thickness, medullation and growth rate of female scalp hair are subject to significant variation according to pigmentation and scalp location during ageing, European Journal of Dermatology. 14 (2004) 28–32.

[97] M. Tajima, C. Hamada, T. Arai, M. Miyazawa, R. Shibata, A. Ishino, Characteristic features of Japanese women's hair with aging and with progressing hair loss, Journal of Dermatological Science. 45 (2007) 93–103.

[98] M.A. LeBeau, M.A. Montgomery, J.D. Brewer, The role of variations in growth rate and sample collection on interpreting results of segmental analyses of hair, Forensic Science International. 210 (2011) 110–116.

[99] F. Pragst, M.A. Balikova, State of the art in hair analysis for detection of drug and alcohol abuse., Clinica Chimica Acta; International Journal of Clinical Chemistry. 370 (2006) 17–49.

[100] B. Moosmann, N. Roth, V. Auwärter, Finding cannabinoids in hair does not prove cannabis consumption., Scientific Reports. 5 (2015) 14906.

[101] G.L. Henderson, Mechanisms of drug incorporation into hair, Forensic Science International. 63 (1993) 19–29.

[102] P.R. Stout, J.A. Ruth, Deposition of [3H]Cocaine, [3H]Nicotine, and [3H]Flunitrazepam in Mouse Hair Melanosomes after Systemic Administration, Drug Metab. Dispos. 27 (1999) 731–735.

[103] K. Polzer, Attitudes About Advances in Sweat Patch Testing in Drug Courts: Insights from a Case Study in Southern California, Journal of Offender Rehabilitation. 49 (2010) 52–73.

[104] G.L. Henderson, M.R. Harkey, C. Zhou, R.T. Jones, P. Jacob, Incorporation of Isotopically Labeled Cocaine and Metabolites into Human Hair: 1. Dose-Response Relationships, Journal of Analytical Toxicology. 20 (1996) 1–12.

[105] F. Pragst, S. Broecker, M. Hastedt, S. Herre, H. Andresen-Streichert, H. Sachs, M. Tsokos, Methadone and illegal drugs in hair from children with parents in maintenance treatment or suspected for drug abuse in a German community., Therapeutic Drug Monitoring. 35 (2013) 737–52.

[106] M.A. LeBeau, M.A. Montgomery, Considerations on the utility of hair analysis for cocaine, Journal of Analytical Toxicology. 33 (2009) 343–344.

[107] C.L. Morris-Kukoski, M.A. Montgomery, R.L. Hammer, Analysis of extensively washed hair from cocaine users and drug chemists to establish new reporting criteria, Journal of Analytical Toxicology. (2014) 628–636.

[108] F. Musshoff, H.P. Junker, D.W. Lachenmeier, L. Kroener, B. Madea, Fully Automated Determination of Cannabinoids in Hair Samples using Headspace Solid-Phase Microextraction and Gas Chromatography-Mass Spectrometry, Journal of Analytical Toxicology. 26 (2002) 554–560.

[109] F. Musshoff, D.W. Lachenmeier, L. Kroener, B. Madea, Automated headspace solid-phase dynamic extraction for the determination of cannabinoids in hair samples, Forensic Science International. 133 (2003) 32–38.

[110] A. Salomone, E. Gerace, F. D'Urso, D. Di Corcia, M. Vincenti, Simultaneous analysis of several synthetic cannabinoids, THC, CBD and CBN, in hair by ultra-high performance liquid chromatography tandem mass spectrometry. Method validation and application to real samples., Journal of Mass Spectrometry : JMS. 47 (2012) 604–610.

[111] M.A. Huestis, J.E. Henningfield, E.J. Cone, Blood cannabinoids. I. Absorption of THC and formation of 11-OH-THC and THCCOOH during and after smoking marijuana, Journal of Analytical Toxicology. 16 (1992) 276–282.

[112] S. Strano-Rossi, M. Chiarotti, Solid-Phase Microextraction for Cannabinoids Analysis in Hair and Its Possible Application to Other Drugs, Journal of Analytical Toxicology. 23 (1999) 7–10.

[113] E.S. Emídio, V. de Menezes Prata, F.J.M. de Santana, H.S. Dórea, Hollow fiber-based liquid phase microextraction with factorial design optimization and gas chromatography–tandem mass spectrometry for determination of cannabinoids in human hair, Journal of Chromatography B. 878 (2010) 2175–2183.

[114] Y. Nakahara, H. Sekine, Studies on confirmation of cannabis use. I. Determination of the cannabinoid contents in marijuana cigarette, tar, and ash using high performance liquid chromatography with electrochemical detection,

Journal of Analytical Toxicology. 9 (1985) 121–124.

[115] E.S. Emídio, V. de Menezes Prata, H.S. Dórea, Validation of an analytical method for analysis of cannabinoids in hair by headspace solid-phase microextraction and gas chromatography–ion trap tandem mass spectrometry, Analytica Chimica Acta. 670 (2010) 63–71.

[116] T. Nadulski, F. Pragst, Simple and sensitive determination of Delta(9)-tetrahydrocannabinol, cannabidiol and cannabinol in hair by combined silylation, headspace solid phase microextraction and gas chromatography-mass spectrometry., Journal of Chromatography. B, Analytical Technologies in the Biomedical and Life Sciences. 846 (2007) 78–85.

[117] G. Skopp, P. Strohbeck-Kuehner, K. Mann, D. Hermann, Deposition of cannabinoids in hair after long-term use of cannabis., Forensic Science International. 170 (2007) 46–50.

[118] J.Y. Kim, S. Suh, M.K. In, K.-J. Paeng, B.C. Chung, Simultaneous determination of cannabidiol, cannabinol, and Δ9-tetrahydrocannabinol in human hair by gas chromatography-mass spectrometry, Archives of Pharmacal Research. 28 (2005) 1086–1091.

[119] J.P. Selten, I.J. Bosman, D. De Boer, N.D. Veen, Y. Van der Graaf, R.A.A. Maes, R.S. Kahn, Hair analysis for cannabinoids and amphetamines in a psychosis incidence study, European Neuropsychopharmacology. 12 (2002) 27–30.

[120] T. Mieczkowski, Hair Analysis IIA research note: the outcome of GC/MS/MS confirmation of hair assays on 93 cannabinoid (+) cases, Forensic Science International. 70 (1995) 83–91.

[121] M.A. Huestis, R.A. Gustafson, E.T. Moolchan, A. Barnes, J.A. Bourland, S.A. Sweeney, E.F. Hayes, P.M. Carpenter, M.L. Smith, Cannabinoid concentrations in hair from documented cannabis users, Forensic Science International. 169 (2007) 129–136.

[122] E. Han, H. Choi, S. Lee, H. Chung, J.M. Song, A comparative study on the concentrations of 11-nor-Δ9-tetrahydrocannabinol-9-carboxylic acid (THCCOOH) in head and pubic hair., Forensic Science International. 212 (2011) 238–41.

[123] J.Y. Kim, J.C. Cheong, J. Il Lee, M.K. In, Improved gas chromatography-negative ion chemical ionization tandem mass spectrometric method for determination of 11-nor-Δ9-tetrahydrocannabinol-9-carboxylic acid in hair using mechanical pulverization and bead-assisted liquid-liquid extraction., Forensic Science International. 206 (2011) 99–102.

[124] C. Moore, F. Guzaldo, T. Donahue, The Determination of 11-nor- 9-Tetrahydrocannabinol-9-Carboxylic Acid (THC-COOH) in Hair using Negative Ion Gas Chromatography-Mass Spectrometry and High-Volume Injection, Journal of Analytical Toxicology. 25 (2001) 555–558.

[125] C. Moore, S. Rana, C. Coulter, F. Feyerherm, H. Prest, Application of two-

dimensional gas chromatography with electron capture chemical ionization mass spectrometry to the detection of 11-nor- Δ9-tetrahydrocannabinol-9-carboxylic acid (THC-COOH) in hair, Journal of Analytical Toxicology. 30 (2006) 171–177.

[126] E. Han, H. Choi, S. Lee, H. Chung, J.M. Song, A study on the concentrations of 11-nor-Δ9-tetrahydrocannabinol-9-carboxylic acid (THCCOOH) in hair root and whole hair, Forensic Science International. 210 (2011) 201–205.

[127] H. Sachs, U. Dressler, Detection of THCCOOH in hair by MSD-NCI after HPLC clean-up, Forensic Science International. 107 (2000) 239–247.

[128] A. Busuttil, J.. Obafunwa, S. Bulgin, Passive inhalation of cannabis smoke: a novel defence strategy?, Journal of Clinical Forensic Medicine. 3 (1996) 99–104.

[129] B. Law, P.A. Mason, A.C. Moffat, L.J. King, V. Marks, Passive inhalation of cannabis smoke., The Journal of Pharmacy and Pharmacology. 36 (1984) 578–581.

[130] J. Mørland, A. Bugge, B. Skuterud, A. Steen, G.H. Wethe, T. Kjeldsen, Cannabinoids in blood and urine after passive inhalation of Cannabis smoke., Journal of Forensic Sciences. 30 (1985) 997–1002.

[131] E.J. Cone, R.E. Johnson, Contact highs and urinary cannabinoid excretion after passive exposure to marijuana smoke., Clinical Pharmacology and Therapeutics. 40 (1986) 247–256.

[132] J. Röhrich, I. Schimmel, S. Zörntlein, J. Becker, S. Drobnik, T. Kaufmann, V. Kuntz, R. Urban, Concentrations of Δ9-tetrahydrocannabinol and 11-nor-9-carboxytetrahydrocannabinol in blood and urine after passive exposure to cannabis smoke in a coffee shop, Journal of Analytical Toxicology. 34 (2010) 196–203.

[133] E.S. Herrmann, E.J. Cone, J.M. Mitchell, G.E. Bigelow, C. LoDico, R. Flegel, R. Vandrey, Non-smoker exposure to secondhand cannabis smoke II: Effect of room ventilation on the physiological, subjective, and behavioral/cognitive effects., Drug and Alcohol Dependence. 151 (2015) 194–202.

[134] P. Zeidenberg, R. Bourdon, G.G. Nahas, Marijuana intoxication by passive inhalation: documentation by detection of urinary metabolites., American Journal of Psychiatry. 134 (1977) 76–77.

[135] M. Perez-Reyes, S. Di Guiseppi, A.P. Mason, K.H. Davis, Passive inhalation of marihuana smoke and urinary excretion of cannabinoids, Clinical Pharmacology & Therapeutics. 34 (1983) 36–41.

[136] E.J. Cone, R.E. Johnson, W.D. Darwin, D. Yousefnejad, L.D. Mell, B.D. Paul, J. Mitchell, Passive inhalation of marijuana smoke: urinalysis and room air levels of delta-9-tetrahydrocannabinol, Journal of Analytical Toxicology. 11 (1987) 89–96.

[137] S.J. Mulé, P. Lomax, S.J. Gross, Active and Realistic Passive Marijuana Exposure

Tested by Three Immunoassays and GCIMS in Urine, Journal of Analytical Toxicology . 12 (1988) 113–116.

[138] E.J. Cone, Marijuana effects and urinalysis after passive inhalation and oral ingestion, National Institute on Drug Abuse Research Monograph. 99 (1990) 88–96.

[139] S. Niedbala, K. Kardos, S. Salamone, D. Fritch, M. Bronsgeest, E.J. Cone, Passive cannabis smoke exposure and oral fluid testing, Journal of Analytical Toxicology. 28 (2004) 546–552.

[140] R.S. Niedbala, K.W. Kardos, D.F. Fritch, K.P. Kunsman, K.A. Blum, G.A. Newland, J. Waga, L. Kurtz, M. Bronsgeest, E.J. Cone, Passive cannabis smoke exposure and oral fluid testing. II. Two studies of extreme cannabis smoke exposure in a motor vehicle, Journal of Analytical Toxicology. 29 (2005) 607–615.

[141] C. Moore, C. Coulter, D. Uges, J. Tuyay, S. van der Linde, A. van Leeuwen, M. Garnier, J. Orbita, Cannabinoids in oral fluid following passive exposure to marijuana smoke, Forensic Science International. 212 (2011) 227–230.

[142] E.J. Cone, G.E. Bigelow, E.S. Herrmann, J.M. Mitchell, C. LoDico, R. Flegel, R. Vandrey, Nonsmoker Exposure to Secondhand Cannabis Smoke. III. Oral Fluid and Blood Drug Concentrations and Corresponding Subjective Effects, Journal of Analytical Toxicology. (2015).

[143] J.W. Hayden, Passive inhalation of marijuana smoke: A critical review, Journal of Substance Abuse. 3 (1991) 85–90.

[144] B. Moosmann, N. Roth, V. Auwärter, Hair analysis for THCA-A, THC and CBN after passive in vivo exposure to marijuana smoke, Drug Testing and Analysis. 6 (2014) 119–125.

[145] G.A.A. Cooper, R. Kronstrand, P. Kintz, Society of Hair Testing guidelines for drug testing in hair, Forensic Science International. 218 (2012) 20–24.

[146] B. Moosmann, N. Roth, V. Auwärter, Hair analysis for Δ(9) -tetrahydrocannabinolic acid A (THCA-A) and Δ(9) -tetrahydrocannabinol (THC) after handling cannabis plant material., Drug Testing and Analysis. (2015).

[147] B. Moosmann, T. Valcheva, M. Neukamm, V. Angerer, V. Auwärter, Hair analysis of synthetic cannabinoids: does the handling of herbal mixtures affect the analyst's hair concentration?, Forensic Toxicology. 33 (2015) 37–44.

[148] L. Mercolini, R. Mandrioli, M. Protti, M. Conti, G. Serpelloni, M.A. Raggi, Monitoring of chronic Cannabis abuse: An LC-MS/MS method for hair analysis, Journal of Pharmaceutical and Biomedical Analysis. 76 (2013) 119–125.

[149] M. Minoli, I. Angeli, A. Ravelli, F. Gigli, F. Lodi, Detection and quantification of 11-nor-Δ9-tetrahydrocannabinol-9-carboxylic acid in hair by GC/MS/MS in Negative Chemical Ionization mode (NCI) with a simple and rapid liquid/liquid extraction, Forensic Science International. 218 (2012) 49.

[150] D. Thieme, H. Sachs, M. Uhl, Proof of cannabis administration by sensitive detection of 11-nor-Delta(9)-tetrahydrocannabinol-9-carboxylic acid in hair using selective methylation and application of liquid chromatography- tandem and multistage mass spectrometry., Drug Testing and Analysis. 6 (2014) 112–8.

[151] E. Han, H. Chung, J.M. Song, Segmental hair analysis for 11-nor-Δ^9-tetrahydrocannabinol-9-carboxylic acid and the patterns of cannabis use., Journal of Analytical Toxicology. 36 (2012) 195–200.

[152] C. Gambelunghe, N. Fucci, K. Aroni, M. Bacci, A. Marcelli, R. Rossi, Cannabis Use Surveillance By Sweat Analysis., Therapeutic Drug Monitoring. (2016).

[153] P. Kintz, V. Cirimele, B. Ludes, Detection of cannabis in oral fluid (saliva) and forehead wipes (sweat) from impaired drivers., Journal of Analytical Toxicology. 24 (2000) 557–561.

[154] V.A. Hill, M.I. Schaffer, G.N. Stowe, Carboxy-THC in Washed Hair: Still the Reliable Indicator of Marijuana Ingestion, Journal of Analytical Toxicology. 40 (2016) 345–349.

[155] J.F.C. Wicks, L.M. Tsanaclis, Hair Analysis for Assessing Cannabis use. Where is the cut-off?, Workshop of the Society of Hair Testing. (2005) 120.

[156] L. Tsanaclis, J.F.C. Wicks, Patterns in drug use in the United Kingdom as revealed through analysis of hair in a large population sample., Forensic Science International. 170 (2007) 121–8.

[157] S. Pichini, E. Marchei, S. Martello, M. Gottardi, M. Pellegrini, F. Svaizer, A. Lotti, M. Chiarotti, R. Pacifici, Identification and quantification of 11-nor-Δ9-tetrahydrocannabinol-9-carboxylic acid glucuronide (THC-COOH-glu) in hair by ultra-performance liquid chromatography tandem mass spectrometry as a potential hair biomarker of cannabis use, Forensic Science International. 249 (2015) 47–51.

[158] W.F. Duvivier, M.R. van Putten, T.A. van Beek, M.W.F. Nielen, (Un)targeted Scanning of Locks of Hair for Drugs of Abuse by Direct Analysis in Real Time–High-Resolution Mass Spectrometry, Analytical Chemistry. 88 (2016) 2489–2496.

[159] B. Moosmann, N. Roth, M. Hastedt, A. Jacobsen-Bauer, F. Pragst, V. Auwärter, Cannabinoid findings in children hair–what do they really tell us? An assessment in the light of three different analytical methods with focus on interpretation of Δ9-tetrahydrocannabinolic acid A concentrations, Drug Testing and Analysis. (2014) 349–357.

[160] M. Uhl, H. Sachs, Cannabinoids in hair: strategy to prove marijuana/hashish consumption., Forensic Science International. 145 (2004) 143–7.

[161] S. Vogliardi, M. Tucci, G. Stocchero, S.D. Ferrara, D. Favretto, Sample preparation methods for determination of drugs of abuse in hair samples: A review., Analytica Chimica Acta. 857C (2015) 1–27.

[162] L. Tsanaclis, J.F.C. Wicks, Differentiation between drug use and environmental contamination when testing for drugs in hair., Forensic Science International. 176 (2008) 19–22.

[163] L. Tsanaclis, J. Nutt, K. Bagley, S. Bevan, J. Wicks, Differentiation between consumption and external contamination when testing for cocaine and cannabis in hair samples, Drug Testing and Analysis. 6 (2014) 37–41.

[164] J. Thorspecken, G. Skopp, L. Pötsch, In vitro contamination of hair by marijuana smoke., Clinical Chemistry. 50 (2004) 596–602.

[165] V. Auwärter, A. Wohlfarth, J. Traber, D. Thieme, W. Weinmann, Hair analysis for Δ9-tetrahydrocannabinolic acid A-New insights into the mechanism of drug incorporation of cannabinoids into hair, Forensic Science International. 196 (2010) 10–13.

[166] J. Greaves, J. Roboz, Mass spectrometry for the novice, CRC Press, 2013.

[167] E. de Hoffmann, V. Stroobant, Mass spectrometry: principles and applications, in: Mass Spectrom. Princ. Appl., 2007.

[168] D.L. Andrews, Encyclopedia of applied spectroscopy, Wiley-VCH Weinheim, Germany, 2009.

[169] A.J. Dempster, A new method of positive ray analysis, Physical Review. 11 (1918) 316.

[170] M. Dole, L.L. Mack, R.L. Hines, R.C. Mobley, L.D. Ferguson, M.B. Alice, Molecular beams of macroions, The Journal of Chemical Physics. 49 (1968) 2240–2249.

[171] M. Yamashita, J.B. Fenn, Electrospray ion source. Another variation on the free-jet theme, The Journal of Physical Chemistry. 88 (1984) 4451–4459.

[172] E.C. Horning, M.G. Horning, D.I. Carroll, I. Dzidic, R.N. Stillwell, New picogram detection system based on a mass spectrometer with an external ionization source at atmospheric pressure, Analytical Chemistry. 45 (1973) 936–943.

[173] T. Portolés, J.G.J. Mol, J. V Sancho, F. Hernández, Advantages of atmospheric pressure chemical ionization in gas chromatography tandem mass spectrometry: pyrethroid insecticides as a case study, Analytical Chemistry. 84 (2012) 9802.

[174] T. Portolés, J. V Sancho, F. Hernández, A. Newton, P. Hancock, Potential of atmospheric pressure chemical ionization source in GC-QTOF MS for pesticide residue analysis, Journal of Mass Spectrometry. 45 (2010) 926–936.

[175] J.H. Gross, Mass spectrometry : a textbook, Third edit, Springer, Cham, 2017.

[176] M. Karas, D. Bachmann, F. Hillenkamp, Influence of the wavelength in high-irradiance ultraviolet laser desorption mass spectrometry of organic molecules, Analytical Chemistry. 57 (1985) 2935–2939.

[177] K. Tanaka, H. Waki, Y. Ido, S. Akita, Protein and polymer analyses up to m/z 100 000 by laser ionization time-of-flight mass spectrometry, Rapid Communications in Mass Spectrometry. (1998).

[178] E. Nordhoff, A. Ingendoh, R. Cramer, A. Overberg, B. Stahl, M. Karas, F. Hillenkamp, P.F. Crain, B. Chait, Matrix-assisted laser desorption/ionization mass spectrometry of nucleic acids with wavelengths in the ultraviolet and infrared, Rapid Communications in Mass Spectrometry. 6 (1992) 771–776.

[179] R. Bradshaw, The intergration of MALDI MSI into the current Home Office Fingermark Examination workflow, PhD thesis, Sheffield Hallam Univerity, 2014.

[180] F. Hillenkamp, J. Peter-Katalinić, J.P.- Katalinić, F. Hillenkamp, MALDI MS : a practical guide to instrumentation, methods, and applications, Second edi, Wiley Blackwell, Weinheim, 2014.

[181] M. Gluckmann, A. Pfenninger, R. Kruger, M. Thierolf, M. Karas, V. Horneffer, F. Hillenkamp, K. Strupat, Mechanisms in MALDI analysis: surface interaction or incorporation of analytes?, International Journal Of Mass Spectrometry. 210 (2001) 121–132.

[182] M. Karas, M. Glückmann, J. Schäfer, Ionization in matrix-assisted laser desorption/ionization: singly charged molecular ions are the lucky survivors, Journal of Mass Spectrometry. 35 (2000) 1–12.

[183] Ic. Lu, C. Lee, Y. Lee, C. Ni, Ionization Mechanism of Matrix-Assisted Laser Desorption Ionization, Annual Review of Analytical Chemistry. 8 (2015) 21–39.

[184] R. Knochenmuss, Ion formation mechanisms in UV-MALDI, Analyst. 131 (2006) 966–986.

[185] R.M. Caprioli, T.B. Farmer, J. Gile, Molecular imaging of biological samples: localization of peptides and proteins using MALDI-TOF MS, Analytical Chemistry. 69 (1997) 4751–4760.

[186] I. V Chernushevich, A. V Loboda, B.A. Thomson, An introduction to quadrupole–time-of-flight mass spectrometry, Journal of Mass Spectrometry. 36 (2001) 849–865.

[187] M.A. Baldwin, K.F. Medzihradszky, C.M. Lock, B. Fisher, T.A. Settineri, A.L. Burlingame, Matrix-assisted laser desorption/ionization coupled with quadrupole/orthogonal acceleration time-of-flight mass spectrometry for protein discovery, identification, and structural analysis, Analytical Chemistry. 73 (2001) 1707–1720.

[188] M. Poetzsch, A.E. Steuer, A.T. Roemmelt, M.R. Baumgartner, T. Kraemer, Single Hair Analysis of Small Molecules Using MALDI-Triple Quadrupole MS Imaging and LC-MS/MS: Investigations on Opportunities and Pitfalls, Analytical Chemistry. 86 (2014) 11758–11765.

[189] A. Miki, M. Katagi, T. Kamata, K. Zaitsu, M. Tatsuno, T. Nakanishi, H. Tsuchihashi,

T. Takubo, K. Suzuki, MALDI-TOF and MALDI-FTICR imaging mass spectrometry of methamphetamine incorporated into hair., Journal of Mass Spectrometry : JMS. 46 (2011) 411–416.

[190] T. Porta, C. Grivet, T. Kraemer, E. Varesio, G. Hopfgartner, Single hair cocaine consumption monitoring by mass spectrometric imaging, Analytical Chemistry. 83 (2011) 4266–4272.

[191] M. Shen, P. Xiang, Y. Shi, H. Pu, H. Yan, B. Shen, Mass imaging of ketamine in a single scalp hair by MALDI-FTMS, Analytical and Bioanalytical Chemistry. 406 (2014) 4611–4616.

[192] N. Shima, K. Sasaki, T. Kamata, S. Matsuta, M. Katagi, A. Miki, K. Zaitsu, T. Sato, T. Nakanishi, H. Tsuchihashi, K. Suzuki, Single-hair analysis of zolpidem on the supposition of its single administration in drug-facilitated crimes, Forensic Toxicology. 33 (2015) 122–130.

[193] T. Nakanishi, T. Nirasawa, T. Takubo, Quantitative Mass Barcode-Like Image of Nicotine in Single Longitudinally Sliced Hair Sections from Long-Term Smokers by Matrix-Assisted Laser Desorption Time-of-Flight Mass Spectrometry Imaging, Journal of Analytical Toxicology. 38 (2014) 349–353.

[194] C. Feng, C. Lu, A new matrix for analyzing low molecular mass compounds and its application for determination of carcinogenic areca alkaloids by matrix-assisted laser desorption ionization time-of-flight mass spectrometry., Analytica Chimica Acta. 649 (2009) 230–5.

[195] N. Bergman, D. Shevchenko, J. Bergquist, Approaches for the analysis of low molecular weight compounds with laser desorption/ionization techniques and mass spectrometry., Analytical and Bioanalytical Chemistry. 406 (2014) 49–61.

[196] S.R. Shanta, T.Y. Kim, J.H. Hong, J.H. Lee, C.Y. Shin, K. Kim, Y.H. Kim, S.K. Kim, K.P. Kim, A new combination MALDI matrix for small molecule analysis: application to imaging mass spectrometry for drugs and metabolites, Analyst. 137 (2012) 5757–5762.

[197] G. Groeneveld, M. de Puit, S. Bleay, R. Bradshaw, S. Francese, Detection and mapping of illicit drugs and their metabolites in fingermarks by MALDI MS and compatibility with forensic techniques, Scientific Reports. 5 (2015).

[198] K. Kuwayama, T. Yamamuro, K. Tsujikawa, H. Miyaguchi, T. Kanamori, Y.T. Iwata, H. Inoue, Utilization of matrix-assisted laser desorption/ionization imaging mass spectrometry to search for cannabis in herb mixtures, Analytical and Bioanalytical Chemistry. 406 (2014) 4789–4794.

[199] A. Su, J. Liu, C. Lin, Rapid drug-screening of clandestine tablets by MALDI-TOF mass spectrometry., Talanta. 67 (2005) 718–24.

[200] C. Cerruti, D. Touboul, V. Guérineau, V. Petit, O. Laprévote, A. Brunelle, MALDI imaging mass spectrometry of lipids by adding lithium salts to the matrix solution, Analytical and Bioanalytical Chemistry. 401 (2011) 75–87.

[201] D. Thieme, H. Sachs, M. Thevis, Formation of the N-methylpyridinium derivative to improve the detection of buprenorphine by liquid chromatography-mass spectrometry, Journal of Mass Spectrometry. 43 (2008) 974–979.

[202] P.J. Trim, M.-C. Djidja, S.J. Atkinson, K. Oakes, L.M. Cole, D.M.G. Anderson, P.J. Hart, S. Francese, M.R. Clench, Introduction of a 20 kHz Nd:YVO4 laser into a hybrid quadrupole time-of-flight mass spectrometer for MALDI-MS imaging., Analytical and Bioanalytical Chemistry. 397 (2010) 3409–19.

[203] D.A. Simmons, Improved MALDI-MS imaging performance using continuous laser rastering, Applied Biosystems Technical Note. (2008).

[204] N. Roth, B. Moosmann, V. Auwärter, Development and validation of an LC-MS/MS method for quantification of Δ9-tetrahydrocannabinolic acid A (THCA-A), THC, CBN and CBD in hair., Journal of Mass Spectrometry. 48 (2013) 227–33.

[205] C. Zhang, H. Zhang, D.W. Litchfield, K.K.-C. Yeung, CHCA or DHB? Systematic Comparison of the Two Most Commonly Used Matrices for Peptide Mass Fingerprint Analysis with MALDI-MS, Spectroscopy. 25 (2010) 48–62.

[206] R. Lemaire, J.C. Tabet, P. Ducoroy, J.B. Hendra, M. Salzet, I. Fournier, Solid Ionic Matrixes for Direct Tissue Analysis and MALDI Imaging, Analytical Chemistry (Washington). 78 (2006) 809–819.

[207] Y.-C. Ho, M.-C. Tseng, Y.-W. Lu, C.-C. Lin, Y.-J. Chen, M.-R. Fuh, Nanoparticle-assisted MALDI-TOF MS combined with seed-layer surface preparation for quantification of small molecules, Analytica Chimica Acta. 697 (2011) 1–7.

[208] S. Kjellström, O.N. Jensen, Phosphoric acid as a matrix additive for MALDI MS analysis of phosphopeptides and phosphoproteins, Analytical Chemistry. 76 (2004) 5109–5117.

[209] M. Shahgholi, B.A. Garcia, N.H.L. Chiu, P.J. Heaney, K. Tang, Sugar additives for MALDI matrices improve signal allowing the smallest nucleotide change (A: T) in a DNA sequence to be resolved, Nucleic Acids Research. 29 (2001).

[210] I. Kim, S. Kim, D. Shin, J. Kim, Matrix Additives in MALDI-TOF MS Analysis of Glycans, Bulletin of the Korean Chemical Society. 37 (2016) 105–107.

[211] Z. Guo, Q. Zhang, H. Zou, B. Guo, J. Ni, A method for the analysis of low-mass molecules by MALDI-TOF mass spectrometry, Analytical Chemistry. 74 (2002) 1637–1641.

[212] D.C. Grant, R.J. Helleur, Surfactant-mediated matrix-assisted laser desorption/ionization time-of-flight mass spectrometry of small molecules., Rapid Communications in Mass Spectrometry. 21 (2007) 837–45.

[213] S.I. Snovida, V.C. Chen, H. Perreault, Use of a 2,5-dihydroxybenzoic acid/aniline MALDI matrix for improved detection and on-target Derivatization of glycans: A preliminary report., Analytical Chemistry. 78 (2006) 8561–8568.

[214] C.D. Calvano, S. Carulli, F. Palmisano, Aniline/α-cyano-4-hydroxycinnamic acid is

a highly versatile ionic liquid for matrix-assisted laser desorption/ionization mass spectrometry, Rapid Communications in Mass Spectrometry. 23 (2009) 1659–1668.

[215] Y. Sugiura, M. Setou, Selective imaging of positively charged polar and nonpolar lipids by optimizing matrix solution composition, Rapid Communications in Mass Spectrometry. 23 (2009) 3269–3278.

[216] L. Bijlsma, J. V. Sancho, F. Hernández, W.M.A. Niessen, Fragmentation pathways of drugs of abuse and their metabolites based on QTOF MS/MS and MS E accurate-mass spectra, Journal of Mass Spectrometry. 46 (2011) 865–875.

[217] J.M.E. Quirke, C.L. Adams, G.J. Van Berkel, Chemical Derivatization for Electrospray Ionization Mass Spectrometry. 1. Alkyl Halides, Alcohols, Phenols, Thiols, and Amines, Analytical Chemistry. 66 (1994) 1302–1315.

[218] J.C. Dunphy, D.G. Pessler, S.W. Morrall, K.A. Evans, D.A. Robaugh, G. Fujimoto, A. Negahban, Derivatization LC/MS for the simultaneous determination of fatty alcohol and alcohol ethoxylate surfactants in water and wastewater samples, Environmental Science & Technology. 35 (2001) 1223–1230.

[219] Y. Lin, C. Chen, G. Wang, Analysis of steroid estrogens in water using liquid chromatography/tandem mass spectrometry with chemical derivatizations, Rapid Communications in Mass Spectrometry. 21 (2007) 1973–1983.

[220] D. Thieme, H. Sachs, M. Thevis, Formation of the N-methylpyridinium derivative to improve the detection of buprenorphine by liquid chromatography-mass spectrometry, Journal of Mass Spectrometry. 43 (2008) 974–979.

[221] R. Murgasova, D.M. Hercules, J.R. Edman, Characterization of polyimides by combining mass spectrometry and selective chemical reaction, Macromolecules. 37 (2004) 5732–5740.

[222] I. Hailat, R.J. Helleur, Direct analysis of sterols by derivatization matrix-assisted laser desorption/ionization time-of-flight mass spectrometry and tandem mass spectrometry, Rapid Communications in Mass Spectrometry. 28 (2014) 149–158.

[223] T. Mukaiyama, T. Tanaka, A Convenient Method for the Preparation of Carboxylic Acid Fluorides, Chemistry Letters. 5 (1976) 303–306.

[224] H.H. Adomat, O.S. Bains, J.M. Lubieniecka, M.E. Gleave, E.S. Guns, T.A. Grigliatti, R.E. Reid, K.W. Riggs, Validation of a sequential extraction and liquid chromatography–tandem mass spectrometric method for determination of dihydrotestosterone, androstanediol and androstanediol–glucuronide in prostate tissues, Journal of Chromatography B. 902 (2012) 84–95.

[225] R. Shroff, A. Muck, A. Svatos, Analysis of low molecular weight acids by negative mode matrix-assisted laser desorption/ionization time-of-flight mass spectrometry., Rapid Communications in Mass Spectrometry. 21 (2007) 3295–300.

[226] S. Laugesen, P. Roepstorff, Combination of two matrices results in improved performance of MALDI MS for peptide mass mapping and protein analysis., Journal of the American Society for Mass Spectrometry. 14 (2003) 992–1002.

[227] B. De Backer, B. Debrus, P. Lebrun, L. Theunis, N. Dubois, L. Decock, A. Verstraete, P. Hubert, C. Charlier, Innovative development and validation of an HPLC/DAD method for the qualitative and quantitative determination of major cannabinoids in cannabis plant material, Journal of Chromatography B. 877 (2009) 4115–4124.

[228] C. Lindholst, Long term stability of cannabis resin and cannabis extracts, Australian Journal of Forensic Sciences. 42 (2010) 181–190.

[229] I. Trofin, G. Dabija, D.-I. Vaireanu, F. Laurentiu, The Influence of Long-term Storage Conditions on the Stability of Cannabinoids derived from Cannabis Resin, Revista de Chimie. 63 (2012) 422–427.

[230] D.J. Harvey, Stability of cannabinoids in dried samples of cannabis dating from around 1896–1905, Journal of Ethnopharmacology. 28 (1990) 117–128.

[231] B. Flinders, E. Cuypers, H. Zeijlemaker, J. Tytgat, R.M.A. Heeren, Preparation of longitudinal sections of hair samples for the analysis of cocaine by MALDI-MS/MS and TOF-SIMS imaging, Drug Testing and Analysis. 7 (2015) 859–865.

[232] I.M. Kempson, W.M. Skinner, P.K. Kirkbride, A method for the longitudinal sectioning of single hair samples, Journal of Forensic Sciences. 47 (2002) 889–892.

[233] B. Flinders, E. Beasley, R.M. Verlaan, E. Cuypers, S. Francese, T. Bassindale, M.R. Clench, R.M.A. Heeren, Optimization of sample preparation and instrumental parameters for the rapid analysis of drugs of abuse in hair samples by MALDI-MS/MS imaging, Journal of the American Society for Mass Spectrometry. 28 (2017) 2462–2468.

[234] K.H. Park, H.J. Kim, B. Oh, E. Lee, J. Ha, Assessment of hair surface roughness using quantitative image analysis, Skin Research and Technology. 24 (2018) 80–84.

[235] Y.-D. Kim, S.-Y. Jeon, J.H. Ji, W.-S. Lee, Development of a classification system for extrinsic hair damage: standard grading of electron microscopic findings of damaged hairs, The American Journal of Dermatopathology. 32 (2010) 432–438.

[236] K. Kuwayama, H. Miyaguchi, T. Yamamuro, K. Tsujikawa, T. Kanamori, Y.T. Iwata, H. Inoue, Micro-pulverized extraction pretreatment for highly sensitive analysis of 11-nor-9-carboxy-Δ(9) -tetrahydrocannabinol in hair by liquid chromatography/tandem mass spectrometry., Rapid Communications in Mass Spectrometry. 29 (2015) 2158–66.

[237] C. Staub, Chromatographic procedures for determination of cannabinoids in biological samples, with special attention to blood and alternative matrices like hair, saliva, sweat and meconium, Journal of Chromatography B: Biomedical

Sciences and Applications. 733 (1999) 119–126.

[238] M.J. Burgueño, A. Alonso, S. Sánchez, Amphetamines and Cannabinoids testing in hair: evaluation of results from a two-year period, Forensic Science International. 265 (2016) 47–53.

[239] E. Lendoiro, Ó. Quintela, A. de Castro, A. Cruz, M. López-Rivadulla, M. Concheiro, Target screening and confirmation of 35 licit and illicit drugs and metabolites in hair by LC–MSMS, Forensic Science International. 217 (2012) 207–215.

[240] C. Coulter, J. Tuyay, M. Taruc, C. Moore, Semi-quantitative analysis of drugs of abuse, including tetrahydrocannabinol in hair using aqueous extraction and immunoassay, Forensic Science International. 196 (2010) 70–73.

[241] G. Merola, S. Gentili, F. Tagliaro, T. Macchia, Determination of different recreational drugs in hair by HS-SPME and GC/MS, Analytical and Bioanalytical Chemistry. 397 (2010) 2987–2995.

[242] J.Y. Kim, S. Suh, M.K. In, K.-J. Paeng, B.C. Chung, Simultaneous determination of cannabidiol, cannabinol, and ΔgD9-tetrahydrocannabinol in human hair by gas chromatography-mass spectrometryin human hair by gas chromatography-mass spectrometry, Archives of Pharmacal Research. 28 (2005) 1086–1091.

[243] E. Han, Y. Park, E. Kim, S. In, W. Yang, S. Lee, H. Choi, S. Lee, H. Chung, J.M. Song, Simultaneous analysis of Δ(9)-tetrahydrocannabinol and 11-nor-9-carboxy-tetrahydrocannabinol in hair without different sample preparation and derivatization by gas chromatography-tandem mass spectrometry., Journal of Pharmaceutical and Biomedical Analysis. 55 (2011) 1096–103.

[244] R. Marsili, S. Martello, M. Felli, S. Fiorina, M. Chiarotti, Hair testing for Δ9-THC-COOH by gas chromatography/tandem mass spectrometry in negative chemical ionization mode, Rapid Communications in Mass Spectrometry. 19 (2005) 1566–1568.

[245] M. Conti, V. Tazzari, M. Bertona, M. Brambilla, P. Brambilla, Surface-activated chemical ionization combined with electrospray ionization and mass spectrometry for the analysis of cannabinoids in biological samples. Part I: Analysis of 11-nor-9-carboxytetrahydro-cannabinol, Rapid Communications in Mass Spectrometry. 25 (2011) 1552–1558.

[246] E. Han, W. Yang, S. Lee, E. Kim, S. In, H. Choi, S. Lee, H. Chung, J.M. Song, Establishment of the measurement uncertainty of 11-nor-D9-tetrahydrocannabinol-9-carboxylic acid in hair., Forensic Science International. 206 (2011) 85–92.

[247] J.Y. Kim, K.I. Moon, Determination of 11-nor-Δ9-tetra-hydrocannabinol-9-carboxylic acid in hair using gas chromatography/tandem mass spectrometry in negative ion chemical ionization mode, Rapid Communications in Mass Spectrometry. 21 (2007) 1339–1342.

[248] M. Chiarotti, L. Costamagna, Analysis of 11-nor-9-carboxy-Δ9-tetrahydrocannabinol in biological samples by gas chromatography tandem mass spectrometry (GC/MS-MS), Forensic Science International. 114 (2000) 1–6.

[249] V. Lobodin, E. Maksimova, R. Rodgers, Gas Chromatography/Atmospheric Pressure Chemical Ionization Tandem Mass Spectrometry for Fingerprinting the Macondo Oil Spill, Analytical Chemistry (Washington). 88 (2016) 6914.

[250] F. Hernández, M. Ibáñez, T. Portolés, M.I. Cervera, J. V Sancho, F.J. López, Advancing towards universal screening for organic pollutants in waters, Journal of Hazardous Materials. 282 (2015) 86–95.

[251] Z. Cheng, F. Dong, J. Xu, X. Liu, X. Wu, Z. Chen, X. Pan, J. Gan, Y. Zheng, Simultaneous determination of organophosphorus pesticides in fruits and vegetables using atmospheric pressure gas chromatography quadrupole-time-of-flight mass spectrometry, Food Chemistry. 231 (2017) 365–373.

[252] T. Portolés, C. Sales, M. Abalos, J. Sauló, E. Abad, Evaluation of the capabilities of atmospheric pressure chemical ionization source coupled to tandem mass spectrometry for the determination of dioxin-like polychlorobiphenyls in complex-matrix food samples, Analytica Chimica Acta. 937 (2016) 96–105.

[253] L. Cherta, T. Portolés, E. Pitarch, J. Beltran, F.J. López, C. Calatayud, B. Company, F. Hernández, Analytical strategy based on the combination of gas chromatography coupled to time-of-flight and hybrid quadrupole time-of-flight mass analyzers for non-target analysis in food packaging, Food Chemistry. 188 (2015) 301–308.

[254] A. Carrasco-Pancorbo, E. Nevedomskaya, T. Arthen-Engeland, T. Zey, G. Zurek, C. Baessmann, A.M. Deelder, O.A. Mayboroda, Gas chromatography/atmospheric pressure chemical ionization-time of flight mass spectrometry: analytical validation and applicability to metabolic profiling, Analytical Chemistry. 81 (2009) 10071–10079.

[255] W.F. Duvivier, R.J.P. Peeters, T.A. van Beek, M.W.F. Nielen, Evidence based decontamination protocols for the removal of external Δ9-tetrahydrocannabinol (THC) from contaminated hair, Forensic Science International. 259 (2016) 110–118.

[256] B. Molnár, I. Molnár-Perl, The role of alkylsilyl derivatization techniques in the analysis of illicit drugs by gas chromatography, Microchemical Journal. 118 (2015) 101–109.

[257] R.H. Lowe, E.L. Karschner, E.W. Schwilke, A.J. Barnes, M.A. Huestis, Simultaneous quantification of Delta9-tetrahydrocannabinol, 11-hydroxy-Delta9-tetrahydrocannabinol, and 11-nor-Delta9-tetrahydrocannabinol-9-carboxylic acid in human plasma using two-dimensional gas chromatography, cryofocusing, and electron impact-mass s, Journal of Chromatography. A. 1163 (2007) 318–27.

[258] W.E. Brewer, S.T. Ellison, S.L. Morgan, Automated Extraction, Derivatization and

GC/MS Determination of Tetrahydrocannabinol and Metabolites in Whole Blood Using Disposable Pipette Extraction, Gerstel Appnote. (2008).

[259] M.J. Baptista, P.V. Monsanto, E.G. Pinho Marques, A. Bermejo, S. Ávila, A.M. Castanheira, C. Margalho, M. Barroso, D.N. Vieira, Hair analysis for Δ9-THC, Δ9-THC-COOH, CBN and CBD, by GC/MS-EI: Comparison with GC/MS-NCI for Δ9-THC-COOH, Forensic Science International. 128 (2002) 66–78.

[260] R. Andrews, S. Paterson, Production of Identical Retention Times and Mass Spectra for Δ9-Tetrahydrocannabinol and Cannabidiol Following Derivatization with Trifluoracetic Anhydride with 1,1,1,3,3,3-Hexafluoroisopropanol, Journal of Analytical Toxicology. 36 (2012) 61–65.

[261] T. Nadulski, F. Sporkert, M. Schnelle, A.M. Stadelmann, P. Roser, T. Schefter, F. Pragst, Simultaneous and sensitive analysis of THC, 11-OH-THC, THC-COOH, CBD, and CBN by GC-MS in plasma after oral application of small doses of THC and cannabis extract, Journal of Analytical Toxicology. 29 (2005) 782–789.

[262] R. Sears, Solid phase extraction of THC, THC-COOH and 11-OH-THC from whole blood, Agilent Application Note. (n.d.).

[263] B. Guthery, T. Bassindale, A. Bassindale, C.T. Pillinger, G.H. Morgan, Qualitative drug analysis of hair extracts by comprehensive two-dimensional gas chromatography/time-of-flight mass spectrometry., Journal of Chromatography. A. 1217 (2010) 4402–10.

[264] D.W. Lachenmeier, L. Kroener, F. Musshoff, B. Madea, Application of tandem mass spectrometry combined with gas chromatography and headspace solid-phase dynamic extraction for the determination of drugs of abuse in hair samples, Rapid Communications in Mass Spectrometry. 17 (2003) 472–478.

[265] C. English, Column Bleed & Septa Bleed – Same Old Thing!, Chromablography. (2013). https://blog.restek.com/?p=10706 (accessed October 29, 2018).

[266] S. V Malysheva, J.D. Di Mavungu, I.Y. Goryacheva, S. De Saeger, A systematic assessment of the variability of matrix effects in LC-MS/MS analysis of ergot alkaloids in cereals and evaluation of method robustness, Analytical and Bioanalytical Chemistry. 405 (2013) 5595–5604.

[267] M.D. Hernando, M. Petrovic, A.R. Fernández-Alba, D. Barceló, Analysis by liquid chromatography–electrospray ionization tandem mass spectrometry and acute toxicity evaluation for β-blockers and lipid-regulating agents in wastewater samples, Journal of Chromatography A. 1046 (2004) 133–140.

[268] M.J. Gómez, M. Petrović, A.R. Fernández-Alba, D. Barceló, Determination of pharmaceuticals of various therapeutic classes by solid-phase extraction and liquid chromatography–tandem mass spectrometry analysis in hospital effluent wastewaters, Journal of Chromatography A. 1114 (2006) 224–233.

[269] B.K. Matuszewski, M.L. Constanzer, C.M. Chavez-Eng, Strategies for the assessment of matrix effect in quantitative bioanalytical methods based on

HPLC− MS/MS, Analytical Chemistry. 75 (2003) 3019–3030.

[270] M.C. Cela-Pérez, F. Bates, C. Jimenez-Morigosa, E. Lendoiro, A. de Castro, A. Cruz, M. Lopez-Rivadulla, J.M. Lopez-Vilarino, M.V. González-Rodríguez, Water-compatible imprinted pills for sensitive determination of cannabinoids in urine and oral fluid, Journal of Chromatography A. 1429 (2016) 53–64.

[271] J. Sánchez-González, R. Salgueiro-Fernández, P. Cabarcos, A.M. Bermejo, P. Bermejo-Barrera, A. Moreda-Piñeiro, Cannabinoids assessment in plasma and urine by high performance liquid chromatography–tandem mass spectrometry after molecularly imprinted polymer microsolid-phase extraction, Analytical and Bioanalytical Chemistry. 409 (2017) 1207–1220.

[272] Y. V Patrushev, Advantages of two-dimensional gas chromatography, Kinetics and Catalysis. 56 (2015) 386–393.

[273] F.T. Peters, O.H. Drummer, F. Musshoff, Validation of new methods, Forensic Science International. 165 (2007) 216–224.

[274] M. Taylor, R. Lees, G. Henderson, A. Lingford-Hughes, J. Macleod, J. Sullivan, M. Hickman, Comparison of cannabinoids in hair with self-reported cannabis consumption in heavy, light and non-cannabis users, Drug and Alcohol Review. 36 (2017) 220–226.

[275] Food and drug Administration, 510(k) SUBSTANTIAL EQUIVALENCE DETERMINATION DECISION SUMMARY DEVICE ONLY TEMPLATE, (n.d.). https://www.accessdata.fda.gov/cdrh_docs/reviews/K040257.pdf?fbclid=IwAR32rB7P2dTi9MDSCUEWNzt04ni_tOz1vQxBsOUvW-w1NNdcylu06QvfKnU (accessed November 11, 2018).

[276] C. Moore, Hair Analysis for Drugs: Cut-off Concentrations Analytes Stability, Drug Testing Advisory Board. (n.d.). https://www.samhsa.gov/sites/default/files/meeting/documents/july_2013_moore_compliant.pdf?fbclid=IwAR3_TNJYiGroFT6zglRYyg-YfYsymXsPd47nvUJZOeebp70gjIHqobeWKEg (accessed November 11, 2018).

[277] F.J. Cox, M. V Johnston, A. Dasgupta, Characterization and relative ionization efficiencies of end-functionalized polystyrenes by matrix-assisted laser desorption/ionization mass spectrometry, Journal of the American Society for Mass Spectrometry. 14 (2003) 648–657.

[278] J. Soltwisch, T.W. Jaskolla, F. Hillenkamp, M. Karas, K. Dreisewerd, Ion yields in UV-MALDI mass spectrometry as a function of excitation laser wavelength and optical and physico-chemical properties of classical and halogen-substituted MALDI matrixes, Analytical Chemistry. 84 (2012) 6567–6576.

[279] T.W. Jaskolla, D.G. Papasotiriou, M. Karas, Comparison between the matrices α-cyano-4-hydroxycinnamic acid and 4-chloro-α-cyanocinnamic acid for trypsin, chymotrypsin, and pepsin digestions by MALDI-TOF mass spectrometry, Journal of Proteome Research. 8 (2009) 3588–3597.

[280] C. Meriaux, J. Franck, M. Wisztorski, M. Salzet, I. Fournier, Liquid ionic matrixes for MALDI mass spectrometry imaging of lipids., Journal of Proteomics. 73 (2010) 1204–18.

[281] P. Källback, M. Shariatgorji, A. Nilsson, P.E. Andrén, Novel mass spectrometry imaging software assisting labeled normalization and quantitation of drugs and neuropeptides directly in tissue sections, Journal of Proteomics. 75 (2012) 4941–4951.

[282] C. Russo, N. Brickelbank, C. Duckett, S. Mellor, S. Rumbelow, M.R. Clench, Quantitative Investigation of Terbinafine Hydrochloride Absorption into a Living Skin Equivalent Model by MALDI-MSI, Analytical Chemistry. 90 (2018) 10031–10038.

[283] C. Marsching, R. Jennemann, R. Heilig, H.-J. Gröne, C. Hopf, R. Sandhoff, Quantitative imaging mass spectrometry of renal sulfatides: Validation by classical mass spectrometric methods, Journal of Lipid Research. 55 (2014) 2343–2353.

[284] M.R. Groseclose, S. Castellino, A mimetic tissue model for the quantification of drug distributions by MALDI imaging mass spectrometry, Analytical Chemistry. 85 (2013) 10099–10106.

[285] S. Schulz, D. Gerhardt, B. Meyer, M. Seegel, B. Schubach, C. Hopf, K. Matheis, DMSO-enhanced MALDI MS imaging with normalization against a deuterated standard for relative quantification of dasatinib in serial mouse pharmacology studies, Analytical and Bioanalytical Chemistry. 405 (2013) 9467–9476.

[286] T. Rao, B. Shen, Z. Zhu, Y. Shao, D. Kang, X. Li, X. Yin, H. Li, L. Xie, G. Wang, Y. Liang, Optimization and evaluation of MALDI TOF mass spectrometric imaging for quantification of orally dosed octreotide in mouse tissues, Talanta. 165 (2017) 128–135.

[287] S.D. Turker, W.B. Dunn, J. Wilkie, MALDI-MS of drugs: Profiling, imaging, and steps towards quantitative analysis, Applied Spectroscopy Reviews. 52 (2017) 73–99.

[288] B.M. Prentice, C.W. Chumbley, R.M. Caprioli, Absolute Quantification of Rifampicin by MALDI Imaging Mass Spectrometry Using Multiple TOF/TOF Events in a Single Laser Shot, Journal of the American Society for Mass Spectrometry. 28 (2017) 136–144.

[289] P. Källback, A. Nilsson, M. Shariatgorji, P.E. Andrén, MsIQuant - Quantitation Software for Mass Spectrometry Imaging Enabling Fast Access, Visualization, and Analysis of Large Data Sets, Analytical Chemistry. 88 (2016) 4346–4353.

[290] D.A. Pirman, R.F. Reich, A. Kiss, R.M.A. Heeren, R.A. Yost, Quantitative MALDI tandem mass spectrometric imaging of cocaine from brain tissue with a deuterated internal standard, Analytical Chemistry. 85 (2013) 1081.

[291] D. Pirman, Quantitative profiling of tissue drug distribution by MS imaging,

Bioanalysis. 7 (2015) 2649–2656.

[292] M. Lagarrigue, R. Lavigne, E. Tabet, V. Genet, J.-P. Thomé, K. Rondel, B. Guével, L. Multigner, M. Samson, C. Pineau, Localization and in situ absolute quantification of chlordecone in the mouse liver by MALDI imaging, Analytical Chemistry. 86 (2014) 5775–5783.

[293] K.M. Park, J.H. Moon, K.P. Kim, S.H. Lee, M.S. Kim, Relative quantification in imaging of a peptide on a mouse brain tissue by matrix-assisted laser desorption ionization, Analytical Chemistry. 86 (2014) 5131–5135.

[294] B. Guthery, A. Bassindale, C.T. Pillinger, G.H. Morgan, The detection of various opiates and benzodiazepines by comprehensive two-dimensional gas chromatography/time-of-flight mass spectrometry, Rapid Communications in Mass Spectrometry. 23 (2009) 340–348.

Appendix I

Sample	THC (H)	CBD (H)	CBN (H)	11-OH (H)	COOH (H)	THC (W)	CBD (W)	CBN (W)	11-OH (W)	COOH (W)	Time since last use	Est lifetime use (cannabis cigarettes)
A	27.84	+	18.19	0.21	ND	22.57	59.31	229.86	1.90	ND	2-3 days	1350
B	13.65	+	9.25	0.27	ND	6.98	115.66	246.38	6.68	ND	2-3 days	1800
C	<LOQ	ND	1.4	ND	0.16	ND	6.59	1.08	ND	ND	>1 week	10
D	31.39	+	15.45	0.32	0.32	8.24	ND	6.85	ND	ND	2-3 days	2214
E	2.12	+	3.12	ND	0.38	ND	268.43	3.27	<LOQ	ND	>1 week	126
F	ND	ND	ND	ND	ND	ND	9.60	0.37	ND	0.05	>1 week	3280
G	ND	ND	1.72	ND	ND	ND	10.46	0.28	ND	ND	4-5 days	1440
H	1.30	ND	1.70	ND	ND	ND	ND	1.02	ND	ND	>1 week	216
I	1.94	ND	4.07	ND	ND	ND	ND	43.36	ND	ND	4-5 days	264
J	1.56	ND	4.87	ND	ND	2.47	14.05	12.43	ND	ND	>1 week	168

Table A-1 cannabinoid concentrations (pg/mg) in hair (H) and wash (W) of self-report frequent cannabis users. ND not detected, + shows that CBD was detected, <LOQ shows that the concentration was above the limit of detection and lower than the limit of quantification.

Sample	THC (H)	CBD (H)	CBN (H)	11-OH (H)	COOH (H)	THC (W)	CBD (W)	CBN (W)	11-OH (W)	COOH (W)	Time since last use	Est lifetime use (cannabis cigarettes)
k	<LOQ	ND	1.70	ND	ND	ND	124.28	1.99	ND	ND	n/a	2
l	<LOQ	ND	2.15	ND	ND	ND	923.34	35.14	ND	ND	>1 week	4
m	ND	ND	1.53	ND	ND	ND	11.65	0.13	ND	ND	>1 week	3
n	<LOQ	ND	1.62	ND	ND	ND	41.42	2.55	0.09	ND	n/a	3
o	<LOQ	ND	1.56	ND	ND	ND	1144.70	5.14	ND	ND	n/a	2

Table A-2 cannabinoid concentrations (pg/mg) in hair (H) and wash (W) of self-report infrequent cannabis users. ND not detected, + shows that CBD was detected, <LOQ shows that the concentration was above the limit of detection and lower than the limit of quantification.

Sample	THC (H)	CBD (H)	CBN (H)	11-OH (H)	COOH (H)	THC (W)	CBD (W)	CBN (W)	11-OH (W)	COOH Wash (W)	Time since last use	Est. lifetime use (cannabis cigarettes)
p	ND	ND	1.512	ND	ND	ND	ND	17.03	ND	ND	n/a	0
q	ND	ND	2.578	ND	ND	ND	30.904	0.20	ND	ND	n/a	0
r	ND	ND	<LOQ	ND	ND	ND	ND	0.10	ND	ND	n/a	0
s	ND	ND	1.902	ND	ND	ND	29.620	0.12	ND	0.10	n/a	0
t	<LOQ	ND	1.578	ND	ND	ND	ND	13.17	ND	ND	n/a	0
u	<LOQ	+	1.297	ND	0.423	ND	ND	0.44	ND	ND	n/a	0
v	<LOQ	ND	1.536	ND	0.304	ND	76.903	2.63	ND	ND	n/a	0
w	ND	ND	ND	ND	ND	ND	75.285	0.99	ND	ND	n/a	0
x	<LOQ	ND	<LOQ	ND	ND	ND	ND	3.91	ND	ND	n/a	0
y	1.567	+	2.09	ND	ND	ND	15.941	7.07	0.53	2.11	n/a	0
z	ND	ND	ND	ND	ND	22.57	211.415	23.26	8.80	5.84	n/a	0

Table A-3 cannabinoid concentrations (pg/mg) in hair (H) and wash (W) of self-reporting non-cannabis users. ND not detected, + shows that CBD was detected, <LOQ shows that the concentration was above the limit of detection and lower than the limit of quantification.

Appendix II

analytical chemistry

Article

pubs.acs.org/ac

Detection and Mapping of Cannabinoids in Single Hair Samples through Rapid Derivatization and Matrix-Assisted Laser Desorption Ionization Mass Spectrometry

Emma Beasley, Simona Francese, and Tom Bassindale*

Centre for Mass Spectrometry Imaging, Biomolecular Research Centre, Sheffield Hallam University, Howard Street, S1 1WB Sheffield, United Kingdom

ABSTRACT: The sample preparation method reported in this work has permitted for the first time the application of matrix-assisted laser desorption ionization mass spectrometry (MALDI-MS) profiling and imaging for the detection and mapping of cannabinoids in a single hair sample. MALDI-MS imaging analysis of hair samples has recently been suggested as an alternative technique to traditional methods of GC/MS and LC/MS due to simpler sample preparation, the ability to detect a narrower time frame of drug use, and a reduction in sample amount required. However, despite cannabis being the most commonly used illicit drug worldwide, a MALDI-MS method for the detection and mapping of cannabinoids in a single hair has not been reported. This is probably due to the poor ionization efficiency of the drug and its metabolites and low concentration incorporated into hair. This research showed that in situ derivatization of cannabinoids through addition of an *N*-methylpyridium group resulted in improved ionization efficiency, permitting both detection and mapping of Δ^9-tetrahydrocannabinol (THC), cannabinol (CBN), cannabidiol (CBD), and the metabolites 11-nor-9-carboxy-Δ^9-tetrahydrocannabinol (THC-COOH), 11-hydroxy-Δ^9-tetrahydrocannabinol (11-OH-THC), and 11-nor-9-carboxy-Δ^9-tetrahydrocannabinol glucuronide (THC-COO-glu). Additionally, for the first time an in-source rearrangement of THC was observed and characterized in this paper, thus contributing to new and accurate knowledge in the analysis of this drug by MALDI-MS.

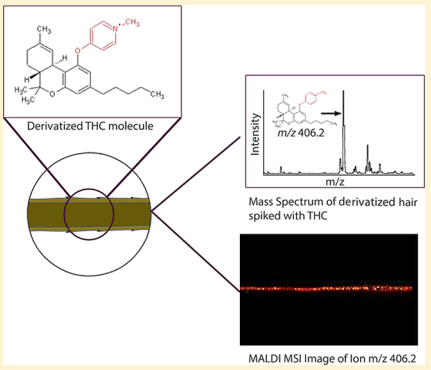

The use of hair as an alternative biological sample in toxicological analysis is well documented. This is due to the fact that hair offers a longer time frame to detect drug use than the more traditional blood or urine. By measuring the length of the hair and approximating the rate of hair growth (1 cm/month on average),[1] it is possible to estimate when specific drug intake occurred, over a time period as long as the length of the hair allows (weeks, months, or even years).[2] This is in stark contrast to blood and urine analysis, where most drugs cannot be detected beyond a few hours to days after intake.[3] Some important applications of hair samples for retrospective detection of drug intake include investigating drug-facilitated crime, workplace testing, child protection cases, and therapeutic monitoring.

Hair analysis is often used to identify cannabis consumption. Cannabis continues to be the most widely used illicit drug in England and Wales, with an estimated 6.7% of adults having used cannabis in the last year,[4] a higher percentage than the European average of 5.7%.[5] Δ^9-Tetrahydrocannabinol (THC) is the main psychoactive constituent of cannabis. THC undergoes a complex hepatic metabolism based on oxidation and subsequent glucuronidation.[6] Since this enzymatic pathway is present only in vivo, metabolite detection has been suggested as a solution to external contamination problems associated with solely analyzing THC content in hair samples.[1] The main oxidative metabolites of THC are 11-hydroxy-Δ^9-tetrahydrocannabinol (11-OH-THC) and 11-nor-9-carboxy-Δ^9-tetrahydrocannbinol (THC-COOH). This molecule then undergoes glucuronidation (phase II metabolism) to form 11-nor-9-carboxy-Δ^9-tetrahydrocannabinol glucuronide (THC-COO-glu)[7] as shown in Figure 1. Other cannabinoids routinely analyzed in hair samples include the *Cannabis sativa* plant degradation products cannabinol (CBN) and cannabidiol (CBD).[8−13]

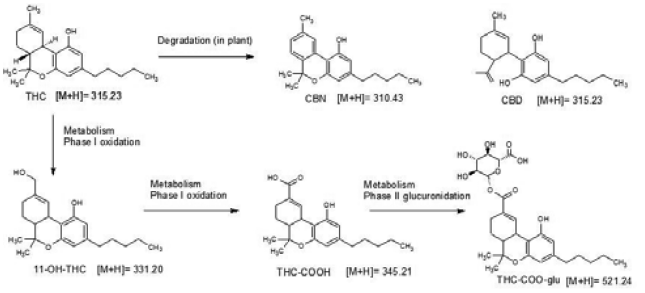

Figure 1. Degradation (ex vivo) and metabolic (in vivo) pathways of THC.

Received: September 8, 2016
Accepted: September 20, 2016
Published: September 20, 2016

DOI: 10.1021/acs.analchem.6b03551
Anal. Chem. 2016, 88, 10328−10334

THC and associated cannabinoids and metabolites can already be detected in hair samples by standard analytical techniques such as gas chromatography (GC)/mass spectrometry (MS)[12,14−18] and liquid chromatography (LC)/MS.[19−23] However, GC/MS requires multiple laborious and time-consuming steps before chromatographic analysis can take place, including digestion, extraction, sample cleanup, and derivatization.

LC/MS has gained in popularity over recent years, as the aforementioned derivatization step is often not needed for successful analysis. However, both methods require a large amount of hair sample (10−50 mg). GC/MS and LC/MS analyses typically give a time of intake accuracy of 1 month due to the common practice of segmenting the hair into 1 cm pieces before analysis.

More recently, direct analysis in real time (DART) has been proposed as a method for the analysis of cannabinoids and cocaine in hair samples;[2,24] however, this method is not able to distinguish between the two isobaric species of THC and CBD, despite tandem mass spectrometric (MS/MS) analysis, because both compounds result in the same product ions. In addition to this, a large sample size is required, and currently the method is applicable only to high levels of THC associated with chronic users because the detection limit is approximately 5 ng/mg of hair. The authors stated that DART "should only be considered as a rapid pre-screening method"; however, this could result in false negative results for lower-level users.

Matrix-assisted laser desorption ionization mass spectrometry (MALDI-MS) has been highlighted as a potential hair analysis method due to several advantages over current techniques, including improved chronological information,[25] simpler sample preparation, and ability to detect drugs on one single hair. Several drugs have already been analyzed in hair samples by MALDI-MS, including methamphetamine[26] and analogues,[27] cocaine,[28−31] ketamine,[32] Zolpidem,[33] and nicotine[34] by utilizing an α-cyano-4-hydroxycinnamic acid (CHCA) matrix without the need for analyte derivatization. Cannabis products were determined in the work of Musshof et al.,[29] but they were unable to determine the difference between the isobaric THC and CBD and did not look for any in vivo metabolites.

In this study, initial experiments suggested the occurrence of an in-source rearrangement of the THC molecule; in addition to low analyte ionization efficiency, this highlighted the low probability of success in mapping cannabinoids in hair samples by MALDI-MS imaging. However, the final method developed included the novel use of 2-fluoro-1-Methylpyridinium *p*-tolunesolfonate (FMTPS) derivatization of hair samples in situ and showed greatly improved detection of cannabinoids and metabolites, allowing these species to be mapped by MALDI-MS imaging.

EXPERIMENTAL SECTION

Materials and Reagents. α-Cyano-4-hydroxycinnamic acid (CHCA), trifluoroacetic acid (TFA), 2-fluoro-1-methylpyridinium *p*-toluenesulfonate (FMPTS), and triethylamine (TEA) were purchased from Sigma−Aldrich. Cannabinol (CBN), cannabidiol (CBD), Δ^9-tetrahydrocannabinol (THC), 11-nor-9-carboxy-Δ^9-tetrahydrocannabinol (THC-COOH), 11-hydroxy-Δ^9-tetrahydrocannabinol (11-OH-THC), Δ^9-tetrahydrocannabinolic acid A (THCA-A), and 11-nor-9-carboxy-Δ^9-tetrahydrocannabinol glucuronide (THC-COO-glu) were purchased as analytical references from Cerilliant (Sigma−Aldrich). Acetonitrile (ACN) and methanol were purchased from Fisher Scientific.

Sample Preparation. CHCA was prepared at 5 mg/mL with the solvent composition being 70:30 ACN/0.2% aqueous TFA. Cannabinoid standards were mixed 1:1 with the matrix solution and deposited in triplicate on the MALDI target. The spots were left to dry at ambient temperature before analysis. Cannabinoid concentrations were 100 μg/mL.

Derivatization of Standards for MALDI Profiling Analysis. Derivatization was carried out according to Thieme et al.[35] Briefly, 40 μL of FMPTS (10 mg/mL in acetonitrile) and 10 μL of triethylamine were mixed by vortexing. This caused the colorless solution to turn canary yellow as previously reported.[35,36] A 20 μL aliquot of each cannabinoid standard (100 μg/mL) was then added, and the solutions were left at room temperature for 5 min. A sample (1 μL) of each solution was then spotted onto a target plate.

Spiking of Hair. Hair samples from an individual who reported not using any illicit drugs were collected by cutting and washed with methanol and water by vortexing. The samples were then cut into 5 cm sections and placed into the bottom of a well in a 24-well cell culture plate in order to keep the spiking solution volume to a minimum while still submerging the hairs. The limitation of 5 cm is due to the size of a MALDI target plate. Spiked samples were prepared by soaking in 300 μL of 0.5 μg/mL cannabinoid standard solution. Blank hair samples were prepared by soaking in 300 μL of methanol. The plate was sealed with tape to avoid evaporation of the standards. All hairs were soaked for 2 h, removed, and allowed to dry for 1 h at room temperature.

User Hair Sample. The hair sample collection was approved by the Sheffield Hallam University Research Ethics committee (SHU ethics number 13-2011). The hair sample was provided from a male volunteer who self-reported smoking cannabis once a week. The hairs were less than 5 cm in length. To wash, the hairs were placed in a clean test tube with methanol (5 mL) and briefly vortexed before being removed. This was repeated twice and the hairs were then left for 2 h at room temperature to dry.

In Situ Derivatization of Cannabinoids. The hair was placed on a glass slide by use of double-sided Sellotape Super Clear tape. Derivatization reagent (2.5 mL) was then sprayed by use of a Neo for Iwata airbrush at a pressure of 30 psi onto an area of 9 cm^2, with the sample in the center of the area. This step was carried out in a fume hood due to hazards associated with use of the triethylamine catalyst.

Deposition of Matrix for Imaging. The hairs were coated in CHCA at 5 mg/mL, with the solvent composition being 70:30 ACN/0.2% aqueous TFA, by use of the SunCollect autospraying system (SunChrom GmbH, Friedrichsdorf, Germany). Fifteen layers were sprayed at a flow rate of 2 μL/min.

INSTRUMENTATION

MALDI Instrumentation and Analytical Conditions. All data were acquired in positive-ion mode on an Applied Biosystems/MDS Sciex hybrid quadrupole time-of-flight mass spectrometer (Q-Star Pulsar-*i*) with an orthogonal MALDI ion source (Applied Biosystems, Foster City, CA) and a neodymium-doped yttrium aluminum garnet (Nd:YAG) laser (355 nm, 1 kHz). The laser power was 30% (1000 Hz, 3.2 μJ), with an elliptical spot size of 100 × 150 μm.[37] Image acquisition was performed in raster image mode.[38] Declustering potential 2 was

DOI: 10.1021/acs.analchem.6b03551
Anal. Chem. 2016, 88, 10328−10334

set at 15 arbitrary units and the focusing potential at 20 arbitrary units, with an accumulation time of 0.999 s. The MALDI-MS/MS images were obtained with argon as the collision gas; the declustering potential 2 was set at 15 and the focusing potential at 20, and the collision energy and collision gas pressure were set at 20 and 5 arbitrary units, respectively.

Images were acquired with oMALDI Server 5.1 software supplied by MDS Sciex (Concord, Ontario, Canada) and processed with Biomap 3.7.5 software (www.maldi-msi.org) to generate black and white images for each m/z ratio of interest. Further image analysis and processing was performed with the public domain software ImageJ (NIH; http://rsb.info.nih.gov/ij), where the previous black and white images were assigned different colors and overlaid to create one final image.

LC/MS Instrumentation and Analytical Conditions. All experiments were performed on a Thermo Finnigan LCQ classic quadrupole ion-trap liquid chromatography mass spectrometer with electrospray ionization (ESI) interfaced to a liquid chromatography system. The system used also consisted of an autosampler and autoinjector. The column used was a Phemonex Lunar C18 (150 mm × 1 mm, 5 μm) with a corresponding guard column. LC/MS/MS chromatographic separation was realized by gradient elution according to a previously published method by Roth et al.[39] Briefly, 0.1% HCOOH in water was used as mobile phase A, and ACN + 0.1% HCOOH was used as mobile phase B. Mobile phase A was gradually reduced over time while mobile phase B was increased from 20% to 95%. The total run time was 15 min, with the THC molecule eluting at 4 min.

RESULTS AND DISCUSSION

Profiling of THC. In preliminary MALDI-MS profiling experiments, analyses were carried out on the cannabinoid standard THC as purchased from the supplier. We immediately observed a detection issue due to interference from a matrix ion peak (m/z 315.10 as seen in Figure 2A, which is more apparent at concentrations lower than 100 μg/mL) in addition to a general low ionization yield in MALDI, as previously reported.[40] For this reason, different matrix systems were tried, including type and amount of matrix [2,5-dihydroxybenzoic acid (DHB), 6-aza-2-thiothymine (ATT), 3-hydroxycoumarin (3-HC), and 2′,4′,6′-trihydroxyacetophenone monohydrate (THAP)], different solvent compositions, different amounts of trifluoroacetic acid (TFA), and the addition of additives [cetrimonium bromide (CTAB), lithium salts, and aniline]. In addition, negative mode analysis was conducted with 9-aminoacridine (9-AA) matrix. None of these experiments improved the detection of THC beyond that achieved with CHCA, and they will not be discussed further in this paper. Another observation from these MALDI profiling spectra was the presence of m/z peaks at 313.22 and 315.23 (Figure 2A). While the peak at 315.23 fitted the expected monoisotopic m/z of THC, the peak at 313.22 was unexplained. However, the absence of a peak at m/z 313.22 in the matrix blanks suggests that it is in fact associated with the THC molecule.

In order to investigate this phenomenon further, LC/MS/MS analysis of the THC standard (100 ug/mL) was carried out. A single peak in the chromatogram confirmed the purity of the THC standard. Interestingly, the peak at m/z 313.22 had 3% of the intensity of the m/z 315.23 peak (seen on MALDI at approximately 110%; Figure 2A), and the isotopic peak at m/z 314.23 was no longer detected. In addition, since this LC/MS

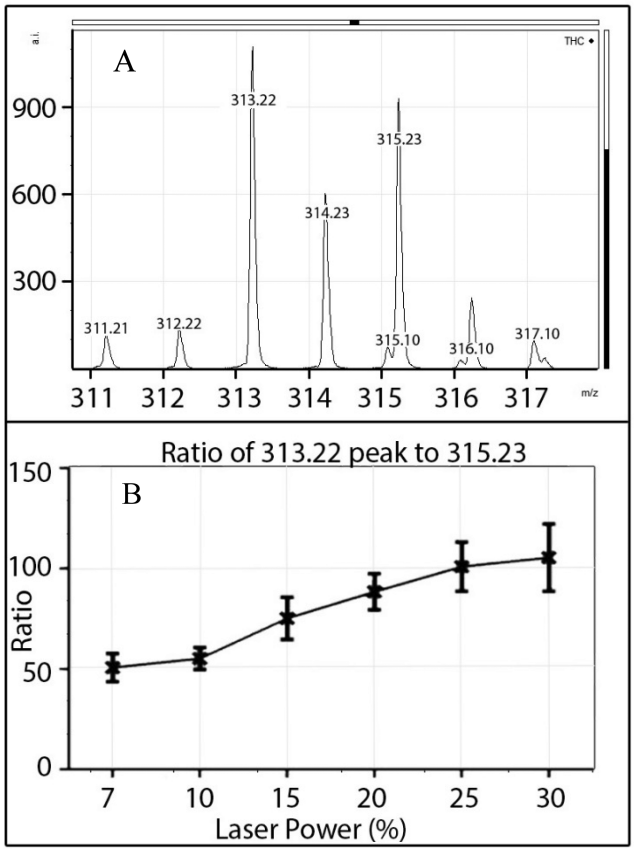

Figure 2. (A) m/z region 311−317 of THC standard with CHCA matrix. (B) Ratio of signal intensity of peaks m/z 313.22 to 315.25 at increasing laser energies.

system utilizes electrospray ionization, it is reasonable to assume that the additional peak at m/z 313.22 is specific to the MALDI ionization process, and we hypothesized that it could be dependent on the laser energy. In fact, experimentally it was observed that increasing laser power causes the ratio of m/z 313.22 to 315.23 signal intensity to increase (Figure 2B).

One possible explanation for this observation is a laser-induced rearrangement of the THC molecule. The loss of hydrogens as free radicals would increase the conjugation of the THC molecule, making it more stable and so the rearrangement would be more favorable. MS/MS spectra of m/z peaks 313.1 and 315.1 obtained by direct infusion of the THC standard also support this theory; the MS/MS spectrum of the parent ion at m/z 315.1 is shown in Figure 3A(i), and that of the rearranged parent ion at m/z 313.1 is shown in Figure 3A(ii). The spectra are very similar to many fragments formed from common mass losses (peaks labeled with stars), demonstrating that these peaks refer to the same (THC) species. Both the parent ions and many of the product ions have a mass shift of −2 Th, suggesting the loss of two hydrogens from the THC parent ion.

Bijlsma et al.[41] reported the fragmentation pathway of THC-COOH, including fragments at m/z 193 and 257, based on MS^E accurate mass data. These fragments would be identical for THC-COOH and THC due to loss of the COOH group from the molecule. In this analysis the m/z 259 and 193 ions were observed in the MS/MS spectrum of the 315.1 parent ion, while we also observed a shift to m/z 257 in the MS/MS spectrum of the 313.1 parent ion. The 193 fragment was

DOI: 10.1021/acs.analchem.6b03551
Anal. Chem. 2016, 88, 10328−10334

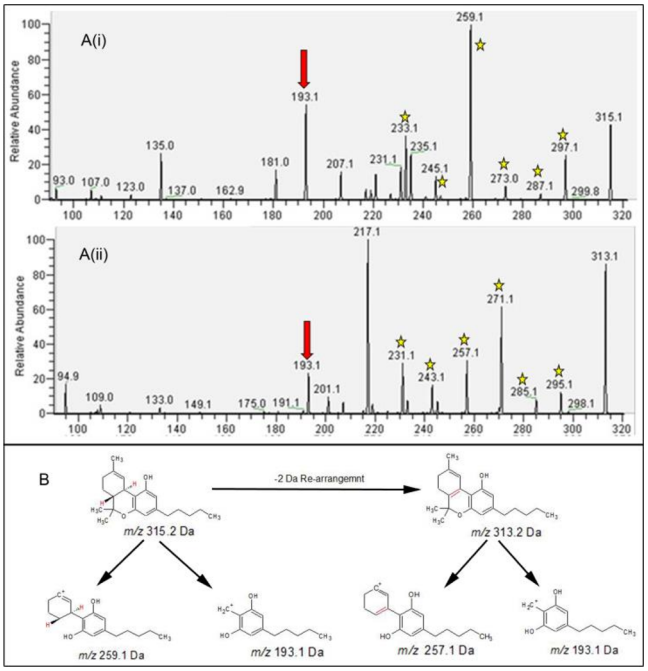

Figure 3. (A) MS/MS spectra of THC. Product ion mass spectra of (i) m/z 315 and (ii) m/z 313 are shown. Both spectra were obtained through direct infusion on an LCQ instrument. Peaks with a star symbol denote a mass shift of 2 Th. (B) Proposed rearrangement of THC and structures of fragments present at m/z 259, 257, and 193 (257 and 193 structures as proposed by Bijlsma et al.[41]).

present in both MS/MS spectra, indicating this fragment does not contain the proposed site of the rearrangement (see Figure 3B).

Derivatization of Cannabinoids. Once the nature of the peak at m/z 313.22 was elucidated, in order to avoid rearrangement due to the laser energy, a chemical modification of THC was carried out. Derivatization has previously been identified as a possible strategy to improve signal intensity and decrease matrix interference.[42,43]

The target for derivatization was the hydroxyl group, since all cannabinoids of interest contain this functional group. After careful review of the literature, the derivatization method using 2-fluoro-1-methylpyridinium *p*-tolunesolfonate (FMPTS) to form an *N*-methylpyridinium derivative, as reported by Quirke et al.[36] for the detection of alcohols by ESI-MS, was chosen. FMPTS derivatization has previously been reported to improve the detection of a range of compounds with alcohol moieties in various sample types including surfactants,[44] estrogens,[45] and the narcotic analgesic burprenorphine,[35] by LC/MS analysis, and polyamides[42] and sterols[46] in MALDI profiling experiments.

This strategy was also selected due to the simplicity of the nucleophilic substitution reaction (which occurs readily at room temperature),[47] the stability of the products formed,[44,48] and also the addition of a permanent charge to the analytes. This is of particular importance, as it allows all cannabinoids to be analyzed in positive-ion mode (despite the nonderivatized THC-COOH being theoretically more suited to negative mode).

Derivatization was successful for all cannabinoids of interest, with all peaks being observed and in agreement with the expected monoisotopic m/z values (Table 1). The derivatized species show an addition of 92 amu, as first reported by Quirke et al.[36] and confirmed by others.[45,46]

Table 1. Theoretical and Experimental m/z Ratios for Derivatized and Nonderivatized Cannabinoid Standards

	[M + H]		derivatized [M + 92]	
cannabinoid	theor	exptl	theor	exptl
THC	315.23	315.23	406.27	406.28
CBN	311.20	311.20	402.24	402.24
CBD	315.23	315.23	406.27	406.28
11-OH-THC	331.23	331.23	422.27	422.26
THC-COOH	345.21	345.21	436.25	436.25
THC-COO-glu	521.24	521.25	612.28	612.28

After derivatization, the ions corresponding to nonderivatized cannabinoids were not observed, suggesting that reaction went to completion (or such that nonderivatized cannabinoids remained present at concentrations below the limit of detection). The expected derivatized THC peak at m/z 406.28 was the most abundant in the spectrum. However, there was evidence that rearrangement still occurred, as a peak at m/z 404.27 was observed, though it was present at only 6% of the intensity of the m/z 406.28 peak, as opposed to approximately 100% when run without derivatization. This suggests that the derivatization largely protects THC from rearrangement, possibly due to steric hindrance or increasing the required amount of laser energy to rearrange the molecule. The peak at m/z 406.28 was also observed in the mass spectrum of the derivatized CBD molecule. This was anticipated as THC and CBD are isobaric species; however, an additional peak at m/z 483.32 was also detected in the CBD spectrum; CBD gains two *N*-methylpyridinium groups, as it has one more hydroxyl group than THC. The peak at m/z 483.32 corresponds to the loss of a methyl group from the doubly derivatized molecule expected to be observed at m/z 498.32. Theoretically there could be two additions of the derivatization group to 11-OH-THC and THC-COOH and up to five additions on the THC-COO-glu molecule as a result of multiple hydroxyl groups being present, though corresponding m/z values were not observed. THC-COO-glu was detected at m/z 612.28 in the mass spectrum, corresponding to a single addition, though the peak at m/z 436.25 was much more abundant, suggesting that the glucuronide group readily fragments from the parent molecule during analysis, resulting in detection of THC-COOH. A further experiment in which the laser power used for analysis was increased showed that the ratio of THC-COO-glu to THC-COOH decreased with increasing laser power (data not shown). Another potential interferent in the assay was THCA-A, the biogenic prescursor to THC. This was analyzed by the same method and showed no trace of ions relating to THC or derivatized THC (data not presented).

It was also noted that for all derivatized samples there was almost complete suppression of CHCA matrix-related peaks, as previously observed by Murgasova et al.[42]

Imaging of Cannabinoids in Hair Samples. Once the detection of cannabinoids through derivatization was optimized, this sample preparation method was adapted to permit mapping of these species in single hair samples by MALDI-MS imaging. Preliminarily, blank and cannabinoid spiked hairs were imaged to verify efficiency of the derivatization method for

DOI: 10.1021/acs.analchem.6b03551
Anal. Chem. 2016, 88, 10328−10334

imaging purposes and were compared to hairs that had not gone through the derivatization step (Figure 4).

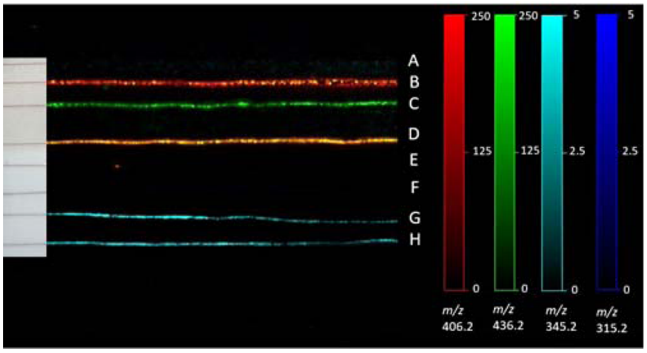

Figure 4. Comparsion between (A–D) derivatized and (E–H) nonderivatized hairs: (A) soaked in methanol and derivatized, (B) soaked in THC standard and derivatized, (C) soaked in THC-COOH standard and derivatized, (D) soaked in a 1:1 mixture of THC and THC-COOH standards and derivatized, (E) soaked in methanol and not derivatized, (F) soaked in THC standard and not derivatized, (G) soaked in THC-COOH standard and not derivatized, and (H) soaked in a mixture of THC and THC-COOH standards and not derivatized.

Unless dramatic modifications are made to contrast and brightness, underivatized hairs soaked in THC standard could not be visualized in the two-dimensional (2D) molecular map, as the ion signals of underivatized THC were of extremely low intensity. Interestingly, THC-COOH could be visualized in the 2D molecular ion map (cyan) in hairs G and H, which were soaked in THC-COOH standard and a mixture of THC and THC-COOH standards, respectively; however, this was also at relatively low intensity (Figure 4). The peak at m/z 406.2, corresponding to derivatized THC, is clearly seen in hair B, which was spiked with THC and subsequently derivatized (red). Similarly, the expected ion at m/z 436.2 was observed in hair C, which was spiked with THC-COOH and subsequently derivatized (green). Hair D, which was spiked with a mixture of THC and THC-COOH and then derivatized, appears yellow in color as both THC and THC-COOH ions are present (a mixture of red and green appears yellow).

Since it was established that derivatization enhances both THC and THC-COOH signals in imaging experiments (as shown in Figure 4), a second mapping experiment with the other cannabinoids was carried out (Figure 5). The peak at m/z 406.2, corresponding to derivatized THC, is clearly seen in hair B, which was spiked with THC and then derivatized (red); the peak at m/z 483.2 was observed in hair C, which was spiked with CBD and derivatized (yellow), the peak at m/z 402.2, corresponding to derivatized CBN, was observed in hair D, which was spiked with CBN and derivatized (blue); the peak at m/z 436.2, corresponding to derivatized THC-COOH, was observed in hair E, which was spiked with THC-COOH and derivatized (green); and finally, the peak at m/z 422.2, corresponding to derivatized 11-OH-THC, was observed in hair F, which was spiked with 11-OH-THC and derivatized (magenta). As with the profiling experiments, THC-COO-glu fragmented to give THC-COOH at m/z 436.2 (green), and its image intensity reflect a 5× lower concentration compared to the other standards due to the concentration in which it is supplied.

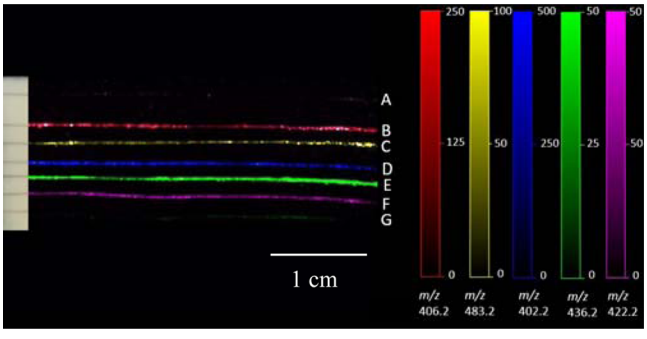

Figure 5. Simultaneous imaging of several cannabinoids of interest: hairs were soaked in (A) methanol, (B) THC, (C) CBD, (D) CBN, (E) THC-COOH, (F) 11-OH-THC, and (G) THC-COO-glu. All hairs were derivatized with FMTPS prior to analysis.

Users' hairs were investigated by the derivatization method coupled with MALDI-MS imaging, employing this optimized method. In particular, MALDI-MS/MS images were obtained of hairs collected from a volunteer who self-reported using cannabis once a week, and the transition from m/z 406.2 derivatized THC parent ion to m/z 110.0 fragment ion was monitored (Figure 6). The product ion at m/z 110.0 corresponds to the hydrated methylpyridinium fragment, which is common to all FTMPS derivatives and has previously been used for confirmation.[44]

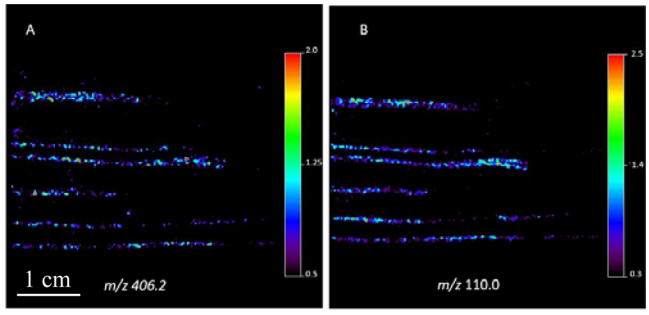

Figure 6. MS/MS image of user hairs: (A) Derivatized THC parent ion at m/z 406.2. (B) Map of fragment ion at m/z 110.

CONCLUSIONS

The use of MALDI imaging and profiling to detect cannabinoids in hair samples following in situ derivatization is presented. The method shows, for the first time, potential to detect cannabinoids from a single hair.

During the development of this method, an interesting, laser-induced THC rearrangement was observed. This caused increased fragmentation of THC and hence low ability to detect the molecule without derivatization. The novel in situ derivatization, completed in minutes at room temperature with FMPTS, showed a greatly increased limit of detection over the nonderivatized analytes and THC, CBD, CBN, and THC metabolites. The ability to detect the metabolites of THC only formed in vivo (THC-COOH, 11-OH-THC, and THC-COO-glu) will enhance the ability of the analyst to distinguish between use and unintentional exposure. During analysis, the THC-COO-glu fragments form THC-COOH, with the consequence that if m/z 436.2 is detected, it cannot be determined which of the analytes was originally present. The m/z 612 peak, however, is unique to THC-COO-glu. This is an

DOI: 10.1021/acs.analchem.6b03551
Anal. Chem. 2016, 88, 10328–10334

advantage over traditional GC/MS methods, where the glucuronide is not generally detected due to the common practice of hydrolysis or digestion of the hair sample, which converts it into THC-COOH.[49]

Prior to integration into a toxicology workflow, a large sample of user hairs should be tested, from different levels of users and with different hair types. The comparison of levels of metabolites detected by traditional methods with the results from MALDI analysis will determine the limit of detection for hair samples and applicability to lower-level users, as well as the possibility of using the method quantitatively in the future. This will allow an assessment of the suitability of the method for users or whether it will be a screen for external contamination. The user hair tested here, from a regular but low-level user, provides proof that the THC at least can be detected.

The method reported has a sample preparation workflow, notwithstanding the derivatization step, that is less time-consuming, due to the lack of extraction step, than traditional GC or LC methods. This method also gives the potential to simultaneously detect THC and metabolites in a single workup and analysis. An additional advantage is the potential of MALDI-MS imaging resolution, allowing increased sensitivity to the time period of use, better than the traditional month-by-month history, although such an approach will require further validation. Analysis of hairs from a known cannabis user has shown applicability of the method to detect THC in real-life samples.

AUTHOR INFORMATION

Corresponding Author

*E-mail t.bassindale@shu.ac.uk.

Notes

The authors declare no competing financial interest.

ACKNOWLEDGMENTS

This work has been funded by a Sheffield Hallam University Vice Chancellors scholarship and the Sheffield Hallam University Biomolecular Research Centre.

REFERENCES

(1) Cooper, G. A. A.; Kronstrand, R.; Kintz, P. *Forensic Sci. Int.* **2012**, *218*, 20−24.
(2) Duvivier, W. F.; van Beek, T. A.; Pennings, E. J. M.; Nielen, M. W. F. *Rapid Commun. Mass Spectrom.* **2014**, *28*, 682−690.
(3) Kintz, P. *Forensic Sci. Int.* **2012**, *218*, 28−30.
(4) Home Office. *Drug misuse: Findings from the 2014/15 crime survey for England and Wales*, 2nd ed., 2015; https://www.gov.uk/government/uploads/system/uploads/attachment_data/file/462885/drug-misuse-1415.pdf.
(5) European Monitoring Centre for Drugs and Drug Addiction. *European Drug Report 2015: Trends and Developments*, 2015; http://www.emcdda.europa.eu/publications/edr/trends-developments/2015.
(6) Sharma, P.; Murthy, P.; Bharath, M. M. *Iran. J. Psychiatry* **2012**, *7*, 149−156.
(7) Mazur, A.; Lichti, C. F.; Prather, P. L.; Zielinska, A. K.; Bratton, S. M.; Gallus-Zawada, A.; Finel, M.; Miller, G. P.; Radomińska-Pandya, A.; Moran, J. H. *Drug Metab. Dispos.* **2009**, *37*, 1496−1504.
(8) Skopp, G.; Strohbeck-Kuehner, P.; Mann, K.; Hermann, D. *Forensic Sci. Int.* **2007**, *170*, 46−50.
(9) Musshoff, F.; Junker, H. P.; Lachenmeier, D. W.; Kroener, L.; Madea, B. *J. Anal. Toxicol.* **2002**, *26*, 554−560.
(10) Strano-Rossi, S.; Chiarotti, M. *J. Anal. Toxicol.* **1999**, *23*, 7−10.
(11) Emídio, E. S.; de Menezes Prata, V.; de Santana, F. J. M.; Dórea, H. S. *J. Chromatogr. B: Anal. Technol. Biomed. Life Sci.* **2010**, *878*, 2175−2183.
(12) Emídio, E. S.; de Menezes Prata, V.; Dórea, H. S. *Anal. Chim. Acta* **2010**, *670*, 63−71.
(13) Nadulski, T.; Pragst, F. *J. Chromatogr. B: Anal. Technol. Biomed. Life Sci.* **2007**, *846*, 78−85.
(14) Pragst, F.; Balikova, M. A. *Clin. Chim. Acta* **2006**, *370*, 17−49.
(15) Huestis, M. A.; Gustafson, R. A.; Moolchan, E. T.; Barnes, A.; Bourland, J. A.; Sweeney, S. A.; Hayes, E. F.; Carpenter, P. M.; Smith, M. L. *Forensic Sci. Int.* **2007**, *169*, 129−136.
(16) Minoli, M.; Angeli, I.; Ravelli, A.; Gigli, F.; Lodi, F. *Forensic Sci. Int.* **2012**, *218*, 49.
(17) Han, E.; Chung, H.; Song, J. M. *J. Anal. Toxicol.* **2012**, *36*, 195−200.
(18) Breidi, S. E.; Barker, J.; Petróczi, A.; Naughton, D. P. *J. Anal. Methods Chem.* **2012**, *2012*, No. 907893.
(19) Mercolini, L.; Mandrioli, R.; Protti, M.; Conti, M.; Serpelloni, G.; Raggi, M. A. *J. Pharm. Biomed. Anal.* **2013**, *76*, 119−125.
(20) Roth, N.; Moosmann, B.; Auwärter, V. *J. Mass Spectrom.* **2013**, *48*, 227−233.
(21) Vincenti, M.; Salomone, A.; Gerace, E.; Pirro, V. *Mass Spectrom. Rev.* **2013**, *32*, 312−332.
(22) Thieme, D.; Sachs, H.; Uhl, M. *Drug Test. Anal.* **2014**, *6*, 112−118.
(23) Míguez-Framil, M.; Cocho, J. Á.; Tabernero, M. J.; Bermejo, A. M.; Moreda-Piñeiro, A.; Bermejo-Barrera, P. *Microchem. J.* **2014**, *117*, 7−17.
(24) Duvivier, W. F.; van Putten, M. R.; van Beek, T. A.; Nielen, M. W. F. *Anal. Chem.* **2016**, *88*, 2489−2496.
(25) Poetzsch, M.; Steuer, A. E.; Roemmelt, A. T.; Baumgartner, M. R.; Kraemer, T. *Anal. Chem.* **2014**, *86*, 11758−11765.
(26) Miki, A.; Katagi, M.; Kamata, T.; Zaitsu, K.; Tatsuno, M.; Nakanishi, T.; Tsuchihashi, H.; Takubo, T.; Suzuki, K. *J. Mass Spectrom.* **2011**, *46*, 411−416.
(27) Kamata, T.; Shima, N.; Sasaki, K.; Matsuta, S.; Takei, S.; Katagi, M.; Miki, A.; Zaitsu, K.; Nakanishi, T.; Sato, T.; Suzuki, K.; Tsuchihashi, H. *Anal. Chem.* **2015**, *87*, 5476−5481.
(28) Porta, T.; Grivet, C.; Kraemer, T.; Varesio, E.; Hopfgartner, G. *Anal. Chem.* **2011**, *83*, 4266−4272.
(29) Musshoff, F.; Arrey, T.; Strupat, K. *Drug Test. Anal.* **2013**, *5*, 361−365.
(30) Cuypers, E.; Flinders, B.; Bosman, I. J.; Lusthof, K. J.; Van Asten, A. C.; Tytgat, J.; Heeren, R. M. A. *Forensic Sci. Int.* **2014**, *242*, 103−110.
(31) Flinders, B.; Cuypers, E.; Zeijlemaker, H.; Tytgat, J.; Heeren, R. M. A. *Drug Test. Anal.* **2015**, *7*, 859−865.
(32) Shen, M.; Xiang, P.; Shi, Y.; Pu, H.; Yan, H.; Shen, B. *Anal. Bioanal. Chem.* **2014**, *406*, 4611−4616.
(33) Shima, N.; Sasaki, K.; Kamata, T.; Matsuta, S.; Katagi, M.; Miki, A.; Zaitsu, K.; Sato, T.; Nakanishi, T.; Tsuchihashi, H.; Suzuki, K. *Forensic Toxicol.* **2015**, *33*, 122−130.
(34) Uematsu, T.; Mizuno, A.; Nagashima, S.; Oshima, A.; Nakamura, M. *Br. J. Clin. Pharmacol.* **1995**, *39*, 665−669.
(35) Thieme, D.; Sachs, H.; Thevis, M. *J. Mass Spectrom.* **2008**, *43*, 974−979.
(36) Quirke, J. M. E.; Adams, C. L.; Van Berkel, G. *Anal. Chem.* **1994**, *66*, 1302−1315.
(37) Trim, P. J.; Djidja, M.-C.; Atkinson, S. J.; Oakes, K.; Cole, L. M.; Anderson, D. M. G.; Hart, P. J.; Francese, S.; Clench, M. R. *Anal. Bioanal. Chem.* **2010**, *397*, 3409−3419.
(38) Simmons, D. A. A practical introduction to MALDI-MS imaging; Applied Biosystems Technical Note, 2008; http://maldi-msi.org/wp/wp-content/uploads/2008/10/Imaging%20Overview%20Doug%20Simmons%20Sept_19_2008.pdf
(39) Roth, N.; Moosmann, B.; Auwärter, V. *J. Mass Spectrom.* **2013**, *48*, 227−233.
(40) Groeneveld, G.; de Puit, M.; Bleay, S.; Bradshaw, R.; Francese, S. *Sci. Rep.* **2015**, *5*, No. 11716.
(41) Bijlsma, L.; Sancho, J. V.; Hernández, F.; Niessen, W. M. A. *J. Mass Spectrom.* **2011**, *46*, 865−875.

DOI: 10.1021/acs.analchem.6b03551
Anal. Chem. 2016, 88, 10328−10334

(42) Murgasova, R.; Hercules, D. M.; Edman, J. R. *Macromolecules* **2004**, *37*, 5732−5740.
(43) Bergman, N.; Shevchenko, D.; Bergquist, J. *Anal. Bioanal. Chem.* **2014**, *406*, 49−61.
(44) Dunphy, J. C.; Pessler, D. G.; Morrall, S. W.; Evans, K. A.; Robaugh, D. A.; Fujimoto, G.; Negahban, A. *Environ. Sci. Technol.* **2001**, *35*, 1223−1230.
(45) Lin, Y.; Chen, C.; Wang, G. *Rapid Commun. Mass Spectrom.* **2007**, *21*, 1973−1983.
(46) Hailat, I.; Helleur, R. J. *Rapid Commun. Mass Spectrom.* **2014**, *28*, 149−158.
(47) Mukaiyama, T.; Tanaka, T. *Chem. Lett.* **1976**, *5*, 303−306.
(48) Adomat, H. H.; Bains, O. S.; Lubieniecka, J. M.; Gleave, M. E.; Guns, E. S.; Grigliatti, T. A.; Reid, R. E.; Riggs, K. W. *J. Chromatogr. B: Anal. Technol. Biomed. Life Sci.* **2012**, *902*, 84−95.
(49) Kuwayama, K.; Miyaguchi, H.; Yamamuro, T.; Tsujikawa, K.; Kanamori, T.; Iwata, Y. T.; Inoue, H. *Rapid Commun. Mass Spectrom.* **2015**, *29*, 2158−2166.

DOI: 10.1021/acs.analchem.6b03551
Anal. Chem. 2016, 88, 10328−10334

J. Am. Soc. Mass Spectrom. (2017) 28:2462–2468
DOI: 10.1007/s13361-017-1766-0

RESEARCH ARTICLE

Optimization of Sample Preparation and Instrumental Parameters for the Rapid Analysis of Drugs of Abuse in Hair samples by MALDI-MS/MS Imaging

Bryn Flinders,[1,4] Emma Beasley,[2] Ricky M. Verlaan,[4] Eva Cuypers,[3] Simona Francese,[2] Tom Bassindale,[2] Malcolm R. Clench,[2] Ron M. A. Heeren[1,4]

[1]FOM-Institute AMOLF, Science Park 104, 1098 XG, Amsterdam, The Netherlands
[2]Center for Mass Spectrometry Imaging, Biomolecular Sciences Research Center, City Campus, Sheffield Hallam University, Howard Street, Sheffield, S1 1WB, UK
[3]KU Leuven Toxicology and Pharmacology", Herestraat 49, PO 9223000, Leuven, Belgium
[4]Maastricht Multimodal Molecular Imaging Institute (M4I), University of Maastricht, Universiteitssingel 50, 6229 ER, Maastricht, The Netherlands

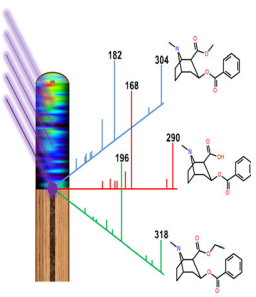

Abstract. Matrix-assisted laser desorption/ionization-mass spectrometry imaging (MALDI-MSI) has been employed to rapidly screen longitudinally sectioned drug user hair samples for cocaine and its metabolites using continuous raster imaging. Optimization of the spatial resolution and raster speed were performed on intact cocaine contaminated hair samples. The optimized settings (100 × 150 μm at 0.24 mm/s) were subsequently used to examine longitudinally sectioned drug user hair samples. The MALDI-MS/MS images showed the distribution of the most abundant cocaine product ion at *m/z* 182. Using the optimized settings, multiple hair samples obtained from two users were analyzed in approximately 3 h: six times faster than the standard spot-to-spot acquisition method. Quantitation was achieved using longitudinally sectioned control hair samples sprayed with a cocaine dilution series. A multiple reaction monitoring (MRM) experiment was also performed using the 'dynamic pixel' imaging method to screen for cocaine and a range of its metabolites, in order to differentiate between contaminated hairs and drug users. Cocaine, benzoylecgonine, and cocaethylene were detectable, in agreement with analyses carried out using the standard LC-MS/MS method.

Keywords: MALDI-MSI, Cocaine, Metabolites, Raster imaging

Received: 2 April 2017/Revised: 2 July 2017/Accepted: /Published Online: 11 August 2017

Introduction

Hair testing is a powerful tool routinely used for the detection of drugs of abuse in toxicology and forensic applications [1–3]. The analysis of hair is highly advantageous as it can provide prolonged detection and chronological information about drug intake or chemical exposure in contrast to the analysis of biological fluids [4]. However, current methodology routinely involves complex and time-consuming homogenization, derivatization, sample-clean up, and extraction techniques followed by gas or liquid chromatography coupled with mass spectrometry (GC-MS or LC-MS). Also these techniques require large amounts of hair sample (10–100 mg) and can only provide the chronological information per month (based on the average growth rate of 1 cm/mo).

Matrix-assisted laser desorption/ionization-mass spectrometry imaging (MALDI-MSI) is well established for the detection and imaging of drugs and pharmaceuticals in tissues. However, it is increasingly being used for the analysis of drugs of abuse in hair, as it offers several advantages over the currently established techniques, such as requiring fewer hair samples, simpler and faster sample preparation, and providing more accurate and visual chronological information in hours or days.

Electronic supplementary material The online version of this article (doi:10.1007/s13361-017-1766-0) contains supplementary material, which is available to authorized users.

Correspondence to: Ron Heeren; *e-mail:* r.heeren@maastrichtuniversity.nl

MALDI-MSI has been used to monitor the distribution of a wide range of compounds, including drugs of abuse, pharmaceuticals, and other compounds in single hair samples, such as cocaine [5], methamphetamine [6, 7], ketamine [8], cannabinoids [9], tilidine [10], zolpidem [11, 12], and nicotine [13]. New techniques have also been introduced into the field, such as infrared-matrix-assisted laser desorption electrospray ionization-mass spectrometry imaging (IR-MALDESI-MSI), which has been used to monitor the distribution of the antiretroviral efavirenz in hair samples from HIV infected patients [14]. Recently, mass spectrometry imaging techniques have been used to address some of the current issues with forensic hair testing, such as the process/rate of drug incorporation [15], the effects of cosmetic treatment [16], and the consequences of different washing procedures [17].

Whilst these examples show it is possible to monitor the distribution of a wide range of compounds in single hair samples, multiple hairs need to be analyzed in order to account for the different growth phases of hair. As a result, depending on the length and number of the hair samples or the spatial resolution, it can take several hours to a few days to acquire images with the conventional spot-to-spot acquisition method. One way to overcome this and improve the speed of analysis is to use "raster imaging" mode. This method of data acquisition is achieved by continuously firing the laser in rows across a sample. The generated data is placed into a bin at selected intervals during the raster, which is based upon the selected spatial resolution and sampling speed [18, 19]. Another issue is the extraction efficiency of the embedded drugs by the matrix solution. As the drugs are considered to be bound to melanin inside the core of the hair, it remains difficult to know whether the drug is completely extracted from the hair by the MALDI matrix, especially through the impermeable outer surface; this can be overcome by longitudinally sectioning the hair samples prior to analysis.

In the work reported here, instrumental and experimental parameters were optimized to rapidly generate high quality images of longitudinally sectioned drug user hair samples using continuous raster imaging. In order to quantify the detected drug, a novel method for preparing a calibration line on longitudinally sectioned hair was developed. To further confirm if the detected drugs and metabolites are indicative of actual ingestion, a multiple reaction monitoring (MRM) method was developed to screen for unique metabolites.

Experimental

Materials

Alpha-cyano-4-hydroxycinnamic acid (CHCA), cocaine (COC), benzoylecgonine (BZE), norcocaine (NCOC), cocaethylene (CE), ecgonine methyl ester (EME), anhydroecgonine methyl ester (AEME), and dichloromethane (DCM) were purchased from Sigma Aldrich (Schnelldorf, Germany). Acetonitrile (ACN), methanol (MeOH), and trifluroacetic acid (TFA) were purchased from Biosolve (Valkenswaard, The Netherlands).

Sample Preparation

Hair samples were collected from volunteer drug users and hair samples of non-users were collected from volunteers and analyzed as negative controls. Hair samples were decontaminated using two 10 mL dichloromethane washes for 1 min by shaking. After washing, the hair samples were left dry at room temperature [20, 21]. Longitudinal sections of hair samples were prepared using the previously reported method [22]. Briefly, the hair sample was affixed onto a metal plate that contains grooves ranging from 20 to 80 μm. Whilst holding the other end of the hair sample with a gloved finger, a holder with a blade fixed at a 20° angle was run along the length of the hair. After visual inspection using a Leica DM RX light microscope (Leica, Wetzlar, Germany) equipped with a Nikon DM100 digital camera (Nikon, Tokyo, Japan), the hair samples were mounted onto a glass slide using double-sided tape. Control hair samples were placed into a 1 mg/mL solution of cocaine (50:50 acetonitrile:water) before mounting onto a glass slide using double sided tape.

Preparation of Standards for Quantitation

Cocaine standards were prepared from a 1 mg/mL stock solution to give the following standards: 0.1, 0.2, 0.5, 1, 2, 5, and 10 ng/μL in 70% acetonitrile. In order to achieve a homogenous and uniform deposition, the cocaine standards were sprayed onto longitudinal sectioned control hair samples using the Suncollect automated pneumatic sprayer (Sunchrom, Friedrichsdorf, Germany) with the aid of stencils made from polylactic acid. The stencils (containing square holes that are 2 mm^2) were made using a Ultimaker Original 3D printer (Ultimaker, Geldermalsen, The Netherlands). The standards were sprayed in a series of 30 layers. The initial layer was sprayed at 10 μL/min, then stepped up from 20 μL/min to 30 μL/min, and subsequent layers were sprayed at 40 μL/min. The hair samples were mounted onto a glass slide using double sided tape.

Matrix Application

The samples were coated with 7 mg/mL CHCA in 50:50 acetonitrile:water with 0.2% TFA using a Bruker ImagePrep (Bruker Daltonics, Bremen, Germany).

Instrumentation

All data were acquired in positive ion mode on an Applied Biosystems/MDS Sciex hybrid quadrupole time-of-flight mass spectrometer (Q-Star Pulsar-*i*) with an orthogonal MALDI ion source (Applied Biosystems, Foster City, CA, USA) and a neodymium-doped yttrium aluminium garnet (Nd:YAG) laser (355 nm, 1 KHz). The laser power was 30 (1000 Hz, 3.2 μJ) and the laser beam had an elliptical spot size of 100 × 150 μm. Image acquisition was performed using the "raster image"

mode [18, 23]. Images were generated using the freely available Novartis Biomap 3.8.0.4 software (www.maldi-msi.org). MALDI-MS spectra were obtained in positive ion mode in the mass range between *m/z* 50 and 1000. Declustering potential 2 was set at 15 arbitrary units and the focus potential at 10 arbitrary units, with an accumulation time of 0.999 s. The MALDI-MS/MS spectra were obtained using argon as the collision gas; the declustering potential 2 was set at 15 and the focusing potential at 20, and the collision energy and collision gas pressure were set at 20 and 5 arbitrary units, respectively.

Dynamic pixel imaging was employed to perform MRM imaging experiments. The method was optimized using standards of cocaine and its metabolites (100 ng/μL in 70% methanol), and the most abundant product ions were selected for imaging. The laser power was 80% (1000 Hz, 8 μJ), the instrument parameters were accumulation time of 0.4 s, seconds/spot 2.4 s, and the mass range was ±2 u for each product ion. Images were generated using the oMALDI server 5.1 software (MDS Sciex, Concord, ON, Canada).

Data Processing

For presentation purposes, mass spectra from the Analyst QS 1.1 software were exported in the form of text files and imported into mMass software, an open-source mass spectrometry software used for mass spectral processing [24].

Results and Discussion

In the initial phase of the study, the optimization of instrumental parameters was carried out:

Optimization of Spatial Resolution and Raster Speed for MALDI-MS/MS Imaging

To determine the optimal spatial resolution and raster speed intact cocaine contaminated hair samples were analyzed in triplicate, and these results were plotted as a function of the average intensity and time, respectively. The results from these experiments are shown in Figure 1.

The average intensity of the product ion of cocaine at *m/z* 182 for each of the spiked hair samples analyzed (n = 3) was determined using the region of interest (ROI) tool in the Biomap 3.8.0.4 imaging software. The results shown in Figure 1 show that analysis of samples at a high spatial resolution results in a decreased sample throughput and sensitivity. This is due to the increased number of rasters and extensive oversampling. Conversely, analysis of samples at a lower spatial resolution results in an increased sample throughput and sensitivity, because of the reduced number of rasters and a fresh area being consistently sampled.

However, it should be noted that when performing the analysis of hair samples at a lower spatial resolution, the results from individual hairs begin to merge. This is observed in the MALDI-MS/MS images (Figure 1c), therefore when preparing hair samples the spacing between the hair samples needs to be taken into account. Whilst high spatial resolution imaging is possible, it may not be necessary, especially across the width of the hair, as the chronological information is obtained longitudinally along the length of the hair. In addition, the incorporation rate and keratinization of drug into the hair can take several days.

Based on the findings of this study, the optimal spatial resolution was determined to be 100 × 150 μm and the optimal raster speed was 0.24 mm/s (416 shots/pixel). Whilst it may appear that imaging the hair samples at 150 × 150 μm, 0.17 mm/s is optimal, the corresponding image shows the hairs begin to merge into one; in addition, there is not much gain in intensity. As the spatial resolution along the length of the hair is 150 μm, each pixel is equivalent to around 12 h of growth. This allows for a much narrower time frame of detection than the standard GC-MS and LC-MS methods, which can only provide information about drug use averaged over a 1 mo period.

Determination of Optimal Sample Orientation

In order to determine if the orientation of the hair samples in relation to the movement of the laser affects the results, six cocaine contaminated hair samples were analyzed in different orientations using the optimized settings. The MALDI-MS/MS images of the cocaine contaminated hair samples are shown in Figure 2.

The MALDI-MS/MS images show cocaine contaminated hair samples analyzed in both the horizontal (Figure 2a) and vertical (Figure 2b and c) orientations. The images show that using the optimized settings clearly differentiates between individual hairs.

The MALDI-MS/MS image shown in Figure 2a shows hair samples analyzed in the horizontal orientation, and the insert shows each hair consists of around to 3–4 pixels. Whereas the image in Figure 2b shows hair samples analyzed in the vertical orientation, the insert shows that each hair consists of 2–3 pixels. The MALDI-MS/MS image in Figure 2c shows better separation, which could be due to the elliptical laser spot size (100 × 150 μm). This is also observed in the insert that shows an expanded view of a single hair prior to smoothing, which consists of around to 2–3 pixels per hair. This experiment shows that hair samples can be analyzed in either orientation; however, the spatial resolution needs to be adjusted accordingly. For subsequent experiments, the hair samples were analyzed in the horizontal orientation with the laser running parallel (150 × 100 μm).

MALDI-MS/MS Imaging of Longitudinal Sectioned Drug User Hair Samples

Once the spatial resolution and raster speed was optimized to produce the best quality image in the shortest time, the method was applied to monitor the distribution of cocaine in a number of longitudinally sectioned hair samples from cocaine users. In order to quantify the amount of cocaine present in the hair

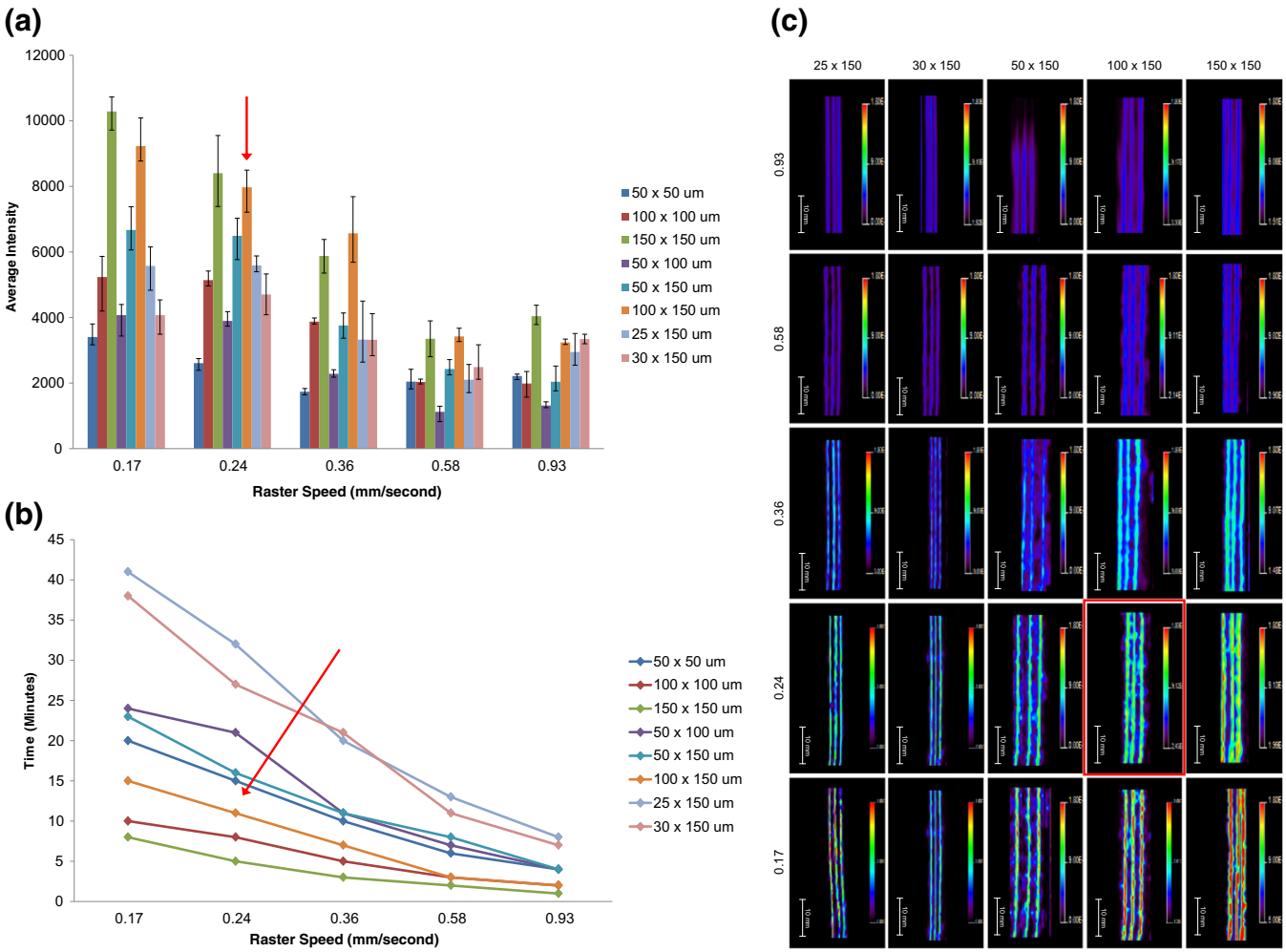

Figure 1. Graphs to determine the optimal spatial resolution and raster speed for imaging the distribution of cocaine in hair samples by MALDI-MS/MS imaging. The graphs show (**a**) the average intensity of the cocaine product ion at *m/z* 182 at each spatial resolution tested at different raster speeds, and (**b**) the time taken for each spatial resolution tested at different raster speeds. (**c**) MALDI-MS/MS images of cocaine contaminated hair samples analyzed used to determine the optimal parameters showing the distribution of the product ion at *m/z* 182. The highlighted image and areas indicated by the red arrows show the determined optimal parameters

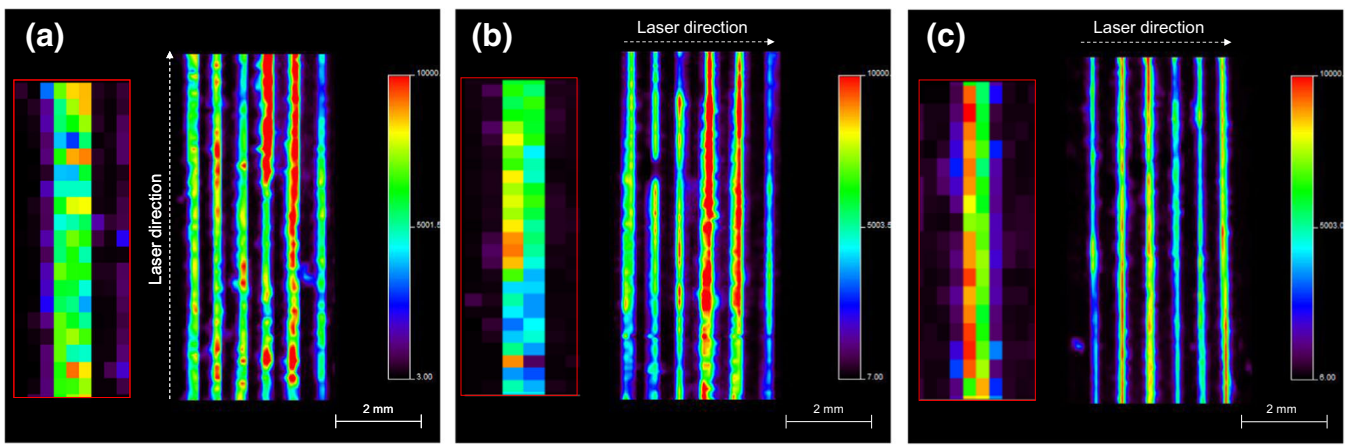

Figure 2. MALDI-MS/MS images of cocaine contaminated hair samples analyzed in different orientations, showing the distribution of the product ion at *m/z* 182. (**a**) Horizontal direction (150 × 100 µm), (**b**) vertical direction (150 × 100 µm), and (**c**) vertical direction (100 × 150 µm). The inserts show the number of pixels per hair

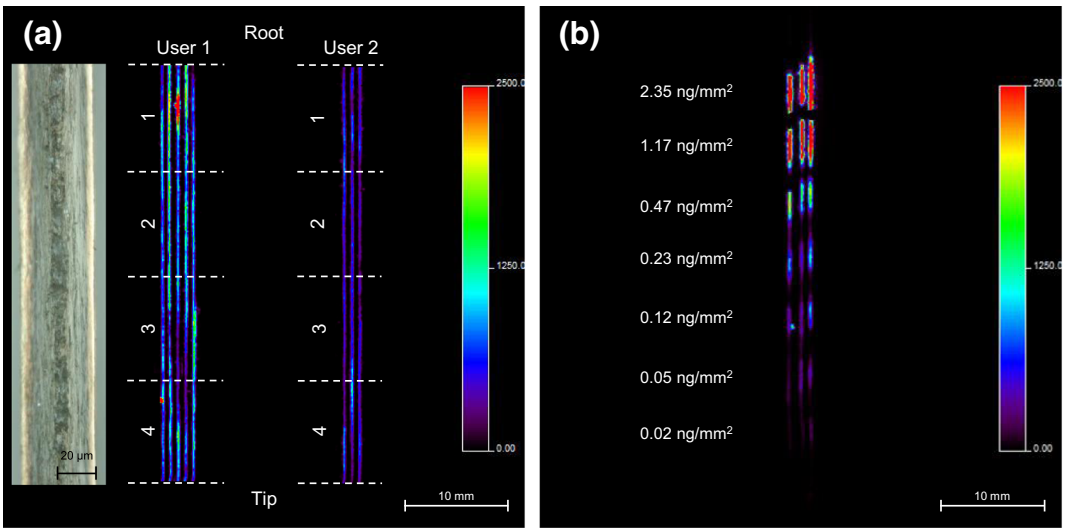

Figure 3. MALDI-MS/MS images of (**a**) longitudinally sectioned drug user hair samples (insert shows optical image of longitudinally sectioned hair), and (**b**) longitudinally sectioned control hair samples sprayed with a cocaine dilution series. The MALDI-MS/MS image shows the distribution of the product ion at *m/z* 182, derived from the precursor ion of cocaine at *m/z* 304

samples, control hair samples sprayed with a cocaine dilution series were also analyzed. The MALDI-MS/MS images of the cocaine user hair samples and cocaine standard hair samples are shown in Figure 3.

The MALDI-MS/MS image (Figure 3a) shows the distribution of the most abundant cocaine product ion at *m/z* 182, which is formed by the neutral loss of benzoic acid from the intact molecule and was detected in both user hair samples. In contrast, it was not detected in the longitudinal sectioned control hair sample; due to the number of hair samples available from the second user, only three hairs were analyzed. The length of the analyzed hair samples was 4 cm; given the average growth rate of human hair is approximately 1 cm per month, this corresponds to a growth period of 4 mo [25]. Since the spatial resolution along the hair is 150 µm, each pixel is equivalent to around 12 h of growth. The analysis of the longitudinally sectioned user hair samples took 3 h and 22 min (136 s per raster). This is around six times faster in comparison to the standard spot-to-spot acquisition method at this spatial resolution, which takes around 18 h. Analysis with the current methodology takes around 1 h; however, the sample preparation takes approximately 1 d. In contrast, the sample preparation for MALDI-MSI takes around 1 h; along with the optimized settings it takes approximately 4 h to perform the entire experiment. This is six times faster than the currently established method. The insert shows a close-up view of a longitudinally sectioned hair sample, prepared using the previously published method [22]. The image clearly shows minimal damage to the hair with the medulla in the center surrounded by the cortex and the cuticle on the edge of the hair.

In order to quantify the amount of cocaine in the longitudinally sectioned user hair samples, a cocaine dilution series was prepared. This was initially spotted onto the glass slide next to the hair samples; however, this resulted in an uncontrollable deposition due to spreading. Therefore, to overcome this issue, the cocaine dilution series was sprayed onto longitudinally sectioned control hair samples using the described method, in order to reproducibly produce uniform and homogenous standards as shown in Figure 3b. The obtained image does suggest that this method of standard deposition has resulted in homogenous and uniform deposition. A decreasing response with respect to the concentration is clearly observable with good reproducibility for each hair sample (see Supplementary Figure S1). The concentration per standard was reported in ng/mm^2, which was calculated from the parameters used to spray the cocaine standards. The analysis of the quantitation hair standards took 1 h and 10 min. It should be noted that the control hair samples used for the calibration curve were not the same color as those from the drug users, and other information such as race and gender was not available. Ideally the hair samples used for quantitation should be matched based on hair color, race, and gender.

Using the ROI tool of the Biomap 3.8.0.4 software, the average intensity of the calibration standards (Supplementary Figure S1) and the four segments from both of the user hairs (Supplementary Figure S2) were determined. The calibration curve was linear over two orders of magnitude ($R^2 = 0.9908$). Using the calibration curve the concentration of cocaine per segment for the first user was determined to be 0.437, 0.389, 0.340, and 0.305 ng/mm^2 (1–4), whereas the concentration of cocaine per segment for the second user was determined to be 0.151, 0.154, 0.1720, and 0.186 ng/mm^2 (1–4). These results indicate both users have a prolonged history of cocaine use and that the first user is a heavier user in contrast to the second user; this is also apparent in in the MALDI-MS/MS image.

MALDI-MS/MS Imaging of Cocaine Metabolites in Drug User Hair Samples

One way to determine if a detected drug is present due to ingestion rather than environmental contamination is to monitor the

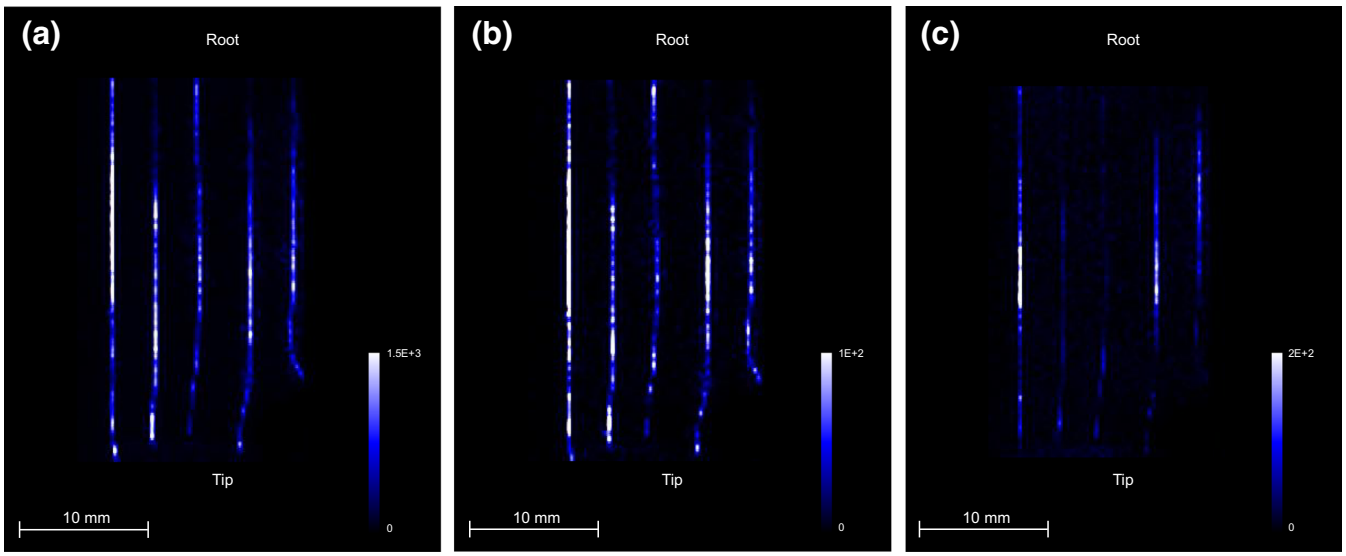

Figure 4. MALDI-MS/MS images of longitudinally sectioned drug user hair samples. The images show the distribution of (**a**) cocaine (*m/z* 304.15→182.12), (**b**) benzoylecgonine (*m/z* 290.15→168.11), and (**c**) cocaethylene (*m/z* 318.17→196.15)

presence of unique metabolites [20, 26]. In the case of cocaine, cocaethylene (a metabolite formed by the simultaneous consumption of cocaine and ethanol), norcocaine (an in-vivo metabolite of cocaine), and anhydroecgonine methyl ester (a pyrolysis product formed when crack cocaine is smoked). Other metabolites, such as benzoylecgonine, the main metabolite of cocaine, can also be formed by environmental degradation [27]. In order to screen the drug user hair samples for cocaine and its metabolites, a MRM imaging method using dynamic pixel imaging was developed. Dynamic pixel imaging is a technique that enables multiple experiments to be performed consecutively in a single acquisition. This is because the target plate is moved around within each pixel, which enables longer acquisition time per pixel and thus multiple experiments to be performed [28]. The transitions for cocaine and its metabolites were as follows: cocaine (*m/z* 304.15→182.12), cocaethylene (*m/z* 318.17→196.15), norcocaine (*m/z* 290.13→136.09), benzoylecgonine (*m/z* 290.15→168.11), ecgonine methyl ester (*m/z* 200.16→182.13), and anhydroecgonine methyl ester (*m/z* 182.13→118.06). The MALDI-MS/MS spectra of cocaine and its metabolites are shown in Supplementary Figure S3.

A requirement for the use of the dynamic pixel imaging method is that the hairs needed to be spaced as far apart as possible in order to distinguish individual hairs. This is due to the figure eight movement of the sample stage during the acquisition, and as a result the best spatial resolution that could be achieved was 250 × 250 μm. The MALDI-MS/MS images of cocaine and its metabolites in the longitudinal sectioned hair samples acquired in this manner are shown in Figure 4.

The length of the analyzed hair samples was 3 cm, and given the average growth rate of human hair is around 1 cm per month, this corresponds to a growth period of 3 mo.. Since the spatial resolution along the hair is 250 μm, this corresponds to 18 h of growth. Cocaine, the major metabolite benzoylecgonine, and the metabolite cocaethylene were detected in the drug user hair sample. This was also confirmed using the routine LC-MS/MS analysis method.

Conclusions

The use of MALDI-MS/MS imaging for the rapid screening of drugs of abuse in hair samples using continuous raster imaging has been presented. Optimization of instrumental and experimental parameters such as the spatial resolution, raster speed, and sample orientations were performed in order to rapidly analyze hair samples without compromising the quality of the images. Whilst these settings are specific to this instrument, they provide a starting point for the optimization of these parameters on other instruments operating in raster imaging mode. Using the optimized settings (100 × 150 μm at 0.24 mm/s), the analysis of the longitudinally sectioned hair samples of two drug users took approximately 3 h, which is six times faster in comparison with the standard spot-to-spot acquisition method at this spatial resolution, which takes around 18 h. In order to quantify the amounts of cocaine in longitudinally sectioned drug user hair samples, a novel method for the preparation of standards was developed. In order to determine if the detected drugs present are from actual abuse rather than external contamination, a MRM imaging method utilizing 'dynamic pixel' imaging in combination with longitudinally sectioned hair was developed. By screening for unique cocaine metabolites that can only be formed in vivo, the confirmation of ingestion of cocaine could be ascertained. Cocaine, benzoylecgonine, and cocaethylene were present, which was consistent with the standard LC-MS/MS method. The work presented here also shows that if required, faster analysis is possible but the spatial resolution and spacing between hair samples needs to be adjusted accordingly.

Acknowledgements

This work is partly funded by the research program of the Foundation of Fundamental Research on Matter (FOM), which is financially supported by the Netherlands Organization for

Scientific Research (NWO). Part of this work (B.F. and R.M.A.H.) was funded by the NWO Forensic Science program (project nr 727.011.004). The MOLHAIR project consortium comprises of FOM Institute AMOLF, Wageningen University, RIKILT, and The Maastricht Forensic Institute (TMFI). This research has in part been made possible with the support of the Dutch Province of Limburg through the LINK program. Traveling grant for a long stay abroad of Dr. E. Cuypers was awarded by Fonds Wetenschappelijk Onderzoek (FWO). The work carried out by E.B, M.R.C, S.F., and T.B is funded by a Sheffield Hallam University Vice Chancellors Scholarship and the Sheffield Hallam Biomolecular Sciences Research Centre PhD studentship awarded to E.B.

Open Access

References

1. Pragst, F., Balikova, M.A.: State of the art in hair analysis for detection of drug and alcohol abuse. Clin. Chim. Acta **370**, 17–49 (2006)
2. Vincenti, M., Salomone, A., Gerace, E., Pirro, V.: Application of mass spectrometry to hair analysis for forensic toxicological investigations. Mass Spectrom. Rev. **32**, 312–332 (2013)
3. Musshoff, F., Madea, B.: New trends in hair analysis and scientific demands on validation and technical notes. Forensic Sci. Int. **165**, 204–215 (2007)
4. Kintz, P., Villain, M., Cirimele, V.: Hair analysis for drug detection. Ther. Drug Monit. **28**, 442–446 (2006)
5. Porta, T., Grivet, C., Kraemer, T., Varesio, E., Hopfgartner, G.: Single hair cocaine consumption monitoring by mass spectrometric imaging. Anal. Chem. **83**, 4266–4272 (2011)
6. Miki, A., Katagi, M., Kamata, T., Zaitsu, K., Tatsuno, M., Nakanishi, T., Tsuchihashi, H., Takubo, T., Suzuki, K.: MALDI-TOF and MALDI-FTICR imaging mass spectrometry of methamphetamine incorporated in hair. J. Mass Spectrom. **46**, 411–416 (2011)
7. Miki, A., Katagi, M., Shima, N., Kamata, H., Tatsuno, M., Nakanishi, T., Tsuchihashi, H., Takubo, T., Suzuki, K.: Imaging of methamphetamine incorporated into hair by MALDI-TOF mass spectrometry. Forensic Toxicol. **29**, 111–116 (2011)
8. Shen, M., Xiang, P., Shi, Y., Pu, H., Yan, H., Shen, B.: Mass imaging of ketamine in a single scalp hair by MALDI-FTMS. Anal. Bioanal. Chem. **406**, 4611–4616 (2014)
9. Beasley, E., Francese, S., Bassindale, T.: Detection and mapping of cannabinoids in single hair samples through rapid derivatization and matrix-assisted laser desorption ionization mass spectrometry. Anal. Chem. **88**, 10328–10334 (2016)
10. Poetzsch, M., Baumgartner, M.R., Steuer, A.E., Kraemer, T.: Segmental hair analysis for differentiation of tilidine intake from external contamination using LC-ESI-MS/MS and MALDI-MS/MS imaging. Drug Test. Anal. **7**, 143–149 (2015)
11. Poetzsch, M., Steuer, A.E., Roemmelt, A.T., Baumgartner, M.R., Kraemer, T.: Single hair analysis of small molecules using MALDI-triple quadrupole MS imaging and LC-MS/MS: investigations on opportunities and pitfalls. Anal. Chem. **86**, 11758–11765 (2014)
12. Shima, N., Sasaki, K., Kamata, T., Matsuta, S., Katagi, M., Miki, A., Zaitsu, K., Sato, T., Nakanishi, T., Tsuchihashi, H., Suzuki, K.: Single hair analysis of zolpidem on the supposition of its single administration in drug-facilitated crimes. Forensic Toxicol. **33**, 122–130 (2015)
13. Nakanishi, T., Nirasawa, T., Takubo, T.: Quantitative mass barcode-like image of nicotine in single longitudinally sliced hair sections from long-term smokers by matrix-assisted laser desorption time-of-flight mass spectrometry imaging. J. Anal. Toxicol. **38**, 349–353 (2014)
14. Rosen, E.P., Thompson, C.G., Bokhart, M.T., Prince, H.M.A., Sykes, C., Muddiman, D.C., Kashuba, A.D.M.: Analysis of anti-retrovirals in single hair strands for evaluation of drug adherence with infrared-matrix-assisted laser desorption electrospray ionization mass spectrometry imaging. Anal. Chem. **88**, 1336–1344 (2015)
15. Kamata, T., Shima, N., Sasaki, K., Matsuta, S., Takei, S., Katagi, M., Miki, A., Zaitsu, K., Nakanishi, T., Sato, T., Suzuki, K., Tsuchihashi, H.: Time-course mass spectrometry imaging for depicting drug incorporation into hair. Anal. Chem. **87**, 5476–5481 (2015)
16. Cuypers, E., Flinders, B., Bosman, I.J., Lusthof, K.J., Van Asten, A.C., Tytgat, J., Heeren, R.M.A.: Hydrogen peroxide reactions on cocaine in hair using imaging mass spectrometry. Forensic Sci. Int. **242**, 103–110 (2014)
17. Cuypers, E., Flinders, B., Boone, C.M., Bosman, I.J., Lusthof, K.J., Van Asten, A.C., Tytgat, J., Heeren, R.M.A.: Consequences of decontamination procedures in forensic hair analysis using metal-assisted secondary ion mass spectrometry. Anal. Chem. **88**, 3091–3097 (2016)
18. Trim, P., Djidja, M., Atkinson, S.J., Oakes, K., Cole, L.M., Anderson, D.M.G., Hart, P.J., Francese, S., Clench, M.R.: Introduction of a 20 kHz Nd:YVO4 laser into a hybrid quadrupole time-of-flight mass spectrometer for MALDI-MS imaging. Anal. Bioanal. Chem. **397**, 3409–3419 (2010)
19. Spraggins, J.M., Caprioli, R.M.: High-speed MALDI-TOF imaging mass spectrometry: rapid ion image acquisition and considerations for next generation instrumentation. J. Am. Soc. Mass Spectrom. **22**, 1022–1031 (2011)
20. Cooper, G.A.A., Kronstrand, R., Kintz, P.: Society of hair testing guidelines for drug testing in hair. Forensic Sci. Int. **218**, 20–24 (2012)
21. Kintz, P.: Segmental hair analysis can demonstrate external contamination in postmortem cases. Forensic Sci. Int. **215**, 73–76 (2012)
22. Flinders, B., Cuypers, E., Zeijlemaker, H., Tytgat, J., Heeren, R.M.A.: Preparation of longitudinal sections of hair samples for the analysis of cocaine by MALDI-MS/MS and TOF-SIMS imaging. Drug Test. Anal. **7**, 859–865 (2015)
23. Simmons, D.A.: Improved MALDI-MS imaging performance using continuous laser rastering. Applied Biosystems Technical Note (2008)
24. Strohalm, M., Kavan, D., Novak, P., Volny, M., Havlicek, V.: mMass 3: a cross-platform software environment for precise analysis of mass spectrometric data. Anal. Chem. **82**, 4648–4651 (2010)
25. LeBeau, M.A., Montgomery, M.A., Brewer, J.D.: The role of variations in growth rate and sample collection on interpreting results of segmental analyses of hair. Forensic Sci. Int. **210**, 110–116 (2011)
26. Schaffer, M., Hill, V., Cairns, T.: Hair analysis for cocaine: the requirement for effective wash procedures and effects of drug concentration and hair porosity in contamination and decontamination. J. Anal. Toxicol. **29**, 319–326 (2005)
27. Cognard, E., Rudaz, S., Bouchonnet, S., Staub, C.: Analysis of cocaine and three of its metabolites in hair by gas chromatography–mass spectrometry using ion-trap detection for CI/MS/MS. J. Chromatogr. B **826**, 17–25 (2005)
28. Multiplexing MALDI mass spectrometry imaging using dynamic pixel imaging. Applied Biosystems Technical Note (2007)